NISTIR 8306

Applied and Computational Mathematics Division

Summary of Activities for Fiscal Year 2019

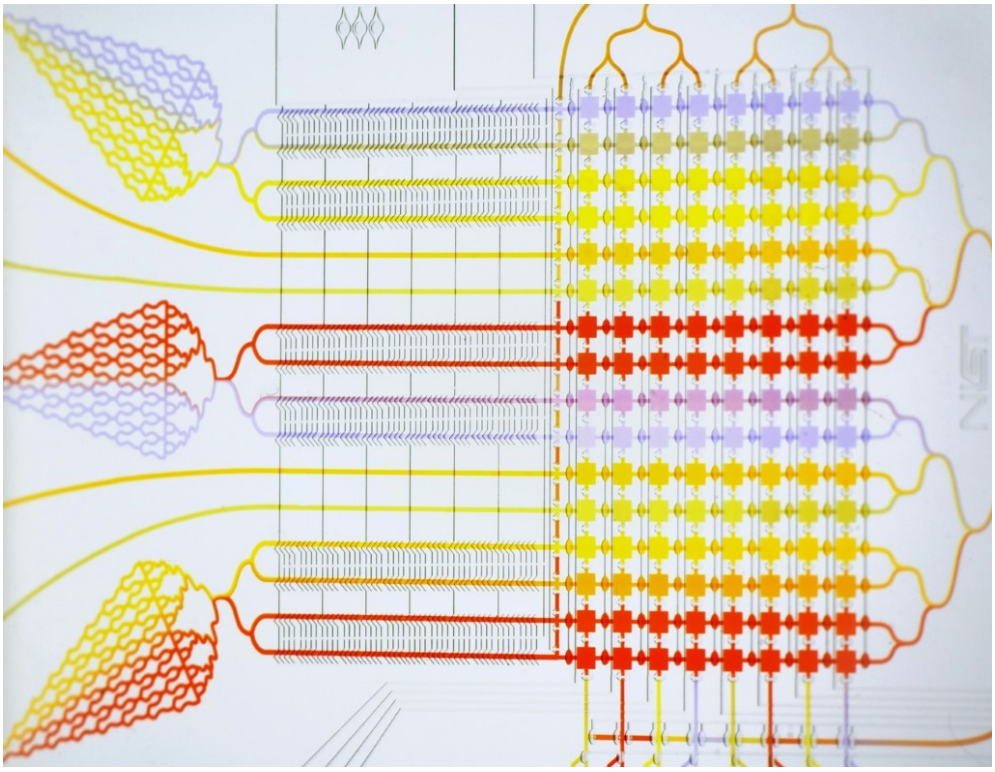

This publication is available free of charge from:
https://doi.org/10.6028/NIST.IR.8306

National Institute of Standards and Technology
U.S. Department of Commerce

NISTIR 8306

Applied and Computational Mathematics Division

Summary of Activities for Fiscal Year 2019

Ronald F. Boisvert, Editor
Applied and Computational Mathematics Division
Information Technology Laboratory

This publication is available free of charge from:
https://doi.org/10.6028/NIST.IR.8306

April 2020

U.S. Department of Commerce
Wilbur L. Ross, Jr., Secretary

National Institute of Standards and Technology
Walter Copan, NIST Director and Under Secretary of Commerce for Standards and Technology

Abstract

This report summarizes recent technical work of the Applied and Computational Sciences Division of the Information Technology Laboratory at the National Institute of Standards and Technology (NIST). Part I (Overview) provides a high-level overview of the Division's activities, including highlights of technical accomplishments during the previous year. Part II (Features) provides further details on three projects of particular note this year. This is followed in Part III (Project Summaries) by brief synopses of all technical projects active during the past year. Part IV (Activity Data) provides listings of publications, technical talks, and other professional activities in which Division staff members have participated. The reporting period covered by this document is October 2018 through December 2019.

For further information, contact Ronald F. Boisvert, 100 Bureau Drive, Mail Stop 8910, NIST, Gaithersburg, MD 20899-8910, phone 301-975-3812, email boisvert@nist.gov, or see the Division's Web site at https://www.nist.gov/itl/math/.

Keywords: applied mathematics; computational science and engineering; high-performance computing; mathematics of metrology; mathematics of biotechnology; materials modeling and simulation; mathematical knowledge management; mathematical modeling; network science; scientific visualization; quantum information science.

Cover Visualization: Microfluidic fabrication techniques allow chemical reaction vessels to be reduced to the size of a human hair, parallelized, and subsequently interconnected. This facilitates high-throughput experimentation and combinatorial testing in chemistry and biology. Illustrated here is an example of a microfluidic device used to establish concentration gradients. Fluid of different colors flows through the input channels (left) and enters the experimental chambers (squares). Because the flow is laminar, diffusion is the only mechanism responsible for mixing (which occurs in the upper branching network and middle mixing regions). In this way it is possible to precisely control concentrations of reactants in combinatorial testing assays. We are developing mathematical models to help inform metrology for microfluidic devices like this. See page 58.

Section Visualizations: The "word cloud," which is found at the start of each Part of this document was created using Wordle, http://www.wordle.net/, and the text of this document as input.

Acknowledgements: Thanks to Lochi Orr for assisting in the compilation of Part IV of this document. Thanks also to Stephen Langer and Brian Cloteaux who carefully read the manuscript and offered many corrections and suggestions for improvement.

National Institute of Standards and Technology Internal Report 8306
Natl. Inst. Stand. Technol. Intern. Rep. 8306, 164 pages (April 2020)

This publication is available free of charge from:
https://doi.org/10.6028/NIST.IR.8306

Contents

Part I

Overview

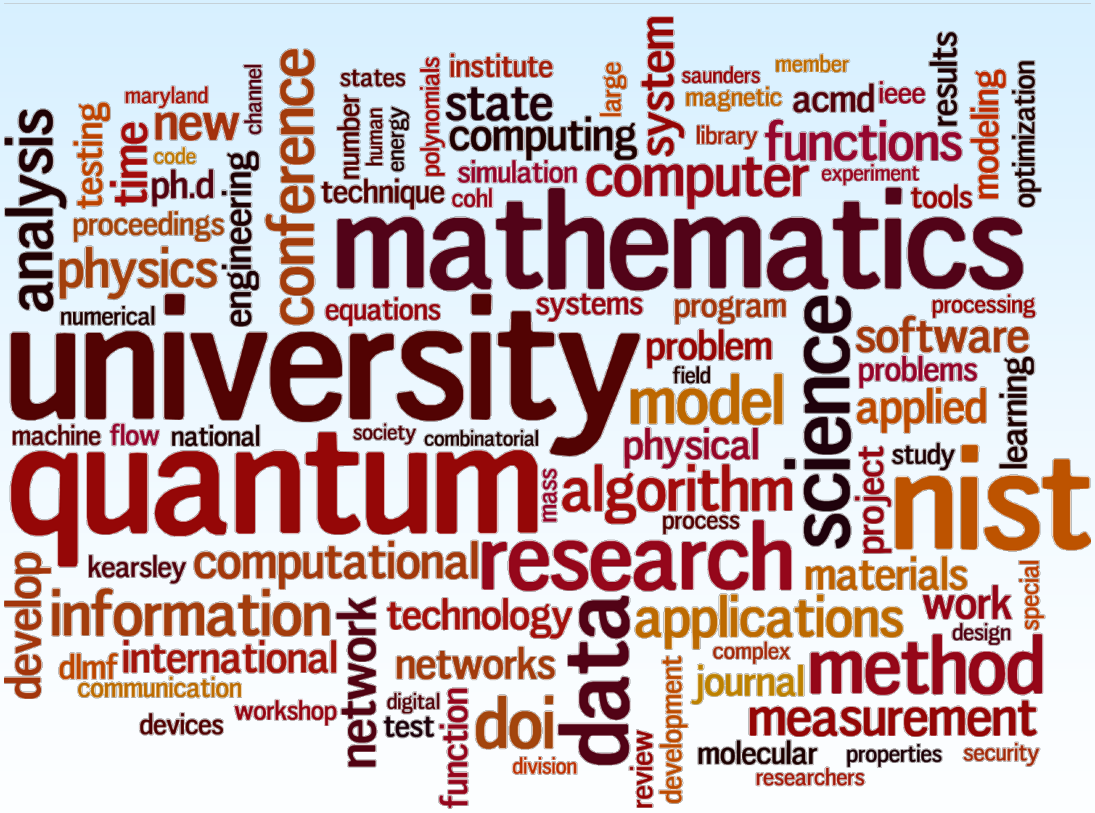

Introduction

Founded in 1901, the National Institute of Standards and Technology (NIST) is a non-regulatory federal agency within the U.S. Department of Commerce. Its mission is to promote U.S. innovation and industrial competitiveness by advancing measurement science, standards, and technology in ways that enhance economic security and improve our quality of life. The NIST Laboratories engage in world-class research, often in close collaboration with industry, that advances the nation's technology infrastructure and helps U.S. companies continually improve products and services. The technical disciplines represented in the NIST Labs include physics, electrical engineering, nanotechnology, materials science, chemistry, bioscience, engineering, fire research, and information technology. The NIST Labs operate in two locations: Gaithersburg, MD, (headquarters—234 hectare/578 acre campus) and Boulder, CO (84 hectare/208 acre campus). NIST employs about 3 400 scientists, engineers, technicians, and support and administrative personnel. NIST also hosts about 2 700 associates from academia, industry, and other government agencies, who collaborate with NIST staff and access user facilities.

The Information Technology Laboratory (ITL) is one of six major organizational units that make up the NIST Labs. ITL's singular purpose is to cultivate trust in information technology and metrology. This is done through the development of measurements, tests, and guidance to support innovation in and deployment of information technology by industry and government, as well as through the application of advanced mathematics, statistics, and computer science to help ensure the quality of measurement science.

The Applied and Computational Mathematics Division (ACMD) is one of seven technical Divisions in ITL. At its core, ACMD's purpose is to nurture trust in metrology and scientific computing. To do so, ACMD provides leadership within NIST in the use of applied and computational mathematics to solve technical problems arising in measurement science and related applications. In that role staff members

- perform research in applied mathematics and computational science and engineering, including analytical and numerical methods, high-performance computing, and visualization;
- perform applied research in computer science and engineering for future computing and communications technologies;
- engage in peer-to-peer collaborations to apply mathematical techniques and tools to NIST problems;
- develop and disseminate mathematical reference data, software, and related tools; and
- work with internal and external groups to develop standards, tests, reference implementations, and other measurement technologies for scientific computing.

Division staff is organized into four groups:

- Mathematical Analysis and Modeling Group (*Timothy Burns, Leader*). Performs research and maintains expertise in applied mathematics, mathematical modeling, and numerical analysis for application to measurement science.
- Mathematical Software Group (*Michael Donahue, Leader*). Performs research and maintains expertise in the methodology and application of mathematical algorithms and software in support of computational science within NIST as well as in industry and academia.
- High Performance Computing and Visualization Group (*Judith Terrill, Leader*). Performs research and maintains expertise in the methodologies and tools of high-performance scientific computing and visualization for use in measurement science.
- Computing and Communications Theory Group (*Ronald Boisvert, Acting Leader; Oliver Slattery, Project Leader*). Performs research and maintains expertise in the fundamental mathematics, physics, computer science, and measurement science necessary to enable the development and analysis of current and future computing and communications systems.

The technical work of the Division is organized into six thematic areas; these are described in the sidebar. Project descriptions in Part III of this document are organized according to these broad themes.

Division Thematic Areas

Broad Areas

Mathematics of Metrology. Mathematics plays an important role in measurement science. Mathematical models are needed to understand how to design effective measurement systems and to analyze the results they produce. Mathematical techniques are used to develop and analyze idealized models of physical phenomena to be measured, and mathematical algorithms are necessary to find optimal system parameters. Mathematical and statistical techniques are needed to transform measured data into useful information. We develop fundamental mathematical methods and tools necessary for NIST to remain a world-class metrology institute, and to apply these to measurement science problems.

High Performance Computing and Visualization. Computational capability continues to advance rapidly, enabling modeling and simulation to be done with greatly increased fidelity. Doing so often requires computing resources well beyond what is available on the desktop. Developing software that makes effective use of such high-performance computing platforms remains very challenging, requiring expertise that application scientists rarely have. We maintain such expertise for application to NIST problems. Such computations, as well as modern experiments, typically produce large volumes of data, which cannot be readily comprehended. We are developing the infrastructure necessary for advanced interactive, quantitative visualization and analysis of scientific data, including the use of 3D immersive environments, and applying the resulting tools to NIST problems.

Current Focus Areas

Materials Modeling. Mathematical modeling, computational simulation, and data analytics are key enablers of emerging manufacturing technologies. The Materials Genome Initiative (MGI), an interagency program with the goal of significantly reducing the time from discovery to commercial deployment of new materials using modeling, simulation, and informatics, is a case in point. To support the NIST role in the MGI, we develop and assesses modeling and simulation techniques and tools, with emphasis on uncertainty quantification, and collaborate with other NIST Laboratories in their efforts to develop the measurement science infrastructure needed by the materials science and engineering community.

Mathematics of Biotechnology. As proof-of-concept academic work in engineering biology meets the market realities of bringing lab science to product initiation, there are questions in how to compare biological products, measure whether desired outcomes are realized, and optimize biological systems for desired behaviors. NIST is working to deliver tools and standards to measure such biological technologies, outputs, and processes from healthcare to manufacturing and beyond. We support this effort with the development and deployment of innovative mathematical modeling and data analysis techniques and tools.

Quantum Information Science. An emerging discipline at the intersection of physics and computer science, quantum information science is likely to revolutionize 21st century science and technology in the same way that lasers, electronics, and computers did in the 20th century. By encoding information into quantum states of matter, one can, in theory, enable phenomenal increases in information storage and processing capability. At the same time, such computers would threaten the public-key infrastructure that secures all of electronic commerce. Although many of the necessary physical manipulations of quantum states have been demonstrated experimentally, scaling these up to enable fully capable quantum computers remains a grand challenge. We engage in (a) theoretical studies to understand the power of quantum computing, (b) collaborative efforts with the multi-laboratory experimental quantum science program at NIST to characterize and benchmark specific physical realizations of quantum information processing, and (c) demonstration and assessment of technologies for quantum communication.

Foundations of Measurement Science for Information Systems. ITL assumes primary responsibility within NIST for the development of measurement science infrastructure and related standards for IT and its applications. ACMD develops the mathematical foundations for such work. This can be very challenging. For example, many large-scale information-centric systems can be characterized as an interconnection of many independently operating components (e.g., software systems, communication networks, the power grid, transportation systems, financial systems). A looming new example of importance to NIST is the Internet of Things. Exactly how the structure of such large-scale interconnected systems and the local dynamics of its components leads to system-level behavior is only weakly understood. This inability to predict the systemic risk inherent in system design leaves us open to unrealized potential to improve systems or to avoid potentially devastating failures. Characterizing complex systems and their security and reliability properties remains a challenging measurement science problem for ITL.

Mathematical Knowledge Management. We work with researchers in academia and industry to develop technologies, tools, and standards for representation, exchange, and use of mathematical data. Of particular concern are semantic-based representations which can provide the basis for interoperability of mathematical information processing systems. We apply these representations to the development and dissemination of reference data for applied mathematics. The centerpiece of this effort is the Digital Library of Mathematical Functions, a freely available interactive and richly linked online resource, providing essential information on the properties of the special functions of applied mathematics, the foundation of mathematical modeling in all of science and engineering.

Highlights

In this section we identify some of the major accomplishments of the Division during the past year. We also provide news related to ACMD staff.

Recent Technical Accomplishments

ACMD has made significant technical progress on many fronts during the past year. Here we highlight a few notable technical accomplishments. Further details are provided in Part II (Features) and Part III (Project Summaries).

Mathematics of Metrology. In the early 1950s, important foundational studies on computational methods for the solution of partial differential equations (PDEs) were carried out at the NBS Institute for Numerical Analysis by such luminaries as Fritz John, Wolfgang Wasow, and John Todd. More recently, we have made remarkable progress on numerical schemes for the even more challenging problem of solving PDEs *backward in time*. Such problems are at the core of many inverse problems found in measurement science. It is well known that any stepwise marching difference scheme consistent with such ill-posed initial value problems is unconditionally unstable, leading to explosive error growth. However, ACMD staff have devised a powerful new approach for solving *ill-posed, time-reversed, multidimensional, nonlinear dissipative evolution equations*, by stabilizing explicit marching difference schemes, which can provide useful backward reconstructions over short time periods in spite of the instability. Such computations had not previously been deemed possible. See page 31.

ACMD researchers were part of successful five-year NIST effort to realize a *1000-fold increase in microcalorimeter sensor throughput*, accomplished via a completely new sensor readout (a microwave multiplexer) enabling much larger detector arrays, and through major new, higher throughput, processing capabilities. Such sensors drive important applications in x-ray materials analysis, nuclear forensics, and astrophysics. A key part of this work led by ACMD was the analysis of the "messy" data flowing from the sensor arrays. See page 40.

We have also taken on a leadership role in promoting the *exchange and reuse of mathematical modeling software within the atomic and molecular physics community*. A prototype gateway for the distribution and maintenance of such codes has been developed. In December 2019 ACMD hosted a workshop with software developers from that community to chart a path forward. See page 43.

High Performance Computing and Visualization. In 2019 NIST released SRM 2497, a *standard reference concrete for rheological measurements*. Certified values for the properties of SRM 2497 were determined using simulations led by ACMD. To obtain the necessary fidelity large-scale parallel computing on an external high-performance computing facility was necessary. Use of the cement paste and mortar SRMs are already referenced in a new ASTM standard test method for measuring the rheological properties of cementitious materials. The ACMD simulation code is now being used to study the flow of dense suspensions in pipes. See page 74.

This year ACMD staff took a leadership role in high-performance at the national level by service as Co-Chair of the White House's National Science and Technology Council *Fast Track Action Committee on Strategic Computing*. The group led an effort with input from government, industrial, and academic stakeholders to update the goals and strategies behind the National Strategic Computing Initiative. Their report was issued in November 2019.[1]

Materials Modeling. Division staff served as Editor of a forthcoming book from World Scientific Publishers entitled *Electrostatic and Magnetic Phenomena: Particles, Macromolecules, Nanomagnetics.* The volume contains a chapter contributed by ACMD on *standard problems in micromagnetics*. See page 66.

[1] *National Strategic Computing Update:Pioneering the Future of Computing*. National Science and Technolgy Council, November 2019. URL: https://www.nitrd.gov/pubs/National-Strategic-Computing-Initiative-Update-2019.pdf

Industrial R&D teams are increasingly reliant on computational tools such as molecular dynamics (MD) to speed up development of next-generation materials. While current computational platforms allow MD to simulate millions of atoms over nanoseconds, this is far short of what is needed to determine macroscale properties. To overcome this, modelers have proposed a variety of strategies that attempt to "project-out" unnecessary degrees-of-freedom to reach larger scales. Unfortunately, such coarse graining schemes are typically ad hoc, without any reference to limiting quantities or quantitative error estimates, which make them problematical in high-throughput industrial settings. To address these issues, ACMD staff have been developing a hierarchy of approaches that link models with increasing degrees of complexity to their all-atom counterparts. The first of these is a method of *coarse graining rigid-body molecules* by reformulating their interaction potential in terms of a generalized multipole expansion. See page 69.

Mathematics of Biotechnology. Bio-related research has been a growing part of the NIST portfolio for some time. Recently, "enabling the future bioeconomy" has been identified as an important strategic direction for future NIST work. To respond to this, ACMD has been increasing its attention and expertise in mathematical modeling in this area. With this annual report we are shining a light on the variety of work we are doing in this area by collecting project descriptions into a separate section.

Developments in biology and biotechnology have fueled the hope of personalizing medical therapies to specific individuals or subsets of the population. Despite the great promise, widespread accessibility is currently limited by an inability to measure specific biomarkers in individuals. An important emerging technology for such measurements is the biological field effect transistor (Bio-FET). We have developed an accurate time-dependent model that couples transport dynamics to kinetic processes at the sensor surface to enable the identification of parameters associated with *Bio-FET measurements*, such as kinetic coefficients and diffusion constants. See page 20.

Two-dimensional nuclear magnetic resonance (NMR) spectroscopy has recently emerged as a tool for characterizing monoclonal antibodies, biologically based therapeutics derived from proteins that are used to treat a wide number of diseases. ACMD staff are working with the NIST/UMD Institute for Bioscience and Biotechnology Research (IBBR) to improve the accuracy and robustness of *2D NMR spectroscopy*. By applying principle component analysis and the unweighted pair group method with arithmetic mean to hundreds of spectra acquired under numerous experimental conditions, ACMD staff have demonstrated that it is possible to accurately and reliably automatically detect sample type and temperature of spectra. These results help move the 2D NMR method from an emerging technology to a harmonized routine measurement that can be applied with great confidence to high precision assessments of the structure of a wide array of protein therapeutics. See page 56.

Microfluidic technologies can, in principle, enable rapid and simultaneous screening of hundreds of diseases with only a few drops of blood. Despite the promise, existing devices have experienced difficulty in producing accurate and repeatable measurements. To address this problem, ACMD staff have worked with MML to develop flowmeters that can continuously measure volumetric flow rates down to approximately 10 nL/min with 5 % (or less) relative uncertainty. A second device can identify zero-flow to within 0.1 nL/min, which is useful for calibrating flow meters and for characterizing flow stability. Accurate measurements at such scales were previously unattainable. These achievements were enabled by insightful physics-based mathematical scaling relationships and symmetry breaking arguments. See page 58.

Human body communication (HBC), in which the body itself is used as a communications medium, is an attractive low complexity technology with promising applications in wearable biomedical sensors. We have developed a flexible and customizable simulation platform to better understand the communication medium for capacitively coupled electrodes in HBC. This knowledge, in turn, can lead to better transceiver design for future applications of this technology. See page 17.

Quantum Information. ACMD staff this year worked with colleagues in PML to demonstrate *quantum gate teleportation* for the first time. If quantum computers are to scale to hundreds and thousands of qubits, then two-qubit gate operations will routinely need to be performed in which each of the target qubits is located in different regions of memory. The team demonstrated a protocol that requires only local operations, classical communication, and shared entanglement to perform a controlled-NOT (CNOT) gate

between ions of the same and mixed species in spatially separated locations in an ion trap. The accomplishment, which was published in *Science*, was noted in *Physics Today*.[2]

There are myriad quantum computing approaches, each having its own set of challenges. The use of arrays of electrostatically defined quantum dots (QDs) at the interface of semiconductor devices is one such approach. Before they can be used, QDs must be "tuned," so that their operation can be controlled. The current practice of tuning QDs manually or in a semi-automated fashion is a relatively time-consuming procedure, inherently impractical for scaling up to systems with many QDs. We are leading the development of *machine learning techniques for state recognition and auto-tuning of quantum dots*. An article reporting this work has been selected as an Editor's Suggestion in *Physical Review Applied.* See page 25.

Foundations of Measurement Science for Information Systems. The benefits of interconnectivity have driven the current explosive growth in networked systems. However, interconnectivity is also inherently associated with risk. ACMD staff are working to understand the effect of the *interplay of risk and benefit of interconnectivity in naturally growing networks*. Our current results suggest that accounting for this interplay allows one to resolve a fundamental issue in the widely accepted preferential attachment model of a growing network. See page 23.

Mathematical Knowledge Management. The NIST *Digital Library of Mathematical Functions* (DLMF), which provides the scientific community a convenient source of reference data on the properties of the special functions of applied mathematics, remains the most popular ACMD-developed resource, serving up more than 5.4M pages of information in calendar year 2019. The DLMF is not a static resource. Four releases containing enhancements and corrections were released this year, and a new chapter on Orthogonal Polynomials of Several Variables, as well as substantial updates to the chapters on Orthogonal Polynomials, Algebraic Methods, and Painlevé Transcendents are currently underway. See page 106.

Recent advances in machine learning have opened up new possibilities for harvesting large collections of scientific documents to find, understand and reuse information. To enable research on *mathematical knowledge processing*, it is important to have a set of documents available in a form appropriate for processing to use for training and testing. To that end, we have applied our LaTeXML tool, which converts TeX to MathML, to the massive corpus at arXiv.org[3]. We have carried out initial experiments on statement classification using that data set. See page 109.

Technology Transfer and Community Engagement

The volume of technical output of ACMD remains high. During the last 15 months, Division staff members were (co-)authors of 65 articles appearing in peer-reviewed journals, 35 papers in conference proceedings, and six published in other venues. 16 additional papers were accepted for publication, while 23 others are undergoing review. Division staff gave 43 invited technical talks and presented 44 others in conferences and workshops.

ACMD continues to maintain an active website with a variety of information and services, most notably the Digital Library of Mathematical Functions, though legacy services that are no longer actively developed, like the Guide to Available Mathematical Software, the Matrix Market, and the SciMark Java benchmark still see significant use. During calendar year (CY) 2019, the division web server satisfied more than 6.2 million requests for pages during more than 767 000 user visits. Another indication of the successful transfer of our technology is references to our software in refereed journal articles. For example, our software system for nano-magnetic modeling (OOMMF) was cited in 150 such papers published in CY 2019 alone; see page 66.

Members of the Division are also active in professional circles. Staff members hold a total of 22 editorial positions in peer-reviewed journals. For example, Barry Schneider is an Associate Editor-in-Chief

[2] https://physicstoday.scitation.org/do/10.1063/PT.6.1.20190715a/full/

[3] https://arXiv.org/

for IEEE's *Computing in Science and Engineering.* Staff members are also active in conference organization, serving on 25 organizing/steering/program committees. Of note, ACMD played an important role as sponsor or (co-)organizer of several significant events this year, including the following:

- *Computational Reproducibility at Exascale*[4], at SC18, Dallas, TX, November 11, 2018. (M. Mascagni and Walid Keyrouz, Co-Organizers)

  This workshop addressed issues of numerical reproducibility as well as approaches and best practices to sharing and running code and the reproducible dissemination of computational results. The main target was computational reproducibility in high performance computing in general, including those issues anticipated as we scale up to exascale machines in the next decade. The participants included government, academic, and industry stakeholders.

- *Computational Reproducibility at Exascale*[5], at SC19, Denver, CO, November 17, 2019. (M. Mascagni and Walid Keyrouz, Co-Organizers)

  This workshop addressed issues of numerical reproducibility as well as approaches and best practices to sharing and running code and the reproducible dissemination of computational results. The main target was computational reproducibility in high performance computing in general, including those issues anticipated as we scale up to exascale machines in the next decade. The participants included government, academic, and industry stakeholders.

- *A Science Gateway for Atomic and Molecular Physics*[6], NIST, Gaithersburg, MD, December 11-13, 2019. (B. Schneider, Local Organizer)

  This workshop was a follow-on to an NSF supported workshop held at Harvard's Institute for Theoretical Atomic, Molecular and Optical Physics (ITAMP) on May 14-16, 2018 entitled, "Developing Flexible and Robust Software in Computational Atomic and Molecular Physics" organized by Barry Schneider (chair), Robert Forrey (Penn State), and Naduvalath Balakrishnan (UNLV). Following the workshop six of the participating research groups interested in atomic and molecular collisions and the interaction of those systems with electromagnetic radiation submitted a joint proposal to the NSF eXtreme Science and Engineering Discovery Environment (XSEDE) to build and maintain a Science Gateway devoted to the codes developed in these groups. The goal was to explore mechanisms to collectively make codes available and easier to use by the partners as well as others in the community. This workshop focused on the next steps. With the proposal granted, the group was joined by Sudhakar Pamidighantam of the XSEDE project for development of the gateway. With some of the codes being ported to various XSEDE platforms, the group decided to focus on describing the science and the computational details of such codes to a larger community with the goal of making them available and useful to others and to also invite people who have similar interests to consider more direct participation in the project.

Service within professional societies is also prevalent among our staff. For example, Bonita Saunders was elected to the Board of Trustees of the Society for Industrial and Applied Mathematics (SIAM). Staff members are also active in a variety of working groups. Ronald Boisvert and Andrew Dienstfrey serve as members of the International Federation for Information Processing (IFIP) Working Group 2.5 on Numerical Software, Donald Porter is a member of the Tcl Core Team, Bruce Miller is a member of W3C's Math Working Group, and Sandy Ressler is a member of the Web3D Consortium. Barry Schneider represents NIST on the High-End Computing (HEC) Interagency Working Group of the Federal Networking and Information Technology Research and Development (NITRD) Program. Further details can be found in Part IV of this report.

[4] http://www.cs.fsu.edu/~cre/cre-2018/index.html

[5] http://www.cs.fsu.edu/~cre/cre-2019/index.html

[6] https://www.nist.gov/news-events/events/2019/12/science-gateway-atomic-and-molecular-physics

Staff News

For the second year in a row, ACMD experienced an unusually large number of staffing changes. Among these are the following.

Arrivals

Matthew Coudron joined the ACMD Computing and Communications Theory Group as a full-time permanent staff member in November 2019. Coudron has a Ph.D. in Theoretical Computer Science from MIT, where he studied with Peter Shor. He comes to NIST after a postdoctoral stay at the Institute for Quantum Computing at the University of Waterloo. Coudron's research interests are in quantum information and computational complexity. He was recently elected a Fellow of the Joint UMD/NIST Center for Quantum Information and Computer Science (QuICS).

Zach Grey began a two-year appointment as a NIST NRC Postdoctoral Associate at the NIST Boulder Labs in December 2019. Zach received a Ph.D. in Computational and Applied Mathematics from the Colorado School of Mines in November 2019. His research interests are in dimension reduction and uncertainty quantification. At NIST he will be working with Andrew Dienstfrey to apply that background to the understanding and quantifying the reliability of artificial intelligence models.

Joseph Klobusicky joined ACMD in September 2019 as a NIST NRC Postdoctoral Associate. He has a Ph.D. in Applied Mathematics from Brown University and comes to NIST after a postdoctoral appointment at Rensselaer Polytechnic Institute. His interests lie in applied probability and analysis. Recent applications have been to stochastic methods in quantitative microbiology and kinetic theory for materials. At NIST he will be working with Anthony Kearsley.

Justyna Zwolak began her tenure as a full-time permanent staff member in the ACMD High Performance Computing and Visualization Group in February 2019. She had previously been a NIST Guest Researcher sponsored by the NIST/UMD Joint Center for Quantum Information and Computer Science (QuICS). Zwolak received a Ph.D. in Mathematical Physics in 2011 from the Nicolaus Copernicus University, Toruń, Poland. Her current research interests are in the use of machine learning techniques for the automated control of physics experiments. A recent application is the tuning of quantum dots for use in quantum computation.

Departures

Sean Colbert-Kelly departed NIST in May 2019, assuming an Associate Mathematician position at the Washington area offices of the RAND Corporation. Colbert-Kelley had held multiple postdoctoral positions in ACMD since 2013, including a NIST NRC Postdoctoral Associateship. His research focused on the analysis of a generalized planar Ginzburg-Landau equation and joint work with NIST MML on the modeling of emulsion stability using a diffuse interface model.

Wesley Griffin, a computer scientist in the ACMD High Performance Computing and Visualization Group since 2012, left NIST in November 2019 for work in private industry. For seven years Griffin was a key contributor to ACMD research in immersive scientific visualization for application to NIST measurement science.

Fern Hunt retired in April 2019 after a 28-year association with NIST. Hunt, who was an expert in the ergodic theory of dynamical systems, engaged in a wide variety of collaborations during her NIST tenure, with applications that included measuring the properties of fractals, predicting the result of high-speed injection of liquid polymers into molds, measuring properties of magnetic materials, modeling optical reflection and scattering from surfaces for photorealistic rendering in computer graphics, measuring the properties of DNA sequences, and identifying influential nodes in networks. She garnered many awards

during her career, including Mathematical Association of America David Blackwell Lecturer (1997), Arthur S. Flemming Award for Outstanding Federal Service in the Field of Science (1999), Mathematical Association of America – Association for Women in Mathematics Falconer Lecturer (2005), Science Spectrum Minorities in Research Science Award (2005), American Mathematical Society Fellow (2018), Association for Women in Mathematics Fellow (2019). Hunt was also a strong proponent of diversity in mathematics; she participated in many conferences focused on the support of women and minority researchers, receiving ITL's first Outstanding Contribution to Diversity Award in 2018. Hunt continues her association with ACMD as a NIST Scientist Emeritus.

Justin Kauffman ended his stay as a NIST NRC Postdoctoral Associate in August 2019 to take a position as Research Assistant Professor at the Northern Virginia Center of Virginia Tech. At NIST he worked on a parallel coupling algorithm between an overset mesh and the hybridizable discontinuous Galerkin method.

Lucas Kocia completed his NIST NRC Postdoctoral Associateship in June 2019, accepting a research position at Sandia Laboratories in Albuquerque, NM. In ACMD his research focused on the use of contextuality as a resource for efficient classical algorithms for quantum simulation.

In Memoriam

William Mitchell, a computer scientist in ITL's Applied and Computational Mathematics Division from 1993-2018, died on October 15, 2019 at age 64 after a year-long struggle with cancer. He is survived by his wife of 36 years, Becky Ross.

Figure 1. *William Mitchell, a research staff member in ACMD from 1993 to 2018 passed away in October 2019 after a year-long struggle with cancer.*

Born on July 25, 1955 in Oneonta, NY, Bill graduated from Clarkson University with a B.S. in mathematics in 1977. He went on to study computer science at Purdue University (M.S., 1983) and the University of Illinois at Urbana-Champaign (Ph.D., 1988). For his Ph.D. Bill studied the numerical solution of elliptic partial differential equations (PDEs). In his thesis he unified three separate hot topics of the day —high order finite element discretizations, adaptive grid refinement, and multigrid linear equation solution —into a coherent and elegant whole using a hierarchical finite element basis for approximation and newest vertex bisection of triangles for adaptivity. Bill implemented his methods in a well-crafted software package, MGGHAT (MultiGrid Galerkin Hierarchical Adaptive Triangles), which he released into the public domain. The methods implemented in MGGHAT were among the most efficient of the day. That software has since been downloaded more than 128,000 times.

Following his studies, Bill spent five years at the General Electric Advanced Technology Laboratory in Moorestown, New Jersey, where he worked primarily on digital signal processing applications, one of which led to a patent. In 1993 Bill joined NIST on the heels of an expansion enabled by the Federal High-Performance Computing and Communications (HPCC) initiative. At NIST Bill worked to adapt his methods for elliptic PDEs to take advantage of increases in performance promised by emerging parallel computer architectures which would enable solving much larger problems. This was quite challenging, since adaptive grid refinement and multigrid, which made his algorithms so efficient, were characterized by data access patterns that stymied straightforward parallelization. Not deterred by this, Bill continued to innovate, developing a novel parallel approach to multigrid (the full domain partition) and a dynamic load balancing method (the refinement-tree based partition), which proved highly effective. A new software package emerged, PHAML (Parallel Hierarchical Adaptive Multi-Level), first released in 2006. Some 2,100 downloads ensued in the very first year, and PHAML has since seen widespread use worldwide to solve problems

in quantum physics, fluid dynamics, heat transfer, astrophysics, and beyond. In the years after, Bill continued to refine his methods and improve his software, using it as a platform for influential studies in the numerical analysis of PDEs and collaborations with colleagues in the NIST Laboratories who had particularly challenging problems to solve. The former included insightful practical comparisons of the performance of a wealth of strategies for adaptive finite element methods. The latter included computation of eigenfunctions describing the interaction of ultra-cold neutral atoms held in an optical trap, analysis of scanning electron microscope images, and simulation of alloy solidification.

Bill always took pride in his software, which was always very well-engineered. He wrote beautiful code. He was also an expert in the modern instantiations of the Fortran programming language, advising many on its proper use, and making contributions to the Fortran standard. For example, as part of his work, Bill needed to access the industry standard OpenGL graphics library, which was written in C. So, he developed a set of bindings (an interface specification) which allowed the access of OpenGL from Fortran. He implemented these in a library, f90gl, which also saw wide distribution. Bill's bindings satisfied an important need, and they were subsequently adopted by the OpenGL community as the standard Fortran bindings for OpenGL.

Bill was also quite active professionally. He was an associate editor of the Journal of Numerical Analysis, Industrial and Applied Mathematics (2006-2018) and its predecessor Applied Numerical Analysis and Computational Mathematics (2001-2005), was on the scientific committee of the International Conference of Numerical Analysis and Applied Mathematics (2003-2018), and organized or chaired minisymposia and technical sessions at numerous conferences. Over his career he published 50 scientific papers and gave over 100 talks. In 1996 he received the Department of Commerce Bronze Medal for Superior Federal Service.

Quite a well-rounded person, Bill had many interests beyond computational science. He was an avid vegetable gardener. He was a fixture at local bowling alleys, where he competed along with NIST colleagues. He was a connoisseur of fine beers, many of which were created in his own home-brew cellar. Every year he and Becky would host an Octoberfest celebration in their backyard for their wide circle of friends featuring Bill's beers and bratwurst created from their own recipe, all enjoyed with lively German oom-pah music playing in the background. Folk music was also a passion of Bill's. He was an accomplished hammered dulcimer player and could often be seen playing with a local Irish ceilidh band. He and Becky (on the violin) were also a performing duo known as Peat and Barley, who entertained at weddings and wineries. Peat and Barley produced several CDs of music, some of which are still available[7].

Bill will be fondly remembered not only for his scientific contributions, but for the joy he brought to his many friends and colleagues.

Recognition

ACMD staff members were recognized with a variety of awards this year, including the following.

Fern Hunt was elected a Fellow of the American Mathematical Society (AMS) in November 2018 "for outstanding applications of mathematics to science and technology, exceptional service to the US government, and for outreach and mentoring." The AMS Fellows program recognizes members who have made outstanding contributions to the creation, exposition, advancement, communication, and utilization of mathematics. Hunt is the first NIST staff member to have received this honor. In October 2019 Hunt also received the honor of being named a Fellow of the Association for Women in Mathematics (AWM) for "exceptional commitment to outreach and mentoring; for her sustained efforts to make the AWM organization more inclusive; for her service to higher education and government; and for inspiring those underrepresented in mathematics with her work in ergodic theory, probability, and computation."

[7] See http://www.peatandbarley.com/

Stephen Jordan, who was a member of the ACMD staff from 2010 to 2018, received the prestigious Presidential Early Career Award for Scientists and Engineers (PECASE) award in 2019 in recognition of his work in quantum information theory. The PECASE Award is the highest honor bestowed by the U.S. government on outstanding scientists and engineers beginning their independent careers.

Ronald Boisvert was named a Fellow of the Association for Computing Machinery (ACM) in December 2019 "for contributions to mathematical software and service to the community." ACM is the largest educational and professional society in the field of computing. ACM's Fellows comprise an elite group that represents less than 1 percent of the Association's global membership.

Alfred Carasso and **Bonita Saunders** were each recognized by the Washington Academy of Sciences in 2019. Carasso received an award for Excellence in Research in Applied Mathematics, while Saunders received an award for Excellence in Research in Mathematics and Computer Science. Each was named a Fellow of the Washington Academy of Sciences.

Michael Donahue and **Donald Porter** received the Jacob Rabinow Applied Research Award at the NIST Awards Ceremony in December 2018. Widely considered NIST's highest award for applied science, the Rabinow award recognizes outstanding achievement in the practical application of the results of scientific or engineering research. Donahue and Porter were recognized for "enabling widespread use of nanomagnetic modeling and simulation to enhance U.S. innovation and product development." The software tool that they created, OOMMF, is the most widely used nanomagnetics modeling system in the world. More than 2,500 journal articles (11 in *Science* and *Nature*) and more than 18 U.S. patent applications reference use of their system, attesting to its impact for U.S. innovation.

ACMD staff showed well in the 2019 ITL Awards program. **Alfred Carasso** received the Outstanding Journal Paper Award for his article "Stabilized Backward in Time Explicit Marching Schemes in the Numerical Computation of Ill-Posed Time-Reversed Hyperbolic/Parabolic Systems," which was published in *Inverse Problems in Science and Engineering.* **Katjana Krhac** and **Kamran Sayrafian** received the Outstanding Conference Paper Award for their article "A Study of Capsule Endoscopy Orientation Estimation Using Received Signal Strength," which was published in the proceedings of the IEEE 29th Annual International Symposium on Personal, Indoor and Mobile Radio Communications held on September 9-12, 2018 in Bologna, Italy. **Chris Schanzle** was recognized for Outstanding Technical Support for "outstanding dedication and initiative in the application of computing resources to high-visibility research projects." **Lochi Orr** received the Outstanding Administrative Support Award for "outstanding initiative, precision, and speed in providing services as a property officer and purchase card

Figure 2. *Within 12 months, Fern Hunt was named both a Fellow of the American Mathematical Society and of the Association for Women in Mathematics.*

Figure 3. *Ronald Boisvert (left) was named a Fellow of the ACM and Stephen Jordan (right) received the Presidential Early Career Award for Scientists and Engineers (PECASE).*

Figure 4. *Bonita Saunders and Alfred Carasso eac received Excellence in Research Awards from the Washington Academy of Sciences in 2019.*

holder." And **Bonita Saunders** received the Outstanding Contribution to Diversity Award "for exemplary service as a role model, mentor, and tutor in support of STEM careers by women and minorities."

Several "best in show" awards were presented to Division staff members by external organizations. **Kamran Sayrafian**, along with ACMD guest researcher **Katjana Krhac** and colleagues at the Polytechnic University of Valencia and the University of Zagreb, received a Best Paper Award at the IEEE Conference on Standards for Communications and Networking held in Paris in October 2018. Their paper was entitled "Impact of Measurement Points Distribution on the Parameters of UWB Implant Channel Model." **Sandy Ressler** took Second Place in the World Standards Day Essay Contest sponsored by the Society for Standards Professionals for an essay entitled "Standards, the Glue for Innovation." The award was presented in Washington, DC on October 18, 2018. **Vladimr Marbukh** and **Kamran Sayrafian** were co-authors with colleagues from the University of Lisbon of the paper "Towards Cross-Layer Optimization of Virtualized Radio Access Networks," which won the Best Paper Award at the European Conference on Networks and Communications held June 18-21, 2019 in Valencia, Spain.

Figure 5. *Vladimir Marbukh (left) and Kamran Sayrafian (second from right) receive the Best Paper Award at the European Conference on Networks and Communications on June 21, 2019 in Valencia, Spain long with co-authors from the University of Lisbon Luis Coreia and Behnam Rouzbehani (second and third from the left).*

Part II

Features

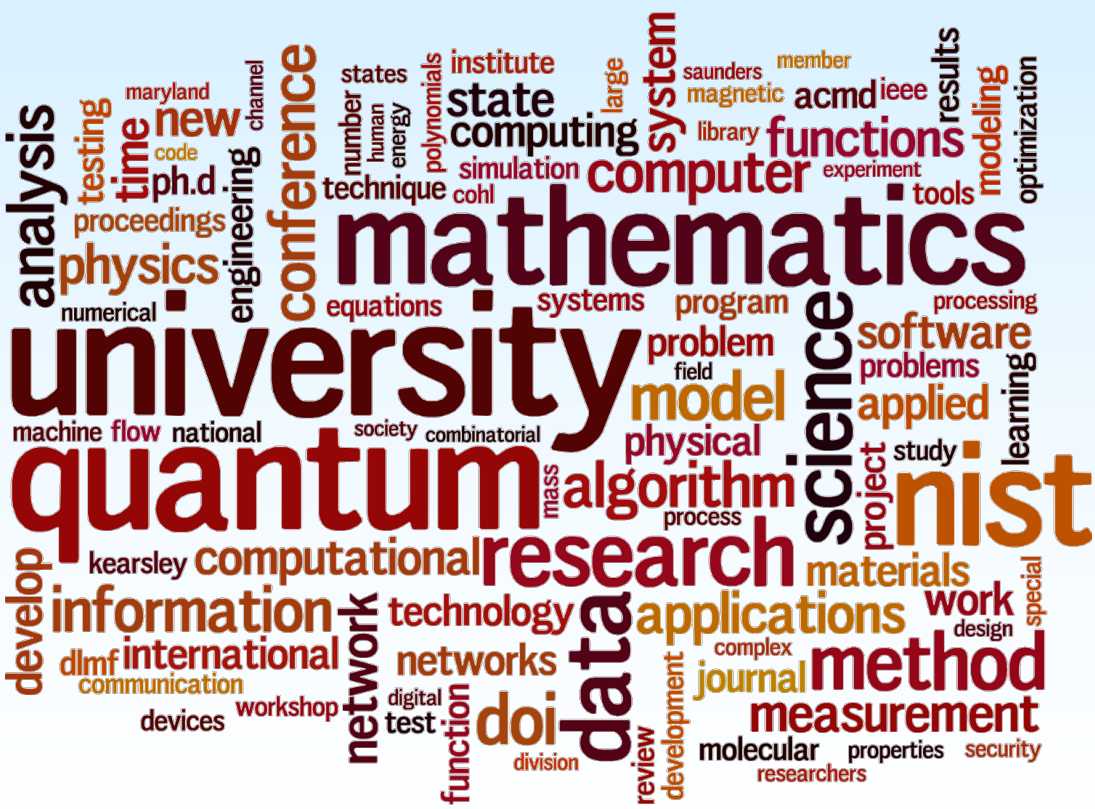

A Simulation Platform to Study the Human Body Communication Channel

Human Body Communication (HBC) is an attractive low complexity technology with promising applications in wearable biomedical sensors. In this research, a simple parametric model based on the finite-element method (FEM) using a full human body model is developed to virtually emulate and examine the HBC channel. FEM modeling allows quantification of the underlying physical phenomena, including the impact of the human body. By adjusting the parameters of the model, a good match with measurement results in the literature is observed. Having a flexible and customizable simulation platform could be very helpful to better understand the communication medium for capacitively coupled electrodes in HBC. This knowledge, in turn, can lead to better transceiver design for future applications of this technology. The platform developed here can also be extended to study communication channel characteristics when the HBC mechanism is used by an implant device.

Katjana Krhac and Kamran Sayrafian

Human Body Communication (HBC) is one of the wireless technologies defined by the IEEE 802.15.6 standard on Body Area Networking (BAN) [1]. In HBC, the human body is used as a communication medium between a pair of transmitter and receiver electrodes that are placed on the body surface. Low complexity and energy consumption are among the reasons that make this technology attractive for wearable and implantable devices. Also, as the transmitted data is mostly confined to the human body area, there is less chance of unauthorized access, and therefore, better security is expected compared to other wireless technologies used for body area networks. In the literature, the general technology has also been referred to as Body Channel Communications (BCC) or Intra-Body Communications (IBC).

These non-RF communication mechanisms include capacitive (or equivalently electric field) and galvanic signal coupling. In the capacitive coupling method, the electrical signal that is applied to the human body (i.e., forward path) is capacitively coupled through the air or the environment where the body is located (i.e., return path). Alternatively, in the galvanic coupling method, the human body would act as a waveguide for the signal that is injected by the alternating current into the body. The term HBC, as outlined in the IEEE 802.15.6, mainly refers to the capacitive coupling methodology. The underlying concept behind HBC is the fact that in the presence of a weak electric field, the human body can act as a signal guide to capacitively couple two electrodes that are in contact with the body surface. The

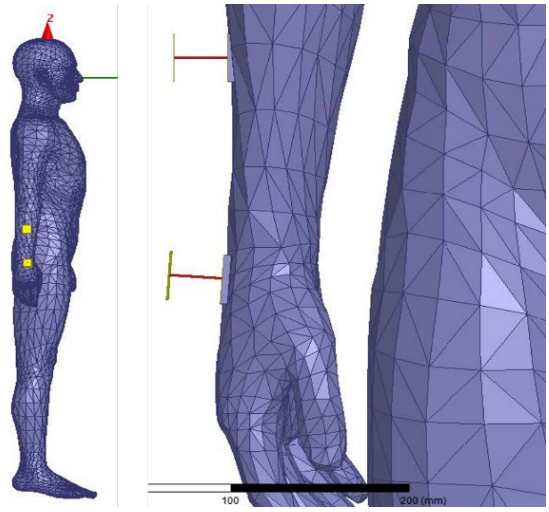

Figure 6. *HBC electrodes on the right arm.*

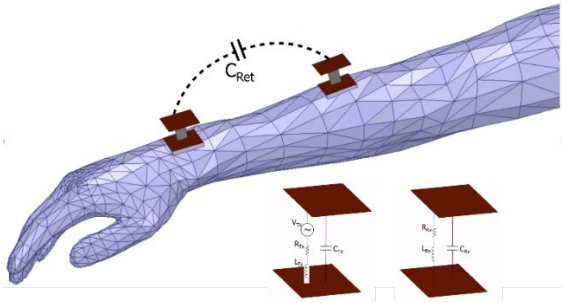

Figure 7. *System schematic.*

coupling through the body is achieved with much less attenuation compared to free space. There have been several studies by researchers to better understand and characterize the HBC channel in the past 10 years. These studies are mostly physical measurement campaigns considering a few common scenarios. Since the environment around the human body (and possibly the body posture) directly affects the wireless link between two HBC electrodes, some discrepancies are often observed among the reported physical measurement results.

Developing a comprehensive simulation platform that can adequately model the HBC channel is quite challenging. This is mostly due to the variables that could impact the return signal path through the air. Methodologies that have been used to investigate and model the electric field propagation mechanism include RC circuits, finite-element method (FEM), circuit-coupled FEM as well as FDTD (finite difference time domain) [2-4]. However, the results obtained through these methodologies have not adequately matched physical measurements obtained through various

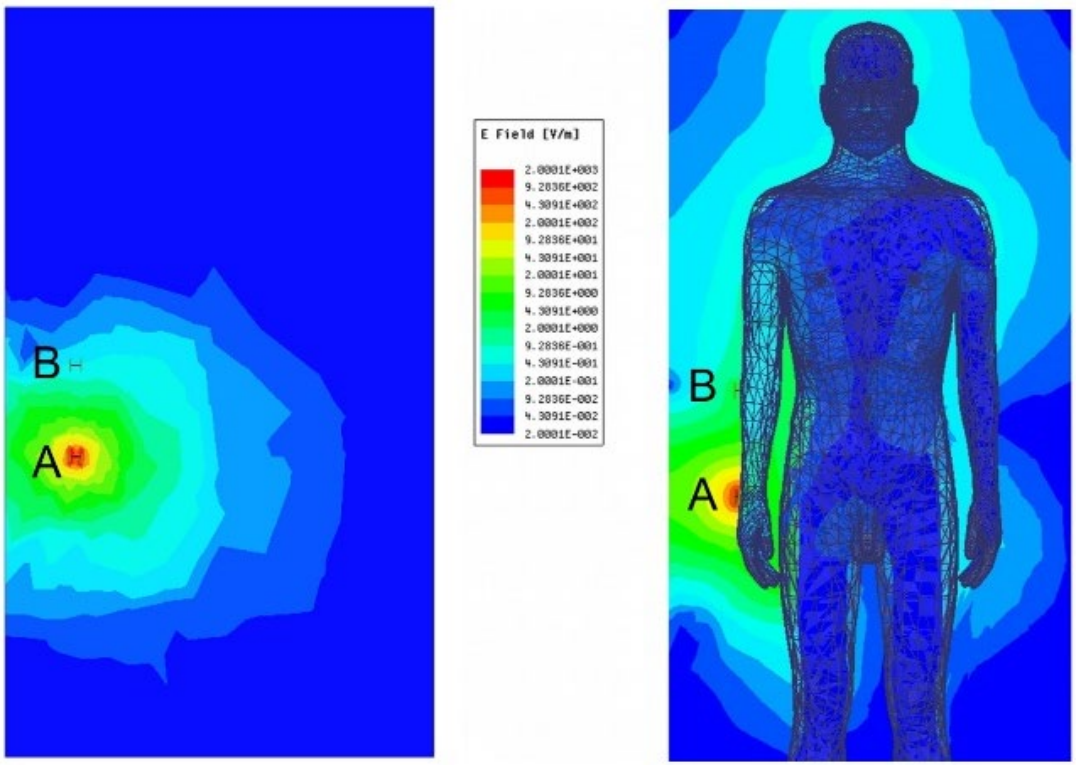

Figure 8. *Electric field distribution around the transmitter electrode (a, left) without the human body and (b, right) with the human body.*

communication scenarios. The common element in most of the results published in the past several years is the passband profile shape of the HBC channel attenuation within the range of 1 MHz to 100 MHz. Depending on the instrumentation or methodology that was used for those measurement, the location of the peak frequency in the passband profile varies from 40 MHz to 70 MHz. In addition, discrepancies are also observed on the average magnitude of the forward transmission coefficient.

Modeling of the HBC channel is a challenging task due to the many parameters that can possibly affect the characteristics of the communication link. Among those, are the size and shape of the electrodes, locations and distance between the receiver and transmitter electrodes, separation between the signal and ground plates of each electrode, body posture, dielectric properties of the human tissues that are in contact with the electrodes, and finally, the environment surrounding the human body. Our objective in this research is to develop a simple parametric FEM-based model that can 1) capture the fundamental concepts of HBC operation/channel; 2) be adjusted to emulate a specific measurement scenario; and 3) be easily extended to study the implant HBC channel.

To obtain this model, we have customized a computational human body model that has been used as part of a novel 3D immersive visualization platform developed at NIST [5]. This body model, which includes frequency dependent dielectric properties of 300+ parts in a male human body, has a resolution of 2 mm. To study HBC, this computational model has been augmented with a skin shell that fits over the exterior body mesh. In addition, variable fat shells (reflecting thin, average and obese persons) have been added to the model. This customization allows us to study the potential impact of the fat layer on the forward path attenuation of an HBC channel.

The HBC electrodes were modeled as two metal plates, one in contact with the skin and the other located directly above and floating in the air. To ensure the full contact of electrodes with the skin tissue in the body model, a small patch (i.e., brick) of skin material has been added directly underneath the electrode to unite the signal plate with the skin exterior. This ensures that the surface of the electrode and the skin are fully coincident. Size, plate separation, distance between the receiver and transmitter electrodes are design variables, and therefore the impact of each one of these parameters can be easily investigated in our model. Figure 6 shows an example of two electrodes placed on the right arm of the human body model in our platform.

The greatest complexity in modeling the HBC channel is incorporating the impact of the parasitic return path and characteristic impedances of the electronic circuits generating the signal (or in case of physical measurement, parasitic of the printed circuit board i.e., PCB). In our FEM-based model, the coupling of the electrodes through the air (i.e., return path) is modeled

by a capacitor (C_{Ret}). We have implemented the capacitive return path using RLC boundary methodology in the electromagnetic solver. The signal leakage path between the electrode plates was also modeled with capacitor C_L. The characteristic impedance of the source was modeled by a cascade of resistor R_T and inductor L_T. These elements are schematically shown in Figure 7.

Using the electromagnetic solver, a variety of different quantities such as the magnitudes of the electric field (inside, on the surface, and outside of the body) and the scattering parameters (e.g., S_{21}) between the two electrodes can be calculated. For example, Figure 8 highlights the basic principle of HBC by displaying the electric field distribution. Figure 8(a), on the left, shows the distribution of the magnitude of the electric field when the transmitting electrode is not in contact with the human body (i.e., operating in the air). On the other hand, when the electrode is place on the human arm, as seen in Figure 8(b), the electric field extends over the entire body surface. This ensures much higher received signal strength, and therefore, a better communication channel between the two electrodes. A signal frequency of 50 MHz was used for the result shown in Figure 8.

The frequency range of interest in HBC is typically 1 MHz to 100 MHz. Higher frequencies could result in the human body acting as an antenna and are also susceptible to external radiation. Therefore, for frequencies higher than 100 MHz, significant channel variation and lower efficiency of the communication system can be expected.

The HBC channel attenuation can be measured by the forward transmission coefficient (i.e., S_{21}) for various scenarios. The S_{21} profile shape and numerical values can be tuned and optimized to match the physical measurement results of a specific experiment. For example, consider the scenario shown in Figure 7, where two electrodes are placed on the human arm with a separation of 15 cm. Figure 9 displays the close match between the simulation results and measurements in the literature for the forward transmission coefficient when C_{Ret} = 5 pF, L_{Tx} = 225 nH and C_L = 35 pF.

This simulation platform allows researchers to further study the HBC channel by considering variations in electrode size and plate separation, as well as placement on the body. It can also serve as a tool to design virtual experiments to better understand the impact of the variable return path distance for a fixed forward path through the human body. As mentioned earlier, low complexity and energy consumption of the HBC will also make this technology an attractive alternative for implantable devices. Physical measurements are no longer possible to examine the channel for implants.

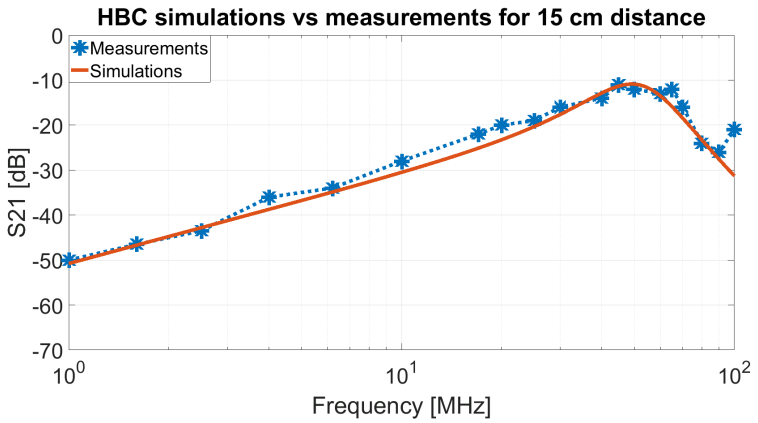

Figure 9. *Comparison of S21 simulation and experiment.*

Therefore, a simulation platform that includes a full human body model will be very useful to study and characterize the implant-HBC channel. The implant communication link is less affected by the environmental variables as both forward and return paths are confined within the human body. Development of the platform discussed here is the first step toward a comprehensive study of the implant-HBC channel.

References

[1] *IEEE Standard for Local and Metropolitan Area Networks, IEEE 802.15.6-2012 – Part 15.6: Wireless Body Area Networks*. 2012. DOI: 10.1109/IEEESTD.2012.6161600

[2] Ž. Lučev Vasić. *Intrabody Communication Based on Capacitive Method*. Doctoral thesis, University of Zagreb, Faculty of Electrical Engineering and Computing, 2014. URL: https://urn.nsk.hr/urn:nbn:hr:168:761582

[3] M. Pereira, G. Alvarez-Botero, and F. Rangel de Sousa. Characterization and Modeling of the Capacitive HBC Channel. *IEEE Transactions on Instrumentation & Measurement* **64**:10 (2015), 2626-2635. DOI: 10.1109/TIM.2015.2420391

[4] J. Park, H. Garudadri, and P. P. Mercier. Channel Modeling of Miniaturized Battery-Powered Capacitive Human Body Communication Systems. *IEEE Transactions on Biomedical Engineering* **64**:2 (2017), 452–462. DOI: 10.1109/TBME.2016.2560881

[5] K. Sayrafian, J. Hagedorn, W. B. Yang, and J Terrill. A Virtual Reality Platform to Study RF Propagation in Body Area Networks. In *IEEE 3rd International Conference on Cognitive Infocommunications (CogInfoCom)*, Kosice, Slovakia, December 2-5, 2012. DOI: 10.1109/CogInfoCom.2012.6421944

Participants

Kamran Sayrafian (ACMD); Katjana Krhac and Dina Simunic (University of Zagreb, Croatia); Gregory Noetscher (NEVA Electromagnetics)

Modeling for Biological Field Effect Transistor Measurements

The traditional approach to much of medicine is a one-size-fits all approach. Due to developments in biology and biotechnology there is now the hope of personalizing therapies to specific individuals or subsets of the population. This new approach to therapeutic protocols holds the promise of superior outcomes at lower doses and therefore a reduction of harmful side effects.

Despite the great promise, widespread accessibility of personalized care is currently limited by an inability to measure specific biomarkers in individuals. Existing techniques are cumbersome, require specialized facilities, and can be prohibitively expensive. The need for low-cost, rapid, and accurate biomarker measurements has led to the development of biological field effect transistors *(Bio-FETs). This technology could extend accessibility of personalized care domestically as well as to the challenging medical treatment landscape in developing countries where low-cost and portable point-of-care-diagnostics are desperately needed to accurately diagnose debilitating diseases like tuberculosis.*

Typical measurements made of reactions occurring inside a BioFET instrument result in time-series data from which information can be extracted to delineate personalized therapeutic strategies. Regretfully, there has been no mathematical modeling framework to interpret such time-series data. As a result, important healthcare decisions have only been made on a qualitative basis. Optimal instrument design requires such a mathematical framework.

This void in understanding has led to a collaboration with the PML Biophysics Group to develop a mathematical modeling framework for Bio-FET experiments. This model has been successfully employed to elucidate previously undiscovered device physics, and follow-on experiments have shown that it provides an effective and novel way of interpreting experimental data.

Ryan Evans and Anthony Kearsley

The ability to tailor therapies to individuals or specific subsets of a population to deliver personalized care has the potential to fundamentally improve healthcare delivery. The most promising therapeutic candidates for such targeted care are new classes of biologic drugs based on naturally occurring molecules, made possible due to rapid advances in genomics and proteomics [1]. Importantly, such therapies can be safer and yield better outcomes at lower doses when treating debilitating conditions such as diabetes, Alzheimer's disease, or certain cancers [2]. Unfortunately, widespread use of personalized care is currently limited by our ability to routinely measure pathology in individuals, including biomarkers, metabolites, tissue histology, and gene expression.

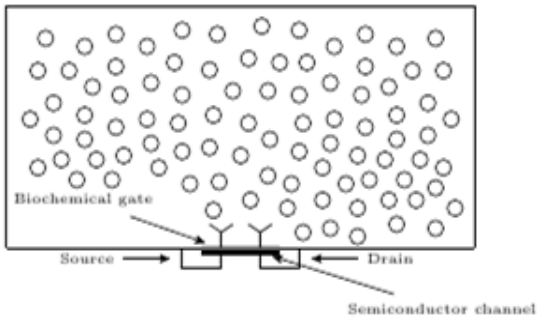

Figure 10. *Schematic of a Bio-FET experiment.*

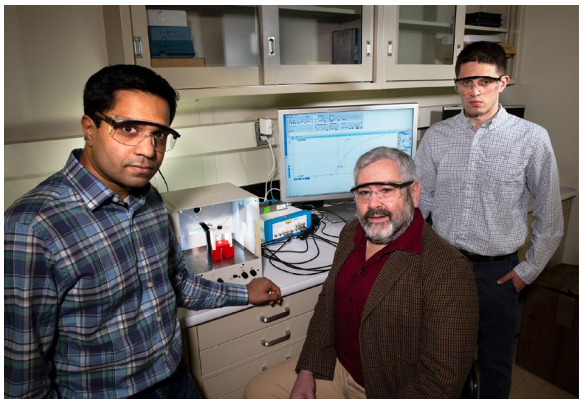

Figure 11. *Arvind Balijepalli, Anthony Kearsley, and Ryan Evans performing a Bio-FET experiment.*

Moreover, existing clinical diagnostics are cumbersome, require specialized facilities, can take days to weeks to perform, and are in many cases prohibitively expensive.

To overcome such problems researchers have developed new portable detection tools, including antibody-based lateral flow assays [3], microelectromechanical sensor (MEMS) based resonators that can detect binding of biomarkers to the sensor surface [4], surface plasmon resonance [5], ring cavity resonators [6], and electronic measurements with biological field effect transistors (Bio-FETs) [7–9]. The latter are particularly well-suited for biomarker measurements due their high charge sensitivity and direct signal transduction, allowing label-free measurements at physiological concentrations. Also, by leveraging semiconductor processing techniques, measurements with FETs can be made massively parallel, cost-effective, and portable.

A Bio-FET is a three-terminal device as represented in Figure 10. A semiconductor channel between the source and drain terminals conducts a current that is strongly modulated by an electrostatic potential applied to the gate. Biomarkers in aqueous solution exhibit a well-defined electrostatic surface potential [10] arising from charged hydrophilic residues that interact with water. When these molecules adsorb to receptor sites

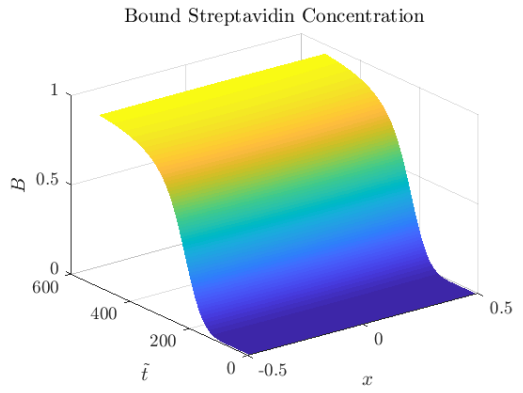

Figure 12. *Space-time curve of reacting species concentration. Here x represents the dimensionless spatial variable and* $\tilde{\boldsymbol{t}}$ *represents the dimensional temporal variable.*

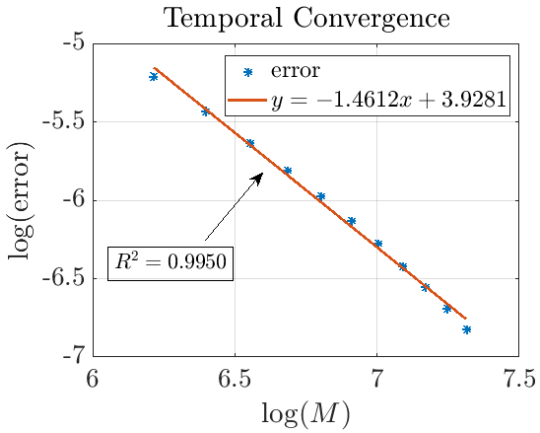

Figure 13. *Error in infinity norm as a function of the number of points in time M.*

confined to the Bio-FET's floor, they strongly modulate the channel current proportionally to the magnitude of their surface potential. This phenomenon allows Bio-FETs to be used to detect and quantify adsorbed biomarkers in solution. Furthermore, functionalizing the Bio-FET, by attaching molecules to the gate surface that have a high inherent affinity for biomarkers of interest, allows measurements with high specificity.

An accurate time-dependent model that couples transport dynamics to kinetic processes at the surface is needed to identify key parameters associated with Bio-FET experiments, such as kinetic coefficients and diffusion constants. Although Bio-FETs measure the time-dependent change in current, and are thus dynamic experiments in nature, most previous modeling efforts assume a steady distribution of biomolecules immobilized to the Bio-FET's floor and focus on characterizing charge transport through the semiconductor [11, 12]. Such models are useful for elucidating semiconductor physics but cannot utilize time-dependent measurements to estimate parameters associated with Bio-FET experiments. One could ostensibly use steady-state data to estimate binding affinities as Edwards discusses in [13] in the context of surface plasmon resonance biosensor experiments, but this requires multiple experiments to obtain accurate estimates and yields only the ratio of the association and dissociation rate constants. A dynamic model can utilize measured time-series data from a single experiment to estimate not only kinetic coefficients, but also other important parameters such as diffusion coefficients.

We presented a time dependent model for Bio-FET experiments in [14], which quantified the evolution of the reacting species concentration in presence of a continuous and uniform injection of ligand at the top boundary. Recently, we have developed a mathematical model for a sealed experiment in which a drop of ligand is injected at an instant of time [15]. This model takes the form of a diffusion equation coupled to a nonlinear equation that describes the evolution of the reacting species concentration. Through a Laplace transform and tools from complex analysis, this coupled set of equations has been reduced to a single nonlinear integro-differential equation (IDE) in terms of the reacting species concentration. Though this equation exhibits a singular convolution kernel that approaches infinity at a rate proportional to $1/\sqrt{t}$ as t approaches 0, a numerical solution to this equation has been developed which achieves greater than first-order accuracy. See Figure 12 for a space-time curve that depicts the numerical IDE solution, and Figure 13 for strong evidence of convergence at a rate of $O(\Delta t^{1.46})$ in time, despite the singular convolution kernel.

To compare the numerical solution of the IDE with experimental data, stochastic regression was employed to separate signal from noise in Bio-FET measurements [16]. This involved modeling the Bio-FET signal as a stochastic differential equation that has a deterministic term and a stochastic term:

$$dX_t = (a_0(t) + a_1(t)X_t)dt + b_0(t)dW_t\,,$$
$$X_t(0) = 0.$$

The coefficients $a_0(t)$, $a_1(t)$, and $b_0(t)$ were determined using a local weighted regression and maximum likelihood estimation as described in [16]. Figure 14 shows an overlay of the measured signal and the estimated deterministic component of the signal $X_t = (a_0(t) + a_1(t)X_t)dt$. Parameters were estimated using a trust region method implemented as lsqnonlin() in MATLAB. The results are shown in Figure 15, which demonstrates that our IDE model exhibits excellent agreement with experimental data.

Current work centers on optimal design. The signals shown in Figure 14 Figure 15 are functions of design variables, such as the biochemical gate radius, solution-well radius, height of the solution-well, and receptor concentration. To maximize diffusive flux into the surface it is desirable to make the receptor concentration and biochemical gate radius as large as possible, but this comes at the cost of increasing a signal distortion effect

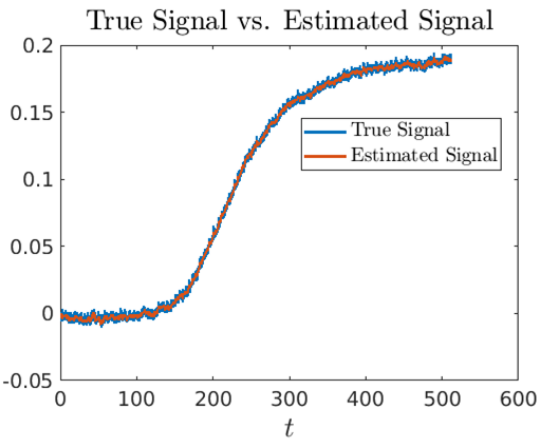

Figure 14. *An overlay of the measured signal (labeled true), and the estimated deterministic component of the signal found through stochastic regression (estimated signal).*

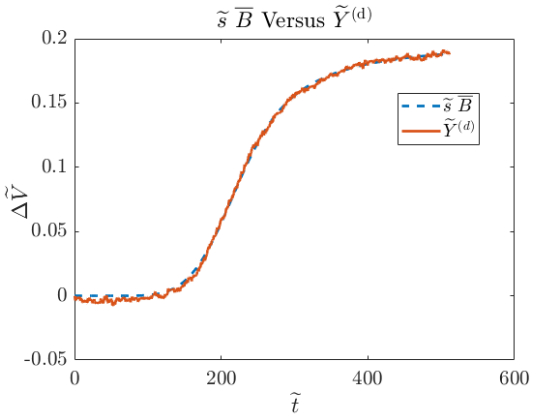

Figure 15. *An overlay of the spatially averaged solution to our IDE model together with the deterministic component of the signal.*

discovered in [15]. The presence of other design variables such as the solution-well radius and height further complicate this highly nonlinear problem. To reconcile these two competing objectives, we are investigating formulating the problem using the Van Stakelberg approach described by Lions [17]. Future work will study competitive binding kinetics at the surface.

References

[1] K. Fosgerau and T. Hoffmann. Peptide Therapeutics: Current Status and Future Directions. *Drug Discovery Today* **20** (2015), 122-128.

[2] B. K. Binukumar, Y.-L. Zheng, V. Shukla, N. D. Amin, P. Grant, and H. C. Pant. TFP5, a Peptide Derived from P35, a CDK5 Neuronal Activator, Rescues Cortical Neurons from Glucose Toxicity. *Journal of Alzheimer's Disease* **39**:4 (2014), 899909.

[3] P. K. Drain, L. Gounder, F. Sahid, and M.-Y. Moosa. Rapid Urine LAM Testing Improves Diagnosis of Expectorated Smear-Negative Pulmonary Tuberculosis in an HIV-Endemic Region. *Scientific Reports* **6** (2016), 19992.

[4] B. Ilic, H. G. Craighead, S. Krylov, W. Senaratne, C. Ober, and P. Neuzil. Attogram Detection Using Nanoelectromechanical Oscillators. *Journal of Applied Physics* **95:7** (2004), 3694-3703.

[5] W. Knoll. Interfaces and Thin Films as Seen by Bound Electromagnetic Waves. *Annual Review of Physical Chemistry* **49**:1 (1998), 569-638.

[6] D. K. Armani, T. J. Kippenberg, S. M. Spillane, and K. J. Vahala. Ultra-high-Q Toroid Microcavity on a Chip. *Nature* **421** (2003), 925-928.

[7] Y. Cui, Q. Wei, H. Park, and C. M. Lieber. Nanowire Nanosensors for Highly Sensitive and Selective Detection of Biological and Chemical Species. *Science* **293** (2001), 1289-1292.

[8] P. Mohanty, Y. Chen, X. Wang, M. K. Hong, C. L. Rosenberg, D. T. Weaver, and S. Erramilli. Field Effect Transistor Nanosensors for Breast Cancer Diagnostics. arXiv:1401.1168 [q-bio.QM], 2014.

[9] F. Pouthas, C. Gentil, D. Cote and U. Bockelmann. DNA Detection on Transistor Arrays Following Mutation-specific Enzymatic Amplification. *Applied Physics Letters* **84**:9 (2004), 1594-1596.

[10] A. Cardone, H. Pant, and S. A. Hassan. Specific and Non-Specific Protein Association in Solution: Computation of Solvent Effects and Prediction of First-Encounter Modes for Efficient Configurational Bias Monte Carlo Simulations. *The Journal of Physical Chemistry B* **117**:41 (2013), 12360-12374.

[11] S. Baumgartner, M. Vasicek, A. Bulyha, N. Tassotti, and C. Heitzinger. Analysis of Field-Effect Biosensors Using Self-Consistent 3D Drift-Diffusion and Monte-Carlo Simulations. *Procedia Engineering* **25** (2011), 40700410.

[12] C. Heitzinger, N. J. Mauser, and C. Ringhofer. Multiscale Modeling of Planar and Nanowire Field-effect Biosensors. *SIAM Journal on Applied Mathematics* **70**:4 (2010), 1635–1654

[13] D. A. Edwards. Estimating Rate Constants in a Convection-Diffusion System with a Boundary Reaction. *SIAM Journal on Applied Mathematics* **63**:1 (1999), 89-112.

[14] R. M. Evans, A. Balijepalli, and A. J. Kearsley. Diffusion-Limited Reaction in Nanoscale Electronics. *Methods and Applications of Analysis* **26**:2 (2019), 149-166.

[15] R. M. Evans, A. Balijepalli, and A. J. Kearsley. Transport Phenomena in Field Effect Transistors. In review.

[16] A. J. Kearsley, Y. Gadhyan, and W. E. Wallace. Stochastic Regression Modeling of Chemical Spectra. *Chemometrics and Intelligent Laboratory Systems* **139** (2014), 26-32.

[17] J. L. Lions. Hierarchic Control. *Proceedings Mathematical Sciences* **104**:1 (1994), 295-304.

Participants

Ryan Evans and Anthony Kearsley (ACMD); Arvind Balijepalli (NIST PML)

Contagion Avoidance on Growing Networks

The current trend towards growing interconnectivity of technological, financial and social infrastructures is driven by economic and convenience benefits. However, recent systemic failures/collapses of various types of networked infrastructures has demonstrated that interconnectivity also increases a system's exposure to risks of undesirable contagion. Understanding and ultimately optimizing the inherent risk/benefit tradeoff of interconnectivity is one of the most urgent and challenging problems faced by the modern society. In our research we attempt to understand the effect of the interplay of risks and benefits of interconnectivity in naturally growing networks.

Brian Cloteaux and Vladimir Marbukh

The economic and convenience benefits of interconnectivity drive the current explosive growth in networked systems. However, as recent catastrophic failures resulting from contagion in numerous large-scale networked infrastructures have demonstrated, interconnectivity is also inherently associated with risk [1]. In our research [2, 3] we attempt to understand the effect of the interplay of risks and benefits of interconnectivity in naturally growing networks.

Our current results suggest that accounting for this interplay allows one to resolve a fundamental issue in the widely accepted *preferential attachment* (PA) model of growing networks. PA assumes that the probability for a newly arriving node to attach to an existing node is an increasing function of the existing node degree d. In particular, the *generalized preferential attachment* (GPA) assumes that the attachment probability is proportional to d^{α} where $\alpha > 0$ [4]. An unresolved issue is that, on the one hand, networks growing under competitive pressures (such as communication networks, power grids, social networks, financial interactions, etc.) are typically characterized by a power law node degree distribution. On the other hand, however, the PA model produces this node degree distribution only for the specific preferential attachment probability proportional to d, i.e., the specific GPA parameter $\alpha = 1$ [4].

Our results suggest that for sufficiently rational agents, attempts to balance the incentive to connect to higher degree nodes and the incentive to avoid undesirable contagion, which is more likely to affect higher degree nodes, results in an effective attachment probability proportional to d for $d \gg 1$ in the GPA model.

In our current work, we assumed a *susceptible-infectious-susceptible* (SIS) contagion model. This selection was motivated by the availability of analytical results for these models. As a first step, we examined the susceptibility of a network to infection that grows under a simple infection risk mitigation scheme: any new node being added to a network does not connect to any currently infected node.

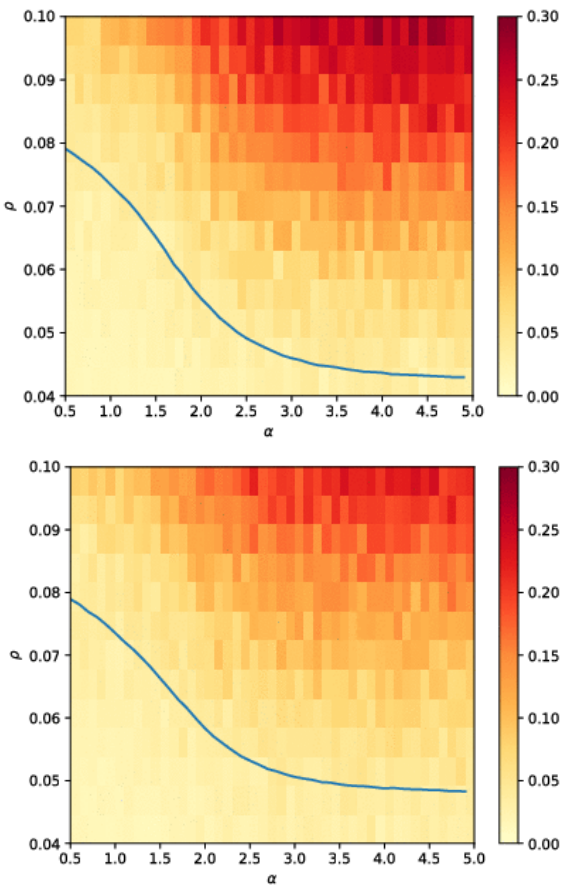

Figure 16. *Comparison of infection rates (shown in color) across various values of α and ρ. The top graph shows the rates for GPA, while the bottom graph shows it for GPA- IA. The line shows the average boundary where infection dies out.*

We began by examining the effect of infection avoidance on overall infection rates. As expected, infection avoidance has a profound effect on both the topology and infection sustainability for an evolving network. Figure 16 shows how infection avoidance dampens infection. In this figure, the top graph (GPA) denotes networks created using standard preferential attachment without any infection avoidance, i.e., the attachment probability is proportional to N^{α}, where N is the node degree, while bottom graph (GPA-IA) denotes the scenario which combines the same GPA with SIS infection avoidance using the infection parameter ρ, i.e., the ratio between the node infection and recovery rates.

A comparison of the upper right-hand corners of the two graphs demonstrates that the percentage of infected nodes in the resulting networks decreases when using infection avoidance. In addition, we are also interested

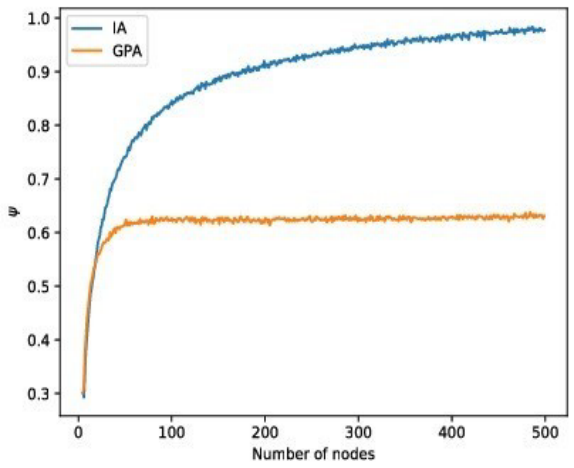

Figure 17. *Exponent ψ for GPA and GPA-IA scenarios.*

in the impact of infection avoidance on the infection-free region in the growing network. This figure indicates an enlargement of infection-free region due to infection avoidance.

We are also interested in the conflict between incentives for connectivity and infection avoidance as a case of *localization*, when in a network with growing number $N \to \infty$ of nodes where only a vanishingly small proportion of nodes $o(N)/N \to 0$ is persistently infected. As one might expect, infection avoidance by sufficiently rational newly arriving nodes keeps the system on the boundary of the localization region.

The phenomenon of localization has major impact on the spread of SIS infection in a network. A network with some level of localization tends to maintain an infection over a subset of the nodes. Networks created using preferential attachment show localization for their hub nodes. We are interested in whether the networks grown through infection avoidance show localization, and how infection avoidance affects the spread of infection in these networks.

Following [5], we quantify the phenomenon of localization by estimating the *inverse participation ratio* (IPR)

$$IPR(N) = \sum_i f_i^4(N),$$

where $f_i(N)$ are the components of the principal eigenvector associated with the network's adjacency matrix that have been normalized by

$$\sum_i f_i^2 = 1.$$

We then fit $IPR(N)$ to a power-law distribution: $IPR(N) \sim N^{-\psi}$. It is known [5], that $\psi = 1$ indicates no localization, $\psi = 0$ indicates complete localization, and $0 < \psi < 1$ indicates partial localization, meaning that only a portion $O(1/N^{1-\psi})$ of nodes are persistently infected.

Figure 17 shows the exponent ψ for two simulation scenarios: (a) conventional GPA [4] where $\alpha = 2.5$, and (b) GPA-IA using the infection parameter $\rho = 1$. This figure strongly indicates that while GPA produces localization, GPA-IA does not. This, and our other findings, demonstrate importance of accounting for the competing incentives driving growing networks and may have important practical implications. In particular, infection localization suggests that detection of the onset of infection and mitigation of infection impact can be achieved by dealing with a small subset of nodes.

Currently we are attempting to verify our conjecture that for certain parameters of the preferential attachment model, infection avoidance keeps the growing network on the verge of the eigenvector localization regime. This conjecture may have important practical implications for infection propagation and mitigation on real networks, since eigenvector localization implies persistent infection presence in a network. Our future plans include enhancing our model by allowing (a) connectivity decisions based not only on the current infected/non-infected node status, but also on the perceived likelihood of being infected, (b) rewiring of already existing connections, (c) node investments in infection risk mitigation, and (d) other types of contagion, e.g., threshold-based.

References

[1] D. Helbing. Globally networked risks and how to respond, *Nature*. 497, 51-59 (01 May 2013). DOI: 10.1038/nature12047

[2] B. Cloteaux and V. Marbukh. SIS Contagion Avoidance in a Network Growing by a Preferential Attachment. In *GRADES-NDA 2019: Proceedings of the 2nd Joint International Workshop on Graph Data Management Experiences & Systems (GRADES) and Network Data Analytics (NDA)*, June 2019, article 11. DOI: 10.1145/3327964.3328502

[3] V. Marbukh. Network Formation by Contagion Averse Agents: Modeling Bounded Rationality with Logit Learning. In *2018 IEEE/ACM International Conference on Advances in Social Networks Analysis and Mining (ASONAM 2018)*, Barcelona, Spain, August 28-31, 2018, 1232-1233. DOI: 10.1109/ASONAM.2018.8508546

[4] P. L. Krapivsky, S. Redner, and F. Leyvraz. Connectivity of Growing Random Networks. *Physical Review Letters* **85** (2000), 4629-4632. DOI: 10.1103/PhysRevLett.85.4629

[5] R. Pastor-Satorras and C. Castellano. Eigenvector Localization in Real Networks and Its Implications for Epidemic Spreading. *Journal of Statistical Physics* **173**:3 (2018), 1110-1123. DOI: 10.1007/s10955-018-1970-8

Participants

Brian Cloteaux and Vladimir Marbukh (ACMD)

Machine Learning for Experimental Quantum Dot Control

Confining electrons in arrays of semiconductor nanostructures, called quantum dots (QDs), is one of many quantum computing approaches. Due to the ease of control of the relevant parameters, fast measurement of the spin and charge states, relatively long decoherence times, and their potential for scalability, QDs are gaining popularity as candidate building blocks for solid-state quantum devices. However, as the number of QD qubits increases, the relevant parameter space grows exponentially, making heuristic control unfeasible. In semiconductor quantum computing, devices now have tens of individual electrostatic and dynamical gate voltages that must be carefully set to isolate the system to the single electron regime and to realize good qubit performance. It is thus highly desirable to have an automated protocol to achieve a target electronic state.

This project aims to develop an autonomous "cold-start" tuning protocol for QD devices. In particular, we are investigating a novel paradigm that combines a machine learning algorithm trained using synthetic data from a physical model with classical optimization techniques to establish an automated closed-loop system for experimental control. Recently, we have experimentally verified that this approach can automatically tune the device to a desired dot configuration. Our results serve as a baseline for future investigation of fully automated device control system and pave the way for similar approaches in a wide range of experiments in physics.

Justyna P. Zwolak

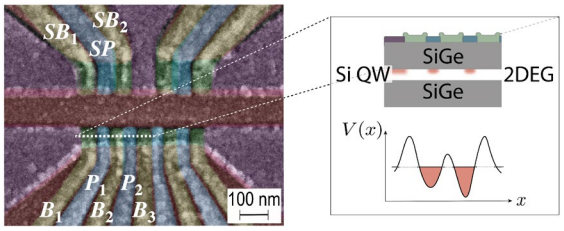

Figure 18. *A false-color scanning electron micrograph of Si/SiGe quadruple dot shows a device identical to the one used during the experimental validation of the proposed autotuner. The top gates (SB_1, SB_2, and SP) are used to form the sensing dot while the bottom gates (B_i for i=1,2,3 and P_j for j=1,2) are used to form and control the qubit dots. The inset, showing a cross section through the device along the dashed white line (top) and a schematic of the electric potential of a tuned double dot (bottom), highlights the double dot used in the experiment. Adapted from [7].*

There are myriad quantum computing approaches, each having its own set of challenges. Arrays of electrostatically defined *quantum dots* (QDs) present at the interface of semiconductor devices is one such approach [1]. Before they can be used, QDs must be "tuned," so that their operation can be controlled. The current practice of tuning QDs manually or in a semi-automated fashion is a relatively time-consuming procedure, inherently impractical for scaling up to systems with many QDs and other applications. Even tuning a double QD constitutes a nontrivial task, with each dot being controlled by at least three metallic gates, each of which influences the number of electrons in the dot, the tunnel coupling to the adjacent lead, and the interdot tunnel coupling. The presence of defects and variations in the local composition of the heterostructure disordering the background potential energy further impedes this process. At the same time, given the progress in the construction of multi-QD arrays in both one and two dimensions (1D and 2D, respectively) [2, 3], it is imperative to replace the current practice of manual tuning to a desirable electronic configuration with a standardized automated method.

Realization of good qubit performance in QDs is achieved via electrostatic confinement of electrons in a two-dimensional electron gas (2DEG) present at the interface of semiconductor heterostructures using dynamically adjusted voltages on multiple electrical gates patterned on top of the device. Figure 18 is an example of a false-color scanning electron micrograph of an Si/SiGe quadruple dot. In this figure, the voltages applied to barrier gates (B_i, i = 1, 2, 3) and plunger gates (P_j , j = 1, 2) define the potential landscape in which the QDs are formed (see insert). In particular, reservoir gates (shown in purple) accumulate electrons into leads with stable chemical potential. Depletion "screening" gates (shown in red) are used to define 1D transport channels in the 2DEG. Barriers define the dot positions by locally depleting carriers within the 1D channel, thereby separating the electron density into disjoint regions, while plungers shift the chemical potential in the dots relative to the chemical potentials of the contacts. In other words, the choice of gate voltages determines the number of dots, their position, and their coupling, as well as the number of electrons present in each dot.

The number of gates scales linearly with the number of dots and the voltage space grows exponentially. In order to reach a stable, few-electron configuration, current experiments set the input voltages heuristically. In particular, the process of tuning QD devices involves identifying the state of the device from a series of measurements, followed by manual adjustment of parameters (i.e., gate voltages) based on the observed outcomes. Figure 19 depicts two sample measurements of the change in the current through the sensing dot as electrons are added to and removed from the qubit dots. The parallel charge transition lines (visible in the top panel)

suggest that the device is in a single dot regime while the X-like features (visible in bottom panel) suggest that the device is in a regime where two dots are formed. As such, the process of tuning relies heavily on a visual inspection and classification of images (a scan of measured data providing information on the current system state) by a human expert. However, such an approach does not scale well with growing array sizes, is prone to random errors, and may result in only an acceptable rather than an optimal state.

Autotuning Protocol. In recent years, convolutional neural networks (ConvNets)—a class of machine learning (ML) algorithms—have emerged as a "go to" technique for automated image classification, giving reliable output when trained on a representative and comprehensive dataset [4]. Taking advantage of the potential of ConvNets, we have proposed an autotuning paradigm that combines a ConvNet-based algorithm trained on simulated charge sensor readout data with an optimization routine to eliminate the need for human intervention in tuning semiconductor QD devices [5]. Using a modified Thomas-Fermi approximation, we developed a model for electron transport in gate-defined quantum dots that mimics the transport characteristics and the charge sensor response of an experimental device [6]. To train the ConvNet, we generated 10 010 random charge sensor measurement realizations, with charge sensor response stored as (30 × 30) pixel maps from the space of plunger gates. By varying between simulations physical parameters of the system (e.g., the device geometry, gate positions, lever arm, and screening length), samples in the training dataset are representative of qualitative features across a wide range of devices. The labels for each simulated measurement are assigned based on the fraction of pixels within given realization in each of the three possible states (i.e., no dot, single dot, or double dot),

$$\mathbf{p}(V_{\mathcal{R}}) = [p_{\text{none}}, p_{\text{SD}}, p_{\text{DD}}] = \left[\frac{N-(|\text{SD}|+|\text{DD}|)}{N}, \frac{|\text{SD}|}{N}, \frac{|\text{DD}|}{N}\right],$$

where |SD| and |DD| are the numbers of pixels with a single dot (SD) and double dot (DD) label, respectively, and N is the size of the image $V_{\mathcal{R}}$ in pixels. As such, $\mathbf{p}(V_{\mathcal{R}})$ can be thought of as a probability vector that a given measurement captures each of the possible states. Currently, the full autotuning protocol, i.e., the process of finding a range of gate voltages where the device is in a desired state, comprises of the following steps which are repeated as necessary.

- *Sandboxing and pre-calibration.* Determining a range of acceptable voltages for all gates (to prevent device damage); establishing voltage level for the barrier gates; tuning of the charge sensor.
- *Measurement and data processing.* Measurement followed by denoising and resizing of the measured 2D scan $V_{\mathcal{R}}$ to assure compatibility with the network.

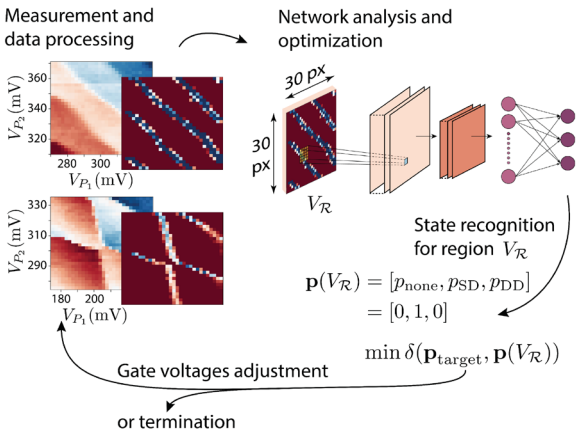

Figure 19. *Visualization of the proposed autotuning protocol. In each iteration, a measured scan is processed and analyzed by a pre-trained ConvNet, resulting in a probability vector* $\mathbf{p}(V_{\mathcal{R}})$ *that quantifies the likelihood of each possible state (i.e., no dot, single dot, or double dot) being captured in the image. A classical optimization is then used to minimize the distance (maximize the "fit") between vector* $\mathbf{p}(V_{\mathcal{R}})$ *and the desired vector* $\mathbf{p}_{target}$*. If the captured state is sufficiently close to the desired one, the optimizer terminates the autotuning process. Otherwise, it returns the position of the consecutive scan and the process it repeated. Adapted from [7].*

- *Network analysis and optimization.* ConvNets analysis of the processed measurement scan resulting in the probability vector $\mathbf{p}(V_{\mathcal{R}})$ followed by optimization (using the simplex-based Nelder-Mead method) of the fitness function

$$\delta(\mathbf{p}_{\text{target}}, \mathbf{p}(V_{\mathcal{R}})) = \left\|\mathbf{p}_{\text{target}} - \mathbf{p}(V_{\mathcal{R}})\right\|_2 + \gamma(V_{\mathcal{R}}),$$

  where $\|\cdot\|_2$ is the L^2 norm and $\gamma(\cdot)$ is a non-negative penalty function constructed to become large when regions are classified as predominantly non-double dot.

- *Termination or gate voltages adjustment.* Either terminating the autotuning protocol or setting the position of a center of a subsequent scan in terms of the gate voltages as decided by the optimizer.

The autotuning is considered successful if the optimizer converges to a voltage range that gives a desired dot configuration.

Experimental Validation. To validate the performance of the autotuner *in situ*, we collaborated with researchers from University of Wisconsin–Madison.

Before testing the autotuner on a real device, we first evaluated the trained network performance on manually labeled experimental images, using an ensemble of (30 × 30) mV scans with 1 mV/pixel resolution and (60 × 60) mV scans with 2 mV/pixel resolution. The accuracy of the neural network in distinguishing between the three possible states was 81.9 %. Then, to test the full autotuning protocol, we performed a series of trial

runs in the (V_{P_1}, V_{P_2}) plunger space. The acceptable voltage range was set to between 0 mV and 600 mV and all attempts to perform measurement outside of these boundaries during a tuning run were blocked with a fixed value of 2 (i.e., a maximum "fit" value) assigned to the fitness function. Figure 19 shows the main steps of the experimental implementation of the autotuner.

For the test, an Si/SiGe quadruple quantum dot device was pre-tuned into an operational mode, with one double quantum dot and one sensing dot active (highlighted in Figure 18). We initiated a series of 25 tuning runs for 11 different starting points within the acceptable rage for V_{P_1} and V_{P_2}. The analysis of the test runs revealed that the success rate depends significantly on where the autotuning protocol is initiated. For runs with at least one plunger set below 375 mV for the initial scan, the overall success rate was 85.7 %. Figure 20 shows a sample successful run of the autotuning protocol. However, when both plungers were set at or above 375 mV, the success rate fell to 18.2 %, with all failing cases resulting from lack of mobility of the tuner within the SD plateau (i.e., "flatness" of the fitness function for the SD region).

To further investigate the reliability of the tuning process, we performed a series of "off-line" tunings, i.e., tunings within premeasured scans that capture all possible state configurations. We found that the size of the initial simplex used in the optimization phase significantly affects the performance of the tuner. In particular, increasing the size of the initial simplex by 25 mV (about 30 %) increased the success rate by 20 %. Scaling the initial simplex dynamically based on the fitness value of the initial measurement, i.e., using larger simplex when starting in points further away from the target area than when initiating relatively close to the target region, resulted in almost 30 % increase of the success rate compared to off-line test with parameters resembling those implemented in the laboratory (i.e., fixed simplex of size 75 mV).

An article reporting this work has recently been published as an Editor's Suggestion in *Physical Review Applied* [7].

Beyond Two Dots. When increasing number of dots, the number of gates that need to be controlled—and thus the number of 2D scans required to assess the state of the device—also grows. Given the recent progress in the construction of multi-dot arrays [2, 3], it is thus imperative to consider new approaches to quantifying the states of QD devices. To address this issue, expanding on our previous work on tuning QD devices using ConvNets, we are now developing a novel approach that eliminates the need for 2D scans. Instead, we propose to capture the state of the device for a given voltage configuration v_0 (i.e., to "fingerprint" the state space at v_0) using a series of 1D traces ("rays") measured from v_0 in multiple directions in the gate voltage space.

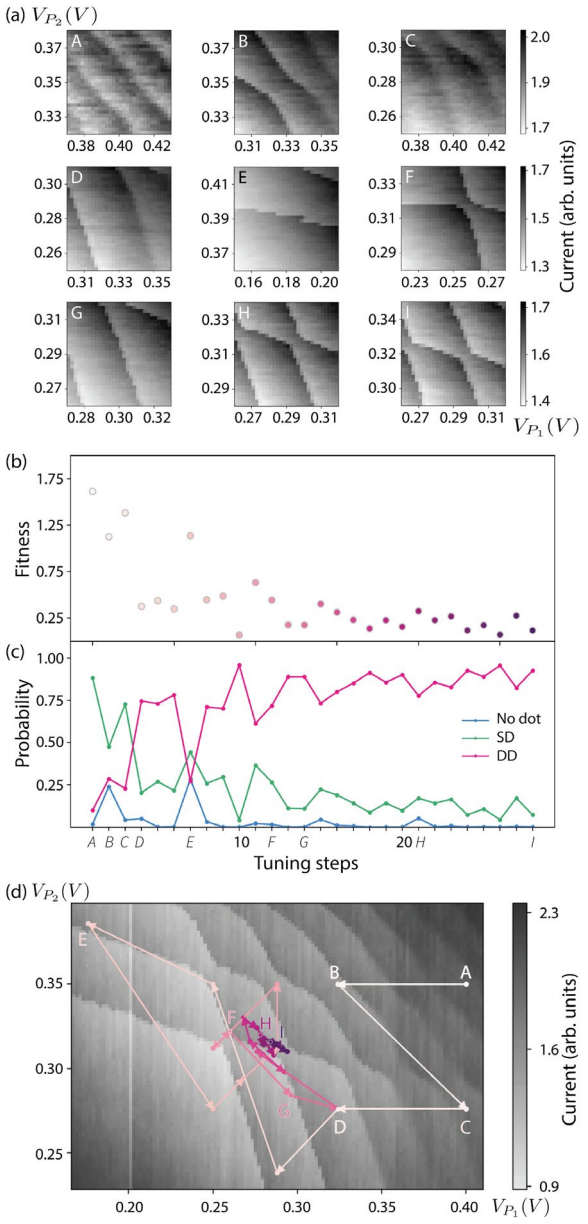

Figure 20. *A sample run of the autotuning protocol. (a) The measured raw scans in the space of plunger gates $(\boldsymbol{V_{P_1}}, \boldsymbol{V_{P_2}})$ show data available to the autotuning protocol at a given step. (b) The change of the fitness value as a function of time. (c) The probability of each state over time as returned by the ConvNet. (d) An overview of the tuning path in the space of plunger gates on a larger scan measured once the autotuning tests were completed. Points A, B, and C define the initial simplex used by the optimizer. Adapted from [7].*

We define a *state fingerprinting procedure* for an N-dot device as follows: For a given point v_0 in the voltage space,

$$v_0 = \left(v_{\mathrm{B1}}^{(0)}, v_{\mathrm{P1}}^{(0)}, v_{\mathrm{B2}}^{(0)}, v_{\mathrm{P2}}^{(0)}, \ldots, v_{\mathrm{BN}}^{(0)}, v_{\mathrm{PN}}^{(0)}, v_{\mathrm{B}(N+1)}^{(0)}\right),$$

The state fingerprint is given by a vector,

$$f_{v_0} = [d(r_1), \ldots, d(r_M)],$$

where $\vartheta = \{r_i\}_{i=1}^{M}$ is a set of M evenly distributed 1D charge sensor response measurements of a fixed length starting at v_0, and a function $d: \vartheta \rightarrow [0,1]$ is used to normalize the "distance" from v_0 to the nearest charge transition line within a given r_i ($i = 1,\ldots,M$).

To test the performance of the fingerprinting approach in differentiating between different states of QD devices, we generated an ensemble of 16 simulated double dot devices (using our Thomas-Fermi-based model) that were used to establish a training dataset for the ML algorithm. For each device, we sampled about 200 points with 12 evenly spaced traces per point (a total of 3 202 points). We then trained a relatively small deep network with three fully connected layers (256, 64, and 32 units) and three classes (no dot, SD, and DD) to an accuracy of 90.7 %. Simultaneously, we were also developing an automated protocol to measure experimental data in a ray-based fashion. In the process, we established a dataset of state fingerprints for 33 experimentally measured points (also using 12 equally spaced rays per point). The fingerprint data allowed us to further test the ML algorithm, resulting in a classification accuracy of 75.8 %.

While more work is needed to, among other things, improve the classifier and develop an efficient protocol for extracting the location of the transition lines from the measured noisy rays, this initial result suggests that the ray-based approach is a promising alternative to 2D scans. More importantly, the ray-based fingerprinting naturally extends to higher dimensional systems, where relying on 2D scans would be unfeasible.

Cold Start Tuning. The autotuning protocol we discuss in the previous sections assumes that the device is pre-calibrated into a regime, where QDs can be formed. To enable fully autonomous tuning, it is necessary to also automate the initialization of the device into the operational regime. Recently, we began to develop a "cold start" tuning protocol to do just that. In the first attempt, we developed a script that automates all the pre-calibration steps typically done by an experimentalist. Currently, we are refining the protocol to address difficulties we encountered during the first experimental test of the tuner. The autotuning protocol defined by the rays and the cold start techniques that we are currently developing will allow for a completely automated calibration and tuning of quantum dot arrays into operational regimes, consequently cutting back on time required to manually work with these devices.

Summary. Working with experimental devices with high-dimensional parameter spaces poses many challenges, from performing reliable measurements to identifying the device state to tuning into a desirable configuration. By combining theoretical, computational, and experimental efforts, this interdisciplinary research sheds new light at how modern ML techniques can assist experiments. To use QD qubits in quantum computers, it is necessary to develop a reliable automated approach to control QD devices, independent of human heuristics and intervention. However, more work is needed to develop a fully automated cold start autotuner for real-life applications.

References

[1] R. Hanson, L. P. Kouwenhoven, J. R. Petta, S. Tarucha, and L. M. K. Vandersypen. Spins in Few-electron Quantum Dots. *Reviews of Modern Physics* **79:**4 (2007), 1217–1265.

[2] D. M. Zajac, T. M. Hazard, X. Mi, E. Nielsen, and J. R. Petta. Scalable Gate Architecture for a One-Dimensional Array of Semiconductor Spin Qubits. *Physical Review Applied* **6**:5 (2016) 054013.

[3] U. Mukhopadhyay, J. P. Dehollain, C. Reichl, W. Wegscheider, and L. M. K. Vandersypen. A 2 × 2 Quantum Dot Array with Controllable Inter-dot Tunnel Couplings. *Applied Physics Letters* **112**:18 (2018), 183505.

[4] A. Krizhevsky, I. Sutskever, and G. E. Hinton. Imagenet Classification with Deep Convolutional Neural Networks. In *Advances in Neural Information Processing Systems 25* (F. Pereira, C. J. C. Burges, L. Bottou, and K. Q. Weinberger, eds.), 1097–1105, 2012.

[5] S. S. Kalantre, J. P. Zwolak, S. Ragole, X. Wu, N. M. Zimmerman, M. D. Stewart, J. M. Taylor. Machine Learning Techniques for State Recognition and Auto-tuning in Quantum Dots. *npj Quantum Information* **5**:6 (2019), 1–10.

[6] J. P. Zwolak, S. S. Kalantre, X. Wu, S. Ragole, J. M. Taylor. QFlow Lite Dataset: A Machine-learning Approach to the Charge States in Quantum Dot Experiments. *PLoS ONE* **13**:10 (2018), 1–17.

[7] J. P. Zwolak, T. McJunkin, S. S. Kalantre, J. P. Dodson, E. R. MacQuarrie, D. E. Savage, M. G. Lagally, S. N. Coppersmith, M. A. Eriksson, and J. M. Taylor. Autotuning of Double-Dot Devices *In Situ* with Machine Learning. *Physical Review Applied* **13**:13 (2020), 034075.

Participants

Justyna P. Zwolak (ACMD); Jacob M. Taylor (NIST PML); Sandesh S. Kalantre (University of Maryland); Mark A. Eriksson, Susan Coppersmith, Thomas McJunkin, J.P. Dodson (University of Wisconsin – Madison)

Part III

Project Summaries

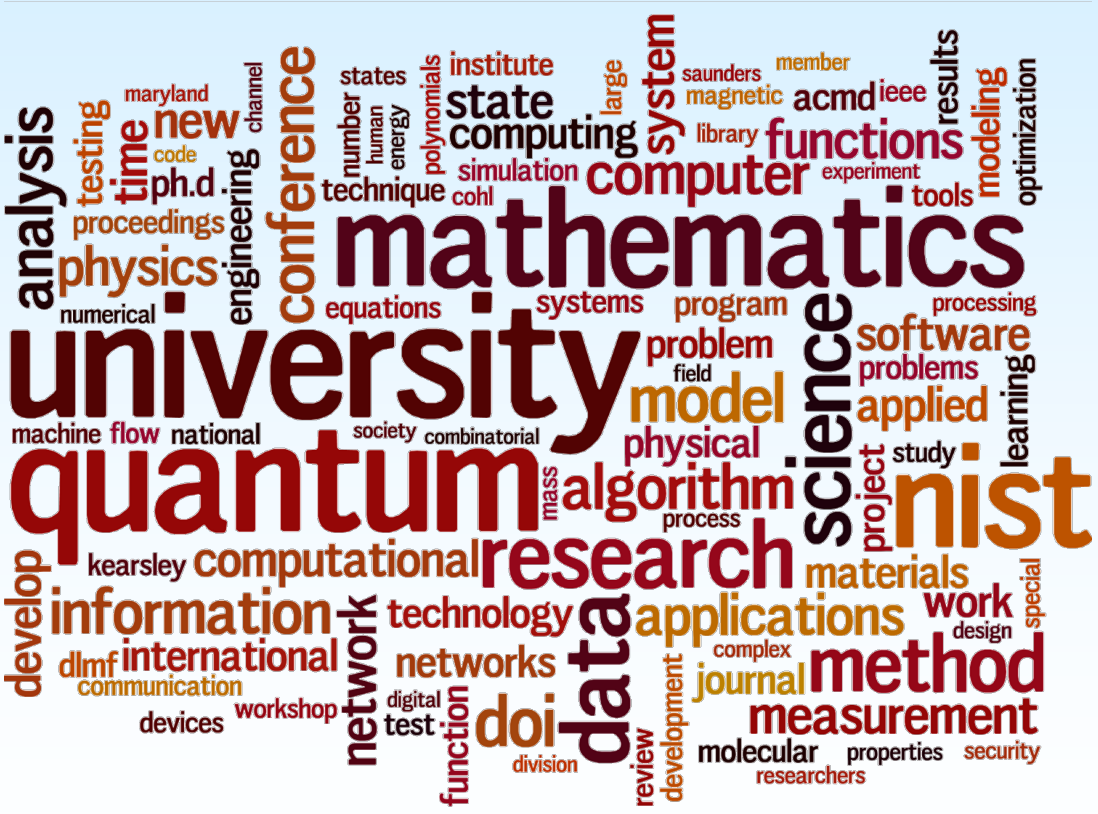

Mathematics of Metrology

Mathematics plays an important role in measurement science. Mathematical models are needed to understand how to design effective measurement systems and to analyze the results they produce. Mathematical techniques are used to develop and analyze idealized models of physical phenomena to be measured, and mathematical algorithms are necessary to find optimal system parameters. Mathematical and statistical techniques are needed to transform measured data into useful information. We develop fundamental mathematical methods and tools necessary for NIST to remain a world-class metrology institute, and to apply these to measurement science problems.

Computing Ill-Posed Nonlinear Evolution Equations

Alfred Carasso

Ill-posed deconvolution problems and associated time-reversed diffusion equations pervade measurement science and are important in numerous applications. In environmental forensics, much success has been achieved using backward advection diffusion equations to locate sources of groundwater contamination [1]. In image science, deblurring nanoscale scanning electron micrographs, as well as galactic scale Hubble Space Telescope imagery, can be accomplished effectively by solving appropriate fractional and logarithmic diffusion equations backward in time [2, 3].

As is well known, any stepwise marching difference scheme consistent with an ill-posed initial value problem is necessarily unconditionally unstable and leads to explosive error growth. However, a powerful new approach has recently been developed for solving ill-posed, time-reversed, multidimensional, nonlinear dissipative evolution equations, based on stabilizing explicit marching difference schemes. An appropriate, easily synthesized, compensating smoothing operator is applied at every time step to quench the instability. The stabilized scheme is unconditionally stable, but slightly inconsistent, and eventually leads to a distortion away from the true solution. However, in many problems of interest, the cumulative error is sufficiently small to allow for useful results. In a series of papers [4-10], such stabilized schemes were successfully applied to interesting classes of time-reversed initial value problems for parabolic equations, viscous wave equations, coupled sound and heat flow, thermoelastic vibrations, 2D viscous Burgers' equations, and most recently, 2D incompressible Navier-Stokes equations. Such computations had not previously been deemed possible.

Backward Recovery In 2D Navier-Stokes Equations. Figure 21, involving a USAF Resolution Chart, illustrates the use of stabilized explicit schemes in solving 2D Navier-Stokes equations backward in time, as developed in [10]. The initial value problem is studied in stream function-vorticity formulation, and the images shown in the first row represent the stream function. The middle row displays corresponding velocity contour plots, while the last row contains vorticity contour plots. Vorticity is obtained by taking the Laplacian of the stream function. The leftmost column in Figure 21 depicts the initial values at time $t = 0$, while the middle column depicts the corresponding Navier-Stokes solution at time $T = 1.0 \times 10^{-3}$. Evidently, considerable erosion and disorganization of sharp features has occurred. In particular, the L_2 norm of the vorticity is reduced to about 1/4 of its initial value. Nevertheless, as shown in the rightmost column, the stabilized explicit scheme, marching backward from

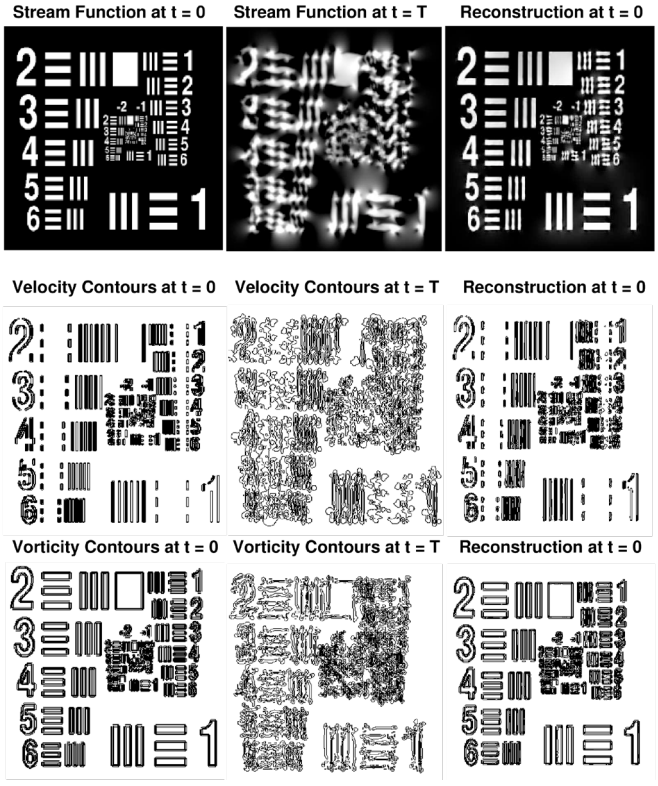

Figure 21. *USAF Resolution Chart illustrating the use of stabilized explicit schemes for the Navier Stokes equations backward in time. Here RE= 11500, Max speed = 115, and* $\boldsymbol{T = 1.0 \times 10^{-3}}$.

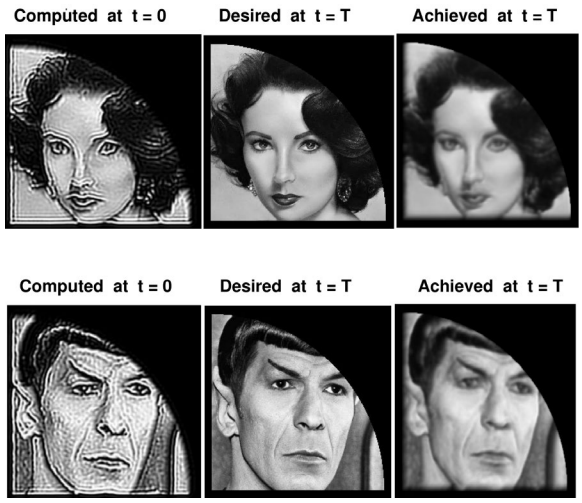

Figure 22. *Inverse design in 2D Burger's equation: compute the initial data at t = 0 that achieves the desired result at t = T.*

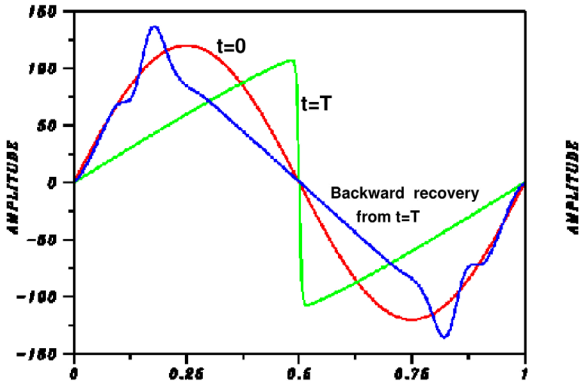

Figure 23. *Non-uniqueness in shock wave reconstruction: Initial sine wave (red) evolves into shock (green) at t = T. Backward reconstruction from t = T produces blue curve at t = 0. Initial blue curve produces a close approximation to the green shock at t = T.*

time T, can produce surprisingly good restorations, leading to L_2 relative errors on the order of twelve to fourteen percent. In this experiment, the Reynolds number $\mathrm{RE} = 1.0 \times 10^4$, and the maximum absolute value of the vorticity is on the order of 1.0×10^5. These values far exceed what would seem reasonable for useful recovery, based on the best-known uncertainty estimates for backward Navier-Stokes solutions developed in [11].

Inverse Design in 2D Viscous Burgers' Equation. The time-reversed viscous Burgers' equation is of considerable interest in connection with inverse design problems in aerodynamics, and data assimilation studies in geophysical fluid dynamics [12-16]. Many of these studies focus primarily on theoretical and computational aspects of the ill-posed 1D problem of finding initial values that can achieve a targeted result at some future time.

However, the 2D problem considered here is more challenging and has not previously appeared in the literature. It involves a coupled system of two nonlinear differential equations in two unknown functions $u(x, y, t), v(x, y, t)$, whose evolutions are necessarily intertwined.

In the example illustrated in Figure 22, where the desired state of the system at the given positive time $t = T$ is shown in the middle column. Such sharp images at time T, cannot be solutions of the 2D Burgers' system with zero Dirichlet data on the domain boundaries. Nevertheless, marching backward from that desired data at time T, using the stabilized explicit scheme developed in [9], produces corresponding feasible initial values at time $t = 0$, shown in the leftmost column. Using these initial values in the well-posed forward problem, leads to the viable approximation shown in the rightmost column in Figure 22.

Non-Uniqueness in 1D Burgers' Shock Wave Reconstruction. As discussed in [17-19], uncertainty estimates in backward in time reconstructions in 1D viscous Burgers' equation, involve bounds on spatial derivatives of the solution, on the time interval where that recovery is sought. The uncertainty is larger with larger spatial derivatives.

In the example in Figure 23, an initial sine curve at time $t = 0$, shown in red, evolves into a smooth approximation to a shock wave at time T, shown in green. Despite highly accurate computations on fine meshes, backward in time reconstruction from the data at time T, does not reproduce the red sine curve. Instead, a substantially different blue curve is obtained at $t = 0$. However, using that blue curve as initial data, leads to a close approximation to the green shock wave at time T.

[1] J. Atmadja and A. C. Bagtzoglou. State of the Art Report on Mathematical Methods for Groundwater Pollution Source Identification. *Environmental Forensics* **2** (2001), 205-214.

[2] A. Carasso, D. S. Bright, and A. E. Vladar. APEX Method and Real-Time Blind Deconvolution of Scanning Electron Microscope Imagery. *Optical Engineering* **41** (2002), 2499-2514.

[3] A. S. Carasso. Bochner Subordination, Logarithmic Diffusion Equations, and Blind Deconvolution of Hubble Space Telescope Imagery and Other Scientific Data. *SIAM Journal on Imaging Sciences* **3** (2010), 954-980.

[4] A. S. Carasso. Compensating Operators and Stable Backward in Time Marching in Nonlinear Parabolic Equations. *International Journal of Geomathematics* **5** (2014), 1-16.

[5] A. S. Carasso. Stable Explicit Time-Marching in Well-Posed or Ill-Posed Nonlinear Parabolic Equations. *Inverse Problems in Science and Engineering* **24** (2016), 1364-1384.

[6] A. S. Carasso. Stable Explicit Marching Scheme in Ill-Posed Time-Reversed Viscous Wave Equations. *Inverse Problems in Science and Engineering* **24** (2016), 1454-1474.

[7] A. S. Carasso. Stabilized Richardson Leapfrog Scheme in Explicit Stepwise Computation of Forward or Backward

Nonlinear Parabolic Equations. *Inverse Problems in Science and Engineering* **25** (2017), 1719-1742.

[8] A. S. Carasso. Stabilized Backward in Time Explicit Marching Schemes in the Numerical Computation of Ill-Posed Time-Reversed Hyperbolic/Parabolic Systems. *Inverse Problems in Science and Engineering* **27** (2019), 134-165.

[9] A. S. Carasso. Stable Explicit Stepwise Marching Scheme in Ill-Posed Time-Reversed 2D Burgers' Equation. *Inverse Problems in Science and Engineering* **27** (2019), 1672-1688.

[10] A. S. Carasso. Computing Ill-Posed Time-Reversed 2D Navier-Stokes Equations using a Stabilized Explicit Finite Difference Scheme Marching Backward in Time. *Inverse Problems in Science and Engineering* (2019) DOI: 10.1080/17415977.2019.1698564

[11] R. J. Knops and L. E. Payne. On the Stability of Solutions of the Navier-Stokes Equations Backward in Time. *Archives of Rational Mechanics and Analysis* **29** (1968), 331-335.

[12] K. Ou and A. Jameson. Unsteady Adjoint Method for the Optimal Control of Advection and Burgers' Equation Using High Order Spectral Difference Method. In *49th AIAA Aerospace Science Meeting*, January 4–7 (2011), Orlando, FL.

[13] N. Allahverdi, A. Pozo and E. Zuazua. Numerical Aspects of Large-Time Optimal Control of Burgers' Equation. *ESAIM Mathematical Modeling and Numerical Analysis* **50** (2016), 1371–1401.

[14] L. Gosse and E. Zuazua. Filtered Gradient Algorithms for Inverse Design Problems of One- Dimensional Burgers' Equation. In *Innovative Algorithms and Analysis* (L. Gosse and R. Natalini eds.), SINDAM Series. Springer (2017), 197–227.

[15] J. Lundvall, V. Kozlov and P. Weinerfelt. Iterative Methods for Data Assimilation for Burgers' Equation. *Journal of Inverse and Ill-Posed Problems* **14** (2006), 505–535.

[16] D. Auroux, P. Bansart and J. Blum. An Evolution of the Back and Forth Nudging for Geophysical Data Assimilation: Application to Burgers' Equation and Comparison. *Inverse Problems in Science and Engineering* **21** (2013), 399-419.

[17] A. Carasso. Computing Small Solutions of Burgers' Equation Backwards in Time. *Journal of Mathematical Analysis and Applications* **59** (1977), 169-209.

[18] D. N. Hào, V. D. Nguyen and V. T. Nguyen. Stability Estimates for Burgers-Type Equations Backward in Time. *Journal of Inverse and Ill Posed Problems* **23** (2015), 41-49.

[19] A. S. Carasso. Reconstructing the Past from Imprecise Knowledge of the Present: Effective Non-Uniqueness in Solving Parabolic Equations Backward in Time. *Mathematical Methods in Applied Sciences* **36** (2012), 249-261.

Computational Tools for Image and Shape Analysis

Günay Doğan (Theiss Research)
Javier Bernal
Charles R. Hagwood (NIST ITL)
James Lawrence
Prashant Athavale (Clarkson University)
Harbir Antil (George Mason University)
Soeren Bartels (University of Freiburg)
Marilyn Y. Vazquez (Ohio State University)
Shuang Li (University of Southern California)
Hasan Hüseyin Eruslu (University of Delaware)
Eve N. Fleisig (Princeton University)
Kevin Su (Stanford University)

The main goal of this project is to develop efficient and reliable computational tools to detect geometric structures, such as curves, regions and boundaries, from given direct and indirect measurements, e.g., microscope images or tomographic measurements, as well as to evaluate and compare these geometric structures or shapes in a quantitative manner. This is important in many areas of science and engineering, where the practitioners obtain their data as images, and would like to detect and analyze the objects in the data. Examples are microscopy images for cell biology or micro-CT (computed tomography) images of microstructures in material science and shoeprint images in crime scenes for footwear forensics. In FY 2019, advances were made in the following two fronts of this project.

Image Segmentation. Image segmentation is the problem of finding distinct regions and their boundaries in given images and is a necessary data analysis step for many problems in cell biology, forensics, and material science, as well as other fields in science and engineering. In FY 2019, Günay Doğan and his collaborators continued to work on multiple strategies for image segmentation.

One of these strategies is the phase field evolution approach for image segmentation pursued by Doğan, and his collaborators, Harbir Antil from George Mason University and Soeren Bartels from University of Freiburg. In this approach, the regions in images and their boundaries are represented implicitly with a phase field function, and the segmentations are obtained by minimizing an associated cost functional. They had implemented an efficient minimization algorithm for this cost functional, relying on Fast Fourier Transform (FFT) operations. Doğan evaluated this algorithm on a variety of test data sets, including specially designed test data, examples of microstructure images, and examples of shoeprints, and obtained very satisfactory results. They are currently preparing a manuscript describing this algorithm [1].

Doğan had worked with Ms. Marilyn Vazquez, a Ph.D. student from George Mason University, currently at Ohio State University, on a segmentation algorithm formulated as data clustering. She had implemented a manifold-based clustering algorithm and used it for segmentation of textured images by clustering local patches from the given image. They completed a report describing this algorithm, demonstrating it on microstructure images. They are currently working on a journal paper describing this work [2].

Doğan worked with two Ph.D. students, Shuang Li from University of Southern California, and Hasan Huseyin Eruslu from University of Delaware. Li had previously developed a new segmentation algorithm using topological derivatives. This algorithm segments images into regions of distinct statistics, modeled with parametric distributions of pixel values. A key feature of this algorithm is a novel region regularization term that helps attain clean spatially coherent region labels. Li performed additional experiments comparing this algorithm to competing ones, such as graph cuts. Doğan and Li wrote a paper describing this algorithm [3].

Eruslu's project was focused on volumetric image segmentation. The goal was to extract boundary surfaces of regions or objects in 3d volumetric images. Eruslu made considerable progress on this project in summer 2018 and returned to continue on the project in summer 2019. He improved the code while moving it to Python 3, made significant performance gains on the line search, curvature computation, mesh regularization, and other components. He implemented additional functionality for efficient region-based segmentation. Extending to more general segmentation models is still work in progress. It will enable segmentation of more complicated 3D images.

Prashant Athavale of Clarkson University visited Doğan in the summer of 2019 to collaborate on preprocessing and segmentation of orientation images of microstructures, including algorithms to inpaint missing data pixels, and denoise misread orientation values.

Shape Analysis. In FY 2019, Doğan worked on optimization algorithms for elastic shape analysis. He had previously developed a fast algorithm to compute an elastic shape distance between two given closed curves, working together with Javier Bernal and Charles Hagwood (ITL SED). The elastic shape distance is a powerful dissimilarity metric to quantify the dissimilarity of two given closed curves [5, 6], and is widely applicable to shape analysis problems in science and engineering. However, the computation of the elastic shape distance is expensive, as it requires solving a difficult optimization problem. Another challenge of the optimization is that the theoretical shape distance definition requires finding the global minimum of the underlying energy, which is very difficult and expensive to do in practice. To overcome these two difficulties, Doğan had developed two reduced energy formulations of the model and devised a new iterative optimization algorithm built on these reduced energy formulations. This algorithm was more efficient than his previously published iterative algorithm and produced high quality minima that translate into more realistic shape distance values. Doğan continued to test and benchmark the algorithm and was able to increase the efficiency of various components. A notable improvement was two orders of magnitude speed-up in rotation optimization achieved by using an analytical singular value decomposition (SVD) routine instead of Matlab's generic SVD function (which actually calls LAPACK's SVD).

Doğan has been working with research volunteer, Kevin Su (currently undergraduate in Stanford University) to develop an improved version of the elastic shape distance algorithm in the Python language. They had previously implemented an efficient version of the dynamic programming (DP) algorithm in Python. DP is the core of the elastic distance computation. They further tuned and optimized the DP algorithm, and applied it to the multiple shape representations, such as unit tangents, curvature, and square root velocity functions.

Bernal worked on elastic registration of curves in higher dimensions, to realize an efficient algorithm for this problem. He recreated the alternating optimization approach of Srivastava et al. [5] for curves in high-dimensional spaces, but also incorporated a high-dimensional generalization of his previous 2D dynamic programming algorithm [8], which computes elastic registrations in linear time. Bernal and James Lawrence formulated a purely algebraic justification of the Kabsch-Umeyama algorithm, which is used to compute optimal rotations. In addition, they developed a procedure to minimize the elastic L^2 distance between two curves, based on ideas in [6], namely alternating computations of optimal registrations, with those of optimal rotations for all starting points of the first curve. As established in [6], carrying out computations this way is not only more efficient on its own, but also allows applications of the FFT for simultaneous computation over all starting points at once. Bernal is currently investigating the generalization of FFT-based rotation optimization to higher dimensions. An application of the resulting code will be to compare lines of proteins in 3D. Future plans include development of algorithm to compute elastic registration of 3D parametrized surfaces. The goal is to identify a shape space of surfaces together with a numerical framework for the computation of geodesics in such a space.

Using different shape representations or different versions of the algorithms lead to different shape dissimilarity metrics, and this brings the question of which metric would perform best. Doğan and research volunteer, Eve Fleisig (currently undergraduate in Princeton University), have been developing a Python program, VEMOS (Visual Explorer for Metrics of Similarity) that can be used to evaluate and compare multiple competing

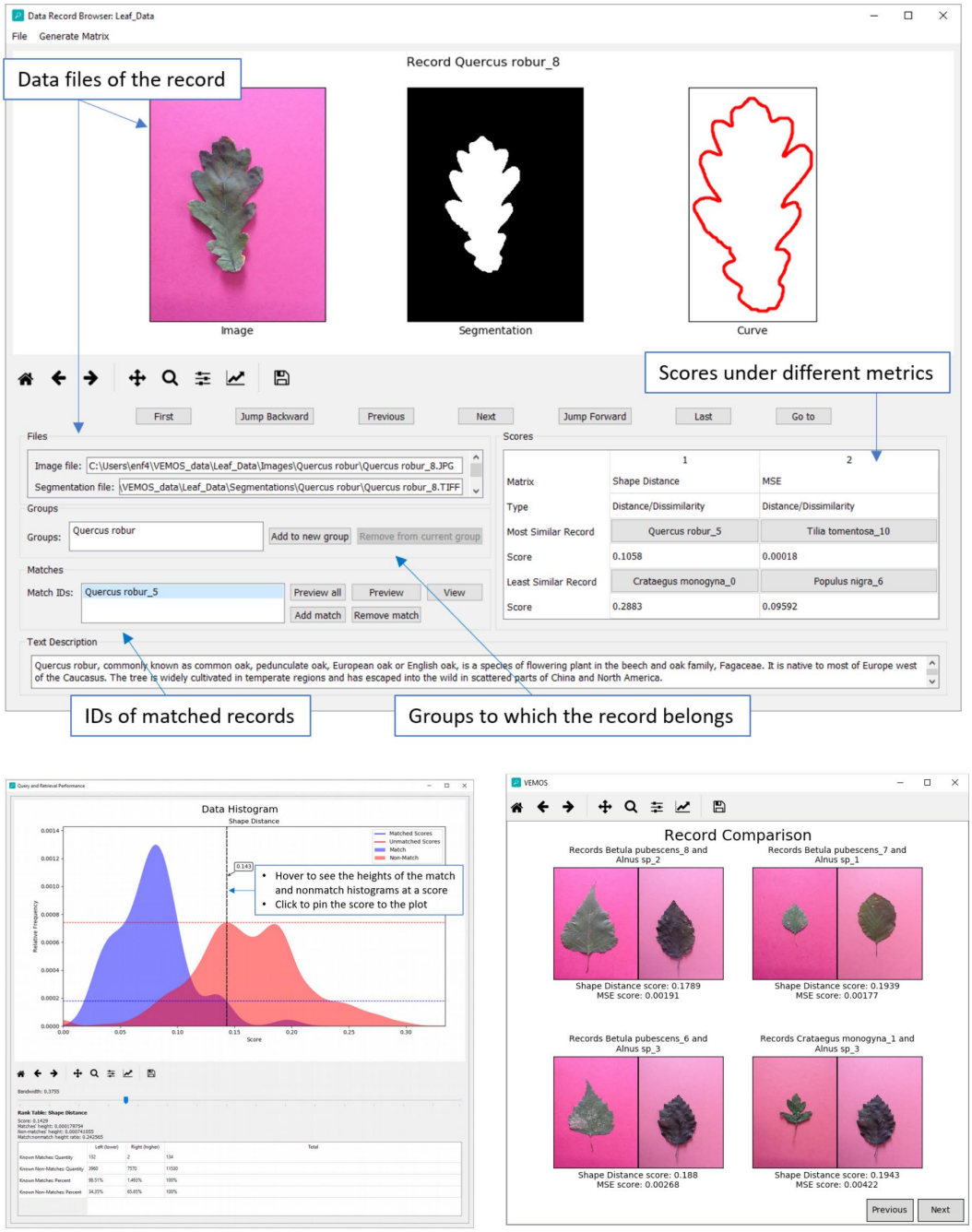

Figure 24. *Screenshots of VEMOS analyzing an example data set (leaves) and associated dissimilarity metrics.*

similarity/dissimilarity metrics, including shape dissimilarity metrics. VEMOS is useful for applications beyond shape distances; it can be used in a versatile manner to evaluate multiple alternative dissimilarity metrics for heterogeneous data sets, including images, shapes, point clouds and other data types. In FY 2019, they added a metric fusion function to create improved metrics from given metrics, also fixed bugs, and improved performance of existing code. They completed a manuscript describing VEMOS [9].

[1] H. Antil, S. Bartels, and G. Doğan. A Phase Field Segmentation Model with Improved Boundary Regularization. In process.

[2] M. Vazquez, T. Sauer, T. Berry, and G. Doğan. Texture Segmentation from a Manifold Learning Perspective. In process.

[3] S. Li and G. Doğan. Image Segmentation by Topology Optimization of Region Statistics. In process.

[4] G. Doğan. An Efficient Langrangian Algorithm for an Anisotropic Geodesic Active Contour Model. In *Scale Space and Variational Methods in Computer Vision*

(F. Lauze, Y. Dong, and A. Dahl, eds.), Lecture Notes in Computer Science **10302** (2017), Springer.

[5] A. Srivastava, E. Klassen, S. Joshi, and I. Jermyn. Shape Analysis of Elastic Curves in Euclidean Space. *IEEE Transactions on Pattern Analysis and Machine Intelligence* **33**:7 (2011), 1415-1428.

[6] G. Doğan, J. Bernal, and C. R. Hagwood. Fast Algorithms for Shape Analysis of Planar Objects. In *Proceedings of the IEEE Conference on Computer Vision and Pattern Recognition (CVPR'15)*, Boston, MA, June 2015.

[7] G. Doğan, J. Bernal, and C. R. Hagwood, FFT-based Alignment of 2D Closed Curves with Application to Elastic Shape Analysis. In *Proceedings of the 1st International Workshop on Differential Geometry in Computer Vision for Analysis of Shapes, Images and Trajectories (DiffCV'15)*, Swansea, United Kingdom, September 2015.

[8] J. Bernal, G. Doğan, and C. R. Hagwood. Fast Dynamic Programming for Elastic Registration of Curves. In *Proceedings of the 2nd International Workshop on Differential Geometry in Computer Vision and Machine Learning (DiffCVML'16)*, Las Vegas, NV, July 1, 2016.

[9] E. Fleisig and G. Doğan. VEMOS: GUI for Evaluation of Distance Metrics of Heterogeneous Data Sets. In process.

Characterization and Computation of Matrices of Maximal Trace Over Rotations

Javier Bernal
James F. Lawrence

A $d \times d$ matrix M is of *maximal trace* over rotation matrices if given any $d \times d$ rotation matrix U, the trace of UM does not exceed that of M. In [1] we have characterized matrices of maximal trace over rotation matrices in terms of their eigenvalues: A $d \times d$ matrix M is of maximal trace over rotation matrices if and only if it is symmetric and has at most one negative eigenvalue, which, if it exists, is no larger in absolute value than the other eigenvalues of the matrix. We then show, also in [1], for $d = 2, 3$, how this characterization can be used in practice to solve important problems in functional and shape analysis.

Suppose $P = \{\mathrm{p}_1, \ldots, \mathrm{p}_n\}$ and $Q = \{\mathrm{q}_1, \ldots, \mathrm{q}_n\}$ are each sets of n points in $\mathbb{R}^d$. With $\|\cdot\|$ denoting the $d-$dimensional Euclidean norm, in the *constrained orthogonal Procrustes problem* [3, 4, 7], a $d \times d$ orthogonal matrix U is found that minimizes

$$\Delta(P, Q, U) = \sum_{i=1}^{n} \|U\mathrm{q}_i - \mathrm{p}_i\|^2,$$

where U is constrained to be a rotation matrix, i.e., an orthogonal matrix of determinant equal to one. This problem generalizes to the so-called *Wahba's problem* which is that of finding a $d \times d$ rotation matrix U that minimizes

$$\Delta(P, Q, W, U) = \sum_{i=1}^{n} w_i \|U\mathrm{q}_i - \mathrm{p}_i\|^2$$

where $W = \{w_1, \ldots, w_n\}$ is a set of n nonnegative weights. Finding solutions to these problems is intimately related to the problem of finding the maximal trace over rotation matrices of a matrix, and being able to find solutions is of importance, notably in the field of functional and shape data analysis [2, 6], where, in particular, the shapes of two curves are compared, in part by optimally rotating one curve to match the other.

In the past three or four decades the algorithm of choice for solving the constrained orthogonal Procrustes problem and Wahba's problem has been the algorithm by Kabsch and Umeyama [3, 4, 7] which is based on the concept of the singular value decomposition of a matrix. The justification of this algorithm as presented separately by Kabsch and Umeyama is not totally algebraic, as it is based on exploiting the optimization technique of Lagrange multipliers. In [5], we have presented a purely algebraic justification of the algorithm through the exclusive use of simple concepts from linear algebra.

Recently we have developed and implemented methods for solving the constrained orthogonal Procrustes problem and Wahba's problem for $d = 2, 3$, without the use of the singular value decomposition concept. Applications of these programs are currently under way in the context of shape analysis, in particular for computing the elastic shape registration of two 3-dimensional curves and the elastic shape distance between them.

[1] J. Bernal and J. Lawrence. Characterization and Computation of Matrices of Maximal Trace over Rotations. *Journal of Geometry and Symmetry in Physics* **53** (2019), 21-53.

[2] G. Dogan, J. Bernal, and C. R. Hagwood. FFT-based Alignment of 2d Closed Curves with Application to Elastic Shape Analysis. In *Proceedings of the 1st International Workshop on Differential Geometry in Computer Vision for Analysis of Shapes, Images and Trajectories (DIFF-CV)*, in conjunction with the British Machine Vision Conference, Swansea, UK, September 10, 2015.

[3] W. Kabsch. A Solution for the Best Rotation to Relate Two Sets of Vectors. *Acta Crystallographica Section A: Crystal Physics* **32**:5 (1976), 922-923.

[4] W. Kabsch. A Discussion of the Solution for the Best Rotation to Relate Two Sets of Vectors. *Acta Crystallographica Section A: Crystal Physics* **34**:5 (1978), 827-828.

[5] J. Lawrence, J. Bernal, and C. Witzgall. A Purely Algebraic Justification of the Kabsch-Umeyama Algorithm. *Journal of Research of the National Institute of Standards and Technology* **124** (2019), 1-6.

[6] A. Srivastava and E. P. Klassen. *Functional and Shape Data Analysis*. Springer, New York, 2016.

[7] S. Umeyama. Least-Squares Estimation of Transformation Parameters Between Two Point Patterns. *IEEE Trans. Pattern Analysis and Machine Intelligence* 13:4 (1991), 376-380

Newton Fractals and Global Optimization

Daniel DeLeon (University of Maryland)
Anthony Kearsley

Inversion of reflection seismograms is often accomplished by formulating a (non-linear) least-squares optimization problem that seeks to find coefficients that explain as well as possible seismic reflection data. These problems are riddled with undesirable local, non-global minimizers caused by noise in seismic measurements. Many years ago, an amazingly inventive approach called Differential Semblance Optimization (DSO) was devised and applied to these types of problems with great success [1] and led to a class of numerical methods based on Newton's method that, for a wide class of noise, converged to a global minimizer even when an initial iterate was far from the solution.

For unconstrained optimization problems like this, if one examines the relationship of initial guesses or starting points to the minimizer to which a numerical algorithm converges, one often finds that the mapping forms a Julia set, that is, a set that consists of values for which arbitrarily small perturbations cause profound changes to the sequence of iterated function values. While one starting point may converge to a desirable global minimizer, a small perturbation in that starting point would cause the numerical algorithm to converge to a less desirable non-global local solution [2]. This phenomenon was also observed when the DSO approach was generalized and applied to minimizing the notorious Lennard-Jones potential, a well-studied model problem for molecular conformation and an unconstrained global optimization problem with many local minima [3].

Measurement-dependent optimization problems often have undesirable minimizers. In this research project, we sought to examine how techniques like those described in [1] and [3] performed when applied to very simple global optimization problems with only one or two variables in hopes to examine which formulations work well, which don't, and why.

Given an unconstrained optimization problem, say

$$\min_x f(x)$$

where f is a function of n variables, $f: \mathbb{R}^n \to \mathbb{R}$ and is assumed to be very smooth and admits local non-global minimizers, consider the very simple reformulation,

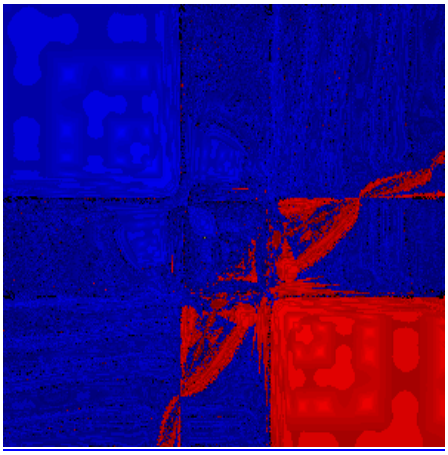

Figure 25. *Convergence of Newton's method for the un-penalized formulation* ($\boldsymbol{\rho} = \mathbf{0}$) *where many starting points converge to both the global and local minimizer.*

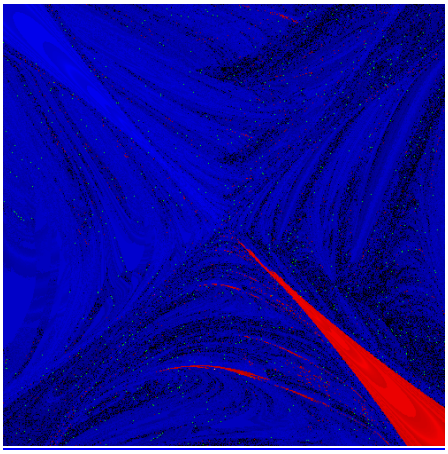

Figure 26. *Convergence of Newton's method for the penalty function where ρ is initialized to be a large number and taken to grow rapidly. The number of starting points converging to the desirable global minimizer increases.*

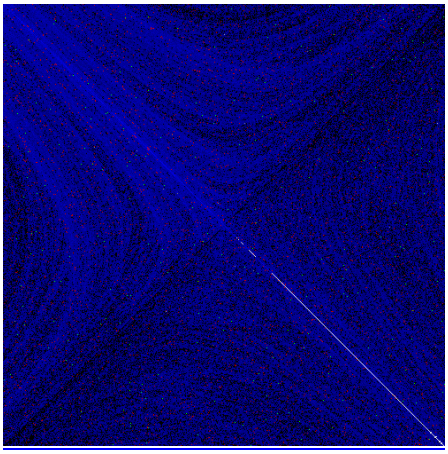

Figure 27. *Convergence of Newton's method for the penalty function where* $\boldsymbol{\rho}$ *is initialized to be a very small number and is increased slowly at every iteration.*

$$\min_{x,y} F_\rho(x,y) = f(x) + f(y) + \rho\varphi(x,y)$$

where $\rho > 0$ is a penalty parameter that tends to $+\infty$ and φ is a function that penalizes the difference between x and y. For example, φ could be the ℓ_2 or the less smooth ℓ_1 or ℓ_∞ norms. There is also a myriad of ways that ρ can be taken to grow to $+\infty$. A differential equation characterizing the trajectory of unconstrained minimizers can be derived and may provide guidance on selecting φ and constructing path following algorithms that result in convergence to a global minimizer.

Consider a simple example, $f(x) = x^6 - 3x^2 + x$ and φ is chosen to be the square of the ℓ_2 distance, $\varphi(x,y) = (x-y)^2$. In this case the original objective function has a single local (non-global) minimizer and one unique global minimizer. The result of this very simple technique can be seen in Figure 25, Figure 26, and Figure 27 where starting points, $(x_0,\ y_0)$ are taken to be in the box defined by $-1.5 \le x_0,\ y_0 \le 1.5$ and the result of using a pure Newton method, no globalization, is applied. Blue designates a starting point that resulted in convergence to the global minimizer and red to the local minimizer. The shading indicates the number iterations before convergence with the lighter shade indicating fewer iterations.

[1] W. W. Symes. A Differential Semblance Algorithm for the Inverse Problem of Reflection Seismology. *Computers and Mathematics with Applications* **22**:4-5 (1991), 147-178. DOI: 10.1016/0898-1221(91)90140-Y

[2] J. Gleick. Chaos: *Making a New Science.* Penguin, New York, 1988.

[3] M. S. Gockenbach, A. J. Kearsley, and W. W. Symes. An Infeasible Point Method for Minimizing the Lennard-Jones Potential. *Computational Optimization and Applications* **8** (1997), 273–286. DOI: 10.1023/A:1008627606581

Estimation of the Derivative and Fractional Derivative of a Function Defined by Noisy Data

Timothy Burns
Bert Rust (retired)

Abel's integral equation

$$Af = I_a^\mu f(x) \equiv \frac{1}{\Gamma(\mu)}\int_a^x (x-y)^{\mu-1} f(y)dy = g(x)$$
$$g(a) = 0$$

where $a \le x \le b$, $0 < \mu < 1$, and Γ is Euler's Gamma function, arises in a number of measurement science applications, including astronomy, spectroscopy, non-contact thermometry, scattering theory, and seismology. Here, we assume that $g = g(x)$ is a smooth function on $[a,b]$, but we are only given noisy samples of the data function, with estimated 2σ error bars at each data point,

$$\mathbf{g}^\epsilon = \mathbf{g} + \epsilon = \{g_1^\epsilon, \ldots, g_m^\epsilon\},$$
$$a < x_1 < \ldots < x_m = b$$

The problem is to determine the *source* function $f = f(x)$. In the limiting case $\mu = 1$,

$$Af = I_a^1 f(x) \equiv \frac{1}{\Gamma(\mu)}\int_a^x f(y)\,dy = g(x)$$
$$g(a) = 0$$

the problem of finding the source function f simplifies to finding the derivative of g,

$$A^{-1}g = D_a^1 g(x) \equiv \frac{dg}{dx} = f(x)$$

which is known to be a difficult ill-posed inverse problem when the data have been contaminated by noise. In the case of the Abel transform, also called the *fractional integration* operator of order μ, the inverse problem of determining the source function f is also ill-posed, and it also involves the derivative of the data function, in a formula that is called the *fractional derivative* of g of order μ,

$$A^{-1}g = D_a^\mu g(x) \equiv$$
$$\frac{1}{\Gamma(1-\mu)}\int_a^x (x-y)^{-\mu}\frac{dg}{dy}(y)\,dy = f(x)$$

It can be shown that, in the presence of noise, ordinary differentiation is the most ill-posed case.

We have revised our method [1] for estimating the fractional derivative of the function g. Our new approach to is to first smooth the data by considering the most ill-posed case, $\mu = 1$. We separate signal from noise in the data using a method that was developed by Rust [2], based on the statistical analysis of time series data. Key assumptions are that the residual corresponding to the noise is a realization of a white noise time series, and the measurements are from a process which preferentially damps high-frequency content in the data. By means of a novel singular value decomposition of the integration operator [3], we use a finite-dimensional spectral projection method, that determines a smooth, closed-form regularization of the data function g, and a corresponding closed-form estimate of the source function f, the derivative of g. Once we have regularized g, we use a little-known singular-value decomposition of the fractional integration operator [4] to find a closed-form estimate of the fractional derivative of g.

[1] T. J. Burns and B. W. Rust. Closed-Form Projection Method for Regularizing a Function Defined by a Discrete Set of Noisy Data and for Estimating its Derivative and Fractional Derivative. arXiv:1805.09849v1, 2018.

[2] B. W. Rust. Truncating the Singular Value Decomposition for Ill-Posed Problems. NIST IR 6131, National Institute of Standards and Technology, Gaithersburg, MD, July 1998.

[3] Z. Zhao, Z. Meng, and G. He. A New Approach to Numerical Differentiation. *Journal of Computational and Applied Mathematics* **232** (2009), 227-239.

[4] R. Gorenflo and K. V. Tuan. Singular Value Decomposition of Fractional Integration Operators in L_2-Spaces with Weights. *Journal of Inverse and Ill-Posed Problems* **3** (1995), 1-10.

TOMCAT: X-ray Imaging of Nanoscale Integrated Circuits for Tomographic Reconstruction

Bradley Alpert
Dan Swetz, Zachary Levine, et al. (NIST PML)
Kurt Larson, et al. (Sandia National Laboratory)
Edward Garboczi (NIST MML)

The NIST Quantum Sensors Group (PML), has been developing cryogenic microcalorimeter spectrometers as a subcontractor in a project for IARPA's RAVEN (Rapid Analysis of Various Emerging Nanoelectronics) program. Recently their participation has expanded into a full project, in collaboration with researchers at Sandia National Laboratory, to undertake the measurement of integrated circuits, with tomographic reconstruction, with the aim of achieving 10 nm spatial resolution of integrated circuits. This extremely ambitious goal is based on a scanning electron microscope (SEM) as the producer of x-rays, a custom sample positioning platform, and novel data processing, exploiting the excellent transition-edge-sensor (TES) energy resolution for the photon-starved, limited angle data.

After an initial project phase to characterize the hardware platform, the photons available for imaging, which are dramatically fewer than would be customary for computed tomography at the intended spatial scale, will not enable reconstruction without significant innovation in algorithms. In addition to established Bayesian reconstruction techniques, based on bounded variation, dictionary-based data augmentation suited to the class of samples will have to be developed. Effective use of the dictionary will also require novel recall from incomplete information. Levine, Garboczi, and Alpert are the NIST researchers participating in the tomography.

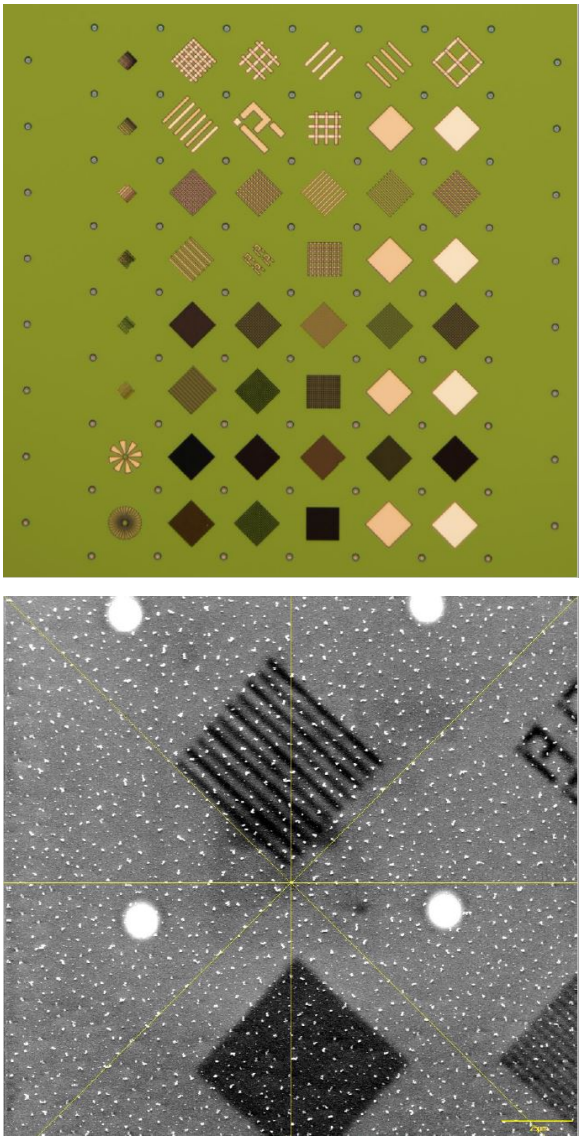

Figure 28. *(Top) Optical image of backside of chip fabricated in NIST cleanroom for initial x-ray tomographic reconstruction. Chip contains several layers, of titanium, silicon nitride, niobium, and silicon dioxide. The patterns are intended to test different reconstruction capabilities and limits. The reference grid has 100 μm spacing. (Bottom) Conventional SEM image of part of the fourth and fifth pattern rows. Image "snow" results from surface roughness. Lower-right scale shows 25 μm. The electron beam of the SEM hits the Ti, and also penetrates to other layers, producing x-rays that are energy-resolved by a TES spectrometer on the opposite side of chip. To collect x-ray data for tomographic imaging, the SEM beam can be scanned; the sample can also be scanned and rotated to collect partial angle data. Analytical challenges include effective utilization of energy-resolved, limited-angle, photon-starved data to recover much smaller-scale structures than present in this initial chip.*

A Thousand-Fold Performance Leap in Ultrasensitive Cryogenic Detectors

Bradley Alpert
Joel Ullom, et al. (NIST PML)
Lawrence Hudson et al. (NIST PML)
Terrence Jach (NIST MML)

Small arrays of cryogenic microcalorimeters developed at NIST have driven breakthroughs in x-ray materials analysis, nuclear forensics, and astrophysics. They have also played a large role in prominent international science collaborations in recent years. Despite these successes, existing cryogenic sensor technology is inadequate for new applications such as in-line industrial materials analysis, energy resolved x-ray imaging, and next-generation astrophysics experiments, which all require faster sensors, much larger arrays, or both.

This year the researchers completed a NIST Innovations in Measurement Science (IMS) project whose goal was a 1000-fold increase in sensor throughput, accomplished via a completely new sensor readout (a microwave multiplexer) enabling much larger detector arrays, and through major new, higher throughput, processing capabilities. The success of this project, especially the microwave multiplexing, has led to additional NIST funding for evaluating the feasibility of new quantum-noise-limited amplifiers and to additional interest by outside collaborations.

These collaborations include one jointly with Sandia National Laboratory, funded by IARPA, for x-ray tomographic imaging of the internal structure of microcircuits at 10 nm resolution; with the SLAC National Accelerator Laboratory, funded by DOE, for development of a spectrometer for an upgrade of the LINAC Coherent Light Source (LCLS-II), an ultra-fast, ultra-bright free electron laser; and with the HOLMES team led at the Italian National Institute for Nuclear Physics and University of Milan, funded by the European Research Council, for measurement of neutrino mass. Each of these efforts requires transition-edge-sensor (TES) microcalorimeter detector arrays operated at higher photon rates than previously achieved, with the LCLS-II collaboration also stipulating better energy resolution than ever achieved with TES detectors.

A side effect of higher photon arrival rates on an array of detectors which share multiplexed readout channels is increased crosstalk. The new microwave multiplexing technology is designed to minimize this effect, but it still poses a challenge to maintaining energy resolution. This year Bradley Alpert developed a simulation with Ben Mates, based on delay differential equations, to improve the modeling of the multiplexing technology and anticipated design changes are expected to reduce crosstalk further.

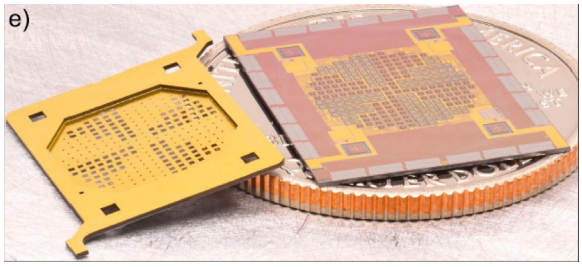

Figure 29. *Photograph of a "hybrid" TES array (right) and its micromachined array of apertures (left) with a U.S. quarter-dollar coin for scale. The pictured array contains 240 TES pixels: 120 each of the 350 μm and 124 μm types. During assembly, the aperture chip is aligned to the detector array via micromachined features such that they are separated by about 20 μm. From [1].*

A fundamental component of the IMS work has been analysis of data from characteristic L-fluorescence lines of lanthanide elements praseodymium, neodymium, terbium, and holmium, whose high-quality measurement was made feasible by the spectrometer improvements due to this project. Alpert has collaborated with Joe Fowler in developing techniques to estimate the effects of instrumental broadening on line shape and line energy uncertainty. A paper describing this work, which will extend NIST standard x-ray reference data, is in final stages of preparation.

Another challenge with large arrays of detectors, which require individual energy calibration due to a variety of energy response curves, is the automatic matching of spectral lines across the array, and their identification. This issue is especially difficult when the emitter is largely unknown, as may occur for the characterization of mixtures of radioactive materials. Alpert has been evaluating approaches for this task in the hope of producing an algorithm that is fully robust to variations in line density and overlap, and various detector response curves.

[1] W. B. Doriese, P. Abbamonte, B. K. Alpert, D. A. Bennett, E. V. Denison, Y. Fang, D. A. Fischer, C. P. Fitzgerald, J. W. Fowler, J. D. Gard, J. P. Hays-Wehle, G. C. Hilton, C. Jaye, J. L. McChesney, L. Miaja-Avila, K. M. Morgan, Y. I. Joe, G. C. O'Neil, C. D. Reintsema, F. Rodolakis, D. R. Schmidt, H. Tatsuno, J. Uhlig, L. R. Vale, J. N. Ullom, and D. S. Swetz. A Practical Superconducting-Microcalorimeter X-Ray Spectrometer for Beamline and Laboratory Science. *Review of Scientific Instruments* 88 (2017), 053108. DOI: 10.1063/1.4983316

[2] A. Nucciotti, B. Alpert, M. Balata, D. Becker, D. Bennett, A. Bevilacqua, M. Biasotti, V. Ceriale, G. Ceruti, D. Corsini, M. De Gerone, R. Dressler, M. Faverzani, E. Ferri, J. Fowler, G. Gallucci, J. Gard, F. Gatti, A. Giachero, J. Hays-Wehle, S. Heinitz, G. Hilton, U. Köster, M. Lusignoli, J. Mates, S. Nisi, A. Orlando, L. Parodi, G. Pessina, A. Puiu, S. Ragazzi, C. Reintsema, M. Ribeiro-Gomez, D. Schmidt, D. Schuman, F. Siccardi, D. Swetz, J. Ullom, and L. Vale. Status of the HOLMES Experiment to Directly Measure the Neutrino Mass. *Journal of*

Low Temperature Physics **193**:5-6 (2018), 1137-1145. DOI: 10.1007/s10909-018-2025-x

[3] D. Li, B. K. Alpert, D. T. Becker, D. A. Bennett, G. A. Carini, H.-M. Cho, W. B. Doriese, J. E. Dusatko, J. W. Fowler, J. C. Frisch, J. D. Gard, S. Guillet, G. C. Hilton, M. R. Holmes, K. D. Irwin, V. Kotsubo, S.-J. Lee, J. A. B. Mates, K. M. Morgan, K. Nakahara, C. G. Pappas, C. D. Reintsema, D. R. Schmidt, S. R. Smith, D. S. Swetz, J. B. Thayer, C. J. Titus, J. N. Ullom, L. R. Vale, D. D. Van Winkle, A. Wessels, and L. Zhang. TES X-ray Spectrometer at SLAC LCLS-II. *Journal of Low Temperature Physics* **193**:5-6 (2018), 1287-1297. DOI: 10.1007/s10909-018-2053-6

[4] J. W. Fowler, C. G. Pappas, B. K. Alpert, W. B. Doriese, G. C. O'Neil, J. N. Ullom, and D. S. Swetz. Approaches to the Optimal Nonlinear Analysis of Microcalorimeter Pulses. *Journal of Low Temperature Physics* **193**:3-4 (2018), 539-546. DOI: 10.1007/s10909-018-1892-5

[5] D. T. Becker, B. K. Alpert, D. A. Bennett, M. P. Croce, J. W. Fowler, J. D. Gard, A. S. Hoover, Y. I. Joe, K. E. Koehler, J. A. B. Mates, G. C. O'Neil, M. W. Rabin, C. D. Reintsema, D. R. Schmidt, D. S. Swetz, P. Szypryt, L. R. Vale, A. L. Wessels, and J. N. Ullom. Advances in Analysis of Microcalorimeter Gamma-Ray Spectra. *IEEE Transactions on Nuclear Science* **66**:12 (2019), 2355-2363. DOI: 10.1109/TNS.2019.2953650

[6] C. J. Titus, D. Li, B. K. Alpert, H.-M. Cho, J. W. Fowler, S.-J. Lee, K. M Morgan, D. S Swetz, J. N. Ullom, A. Wessels, and K. D. Irwin. Count Rate Optimizations for TES Detectors at a Femtosecond X-ray Laser. submitted.

[7] J. W. Fowler, B. K. Alpert, Y. I. Joe, G. C. O'Neil, D. S. Swetz, and J. N. Ullom. A Robust Principal Component Analysis for Messy Microcalorimeter Data. submitted.

Numerical Solutions of the Time Dependent Schrödinger Equation

Barry I. Schneider
Heman Gharibnejad
Luca Argenti (University of Central Florida)
Nicholas Douguet (Kennesaw State University)
Jeppe Olsen (Aarhus University)

We have been collaborating with various scientists for a number of years developing numerically robust methods for solving the time-dependent Schrödinger equation. Luca Argenti, an Assistant Professor from the University of Central Florida, and his former postdoc, Nico Douguet, now at Kennesaw State University in Atlanta, joined the effort in 2016. Heman Gharibnejad, a NIST NRC postdoctoral associate, who joined the group in January of 2017 to collaborate on our ongoing efforts, became a Research Associate at the University of Maryland this past year. He will continue working on the project part time even though he is leaving NIST at the beginning of 2020. There are three related research threads underway.

1. Developing a hybrid finite element discrete variable (FEDVR)-Gaussian approach to treat the interaction of attosecond (10^{-18} sec) radiation with molecular targets.
2. Examining the performance of various numerical time propagation techniques for the TDSE.
3. Elucidating various aspects of core-hole ionization and excitation in N_2O.

The hybrid finite element approach that has been developed is quite general, but the applications to date have concentrated on describing the single and double ionization of electrons exposed to intense, ultrafast, laser radiation in many-body atomic and molecular systems. These attosecond (10^{-18} sec) pulses provide a new window to study the electronic motion in atoms and molecules on their natural timescale. To put this in context, the motion of electrons responsible for chemical binding and electron transfer processes in nature have a characteristic timescale of about 100 attoseconds. (It takes an electron 152 attoseconds to go around the hydrogen atom.) These processes can only be described using time-dependent quantum mechanics. Where appropriate, this needs to be coupled to Maxwell's equations to describe macroscopic phenomena. Our overall goal is to image quantum phenomena with sub-femtosecond temporal and sub-Angstrom spatial resolution. Eventually, one can contemplate producing "molecular movies" of this motion in much the same way as it is done in molecular dynamics simulations of heavy particle processes.

The basic methodology as applied to atoms and simple diatomic molecules has been described in [1-3, 5-11]. Reference [4] provides a detailed review of the work. The essential aspects have been

- development of the finite element discrete variable method (FEDVR) to spatially discretize the coordinates of the electrons, and
- use of the short iterative Lanczos method to propagate the wavefunction in time.

The method has been efficiently parallelized using MPI and scales linearly with the size of the FEDVR basis. Large scale calculations have been performed on a number of atoms and molecules using resources provided by the NSF Extreme Science and Engineering Discovery Environment (XSEDE). The group has received a competitively awarded allocation of more than 3.0 million service units for the current fiscal year.

We have begun a study to employ a mixed basis of Gaussian functions at short range and FEDVR functions at long range to extend our methods to complex polyatomic molecules. This approach has several important advantages over using a single basis over all of

space. First, the use of nuclear-centered Gaussians preserves the local atomic symmetry around each nucleus and avoids the poor convergence of using a single-center FEDVR basis at all distances. Second, once the electron is far enough away from the nuclear cusps, a single center expansion converges quickly and, importantly, can represent the electrons out to very large distances using an approach that is very amenable to domain decomposition. The major issue is to compute the one and two electron integrals between the two types of basis functions. Since 2017, we have been developing a new and efficient formalism, using transition density matrices extracted from a high-level quantum chemistry code, to compute the additional integrals. Jeppe Olsen from Aarhus University, an extremely talented quantum chemist, has been collaborating with us on the project. The NIST-UCF-KSU-Aarhus group has met a number of times at NIST and Orlando and has made substantial progress. It should be noted, that this is a very complex many-body problem and even with the most talented of researchers, it is a long-term effort. We are in the process of implementing our approach and interfacing with the quantum chemistry code of Olsen.

Two NIST SURF students, Mark Leadingham and Henry Schmale, helped to develop a simple one-dimensional model of the hydrogen atom in an intense electric field to test some of the numerical methods used for time propagation. The model serves well to illustrate the problems that would be faced in higher spatial dimensions while being simple enough for talented undergraduates to tackle in a summer research program. A paper [14] has appeared in *Computer Physics Communications* on this research. The model uses a soft core to treat the interactions of the electron with the nucleus and a three-point finite difference approach to the second derivative operator. While this problem has been studied before, and the model is a reasonable representation of the three-dimensional hydrogen atom, our objective was to determine how various time propagation schemes performed as well as to suggest a new approach that might be more robust than those currently being used.

The study found that while very simple propagation schemes such as the Crank-Nicholson (CN), variants of the split-operator (SO) method and real-space propagation (RSP) methods are very efficient per time step, the size of the time steps must be quite small to obtain accurate results. In contrast, more elaborate schemes, such as the short-iterative-Lanczos (SIL) method, are more expensive per time step but allow time steps two orders of magnitude larger than CN, SO or RSP for the same accuracy. While we suspected that might be the case, only a careful study confirmed the results. The conclusion was that the SIL performed much more efficiently in practice than the other methods. The basic reason is that the SIL only depends on the natural time scale of the laser field and not on issues of the spectrum of the operator being discretized. The SIL does not rely on a second order expansion to be accurate. We have also examined higher order spatial discretization schemes and also have found them to be even more efficient and accurate than the three-point approach. We are now looking into an integral equation technique that would combine the best of the SIL with perhaps even larger time steps for high accuracy.

This past year we initiated a shorter-term project to examine core ionization in N_2O using an older code, MESA. This project will allow us to test parts of our new approach and in addition, contributes understanding to an ongoing research by some experimental colleagues in Japan who solicited our assistance in understanding their experiments. Finally, another invited paper [15] reviewing computational methods in atomic and molecular physics has been published in the new on-line journal *Nature Reviews Physics*.

[1] J. Feist, S. Nagele, R. Pazourek, E. Persson, B. I. Schneider, L. A. Collins, and J. Burgdörfer. Nonsequential Two-Photon Double Ionization of Helium. *Physical Review A* **77** (2008), 043420.

[2] X. Guan, K. Bartschat, and B. I. Schneider. Dynamics of Two-photon Ionization of Helium in Short Intense XUV Laser Pulses. *Physical Review A* **77** (2008), 043421.

[3] X. Guan, K. Bartschat, and B. I. Schneider. Two-photon Double Ionization of H_2 in Intense Femtosecond Laser Pulses. *Physical Review A* **82** (2010), 041407.

[4] B. I. Schneider, J. Feist, S. Nagele, R. Pazourek, S. Hu, L. Collins, and J. Burgdörfer. Recent Advances in Computational Methods for the Solution of the Time-Dependent Schrödinger Equation for the Interaction of Short, Intense Radiation with One and Two Electron Systems, in Dynamic Imaging. In Quantum Dynamic Imaging, (A. Bandrauk and M. Ivanov eds.), CRM Series in Mathematical Physics, Springer, New York, 2011.

[5] X. Guan, E. Secor, K. Bartschat, and B. I. Schneider. Double-slit Interference Effect in Electron Emission from H_2^+ Exposed to X-Ray Radiation. *Physical Review A* **85** (2012), 043419.

[6] X. Guan, K. Bartschat, B. I. Schneider, L. Koesterke, Resonance Effects in Two-Photon Double Ionization of H_2 by Femtosecond XUV Laser Pulses. *Physical Review A* **88** (2013), 043402.

[7] J. Feist, O. Zatsarinny, S. Nagele, R. Pazourek, J. Burgdörfer, X. Guan, K. Bartschat, and B. I. Schneider. Time Delays for Attosecond Streaking in Photoionization of Neon. *Physical Review A* **89** (2014), 033417.

[8] X. Guan, K. Bartschat, B. I. Schneider, and L. Koesterke. Alignment and Pulse-duration Effects in Two-photon Double Ionization of H_2 by Femtosecond XUV Laser Pulses. *Physical Review A* **90** (2014), 043416.

[9] B. I. Schneider, L. A. Collins, X. Guan, K. Bartschat, and D. Feder. Time-Dependent Computational Methods for Matter Under Extreme Conditions. *Advances in Chemical Physics* **157** (2015), Proceedings of the 240 Conference: Science's Great Challenges, (A. Dinner, ed.), John Wiley.

[10] B. I. Schneider, X. Guan, and K. Bartschat. Time Propagation of Partial Differential Equations Using the Short Iterative Lanczos Method and Finite-Element Discrete Variable Representation. *Advances in Quantum Chemistry* **72** (2016), 95-127.

[11] B. I. Schneider. How Novel Algorithms and Access to High Performance Computing Platforms are Enabling Scientific Progress in Atomic and Molecular Physics. *Journal of Physics: Conference Series* **759** (2016), 012002.

[12] B. I. Schneider. 45 Years of Computational Atomic and Molecular Physics: What Have We (I) Learned. *Journal of Physics: Conference Series* **875** (2017).

[13] B. I. Schneider, L. A. Collins, K. Bartschat, X. Guan, and S. X. Hu. A Few Selected Contributions to Electron and Photon Collisions with H_2 and H_2^+. *Journal of Physics* **50** (2017), 214004.

[14] H. Gharibnejad, B. I. Schneider, M. Leadingham, and H. J. Schmale. A Comparison of Numerical Approaches to the Solution of the Time-Dependent Schrödinger Equation in One Dimension. *Computer Physics Communications* (2019), 106808, to appear.

[15] B. I. Schneider and H. Gharibnejad. Numerical Methods Every Atomic and Molecular Theorist Should Know. *Nature Reviews Physics*, December 2019.

A Science Gateway for Atomic and Molecular Physics

Barry I. Schneider
Klaus Bartschat (Drake University)
Kathryn Hamilton (Drake University)
Oleg Zatsarinny (Drake University)
Igor Bray (Curtin University, Australia)
Armin Scrinzi (Ludwig-Maximilians U., Germany)
Fernando Martiın (U. Autonoma de Madrid, Spain)
Jesus Gonzalez Vasquez (U. Autonoma de Madrid)
Jimena Gorfinkiel (Open University, UK)
Jonathan Tennyson (University College London,UK)
Sudhakar Pamidighantam (Indiana University)

https://ampgateway.org/

An international effort is now underway to develop and maintain a Science Gateway for Atomic and Molecular Physics [1]. The purpose of the gateway is to collect and make available to the community a set of advanced computational tools that are actively being used to study atomic and molecular collisions and the interaction of radiation with atoms and molecules. The availability of collision data is critical to many areas of physics including astrophysics, fusion energy, the study of lighting and microelectronics.

Codes for modeling and simulation of such phenomena have been developed in specific groups by graduate students and postdocs but are often poorly documented, and unavailable outside the group developing the software. This leads to "reinventing the wheel" in too many instances. Maintaining these computational tools, as well as enhancing their capabilities, is one of the major goals of the project and is critical to ensure continued scientific progress in atomic and molecular physics (AMP).

Another important goal is to enable the code developers themselves to compare the calculations of specific well-defined problems using different methodologies. This enables the verification of results of different codes and encourages comparison with experiment, when available. It has already been demonstrated that a few of these codes are often more accurate than experiment and thus provide a predictive capability when experimental results are unavailable.

At the outset, the group acknowledged that, in contrast to some other communities, the AMP community has lagged behind in developing community supported software packages that are robust and used by others. The group was convinced the time had arrived to change existing practices and make these tools available and easily used by future generations of AMP scientists as well as the developers themselves.

The group wrote a proposal to the NSF XSEDE program to fund some initial development of the gateway. The proposal was successful and, importantly, provided the developers with some hands-on assistance from the Extended Collaborative Support Services arm of XSEDE. This was vital to the success of the effort. In particular, we acknowledge the important contribution of Sudhakar Pamidighantam of IU in making our efforts a success.

There have already been some important advances. All of the six major codes chosen for initial deployment have been ported to at least three XSEDE supercomputers. There is a web interface to the gateway to perform calculations with these codes. While the current interface is still in its infancy, we are aware of what needs to be done and progress is ongoing.

A very important recent development was the AMP Gateway workshop held at NIST on December 11-13, 2019. The workshop was jointly supported by the Molecular Software Science Institute (MOLSSI) at Virginia Tech, the NSF, and NIST. Some thirty participants came together to discuss what has been accomplished and to present ideas for the future. The developers gave presentations on the science behind the codes and how to use the codes via the gateway. Pamidighantam spoke on the details of gateway and how it can be used effectively, even for individuals desiring

specific results but uninterested in the specifics of a given code. Other participants presented details of codes that have not yet been implemented on the gateway, and several have now expressed strong interest in joining the project. The workshop concluded with a discussion of what was needed for the future. This included the need for longer term support from XSEDE for computer and human resources as well as a possible proposal to the NSF cyberinfrastructure program.

[1] B. I. Schneider, K. Bartschat, O. Zatarinny I. Bray, A. Scrinzi, F. Martin, M. Klinker, J. Tennyson, J. Gorfinkiel, and S. Pamidighanta., A Science Gateway for Atomic and Molecular Physics. arXiv:2001.02286

Predicting Molecular Weight from Mass Spectra

Anthony J. Kearsley
Arun S. Moorthy (NIST MML)
Gary Mallard (NIST MML)
William E. Wallace (NIST MML)
Stephen E. Stein (NIST MML)

Measuring the characteristics of individual molecules or compounds is fundamental to modern chemistry. The most commonly employed measurement instrument employed to accomplish this task is a mass spectrometer which decomposes molecules or compounds into ions and manages them with controlled external electric and magnetic fields [1]. Typically, ions are then detected electronically, resulting in the output of a mass spectrum, usually a bar graph, in which each bar represents an ion having a specific mass-to-charge ratio (m/z) and the height of the bar or peak indicating relative ion abundance. One piece of information often sought from mass spectra is an estimate of molecular mass.

Recently we conducted a comparison of three different computational methods for predicting the nominal molecular weight of a compound from a mass spectrum. The three methods compared were the so called "Simple Method" which follows a set of rules to interpret spectral peaks. It requires only a spectrum in order to produce an approximate nominal molecular weight. The second method referred to as the "Hitlist Method" uses the results of a mass spectral library search [2] to generate a molecular weight prediction with an assigned probability. This method requires a spectrum and a reference spectral library to estimate a nominal molecular weight. A final method, known as the "Iterative Hybrid Search Method," executes several hybrid library searches [3, 4] of a given mass spectrum, before it generates a molecular weight prediction and an assigned probability.

In our study we observed that the hitlist method (86 %) outperformed the simple (67 %) and iterative hybrid (68 %) for correct identifications in a global

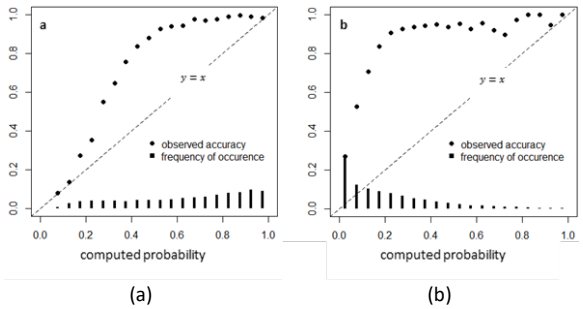

Figure 30. *Summary of performance results for molecular weight prediction algorithms (a) Hitlist Method, and (b) Iterative Hybrid Search Method. The Hitlist Method predicted molecular weights with computed probability greater than 0.8 (3628 examples) were correct more than 99% of the time. The Iterative Hybrid Search predicted molecular weight with computed probability greater than 0.8 (113 examples) were accurate ~99 %.*

assessment. Of course, each method requires different amounts of information to be employed and there are important applications, like forensic chemistry, where one method may be more appropriate than another. Some results are summarized in Figure 30 where the (a) portion reports results from the hitlist method and the (b) portion on the iterative hybrid search method for a collection of 10410 test spectra taken from [5].

[1] J. T. Watson and O. D. Sparkman. *Introduction to Mass Spectrometry: Instrumentation, Applications and Strategies for Data Interpretation.* John Wiley & Sons, 2007.

[2] S. E. Stein and D. R. Scott. Optimization and Testing of Mass Spectral Library Search Algorithms for Compound Identification. *Journal of the American Society for Mass Spectrometry* **5**:9 (1994), 859-866. DOI: 10.1016/1044-0305(94)87009-8

[3] A. S. Moorthy, W. E. Wallace, A. J. Kearsley, D. V. Tchekhovskoi, and S. E. Stein. Combining Fragment-Ion and Neutral-Loss Matching during Mass Spectral Library Searching: A New General-Purpose Algorithm Applicable to Illicit Drug Identification. *Analytical Chemistry* **89**:4 (2017), 13261-13268. DOI: 10.1021/acs.analchem.7b03320

[4] M. C. Burke, Y. A. Mirokhin, D. V. Tchekhovskoi, S. P. Markey, J. L. Heidbrink Thompson, C. Larkin, and S. E. Stein. The Hybrid Search: A Mass Spectral Library Search Method for Discovery of Modifications in Proteomics. *Journal of Proteome Research* **16**:5 (2017), 1924-1935. DOI: 10.1021/acs.jproteome.6b00988

[5] S. E. Stein. *NIST/EPA/NIH Mass Spectral Library (NIST 17) and NIST Mass Spectral Search Program (Version 2.3) User Manual*. 2017.

Prediction of Retention Times in Gas Chromatography Using Machine Learning

Barry I. Schneider
Chen Qu (University of Maryland)
Thomas Allison (NIST MML)
Walid Keyrouz (NIST ITL)
Anthony Kearsley

We have been working on machine learning techniques to better predict the Kovats retention indices of molecules used in gas chromatography.

Gas chromatograph (GC) is widely used to separate molecules in a mixture. It utilizes a capillary column which has a stationary phase (e. g., 5 % phenyl polysiloxane). Due to the different affinity of the molecules to the stationary phase of the column, the molecules can be separated as the sample travels the length of the column. The molecules are retained by the column and then are discharged from the column at different times (called the retention time). The Kovats retention index (RI) [1] can be viewed as a "normalized" retention time, which is almost independent of the conditions of the experiment (e. g., length and diameter of the columns and the temperature). It is basically a unique property of a molecule, though RI alone is not sufficient to identify a compound. When combined with mass spectrometry (MS), GC-MS is a powerful approach to identify substances. The theoretical prediction of the retention indices of molecules in the GC is a critical first step in this two-step process.

NIST has maintained a database of RI of different molecules and has developed an approach based on group-additivity to predict RI. [2] While this approach has had reasonable success, we are seeking a more general and accurate model by utilizing techniques from machine learning and artificial intelligence.

To begin, we preprocess the NIST RI database to create a data set that is used in the subsequent research. We focused on one particular type of column in GC (semi-standard non-polar), because the majority of the data uses this type of column and other species of columns are underrepresented in the NIST database. We further removed molecules with too large or small RI: the distribution of RI is basically a Gaussian and both "tails" are under-represented. In addition, we only considered molecules containing H, C, N, O, F, Si, S, Cl, Br, as there is insufficient data for other elements. The Python package RDKit[8] was used to process the data. The final data set contains about 66 000 molecules.

Different neural network (NN) models were trained on the data set we obtained. Most NNs require an input of a fixed length, but since the data set contains molecules of different sizes, we need to consider models that have non-fixed input size. The following approaches have been considered:

- *Multi-layer perceptron.* The input feature vector for this NN was generated following the proposal of Collins et al. [3], which combines the connectivity count and histograms of bond lengths and angles. By using histograms, the length of the feature vector is independent of the size of the molecule.
- *SchNet.* [4] This model assumes that the RI can be approximated as the sum of atomic contributions.
- *Graph NN.* Specifically, MEGNet [5] was used. A graph is a natural representation of a molecule: the atoms are regarded as vertices and the atom pairs are regarded as edges. Graph NNs achieve good results in predicting many properties of molecules.

We randomly split the data set into training, validation, and test subsets (with ratio 8:1:1 or 7:2:1) to avoid overfit. Training was carried out on Enki, NIST's IBM Power 9 supercomputer, using the Tensorflow package[9]. Among the three approaches considered, the graph NN achieved the smallest validation and test error (root-mean-square (RMS) of around 95) so it was selected for further improvement. Importantly, this is already a significant improvement compared to the older group-additivity model, which has an RMS of ≈125.

The graph NN model still has several drawbacks. The test error is still large, and the training requires a large amount of computation resources. It requires more than 100 GB memory and it takes roughly 2 days for the training. Further improvement of the model was achieved by the following means:

- Removing data that are potentially erroneous. Almost all data sets have such data points, and the accuracy can be greatly enhanced if they are removed. Here we remove a molecule when its experimental RI is significantly different from the prediction of the group-additivity model. Only 1 000 out of 66 000 molecules were removed, but the validation and test RMS errors are reduced to around 80, and the mean unsigned error is about 48.
- Using only the 2D structure of the molecule instead of the 3D coordinates and applying a cut-off for pairs of atoms leads to the following significant improvements:
    - It is not necessary to perform electronic structure calculations to find the optimized 3D structure of a molecule, making the model much more friendly for users.
    - The cut-off greatly reduces the memory usage as only atom pairs within the cut-off need

[8] http://www.rdkit.org

[9] http://tensorflow.org/

to be considered. The training can now be performed within 10 hours, far more rapidly than before.

- The reduction in memory usage allows us to add more layers to the NN model, reducing the training, validation, and test errors.
- The root-mean-square and mean unsigned errors were further reduced to around 72 and 42, respectively.

The cutoff is applied so that we only consider pairs of atoms that are within a certain spatial distance (for example, only consider pairs whose inter-atomic distance is less than 6 Angstrom), or within a certain graph distance (for example, only consider two atoms that are separated by no more than 4 bonds). When we have the 3D coordinates of the molecule, we can apply either the spatial distance cutoff or the graph distance cutoff, and if we only have a 2D graph of the molecule, we apply the graph distance cutoff. Using the cutoff substantially reduces the number of vectors used to describe each pair of atoms, RAM, and training time with essentially no effect on the results.

Finally, we believe that the lack of stereochemical information largely contributes to the error of the current model. Stereoisomers are not properly labelled in the NIST RI database, so they cannot be distinguished in the graph model. However, they can have different RIs, and this can cause very large error. The ultimate solution is a better database with all stereochemistry properly accounted for. However, this is practically impossible and so we are currently focused on finding other approaches to reduce the error caused by stereochemistry.

[1] E. Kovats. Gas-chromatographische Charakterisierung organischer Verbindungen. Teil 1: Retentionsindices aliphatischer Halogenide, Alkohole, Aldehyde und Ketone. *Helvetica Chimica Acta* **41** (1958), 1915-1932.

[2] S. E. Stein, V. I. Babushok, R. L. Brown, and P. J. Linstrom. Estimation of Kováts Retention Indices Using Group Contributions. *Journal Chemical Information and Modeling* **47** (2007), 975-980.

[3] C. R. Collins, G. J. Gordon, O. A. von Lilienfeld, and D. J. Yaron. Constant Size Descriptors for Accurate Machine Learning Models of Molecular Properties. *Journal of Chemical Physics* **148** (2018), 241718.

[4] K. T. Schütt, H. E. Sauceda, P.-J. Kindermans, A. Tkatchenko, and K.-R. Müller. SchNet – A Deep Learning Architecture for Molecules and Materials. *Journal of Chemical Physics* **148** (2018), 241722.

[5] C. Chen, W. Ye, Y. Zuo, C. Zheng, and S. P. Ong. Graph Networks as a Universal Machine Learning Framework for Molecules and Crystals. *Chemistry of Materials* **31**, 3564-3572.

Large Scale Dynamic Building System Simulation

Aaron Chen (Drexel University)
Anthony Kearsley
Amanda Pertzborn (NIST MML)
Jin Wen (Drexel University)

The building sector represents the largest primary energy-consuming sector in the United States, responsible for 41 % of the country's primary energy, in comparison to 28 % for the transportation sector and 32 % for industry. Moreover, buildings consume 74 % of the electricity in the United States, which makes the building sector significant to the overall smart grid infrastructure. Given the rapid development of the smart grid and the potential of buildings to store and generate

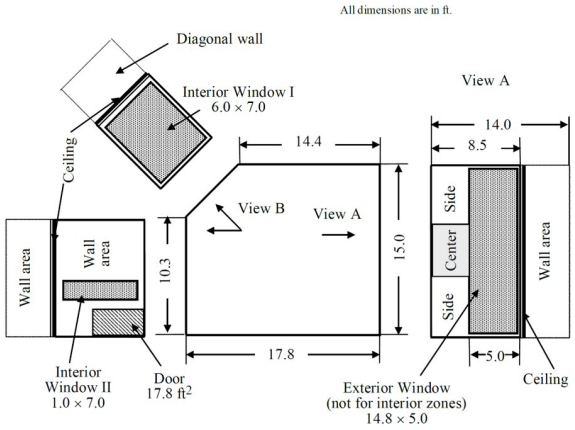

Figure 31. *A floor and window view of a typical zone.*

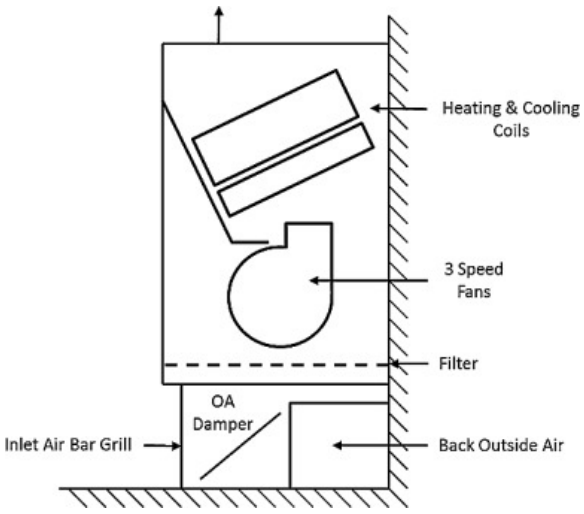

Figure 32. *Schematic of a simple fan/coil unit.*

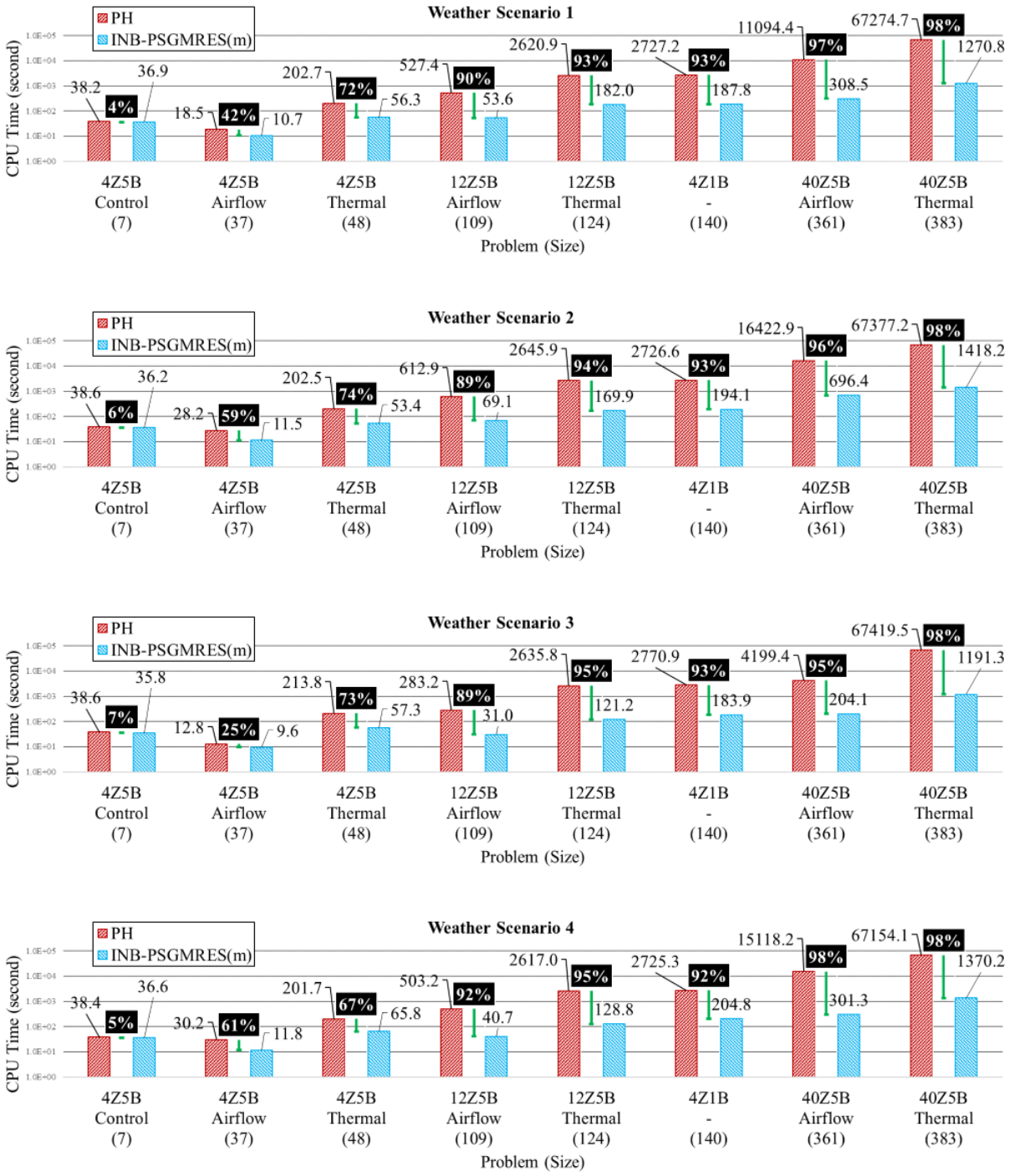

Figure 33. *A comparison of required CPU-time for both Powell's Hybrid Method (PH) and the more complicated technique proposed in [1].*

electricity through demand shifting and transactive control, there is an urgent need to improve the dynamic interactions between buildings and the smart grid, which further calls for robust and accurate dynamic building energy system modeling and simulation.

Traditional dynamic building simulations typically focus on a single building. However, dynamic building simulations used for smart grid applications simulate large and complex building energy systems and their interactions among building clusters that are composed of multiple buildings. These result in large systems of coupled, potentially ill-conditioned nonlinear systems (easily including thousands of equations), that will need

to be solved rapidly. Efficient, robust and accurate solution of large sparse nonlinear algebraic and differential equation systems is becoming more and more essential to meet the demands to simulate large scale multiple-building heating ventilation and air conditioning (HVAC) scenarios that are coupled to various complex energy sources either through the smart grid or other means, such as district heating/cooling.

In practice, these simulations are decomposed into geometric zones (see Figure 31) where one expects air flow and thermal conductivity to be similar. Typically, these zones are comprised of rooms or collections of closely connected rooms. HVAC systems control temperature and air flow in these zones through coupled boundary conditions that are matched in what is called a "super-block." It is interesting that something as simple as a fan/coil unit (see Figure 32) can result in an approximation whose discretized system is quite hard to solve. More detailed mathematical models which would more accurately predict the physics of a simple fan coil unit would result in simulations that would be prohibitively expensive. Less detailed mathematical models yield more well-conditioned systems that can be solved quickly but do not provide the flexibility of, for example, more complicated scenarios through various degrees of occupancy, seasons or other factors that must be considered.

In [1], Chen develops a class of large-scale Krylov methods for solving these nonlinear systems using automatically built preconditioners. Comprised of smaller models, like the one used to predict fan/coil dynamics, the resulting large-scale systems are assembled at the same time as a preconditioner, both of which would be made available to a building engineer seeking to simulate and evaluate a building HVAC system. Not surprisingly, poor variable scaling [2] can also lead to a deterioration in numerical performance but results presented in [1] suggest that pre-conditioning of inexact Krylov methods can outperform more traditional dense solution techniques [3] as problem sizes grow. Figure 33 demonstrates that the numerical method proposed in [1], here called INB-PSGMRES(m), outperforms Powell's hybrid method (PH) [4] irrespective of seasonal changes. Here m denotes the dimension of the Krylov subspace, traditionally a parameter that is tuned. Of course, the comparison of CPU time is not exactly a straightforward one. The PH method was not designed for problems of this size. However, it provides strong evidence that methods like those proposed in [1] are very much appropriate for these simulations.

[1] Z. Chen. *Advanced Solver Development for Large-Scale Dynamic Building System Simulation*. Ph.D. Thesis, Drexel University, Philadelphia PA, 2019.

[2] Z. Chen, J. Wen, A. J. Kearsley, and A. J. Pertzborn. Scaling Methods for Dynamic Building System Simulation in an HVACSIM+ Environment. In *Proceedings of the 15th International Building Performance Simulation Association (IBPSA) Conference*, San Francisco, CA, 2017, 2059-2065.

[3] S. Pourarian, A. Kearsley, J. Wen, and A. Pertzborn. Efficient and Robust Optimization for Building Energy Simulation. *Energy and Buildings* **122** (2016), 53-62.

[4] M. J. Powell. A Hybrid Method for Nonlinear Equations. *Numerical Methods for Nonlinear Algebraic Equations* **7** (1970), 87-114.

Tall Building Database-Assisted Design

Dong Hun Yeo (NIST EL)
Florian A. Potra
Emil Simiu (NIST EL)

Large discrepancies between independent wind engineering laboratories' estimates of wind effects on tall structures and the failure of efforts to trace unambiguously the sources of those discrepancies have prompted NIST to develop a research program on the design of tall structures for wind loads. The research program aims to (a) improve the accuracy of estimates of wind effects with specified mean recurrence intervals (MRIs) by solving in a physically and probabilistically rigorous manner outstanding problems associated with the effects of wind directionality and the stochastic nature of the aerodynamic loading; (b) achieve a more effective integration of wind and structural engineers' contributions to the design process; (c) enable the structural engineer to be fully in charge of the structural design process, including the dynamic analyses, heretofore split between wind and structural engineers; and (d) ensure that each phase of the wind and structural engineers' contributions to the structural design is compatible with Building Information Modeling (BIM) requirements and can be effectively scrutinized by structural engineers and project stakeholders.

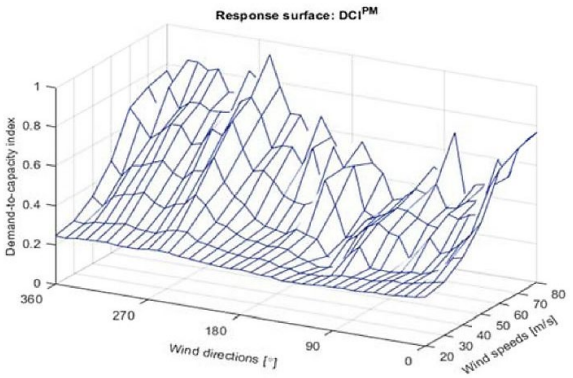

Figure 34. *Example of a peak DCI response surface.*

NIST research has resulted in the development of the procedure called Database-assisted Design (DAD) and of a variant of the DAD procedure called Equivalent Static Wind Loads (ESWL) [1]. In the ESWL approach, which is only applicable to buildings with simple shapes (e.g., prismatic buildings), static wind loads are calculated that induce in the structural members demand-to-capacity indexes (DCIs) approximately equal to the more accurately estimated peak DCIs induced by the fluctuating loads [2].The clarity of both procedures enables their effective scrutiny by structural engineers and project stakeholders and assures their compatibility with the BIM environment for automated structural design.

The DCI is defined as the left-hand side of the design interaction equations used for the sizing of members subjected to more than one type of internal force (e.g., to a bending moment and an axial force). For a well-designed member the DCI is close to unity, subject to serviceability constraints. Consider, for example, a given member cross section for which it is required to determine the peak DCI with a specified design MRI *N*. To do so it is necessary, as a first step, to develop that cross section's peak DCI *response surface*, that is, the surface representing the peak DCI corresponding to any wind speed and direction. An example of a peak DCI response surface is shown in Figure 34. The objective of optimal structural design is to determine the sizes of all members so that the DCI is sufficiently close to one for all members, the serviceability constraints are satisfied, and the weight of the whole structure is minimized. This complicated optimization problem can be solved by carefully adapting a variant of an interior point method.

[1] D. Yeo, F. A. Potra, and E. Simiu. Tall Building Database-assisted Design: A Review of NIST Research. *International Journal of High-Rise Buildings* **8**:4 (2019), 1-9. DOI: 10.21022/IJHRB.2019.8.4.265

[2] S. Park, E. Simiu, and D. Yeo. Equivalent Static Wind Loads vs. Database-Assisted Design of Tall Buildings: An Assessment. *Engineering Structures* **186** (2019), 553-563.

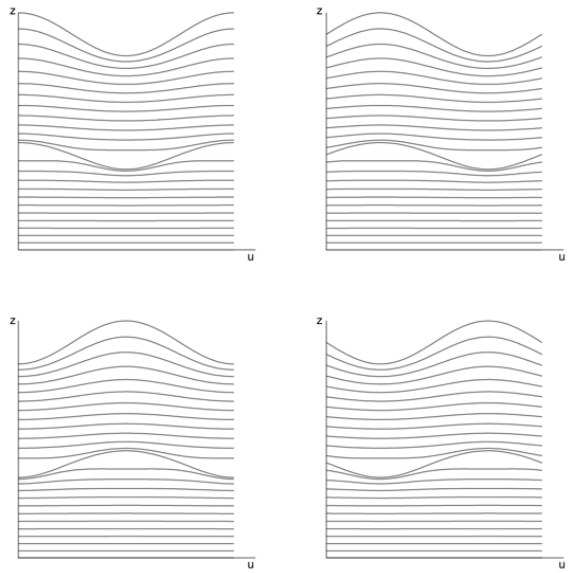

Figure 35. *Computation of a plasma equilibrium in a "slab" geometry. The plots show various flux surfaces at four toroidal angles v = 0, v = 1/4, v = 1/2, and v = 3/4 (from left to right and from top to bottom). The magnetic field lines lie in the flux surface, and the charged ions tightly orbit the field lines, providing magnetic confinement. The gap in the spacing of the flux surfaces in the center of each plot indicates the presence of a singular current sheet at a rational flux surface. The goal is to design the shape of the boundaries to avoid the generation of such current sheets, which are detrimental to the plasma confinement.*

Modeling Magnetic Fusion

Geoffrey McFadden
Eugenia Kim (New York University)
Antoine Cerfon (New York University)

The controlled nuclear fusion of a hot plasma of hydrogen isotopes that is confined by a strong magnetic field is currently an area of intense experimental and theoretical research. Provided that many technological challenges can be overcome, this approach may someday provide a source of commercial energy that avoids many of the drawbacks of conventional nuclear reactors.

Quite often a toroidal geometry for the plasma is envisioned in which the ions fuse to form helium and release energetic neutrons that act as a source of energy. A number of computational methods to model such magnetic fusion devices have been developed by researchers at NYU and elsewhere to allow effective numerical simulations of the most essential features of modern tokomak and stellarator experiments.

We are currently participating in the continuing development of a code, NSTAB, that computes three dimensional equilibria of toroidal plasmas, and determines their nonlinear stability [1, 2]. A crucial assumption is that of "nested" flux surfaces, which describe the geometry of the magnetic field lines that permeate the plasma. This assumption precludes the possibility of magnetic "islands" that would result in undesirably rapid particle transport across magnetic surfaces. However, the assumption of nested flux surfaces can lead to the formation of singular current sheets at magnetic surfaces where the field lines are closed with a rational winding number. So-called *quasi-symmetric configurations* [2] are designed to avoid these undesirable singularities at rational surfaces by carefully choosing the shape of the plasma boundary in such a way as to avoid resonances at these surfaces.

To better study this procedure, we have developed a simplified version of NSTAB that applies in a rectangular geometry and avoids the complication of the magnetic axis that occurs in toroidal geometries [3, 4]. A variation principle based on energy minimization is used to derive governing equations, which are nonlinear partial differential equations of a non-standard type. In Figure 35 we show a sample calculation in which a singularity at a rational flux surface with a winding number of unity is generated by a wall perturbation with wavenumber $(k_x, k_y) = (1,1)$. These studies are intended to provide design principles that can be used to generate quasi-symmetric stellarators with improved performance in future fusion power plants.

[1] M. Taylor. A High Performance Spectral Code for Nonlinear MHD Stability. *Journal of Computational Physics* **110** (1994), 407-418.

[2] P. R. Garabedian and G. B. McFadden. Design of the DEMO Fusion Reactor Following ITER. *Journal of Research of the National Institute of Standards and Technology* **114** (2009), 229-236.

[3] E. Kim, G. McFadden, and H. Weitzner. "Computational Study of Magnetohydrodynamic Equilibria with Emphasis on Fragility of Flux Surfaces." 60th Annual Meeting of the APS Division of Plasma Physics, Portland, OR, November 7, 2018.

[4] E. Kim, G. McFadden, and A. Cerfon. Elimination of MHD current sheets by modifications to the plasma wall in a fixed boundary model. *In review.*

Electronic Energy Loss Cross Sections and the Stopping Power of High-energy Heavy Ion Projectiles in Diatomic Molecular Mediums

Heman Gharibnejad
David R. Schultz (University of Northern Arizona)
Thomas E. Cravens (Kansas University)
Stephen J. Houston (Kansas University)

The motivation for this research goes back to efforts to model large gaseous planetary atmospheres in our solar system. During the flybys of Jupiter in 1979, NASA's Voyager spacecraft detected a significant ion population within Jupiter's atmosphere. These observations are consistent with physical chemistry models inferring the presence of O^+, S_2^+, O_2^+, S_3^+, and S^+ [1]. The observations of such ions were later supported by data from the subsequent probes, such as Ulysses (1992), Galileo (1995-2003), Cassini (2000), and the Juno spacecraft (2016-2021). The source of energetic ions is Jupiter's Galilean satellites, principally its volcanic moon Io. Another channel for energetic ions is the interaction of solar wind, consisting of hydrogen, alpha particles, electrons, and protons, with Jupiter's magnetic field.

The heavy ions, present in the magnetosphere, also precipitate into the Jovian atmosphere as evidenced by the existence of both north and south polar x-ray auroras identified [1] as originating from de-excitation emission following charge transfer between the precipitating ions and molecules of the upper atmosphere, principally molecular hydrogen. In this process low-charge-state, heavy ions are accelerated by Jupiter's prodigious magnetic field to just below 1 MeV/u energies (where u is the atomic mass of the species). The ions then strip to high-charge states in collisions with H_2, slow down in their passage through the atmosphere, and produce secondary electrons, cause dissociation and photon emission of H_2, and from the precipitating ions. These atomic processes heat the atmospheric molecules and contribute to the atmospheric ion and electron currents.

The main objective of our research is to obtain comprehensive cross sections and energy losses of high energy hydrogen and heavy ionic plasma colliding with diatomic hydrogen molecules. Such cross sections give astronomers better models to understand atmospheric processes and X-ray production in gaseous planets. Unfortunately, a comprehensive data set of such cross sections is either not available or there only exists disparate experimental and theoretical results in the literature for a few processes. Moreover, distinguishing between different processes is extremely difficult in experiments and is a task more suited to theoretical studies.

Calculation of the full range of these processes, projectile charge states, and impact energies is presently only achievable using the classical trajectory Monte Carlo (CTMC) method, as described in the previous work for oxygen [2, 3]. The scarcity or the non-existence of measurements to test the very wide range of data for inelastic processes required for ion-electron-transport simulations precludes a direct test of the present comprehensive set of inelastic cross sections and energy losses. However, as part of verification, use of an ion-transport simulation with the present integral cross sections and average energy losses allows the calculation of the stopping power [5] representing the energy loss and charge evolution as sulfur ions pass through molecular hydrogen gas. The stopping-power is a measure that can be compared with available measurements and accepted values as a function of impact energy.

In a recent work [3] we investigated the possibility of having mixtures of reaction channels happening simultaneously as opposed to separately. As an example of simultaneous processes, probability of single ionization vs. single ionization combined with excitation or stripping was explored. Last year we also completed our study of hydrogen channels [4]. The sulfur data is also compiled, making extensive use of the ACMD's KNL

compute nodes (dirac). Our astronomer colleagues, T. Cravens and S. J. Houston, simulated [6] oxygen and sulfur precipitation by taking into account the new cross sections and predicted X-ray fluxes, efficiencies and spectra for various initial ion energies. Their results showed good agreement between in situ observations of X-ray spectrum for oxygen, but not sulfur. We therefore need to carefully review the sulfur data and make comparisons with existing experimental results before the data publication.

Another avenue of computational research is exploring the possibility of producing cross sections through machine learning and Gaussian procedures instead of computationally lengthy and expensive Monte Carlo dynamic simulations.

[1] L. P. Dougherty, K. M. Bodisch, and F. Bagenal. Survey of Voyager Plasma Science Ions at Jupiter: Heavy Ions. *Journal of Geophysical Research: Space Physics* **122**:8(2017), 8257–8276.

[2] D .R. Schultz, N. Ozak, T. E. Cravens, and H. Gharibnejad. Ionization of Molecular Hydrogen and Stripping of Oxygen Atoms and Ions in Collisions of $O^{q+}+H_2$ (q=0-8): Data for Secondary Electron Production from Ion Precipitation at Jupiter. *Atomic Data and Nuclear Data Tables* **113** (2017), 1 – 116.

[3] D. R. Schultz, H. Gharibnejad, T. E. Cravens, and S. J. Houston. Data for Secondary-Electron Production from Ion Precipitation at Jupiter II: Simultaneous and Non-Simultaneous Target and Projectile Processes in Collisions of $O^{q+}+H_2$ (q=0-8). *Atomic Data and Nuclear Data Tables* **12** (2019), 1-69.

[4] D. R. Schultz, H. Gharibnejad, T. E. Cravens, and S. J. Houston. Data for Secondary-Electron Production from Ion Precipitation at Jupiter III: Target and Projectile Processes in H^+, H, and H^- + H Collisions**.** *Atomic Data and Nuclear Data Tables*, to appear.

[5] J. F. Ziegler, M. D. Ziegler, and J. P. Biersack. SRIM: The Stopping and Range of Ions in Matter. *Nuclear Instruments and Methods in Physics Research Section B: Beam Interactions with Materials and Atoms* **268**:11 (2010), 1818–1823.

[6] S. J. Houston, T. E. Cravens, D. R. Schultz, H. Gharibnejad, W. R. Dunn, D. K. Haggerty, A. M. Rymer, B. H. Mauk, and N. Ozak. Jovian Auroral Ion Precipitation: X-Ray Production from Oxygen and Sulfur Precipitation. *Journal of Geophysical Research: Space Physics* **124** (2019).

Mathematics of Biotechnology

As proof-of-concept academic work in engineering biology meets the market realities of bringing lab science to product initiation, there are questions in how to compare biological products, measure whether desired outcomes are realized, and optimize biological systems for desired behaviors. NIST is working to deliver tools and standards to measure such biological technologies, outputs, and processes from healthcare to manufacturing and beyond. We support this effort with the development and deployment of innovative mathematical modeling and data analysis techniques and tools.

Quantitative MRI

Andrew Dienstfrey
Zydrunas Gimbutas
Kathryn Keenan (NIST PML)
Karl Stupic (NIST PML)
Stephen Russek (NIST PML)

Magnetic resonance imaging (MRI) enables non-invasive imaging of biological soft tissue *in vivo*. Quantitative MRI (qMRI) refers to an extension of MRI in which scanning protocols and data analysis are implemented to obtain an *in vivo* map of measurable quantities whose magnitudes are reported in terms of standard physical units. For example, tumor volumes are reported in units of mm^3, blood perfusion in units of ml g^{-1} min^{-1}, apparent diffusion coefficient in mm^2 s^{-1}, and temperature in K. In addition to these biophysical quantities, proton spin relaxation times specific to magnetic resonance physics, known as T_1 and T_2 are reported in seconds, are being considered as biomarkers for a wide range of pathologies including traumatic brain injury, multiple sclerosis, and liver disease.

Increasing focus on qMRI for medical diagnosis and treatment requires a robust measurement infrastructure to ensure cross-comparability and temporal stability of derived values. In FY 2019 we continued our collaboration with researchers from NIST's Applied Physics Division (686) to extend SI traceability and quality assurance protocols for this essential medical imaging technology. An important component of this infrastructure are phantoms, specially designed objects with known properties which can be used to evaluate and tune the performance of imaging devices.

The NIST MRI system phantom was designed in collaboration with the International Society of Magnetic Resonance in Medicine (ISMRM). The phantom is the first of its kind maintained by a national metrology institute, and is unique in exhibiting SI-traceability, a high level of precision, and long-term stability. The system phantom can be used as a reference for parameters including geometric distortion, resolution, and proton spin relation times. A schematic of the phantom is shown in Figure 36. This calibration structure is useful to transition MRI from a qualitative imaging technique to a precise metrology with documented accuracy and uncertainty. [1]

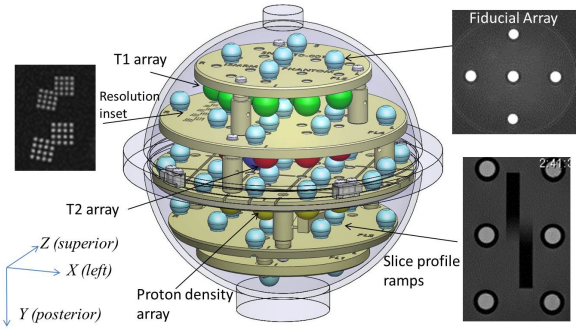

Figure 36. *Schematic of NIST/ISMRM System Phantom.*

In FY2019 we completed a study assessing the effects of an "all but superconducting magnet" scanner upgrade on T_1 measurement in a clinical setting [2]. Upgrades to software and hardware are inevitable over the lifetime of a magnetic resonance scanner. For longitudinal work, upgrades could possibly introduce measurement differences in the data from before and after the system upgrade, potentially jeopardizing complex and expensive studies.

Inversion recovery (IR) and variable flip angle (VFA) are two common qMRI protocols for T_1 measurement in clinical practice. In both cases, T_1 is estimated as a model parameter that links directly-measured MR signals to experimental variables—inversion time (TI_k) and flip angle (α_m)—in the IR and VFA protocols respectively.

The measurement model for the IR experiment is

$$y_k = \left|M_0\left(1 - be^{-(TI_k/T_1)}\right)\right| + n_k.$$

Here y_k is the measured signal at the k-th inversion time, M_0 is the magnitude of the magnetization signal within the ROI, b is related to the fraction of spins inverted in the initial 180 pulse, and n_k represents measurement noise. For a given set of TI_k and associated values y_k, the parameters $T_1, M_0, and\ b$ are unknown and need to be estimated. Nonlinear least squares is a natural approach. However, the absolute value in the IR signal model entails a loss of differentiability at measurement points where the signal is near zero. To avoid this, we modified the objective and

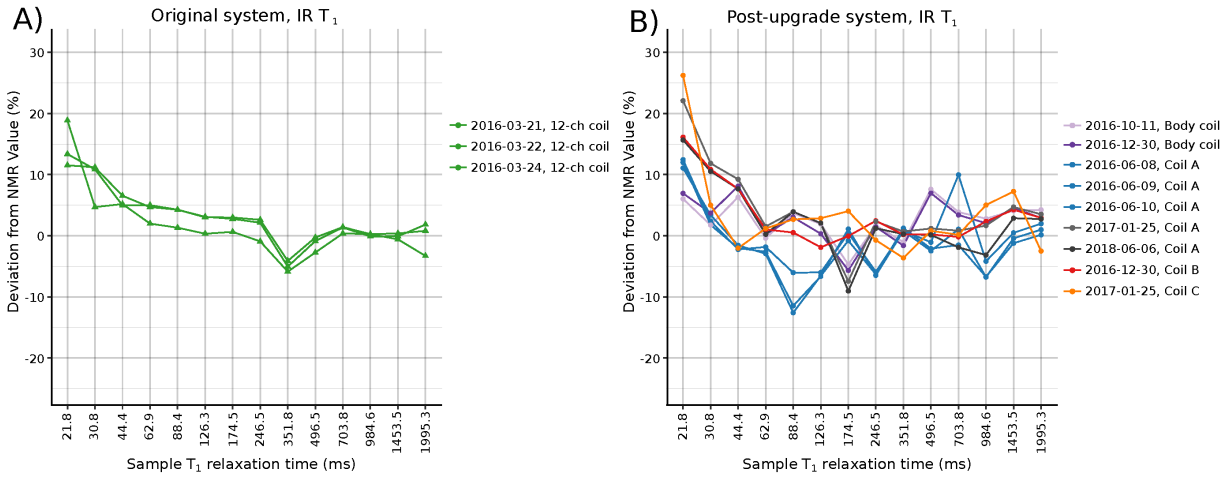

Figure 37. *IR measurement of T_1 pre- and post-upgrade in comparison to NMR reference values.*

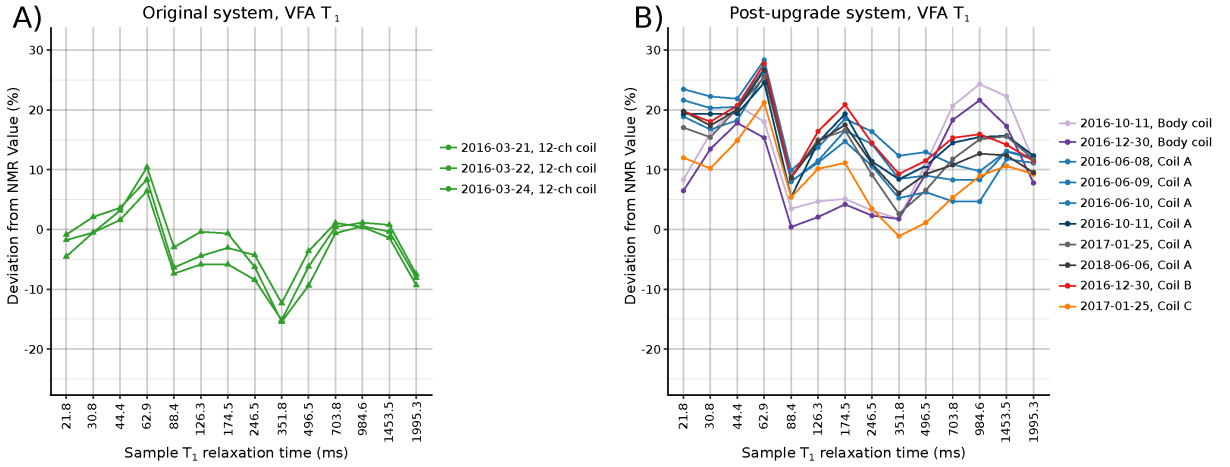

Figure 38. *VFA measurements of T_1 pre- and post-upgrade in comparison to NMR reference values.*

solved the following, nonlinear least squares problem to estimate T_1, M_0, *and* b:

$$\min \sum_{k=1}^{K} \left(y_k^2 - \left(M_0 \left(1 - b e^{-TI_k/T_1} \right) \right)^2 \right)^2 .$$

This smooth problem was solved via Newton iteration refinement of an initial guess found by search over a dense grid in the 3D parameter space. Through extensive numerical experiments, we determined that the differences between solving the smoothed least-squares problem and the original (non-smooth) problem involving the absolute value are minimal.

Analysis of VFA data proceeds along similar lines. In this case, the measured MRI signal is modeled as a function of flip-angle

$$z_m = A \sin \alpha_m \frac{1 - e^{-TR/T_1}}{1 - e^{-TR/T_1} \cos \alpha_m} + n_m$$

where TR is a fixed experimental parameter, n_m is measurement noise, and A represents signal strength for the sample. Once again, estimates of T_1 and A are determined by non-linear least squares minimizing the sum

$$\sum_{m=1}^{M} \left(z_m - A \sin \alpha_m \frac{1 - e^{-TR/T_1}}{1 - e^{-TR/T_1} \cos \alpha_m} \right)^2 .$$

The T_1 measurements from IR and VFA scans are compared to phantom reference values obtained by NIST's MRI Biomarker Measurement Service based on NMR [3]. Discrepancies between MRI measurements and these reference values are shown in Figure 37 and Figure 38.

The results show significant differences in T_1 measurement post-upgrade in both IR and VFA protocols. For both, there is much greater variability in the percent deviation in comparison to reference values. For the IR protocol these deviations exceed 20 % for the lower T_1 values. Excluding these two data points, there is no

discernible bias across the remaining nominal T_1 values. By contrast, the VFA measurements exhibit a pronounced shift toward higher T_1 across all nominal points.

The scanner upgrade for this study was not unusual and involved aging coil replacements and software updates. Critically, the system passed all vendor quality assurance (QA) protocols pre- and post-upgrade. This study demonstrates that these QA guidelines are insufficient to determine T_1 measurement precision within a medically relevant range. All results were reported in a paper published in FY 2019 [2].

In the upcoming year we plan to continue analyzing data collected by a growing network of collaborators performing scans of the NIST/ISMRM System Phantom. We currently have multi-vendor datasets which we are analyzing for T_1 measurement variability using the same software analysis tools developed for this study. Additional software is being developed to assess geometric distortion. Separately, we are researching the use of deep neural networks to assess geometric distortion directly from k-space data. We hope to report progress on these activities in the future.

[1] K. F. Stupic, M. Ainslee, M. A. Boss, *et. al.* A Standard System Phantom for Magnetic Resonance Imaging. In preparation.

[2] K. E. Keenan, Z. Gimbutas, A. Dienstfrey, and K. F. Stupic. Assessing Effects of Scanner Upgrades for Clinical Studies. *Journal of Magnetic Resonance Imaging* **50**:6 (2018), 1948-1954.

[3] M. Boss, A. Dienstfrey, Z. Gimbutas, K. E. Keenan, A. B. Kos, J. D. Splett, K. F. Stupic, and S. E. Russek. Magnetic Resonance Imaging Biomarker Calibration Service: Proton Relaxation Times. NIST Special Publication 250-97, 2018.

Mass Spectral Similarity Mapping Applied to Fentanyl Analogs

Anthony Kearsley
Arun Moorthy (NIST, MML)
Gary Mallard (NIST MML)
William Wallace (NIST MML)

Compound identification is a fundamental task in forensics chemistry. A common tool of this process is mass spectral library searching. That is, given a database of mass spectra of known compounds and a mass spectrum of an unknown compound, mass spectral library searching seeks to identify the unknown compound by calculating similarities/dissimilarities. Typically, mass spectral library searching returns a hitlist or list of likely compound matches. Ideally, top hits will provide an analyst adequate information to correctly infer the identity of an analyte.

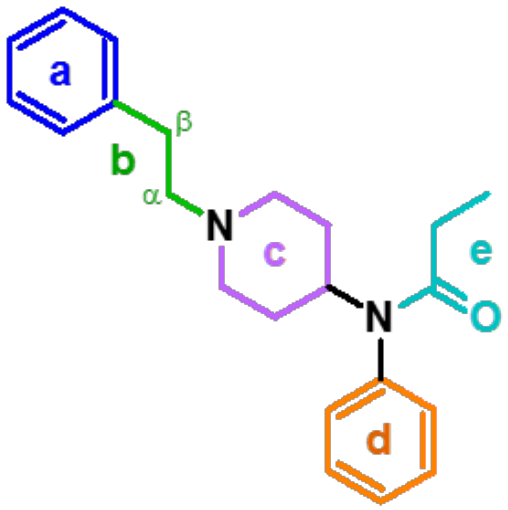

Figure 39. *Molecular structure of fentanyl with potential sites for modification (as defined by the DEA [1]) labeled.*

It is important to note that the eventual classification of the analyte is still a human task —the burden of identification resides with the analyst. This is of particular interest in forensic chemistry applications. For example, incidents of opioid abuse continue to grow, leading to a rise of fentanyl and related analogs like synthetic opioids with fast onset and high therapeutic indexes [1]. Forensic practitioners struggle to provide confident identifications when encountering novel designer fentanyl analogs.

To aid in this activity, a natural extension to traditional mass spectral library searching is being developed that, in addition to returning a hit list of database entries with similar spectra to the analyte spectrum, generates a map of spectral similarity between the hit list and the actual mass spectra themselves. The map can then be scrutinized using a variety of numerical techniques. The objective of this extension is to provide analysts with additional information which can improve confidence in identifying analytes, and, may eventually lead to automated classification with quantifiable uncertainty.

Fentanyl analogs can be classified by the type and location of the structural modifications by which they differ from a fentanyl molecule. For example, examining Figure 39, it can be observed that α-methyl fentanyl contains a methyl addition on the α position of modification site “b”. The defined modification sites and structural scaffold are an interpretation derived from the definitions provided in [2]. One interesting notion is that of fentanyl analog type indicating the number of structural locations (modification sites) by which an analog differs from the molecule fentanyl. For example, α-methyl fentanyl is considered a Type I fentanyl analog, as it differs from fentanyl at a single modification site. Type II analogs have modifications in two locations, and

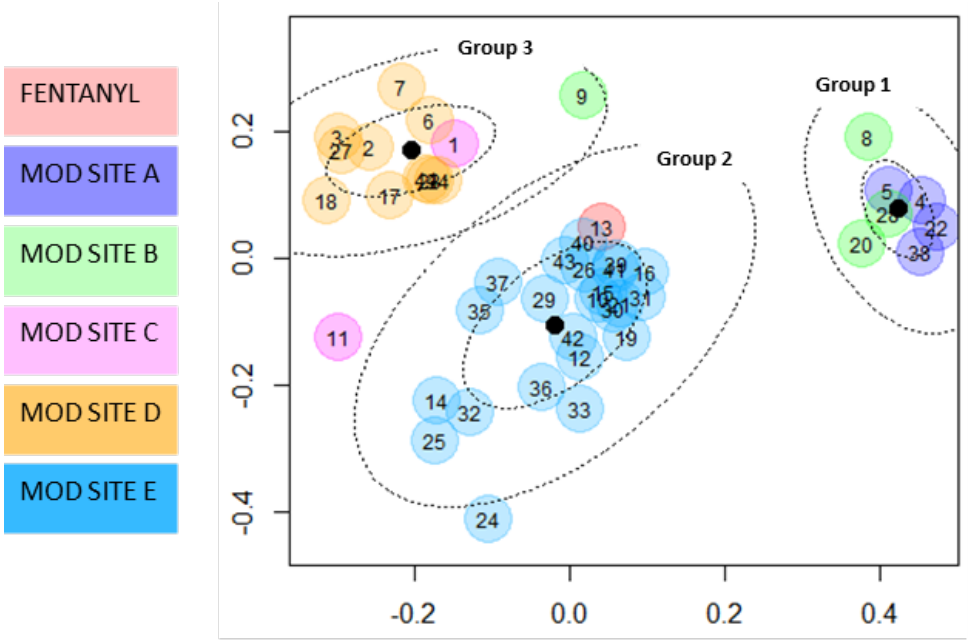

Figure 40. *Spectral similarity space of the Type I fentanyl analog reference set visualized by non-metric Multidimensional Scaling of dissimilarity matrices generated by hybrid match factors. Each point in the spectral similarity space represents a spectrum of a molecule and its coloring indicates at which modification site it differs from fentanyl (labeled 13, in red). Groups 1-3 were discovered through k-means clustering of the spectral similarity space data, with bold black dots indicating cluster centers and dotted outlines indicating the 50 % (inner) and 95 % (outer) confidence ellipse around each center.*

so forth for Types III-V. The spectra and structure information for all Type I fentanyl analogs, along with the spectrum for the molecule fentanyl, contained in the Scientific Working Group for the Analysis of Seized Drugs (SWGDRUG) Mass Spectral Library version 3.3[10] can be used to form a reference set for comparisons.

Preliminary results suggest the notion of using a map instead of only a hitlist can provide very useful analysis. Using Type I fentanyl as an example, a reference set can be generated. In an attempt to classify compounds, the hybrid similarity match factors [3] are exclusively used to approximate spectral similarity when generating maps together with multidimensional scaling (MDS) [4], which is a procedure for representing dissimilarity among pairs of objects as distances between points in a low-dimensional space while preserving correlations from the original data as best as possible. Using MDS to project the Type I fentanyl analog dissimilarity matrices down to two dimensions, one can visualize more easily as seen in Figure 40, which illustrates the spectral similarity space of the Type I fentanyl analog reference set using non-metric MDS.

[1] J. B. Morrow, J. D. Ropero-Miller, M. L. Catlin, A. D. Winokur, A. B. Cadwallader, J. L. Staymates, S. R. Williams, J. G. McGrath, B. K. Logan, M. M. McCormick, K. B. Nolte, T. P. Gilson, M. J. Menendez, and B. A. Goldberger. The Opioid Epidemic: Moving Toward an Integrated, Holistic Analytical Response. *Journal of Analytical Toxicology* **43** (2018), 1-9.

[2] Federal Register **83**:25, February 6, 2018, 5188–5192.

[3] A. S. Moorthy, W. E. Wallace, A. J. Kearsley, D. V. Tchekhovskoi, and S. E. Stein. Combining Fragment-Ion and Neutral-Loss Matching during Mass Spectral Library Searching: A New General Purpose Algorithm Applicable to Illicit Drug Identification. *Analytical Chemistry* **89**:24 (2017), 13261-13268.

[4] A. J. Kearsley, R. A. Tapia, and M. W. Trosset. The Solution of the Metric STRESS and SSTRESS Problems in Multidimensional Scaling using Newton's Method. *Computational Statistics* **13**:3 (1998), 369–396.

[10] https://swgdrug.org

Chemometrics for 2D-NMR and Mass Spectrometry

Anthony Kearsley
Ryan M. Evans
Chris Schanzle
John Marino (UMD/NIST IBBR)
Frank Delaglio (UMD/NIST IBBR)
Luke Arbogast (UMD/NIST IBBR)
Robert Brinson (UMD/NIST IBBR)
John Schiel (UMD/NIST IBBR)
Trina Mouchahoir (UMD/NIST IBBR)

Nuclear magnetic resonance (NMR) spectroscopy and mass spectrometry are foundational tools of analytical chemistry and have far-reaching applications. Mass spectrometry is currently being used to identify illicit drug compounds, and two-dimensional NMR has recently emerged as a tool for characterizing monoclonal antibodies [1-3], biologically based therapeutics derived from proteins used to treat a wide number of diseases from rheumatoid arthritis to certain kinds of cancer.

Analysis of NMR or mass spectra typically requires an expert and is commonly done through visual inspection. For example, consider a set of two-dimensional NMR spectra of monoclonal antibodies (see Figure 41). Since NMR spectra encapsulate a type of chemical *signature*, scientists are interested in comparing NMR spectra with a known reference to establish safety and efficacy. This is crucial in industrial settings to evaluate heterogeneity arising from manufacturing process modifications. Though expert feedback can be invaluable, visual inspection is ultimately subjective and error prone, especially when analyzing hundreds of spectra. Thus, quantitative analysis of NMR spectroscopy and mass spectrometry data is of fundamental importance.

The NIST/UMD Institute for Bioscience and Biotechnology Research (IBBR) is the home to a research group, led by J. Marino, that seeks to improve accuracy

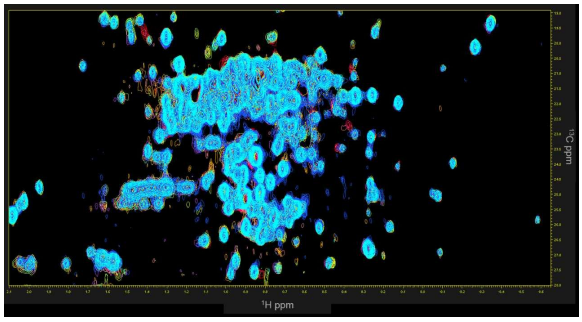

Figure 41. *Multiple overlay of NMR spectra.*

and robustness of two-dimensional NMR spectroscopy for characterizing monoclonal antibodies. This project recently conducted a benchmark international inter-laboratory study with scientists from twenty-six different laboratories in nine different countries spanning five continents. This large group performed a variety of NMR experiments on samples derived from the NIST-mAb, a monoclonal antibody that has become a standard reference material (SRM 8671).

Hundreds of spectra were acquired under numerous experimental conditions, by varying factors such as sample type, instrument manufacturer, magnet strength, and temperature. Spectral information was concisely summarized in the form of *peak tables*, which consist of a weighted l_2 norm of significant peak locations for each spectrum. By applying principle component analysis (PCA) and the unweighted pair group method with arithmetic mean (UPGMA) to a set of peak tables, it was demonstrated that it is possible to accurately and reliably detect sample type and temperature of spectra from this study (see Figure 42). It was confirmed that differences resulting from variations in sample type and temperature are minor, and that two-dimensional NMR can characterize the NISTmAb across a wide variety of experimental conditions in a highly repeatable and reproducible manner [4]. These results move the 2D NMR method from an emerging technology to a harmonized,

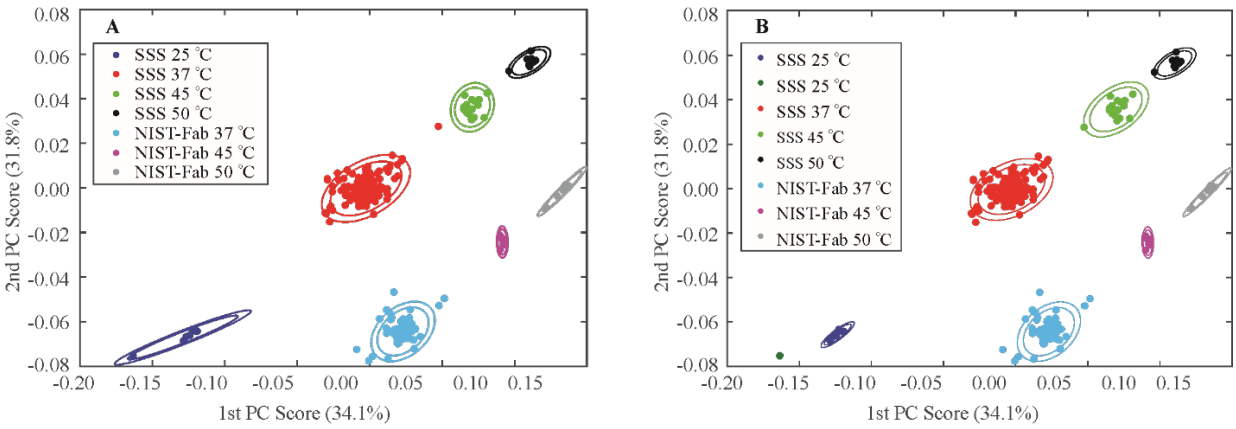

Figure 42. *Left: manual classification of peak tables of NMR spectra according to sample type and temperature in principle component space. Right: classification of NMR spectra in principle component space using UPGMA. Observe that the two figures are nearly identical.*

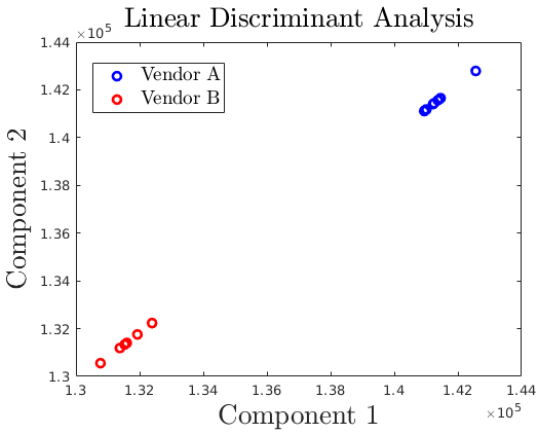

Figure 43. *Classification of mass spectra according to vendor.*

routine measurement that can be generally applied with great confidence to high precision assessments of the structure of a wide array of protein therapeutics.

These results were predicated upon successfully pairing a proper machine learning algorithm with an appropriate measure of distance between spectra. Since the data were elements of two-dimensional Euclidean space, it was natural to use the Euclidean distance. However, when comparing raw 2D-NMR spectra, it is not at all clear that this is the right choice. Although use of the Euclidean metric has been explored [5], this is a *bin-by-bin* distance and Figure 42 suggests that a *cross-bin* distance may be more appropriate. Both techniques rely on quantizing the spectrum under consideration and mapping each intensity value at every discrete location to a unique bin. While bin-to-bin distances compare only bins at adjacent locations, cross-bin distances are non-local and compare each bin to its neighbors. The first Wasserstein metric is an example of a cross-bin distance that has been used for image identification [6], and in the present case it has the elegant interpretation as the minimum amount of work required to turn one spectrum into another. Current research focuses on comparing the first Wasserstein metric with other metrics like χ^2 and l_2 and finding an appropriate machine learning algorithm with which to pair these metrics, in order to develop superior techniques for classifying monoclonal antibody spectra. Future work will include comparing these techniques with the Tucker3 decomposition [7].

Another facet of this research project involves mass spectrometry, which can be used as a complementary tool for characterizing monoclonal antibodies. When using mass spectrometry to analyze these therapies, it is important to establish validity of a given method, i.e., that it is repeatable and reproducible to high precision. This is also known as *system suitability*.

Schiel and Mouchahoir are currently spearheading a novel inter-laboratory study at the IBBR to establish the significance of system suitability in the context of mass spectrometry experiments that involve monoclonal antibodies. This study is comprised of fifteen participants from different laboratories, each of whom has performed a mass spectrometry experiment on a monoclonal antibody. Using linear discriminant analysis (LDA), we have shown that it is possible to partition each spectrum according to the vendor of the instrument with which it was measured (see Figure 43). This preliminary finding shows that we can effectively classify participants according to certain attributes.

Future work will investigate the classification of participants according to attributes. Of interest is the possibility of separating spectra into distinct classes: those deemed to be well-measured and reproducible, and those that are not. Quantitative analysis is expected to play an integral role in establishing the significance of system suitability of mass spectrometry experiments involving monoclonal antibodies.

[1] Y. Aubin, G. Gingras, and S. Sauvé. Assessment of the Three-Dimensional Structure of Recombinant Protein Therapeutics by NMR Fingerprinting: Demonstration on Recombinant Human Granulocyte Macrophage-Colony Stimulation Factor. *Analytical Chemistry* 80:7 (2008), 2623-2627.

[2] L. W. Arbogast, R. G. Brinson, and J. P. Marino. Mapping Monoclonal Antibody Structure by 2D 13C NMR at Natural Abundance. *Analytical Chemistry* **87**:7 (2015), 3556-3561.

[3] R. Kiss, Á. Fizil, and C. Szántay Jr. What NMR Can Do in the Biopharmaceutical Industry. *Journal of Pharmaceutical and Biomedical Analysis* **147** (2018), 367-377.

[4] R. G. Brinson, J. P. Marino, F. Delaglio, L. W. Arbogast, R. M. Evans, A. Kearsley, G. Gingras, H. Ghasriani, Y. Aubin, G. K. Pierens, X. Jia, M. Mobli, H. G. Grant, D. W. Keizer, K. Schweimer, J. Ståhle, G. Widmalm, E. R. Zartler, C. W. Lawrence, P. N. Reardon, J. R. Cort, P. Xu, F. Ni, S. Yanaka, K. Kato, S. R. Parnham, D. Tsao, A. Blomgren, T. Rundlöf, N. Trieloff, P. Schmieder, A. Ross, K. Skidmore, K. Chen, D. Keire, D. I. Freedberg, T. Suter-Stahel, G. Wider, G. Ilc, J. Plavec, S. A. Bradley, D. M. Baldisseri, M. L. Sforça, A. Carolina de Mattos Zeri, J. Y. Wei, C. M. Szabo, C. A. Amezcua, J. B. Jordan, and M. Wikström. Enabling Adoption of 2D-NMR for the Higher Order Structure Assessment of Monoclonal Antibody Therapeutics. *mAbs* **11**:1 (2019), 94-105.

[5] B. Japelj, Boštjan, G. Ilc, J. Marušič, J. Senčar, D. Kuzman, and J. Plavec. Biosimilar Structural Comparability Assessment by NMR: From Small Proteins to Monoclonal Antibodies. *Scientific Reports* **6** (2016), 32201.

[6] Y. Rubner, C. Tomasi, and L. J. Guibas. The Earth Mover's Distance as a Metric for Image Retrieval. *International Journal of Computer Vision* **40**:2 (2000), 99-121.

[7] K. Chen, J. Park, F. Li, S. M. Patil, and D. A. Keire. Chemometric Methods to Quantify 1D and 2D NMR Spectral Differences Among Similar Protein Therapeutics. *AAPS PharmSciTech* **19**:3 (2018), 1011-1019.

Metrology for Microfluidics

Paul Patrone
Joseph Klobusicky
Anthony Kearsley
Gregory A. Cooksey (NIST PML)

Advances in microfluidics promise to fundamentally change the way many scientific disciplines operate by enabling precise control over the motion of fluids and solutes in micron-scale systems. For example, microfluidic fabrication techniques allow chemical reaction vessels to be reduced to the size of a human hair, parallelized, and subsequently interconnected. This facilitates high-throughput experimentation and combinatorial testing; see Figure 44. Moreover, the medical community has recognized that related approaches can, in principle, enable rapid and simultaneous screening of hundreds of diseases with only a few drops of blood. Indeed, the lure of disrupting this $75 billion medical testing industry has led to significant venture capital investments in high-profile startups that specialize in microfluidics for lab-on-a-chip applications. Despite the promise, few commercial implementations of such devices have emerged, leading the community to reflect on the fundamental measurement challenges that have stalled progress.

To address these shortcomings, ITL and PML staff have adopted an approach that tightly integrates mathematical analysis, modeling, physics, and bioengineering to tackle all aspects of the measurement problem simultaneously. Furthering work from FY 2018, several of us continued the development of a pair of flowmeters that can continuously measure volumetric flow rates v_ν down to scales that were previously unattainable. The first of these devices can measure v_ν down to approximately 10 nL/min with 5 % (or less) relative uncertainty using physics-based scaling relationships to extrapolate measurements of a previously calibrated flow meter. The second device uses symmetry breaking arguments to identify zero-flow to within 0.1 nL/min, which is useful in general for calibrating flow meters and for characterizing flow stability; see Figure 45. This work has led to a pair of patent applications and several publications [1-5].

More recently, we have been investigating the usefulness of the zero-flow meter as an alternative to flow velocimetry. The latter technique characterizes a flow profile by measuring the velocities of tracer particles that follow individual streamlines. This approach becomes problematic at small scales, however, if the tracers interact with the flow and/or each other. The zero-flow meter avoids such problems by using fluorescent solutes that are orders of magnitude smaller than tracers and have negligible effects on the fluid flow. However, the fluorophores are uniformly distributed in the fluid, so that a strong laser is needed to bleach

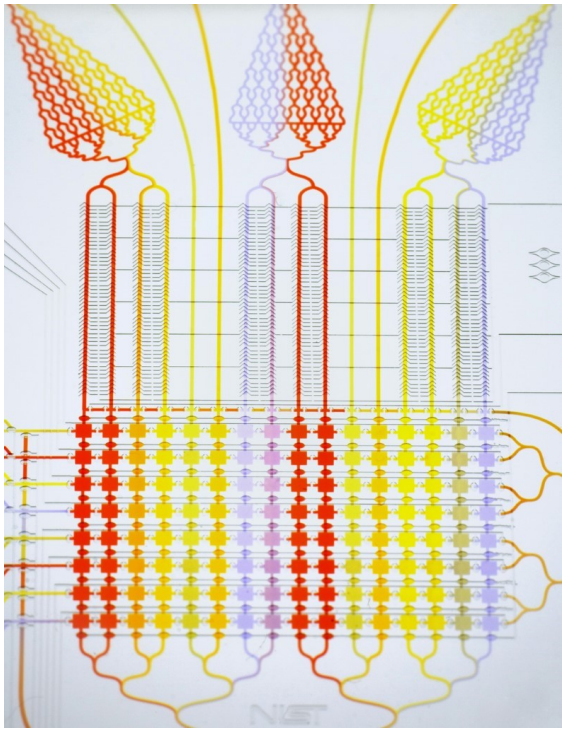

Figure 44. *Example of a microfluidic device used to establish concentration gradients. Fluid of different colors flows through the input channels (top) and enters the experimental chambers (squares). Because the flow is laminar, diffusion is the only mechanism responsible for mixing (which occurs in the upper branching network and middle mixing regions). In this way it is possible to precisely control concentrations of reactants in combinatorial testing assays.*

(i.e., deactivate) them and establish concentration gradients that map out the flow profile. Mathematically, we model this system with the partial differential equation (PDE) of the form

$$D\nabla^2 c - v_\nu u(x,y)\partial_z c = 0$$

where D is the fluorophore diffusion coefficient, c is the concentration of fluorophores, v_ν is the volumetric flow rate, and $u(x,y)$ is the velocity profile corresponding to Poiseuille flow in a duct of arbitrary geometry. This PDE is supplemented by zero-flux boundary conditions on the microchannel walls and the Dirichlet conditions $c = 0$ and $c = 1$ at $z = 0$ and $z = 1$, respectively. The first of these corresponds to the physical situation in which the laser is so strong that it bleaches virtually all particles on contact, while the second models a reservoir of fluorophores, which we can realize experimentally with high fidelity. Analytically we have determined that when D is sufficiently small and the laser sufficiently strong, back-diffusion of the deactivated fluorophores occurs within a small boundary layer on the order of D/v_ν. The singular perturbation theory solution of the PDE in this layer has the form

$$c = c_0[1 - \exp(-z v_\nu u(x,y) w^2/D)]$$

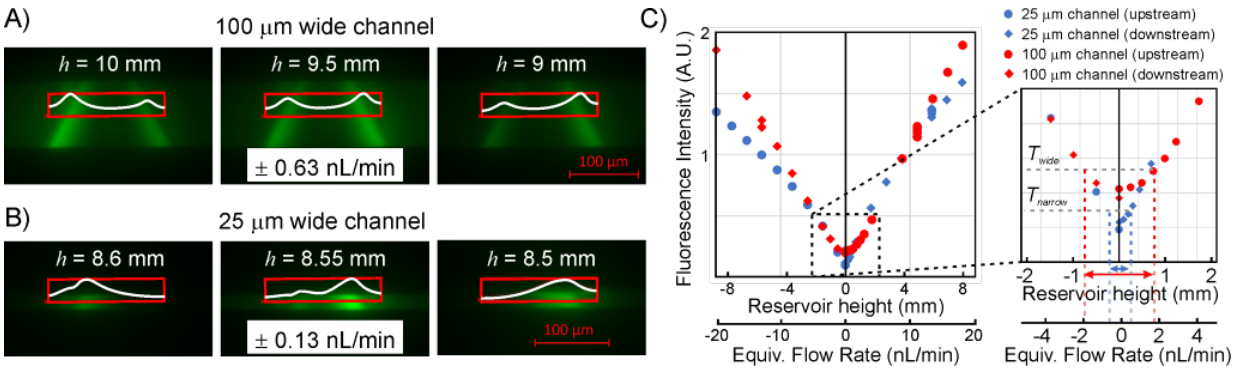

Figure 45. *Determination of uncertainty in height around zero flow. Microscopy images show fluorescence intensity (green) at different heights near zero flow in wide (A) and narrow (B) channel interrogation regions. The white curve shows a line scan of fluorescence intensity across the illumination region (along the bottom line of the red box). When flow is near zero, all fluorescein in the channel is bleached, except for fresh fluorescein diffusing into the edges of the laser path. Brighter intensity on the left is used to indicate positive flow, brighter intensity on the right indicates negative flow. Zero flow is a point somewhere between. (C) Steady-state fluorescence values from waveguides upstream (equivalent to being positioned on the left in the images) and downstream (right in the images) of the excitation beam are shown for the two microchannel widths at different heights of the fluid reservoir (e.g., the flow controller). The equivalent flow rate was determined from the conductance of the system (2.5 nL min^{-1} mm^{-1}). Inset shows magnification of the critical region and application of thresholds, T_{wide} and T_{narrow} (gray dotted lines), to isolate the minimum of the signal and determine the height, and corresponding flow, uncertainty ((blue dotted lines show 25 μm channel; red dotted lines show 100 μm channel).*

where w is the characteristic width of the channel. Interestingly, this solution has the property that its level sets map out the shape of the flow profile. Thus, imaging of the fluorescence concentration in this boundary layer should amount to direct imaging of the streamlines. Experimental work is on-going to verify this theory and better assess uncertainties associated with this method.

[1] P. N. Patrone, G. Cooksey, and A. Kearsley. Dynamic Measurement of Nanoflows: Analysis and Theory of an Optofluidic Flowmeter. *Physical Review Applied* **11** (2019), 034025. DOI: 10.1103/PhysRevApplied.11.034025

[2] G. A. Cooksey, P. N. Patrone, J. R. Hands, S. E. Meek, and A. J. Kearsley. Dynamic Measurement of Nanoflows: Realization of an Optofluidic Flow Meter to the Nanoliter-per-Minute Scale. *Analytical Chemistry* **91** (2019), 10713-10722. DOI: 10.1021/acs.analchem.9b02056

[3] G. A. Cooksey, P. N. Patrone, J. R. Hands, S. E. Meek, and A. J. Kearsley. Dynamic Measurement of Nanoliter per Minute Flow by Scaled Dosage of Fluorescent Solutions. In *Proceedings of the 22nd International Conference on Miniaturized Systems for Chemistry and Life Sciences (MicroTas 2018),* Kaohisung, Taiwan, November 11-15, 2018.

[4] G. A. Cooksey, P. N. Patrone, and A. J. Kearsley. Optical flow meter for determining a flow rate of a liquid. U.S. Patent Application Number 15/967966, 2017.

[5] G. A. Cooksey and P. N. Patrone. Zero Flow Detector, NIST Invention Disclosure, 2019.

Mathematics of Metrology for Cytometry

Paul N. Patrone
Anthony J. Kearsley
Matthew DiSalvo (NIST PML)
Gregory A. Cooksey (NIST PML)

For more than 30 years, flow cytometry has been a mainstay tool for cancer detection, drug development, and biomedical research. It has remained a primarily qualitative metrology platform because measurement uncertainties associated with this technique are so large. While exact economic figures are difficult to estimate, this has clearly had a significant impact on the roughly $200 billion of waste in the healthcare industry and contributed to the broader reproducibility crisis in biomedical research [1].

From a metrology standpoint, the challenge of making cytometry an accurate and precise tool arises from the competing requirement that it have high throughput. Typical biological samples have on the order of millions to hundreds of millions of cells, which must be analyzed over a time frame of a few hours. To achieve this throughput, cytometers direct cells through a microfluidic channel at high-speed, past an optical interrogation region that collects fluorescence light from antibodies attached to surface proteins. The total fluorescence collected from each cell should then, in principle, be proportional to the total number of markers on its surface. But in practice, this idealized picture is complicated by the cumulative effects of the physical phenomena involved: fluid-dynamic forces cause cells

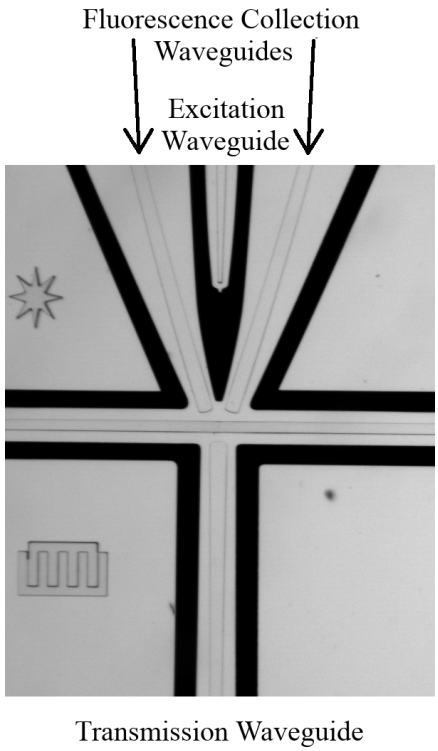

Figure 46. *Characteristic microfluidic cytometer. The excitation laser is projected down a central waveguide that coincides with a symmetry axis of the device. Fluorescence detection waveguides straddle the excitation waveguide on both the left and right. Thus, the fluorescence vs time data acquired from these two channels should be mirror images of one another.*

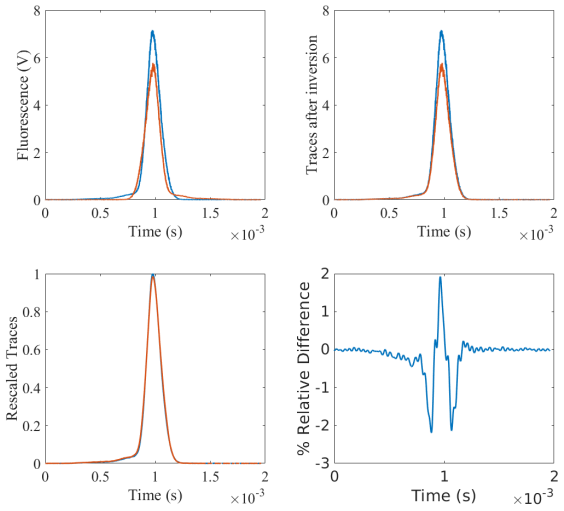

Figure 47. *Fluorescence data collected from the waveguides to the left and right of the excitation waveguide in the figure above.* Top left: *original fluorescence traces.* Top right: *the same traces after inverting the orange curve.* Bottom left: *rescaled traces after affine transformation*. Bottom right: *difference between the curves on the bottom left plot expressed as a percentage. Note that the excellent point-wise agreement between the curves suggests that we have duplicated the measurement to within precision of a few percent or less. Such measurements are necessary to validate the lower limits with which a cytometer can distinguish events.*

to move across streamlines and/or have unpredictable trajectories; optical geometric collection efficiencies depend on position in the interrogation region; and signal acquisition and processing tools introduce non-linear effects and measurement uncertainties through discrete sampling. These challenges, in addition to the complexity of exactly replicating the necessary measurement infrastructure at the micron scale, have made it virtually impossible to reproduce measurements on a single cell, a necessary first step towards fully assessing and controlling uncertainties in cytometry.

To address this challenge, ACMD and PML staff have been collaborating on development of a microfluidic-based cytometer whose design explicitly allows control and study of repeat measurements of cells. A characteristic device is shown in Figure 46. Of note, the system is designed to have reflection symmetry about the excitation laser waveguide; thus, for a homogeneous object, the signals collected by the two fluorescence waveguides should be mirror images of each other; see Figure 47. From a physics perspective, this device allows fundamental limits for reproducibility to be established for any given measurement. For example, letting $s_1(t)$ and $s_2(t)$ be the time traces of the two fluorescence signals, we may consider a variation on the L2 metric of the form

$$\epsilon^2 = \min_{\Delta t} \sum_t [s_1(t) - s_2(-t + \Delta t)]^2$$

where Δt accounts for the time of a cell to transit from some position to its mirror image about the excitation laser axis. If the two signals are the same up to their noise realizations, we deduce that the fundamental limit to distinguish any two signals is given by an equation of the form

$$\epsilon_\star^2 = 4 \sum_t \eta(t)^2,$$

where $\eta(t)$ is the noise in the measurement as a function of time. By this we mean that if you look at the difference of any two signals in an appropriate norm, on average, you cannot see differences that are less than $\epsilon_\star^2$. Alternatively, $\epsilon_\star^2$ determines the lower bound on uncertainty in the measurement

Ongoing work is directed to studying additional details of this modeling, along with the choice of other metrics useful from a metrology standpoint.

[1] W. H. Shrank, T. L. Rogstad, and N. Parekh. Waste in the US Health Care System: Estimated Costs and Potential for Savings. *JAMA* **322**:15 (2019), 1501-1509.

Asymptotics in Molecular Motors Models

Joseph Klobusicky
Peter Kramer (Rensselaer Polytechnic Institute)
John Fricks (Arizona State University)

Molecular motors are essential for the directed transport of large compounds across a cell [1] in eukaryotes (organisms containing a nucleus with chromosomes). A vesicle and the molecular compound it encloses, collectively referred to as a cargo, travel along a microtubule by attaching to one or several molecular motors. The motors which we study, called kinesins, consist of two heads which attach to the microtubule, a tail which attaches to the cargo, and a coiled-coil tether connecting the heads and tail.

By representing the position of N motors in the direction of the microtubule by X_i, and of the cargo by Z, we may write a system of stochastic differential equations describing ensemble evolution for each of the possible attachment states of the motor ensemble. For instance, in the case of a fully attached system, equations take the form

$$dX_i = v_i g\big(\kappa(Z - X_i)\big)dt + \sigma^i dW^i(t), \quad i = 1, \dots, N,$$

$$\gamma dZ = \sum_{j=1}^{N} \kappa(X_i - Z)dt - F_T dt + \sqrt{2k_B T\gamma}\, dW^z(t).$$

In the drift term for X_i, v_i is an unencumbered velocity of a single motor. The function g is a (typically) nonlinear force velocity relation, which in our case accepts a spring force of $\kappa(Z - X_i)$ with a spring constant of κ. For the diffusion term, σ^i represents motor diffusion arising from the mechano-chemical reactions involved with motor procession along the microtubule, and $W^i(t), i = 1, \dots, N$ are N independent standard Brownian motion. The equation for the cargo position Z is an overdamped Langevin equation, which feels forces from the N attached motors and a possible laser trap force applied during an experiment. As the cargo is not anchored to the microtubule, it is subject to thermal fluctuations, which depend on the friction constant γ for the cargo and the Boltzmann constant $k_B T$. Finally, $W^z(t)$ is another Brownian motion independent of $W^i(t), i = 1, \dots, N$.

A main goal for modeling molecular motors is to obtain statistics of effective velocity and diffusion for ensembles, given only information about single motor ensembles. Explicit formulas for these statistics are intractable, as we are generally dealing with nonlinear systems of stochastic differential equations (SDEs). To further complicate matters, the transition rate between attachment states is often dependent on distances between Z and each X_i. Mathematically, this can be described by a Cox process, for which explicit expressions of switching times are rare. At the event of motor attachment or detachment, the cargo will on average shift its position in an approximate jumping motion. See Figure 48 for an illustration on a two-motor ensemble.

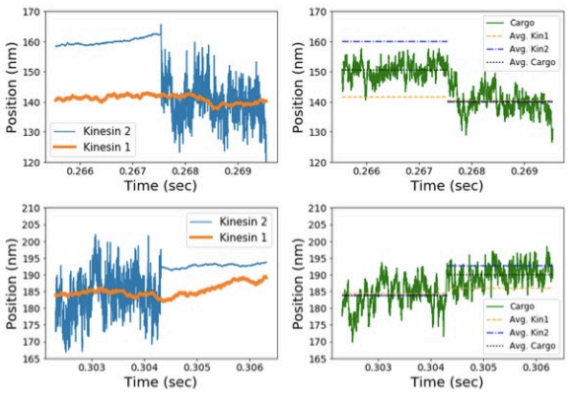

Figure 48. *Behavior of a two-motor ensemble at attachment and detachment times. Each figure shows time versus position of either motors or cargo. Upper left: a kinesin 2 motor detaches from a microtubule at approximately .2675 s. Bottom left: a kinesin 2 motor attaches from a microtubule at approximately .3045 s. Right: the position of cargo before and after attachment (upper right) and detachment (lower right).*

To obtain approximations of ensemble statistics, we use methods of stochastic averaging. The main assumption for stochastic averaging is a separation of scales, meaning that some variables fluctuate faster than others. Through a nondimensionalization, we find that unattached motors are the fastest variables, followed by the cargo, and finally attached motors. Through "freezing" the position of slow variables and integrating out the position of fast variables, we may reduce evolution equations for each state of a two-motor ensemble to a single, constant coefficient SDE. Transition rates may also be averaged to constants. Using the simplified Markov chain model, we may then appeal to known formulas in renewal-reward theory to find expected recurrence times for attached states, and thus equations for effective velocity and diffusivity. Results for this work are contained in [2], which we plan to submit soon.

[1] B. Alberts. *Molecular Biology of the Cell*. CRC Press, 2017.

[2] J. Klobusicky, J. Fricks, and P.R. Kramer. Effective Behavior of Cooperative and Nonidentical Molecular Motors. In process.

Mathematical Models for Cryobiology

Daniel Anderson
James Benson (University of Saskatchewan, Canada)
Anthony Kearsley

Cryobiology, the study of biological specimens at cryogenic temperatures, plays an enormous role in a wide range of fields. In the field of medicine, cryobiology is the basis for cryopreservation in assisted reproduction, organ transplantation, biobanking and personalized medicine. Cryo-banking is used in the agriculture industry as well as for initiatives aimed at preserving rare and endangered plant and animal species and in the development of more productive agricultural yields. Applications in forensics arise in the processing and preservation of frozen biological samples that are often important and fragile evidence in criminal investigations. The breadth and depth of these applications reflect the complexity of the biological, chemical, and physical aspects required to describe and model these problems. Mathematical and computational modes can be used to probe these complex systems and, in conjunction with sophisticated control and optimization schemes, can establish more effective protocols for cryopreservation.

The maintenance of a viable cell during cryopreservation is complicated by two primary factors. Cooling the cell too quickly increases the likelihood of intracellular ice formation and cell damage or death while cooling the cell too slowly can overexpose the cell to high solution concentrations and lead to chemical toxicity. Mathematical modeling in cryobiology thus requires a detailed understanding of thermal and chemical transport in bulk phases as well as across a semi-permeable cell membrane. Additionally, phase transformation of these multicomponent solutions must also be included. Achieving the goal of cryopreserving a cell requires a delicate balance between these two damage mechanisms, and thus a delicate optimization problem. Our ongoing research project has resulted in a series of papers, exploring foundational aspects of biochemical and physical modeling in cryobiology, computational methods for the solution of these models, and applications of these ideas to cryopreservation of cells.

In our first paper [1] we laid the foundations of the necessary chemical thermodynamics underpinning the transport processes during cryopreservation. This work specifically developed a detailed characterization of quantities such as chemical potentials for multicomponent systems of experimental and theoretical interest to cryobiologists. The multiphase, multi-species transport equations were developed along with a consistent characterization of cell membrane dynamics and solid-liquid phase transitions [2]. A critical aspect of our work was to obtain, from first principles, mathematical models that address both spatial and temporal dynamics of

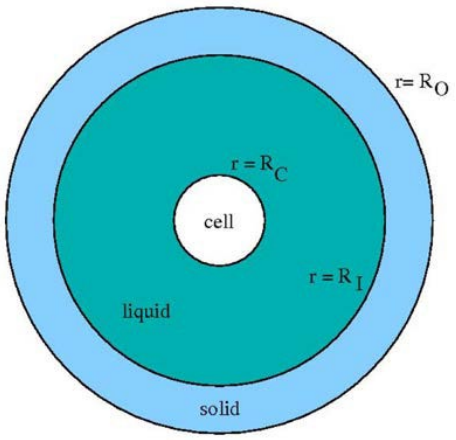

Figure 49. *Spherical cell inside a liquid-solid structure.*

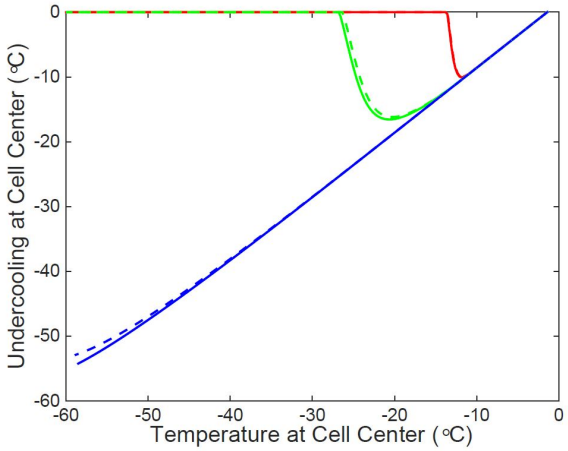

Figure 50. *Three different freezing protocols showing undercooling at the cell center versus the temperature at the cell center for Protocol 1 (red curves), Protocol 2 (green curves) and Protocol 3 (blue curves) for two cases: complete solute rejection (solid curves) and partial solute rejection (dashed curves).*

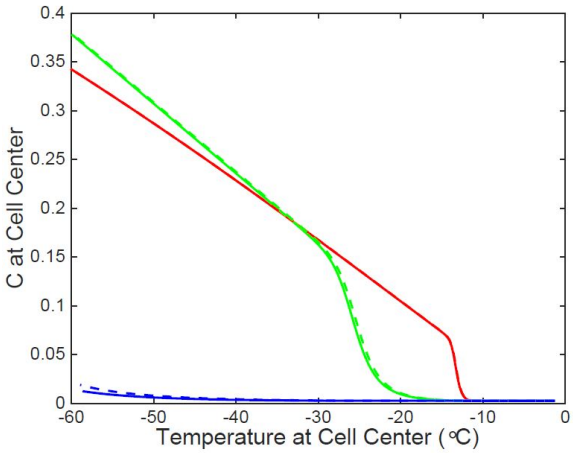

Figure 51. *Dimensionless concentration of cryoprotectant measured at the cell center versus temperature for three different freezing protocols. Protocol 1 (red curves), Protocol 2 (green curves) and Protocol 3 (blue curves) for two cases: complete solute rejection (solid curves) and partial solute rejection (dashed curves).*

chemical species and heat transport. Various aspects of the freezing of a spherical biological cell (see Figure 49) were addressed in [3] and [4]. In [3] we explored the influence of confinement created by an inward growing solidification front on the extracellular and intracellular environments. In [3] and [4] we showed that well-known effects in materials science of partial solute rejection at a solidification front can have non-trivial and non-intuitive influences on the intracellular state. This was a profound observation and led to the development of objective functions which have been developed to measure both intracellular undercooling and chemical toxicity and are sensitive to cooling rates (see Figure 50 and Figure 51) and also to details of the solidification process that have not, until now, been incorporated into cryopreservation models. These control functions appear more suited to deriving cooling protocols than previously employed toxicity functions [5].

The groundwork established in these papers, including a detailed description of computational algorithms in [4], will be the launching point for a control and optimization study to help develop improved cryopreservation heating and cooling protocols.

[1] D. M. Anderson, J. D. Benson, and A. J. Kearsley. Foundations of Modeling in Cryobiology I: Concentration, Gibbs Energy, and Chemical Potential Relationships. *Cryobiology* **69** (2014) 349-360. DOI: 10.1016/j.cryobiol.2014.09.004

[2] D. M. Anderson, J. D. Benson, and A. J. Kearsley. Foundations of Modeling in Cryobiology II: Heat and Mass Transport in Bulk and at Cell Membrane and Ice-liquid Interfaces. *Cryobiology* **91** (2019), 3-17. DOI: 10.1016/j.cryobiol.2019.09.014

[3] D. M. Anderson, J. D. Benson, and A. J. Kearsley. Foundations of Modeling in Cryobiology III: Heat and Mass Transport in a Ternary System. *Cryobiology* (2019), to appear. DOI: 10.1016/j.cryobiol.2019.09.013

[4] D. M. Anderson, J. D. Benson, and A. J. Kearsley. Numerical Solution of Inward Solidification of a Dilute Ternary Solution Towards a Semi-permeable Spherical Cell. *Mathematical Biosciences* **316** (2019) 108240. DOI: 10.1016/j.mbs.2019.108240

[5] J. D. Benson, A. J. Kearsley, and A. Z. Higgins. Mathematical Optimization of Procedures for Cryoprotectant Equilibration using a Toxicity Cost Function. Cryobiology 64 (2012) 144-151. DOI: 10.1016/j.cryobiol.2012.01.001

Data Analysis and Uncertainty Quantification for Biological Systems

Paul Patrone
Anthony Kearsley
James A. Liddle (NIST PML)
Jacob Majikes (NIST PML)
Lili Wang (NIST MML)

Development of metrology for biological and bio-engineering systems provides some of the richest and most difficult opportunities for mathematical modeling and uncertainty quantification. The complexity of such measurements requires highly interdisciplinary teams that can address problems ranging from the task of keeping cells alive to analyzing the physics of measurements and mathematics of signal processing. In many instances, however, the scientific community has remained stovepiped, without sufficient interaction between experts in all fields needed to simultaneously confront these challenges. Unfortunately, this had led to a situation in which many biological measurements lack meaningful uncertainty estimates and/or tools necessary to determine such information.

To address this problem, ACMD and other NIST staff have initiated a series of collaborative research projects whose main goals are to develop analysis and uncertainty quantification (UQ) tools for widely used measurement techniques in biology. A key theme unifying these projects is the recognition that robust analysis and UQ strategies must leverage mathematical principles if they are to be immune to the variable conditions found in biological systems. Thus, concepts from functional analysis and optimization play fundamental roles in this work.

The first project continues work from FY 2018 and aims to develop methods for analyzing real-time polymerase chain reaction (PCR) data. Such measurements can be used, for example, to detect mutations in DNA by characterizing the temperature at which it melts (i.e., opens). A typical PCR protocol uses fluorescent markers that only emit light when the DNA strand is in a closed or open state (but not both), so that the fluorescence as a function of temperature provides an indirect probe of the fraction of melted strands. In typical systems, however, small sample sizes and pipetting errors make it virtually impossible to repeat experimental conditions, so that appreciable differences in measurement signals are common. Background effects, especially when they are temperature dependent, add further complications.

To overcome this lack of reproducibility, we developed a data analysis and UQ strategy that can determine when and to what extent there is a “universal signal”

connecting a collection of similarly prepared samples. The underlying intuition behind this approach is the recognition that differences in sample sizes (e.g., due to pipetting errors) should only affect the magnitude of signal, but not the physics that generated it. Thus, we postulate that all signals $S_i(T)$ can be related by an equation of the form

$$U(T) = \tau_{0,i} S_i(T) + \sum_{n=1}^{N} \tau_{n,i} B_n(T) \qquad (1)$$

where i is measurement index, $U(T)$ is the universal (or scaled) form of the signal, the $B_n(T)$ are background corrections, and the $\tau_{n,i}$ are affine parameters that depend on the measurement signals and bring them all into agreement with the universal signal. To determine the $\tau_{n,i}$, we minimize an objective function of the form

$$L = \sum\nolimits_{i,j,T} \left(U_i(T) - U_j(T)\right)^2$$

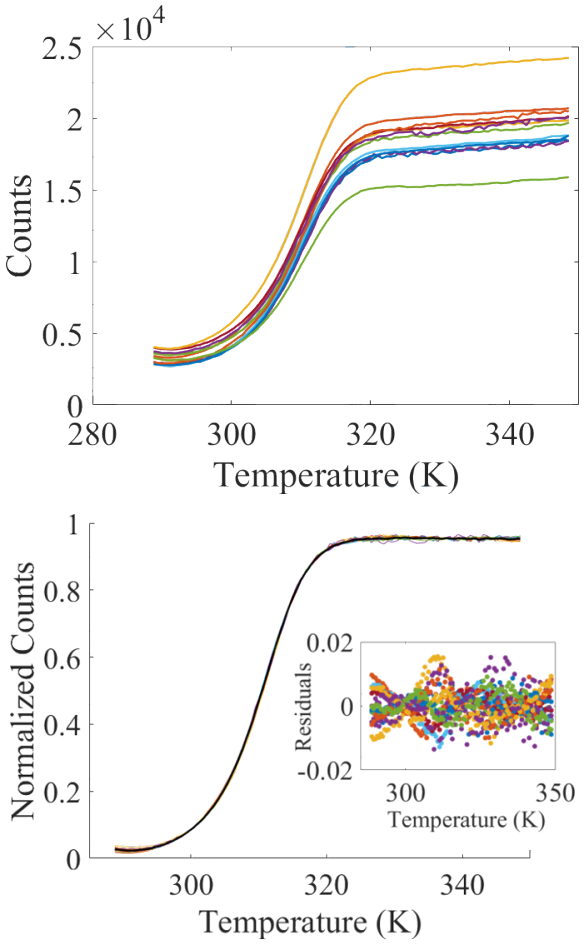

Figure 52. *Raw PCR data (top) and transformed data (bottom). Despite the fact that the raw data exhibits O(1) relative variation, the transformed signals all agree to within a few percent pointwise in temperature after data collapse*

where $U_i(T)$ is the realization of $U(T)$ generated from $S_i(T)$ via an affine transformation in the spirit of Eq. 1. Note that this objective considers all combinations of transformed signals, although it requires regularization and the addition of constraints to ensure a well-posed problem. Additional constraints, e.g. formulated in terms of relative errors, can be used to test the feasibility of achieving collapse with a given uncertainty in the universal signal. The bottom subplot of Figure 52 illustrates the outcome of this optimization applied to collection of datasets in the top sub-plot; see also [1] and [2]. On-going work aims to facilitate technology transfer to commercial PCR instrument manufacturers.

The second project addresses the task of uncertainty quantification for cytometry as part of a NIST Innovation in Measurement Sciences project entitled, *NIST-in-a-Drop: Revolutionizing Measurements of Single-Cell Kinetics*. This project seeks to characterize the properties of large cell populations (e.g., whether they express cancer or other disease markers) by determining the number of fluorescent antibodies attached to proteins on the cell membranes. However, the measurement process introduces several sources of uncertainty associated with variation in sample preparation, antibody lots, calibration conditions, and data analysis. Given that these phenomena interact in a nonlinear fashion, it is difficult to quantify the scale and cumulative effects of these uncertainties. Unfortunately, there are neither detailed empirical studies nor suitably developed tools that would facilitate this task.

To address this problem, we developed a design-of-experiment and hierarchical modeling framework for cytometry that can estimate the relative contributions of multiple sources of uncertainty that cannot be separated by experimental procedures alone. The main idea behind this approach is to formulate a physics-based model of a cytometer measurement of the form

$$v_{i,j,k,l} = m_i F(A_j) + b_k + N_l(0, \epsilon^2)$$

where the i,j,k,l index cell lot, antibody lot, instrument operator, and experiment, respectively, m_i is the mean number of biological markers per cell, $F(A_j)$ is a nonlinear function that characterizes the binding fraction of antibodies, b_k is an operator bias, and $N_l(0, \epsilon^2)$ is a normal random variable characterizing inherent variability in the measurement process. Experimentally we can fix the realizations of these random variables, e.g., by using a single antibody lot for several experiments. In this way, we generated all 27 combinations of measurements sampling the three realizations of the cell lot, antibody lot, and operators. Using a maximum likelihood analysis, for example, it is then possible to estimate the values of the different realizations and thereby also approximate their underlying distributions. Such information can then be used to target specific experimental parameters for uncertainty reduction or better understanding of the total variability in

cytometry measurements. This work is currently being prepared for publication in conjunction with FDA and Fluidigm.

[1] P. N. Patrone, A. J. Kearsley, J. M. Majikes, and J. A. Liddle. Analysis and Uncertainty Quantification of DNA Fluorescence Melt Data: Applications of Affine Transformations. *In review*.

[2] J. M. Majikes, P. N. Patrone, D. Schiffels, M. Zwolak, A. J. Kearsley, S. Forry, and J. A. Liddle. Revealing Thermodynamics of DNA Origami Folding via Affine Transformations. *In review*.

Materials Modeling

Mathematical modeling, computational simulation, and data analytics are key enablers of emerging manufacturing technologies. The Materials Genome Initiative (MGI), an interagency program with the goal of significantly reducing the time from discovery to commercial deployment of new materials using modeling, simulation, and informatics, is a case in point. To support the NIST role in the MGI, we develop and assesses modeling and simulation techniques and tools, with emphasis on uncertainty quantification, and collaborate with other NIST Laboratories in their efforts to develop the measurement science infrastructure needed by the materials science and engineering community.

Micromagnetic Modeling

Michael Donahue
Donald Porter
Robert McMichael (NIST PML)
Justin Shaw (NIST PML)
Hans Nembach (NIST PML)
Cindi Dennis (NIST MML)

http://math.nist.gov/oommf/

Advances in magnetic devices such as recording heads, field sensors, spin torque oscillators, and magnetic non-volatile memory (MRAM) are dependent on an understanding of magnetization processes in magnetic materials at the nanometer level. Micromagnetics, a mathematical model used to simulate magnetic behavior, is needed to interpret measurements at this scale. ACMD is working with industrial and academic partners, as well as with colleagues in the NIST MML and PML, to improve the state-of-the-art in micromagnetic modeling.

We have developed a public domain computer code for performing computational micromagnetics, the Object-Oriented Micromagnetic Modeling Framework (OOMMF). OOMMF serves as an open, well-documented environment in which algorithms can be evaluated on benchmark problems. OOMMF has a modular structure that allows independent developers to contribute extensions that add to its basic functionality. OOMMF also provides a fully functional micromagnetic modeling system, handling three-dimensional problems, with extensible input and output mechanisms. In FY 2019 alone, the software was downloaded by more than 2 900 users and employed by over 200 additional users through the nanoHUB service[11]. The use of OOMMF was acknowledged in more than 150 peer-reviewed journal articles. OOMMF has become an invaluable tool in the magnetics research community.

Key developments over the last year include the following:

- Completed a book chapter on standard problems in micromagnetics [1].
- Released extended precision numerics and an alternative approach to the demagnetization energy calculation based on hybrid fine/coarse grid computations in version OOMMF 2.0a2[12].
- Increased support for periodic boundary conditions.
- Logarithmic axis scaling added to graphing utility program.
- Issued maintenance release OOMMF 1.2b3[13].

OOMMF is part of a larger activity, the Micromagnetic Modeling Activity Group (muMAG), formed to address fundamental issues in micromagnetic modeling through two activities: the development of public domain reference software, and the definition and dissemination of standard problems for testing modeling software. ACMD staff members are involved in development of the standard problem suite as well. The history of muMAG standard problems is the subject of a book chapter soon to be published [1]; M. Donahue serves as editor of the volume containing that chapter [2].

In addition to the continuing development of OOMMF, the project also does collaborative research using OOMMF. One such collaboration, with researchers at the University of Akron, involves using micromagnetic simulations to improve performance in electric motors [3, 4]. M. Donahue is a team member on the NIST Innovations in Measurement Science nanothermometry project Thermal MagIC[14], and he also provides technical guidance on micromagnetic modeling for the DARPA M3IC (Magnetic, Miniaturized, and Monolithically Integrated Components) project[15], which aims to integrate magnetic components into the semiconductor materials fabrication process to improve electromagnetic systems for communications, radar, and related applications.

In total, the ACMD micromagnetic project produced a book chapter [1], two journal articles [3, 4], and three conference presentations [5, 6, 7] this year.

[11] https://nanohub.org/
[12] https://math.nist.gov/oommf/software-20.html
[13] https://math.nist.gov/oommf/software-12.html
[14] https://www.nist.gov/programs-projects/thermal-magic-si-traceable-method-3d-thermal-magnetic-imaging-and-control
[15] https://www.darpa.mil/program/magnetic-miniaturized-and-monolithically-integrated-components

The research of the Micromagnetic Modeling project was honored at the 46th Annual NIST Awards Ceremony on December 12, 2018. M. Donahue and D. Porter received the Jacob Rabinow Applied Research Award, an annual NIST award for outstanding achievements in the practical application of the results of scientific engineering research.

[1] D. G. Porter and M. J. Donahue. Standard Problems in Micromagnetics. In *Electrostatic and Magnetic Phenomena: Particles, Macromolecules, Nanomagnetics*. World Scientific Publishing, to appear.

[2] M. J. Donahue (ed.). *Electrostatic and Magnetic Phenomena: Particles, Macromolecules, Nanomagnetics*. World Scientific Publishing, to appear.

[3] F. Ahmadi, Y. Sozer, M. J. Donahue, and I. Tsukerman. A Low-loss and Lightweight Magnetic Material for Electrical Machinery. *IET Electric Power Applications*, to appear.

[4] F. Ahmadi, M. J. Donahue, Y. Sozer, and I. Tsukerman. Micromagnetic Study of Magnetic Nanowires. *AIP Advances*, to appear.

[5] A. J. Biacchi, E. De Lima Correa, F. Zhang, T. Moffat, W. Tew, M. J. Donahue, S. Woods, C. Dennis, and A. R. Hight Walker. "Tuning the Properties of Colloidal Magnetic Particles for Thermometry on the Nanoscale." 64th Annual Conference on Magnetism and Magnetic Materials (MMM 2019), Las Vegas, NV, November 8, 2019.

[6] F. Ahmadi, M. J. Donahue, Y. Sozer, and I. Tsukerman. "Micromagnetic Study of Soft Magnetic Nanowires." 64th Annual Conference on Magnetism and Magnetic Materials (MMM 2019), Las Vegas, NV, November 7, 2019.

[7] M. J. Donahue and D. G. Porter. "Quantitative Evaluation and Reduction of Error in Computation of the Demagnetization Tensor." 64th Annual Conference on Magnetism and Magnetic Materials (MMM 2019), Las Vegas, NV, November 7, 2019.

OOF: Finite Element Analysis of Material Microstructures

Stephen A. Langer
Andrew C.E. Reid (NIST MML)
Günay Doğan (Theiss Research)
Shahriyar Keshavarz (Theiss Research)

http://www.ctcms.nist.gov/oof/

The OOF Project, a collaboration between ACMD and MML, is developing software tools for analyzing real material microstructure. The microstructure of a material is the (usually) complex ensemble of polycrystalline grains, second phases, cracks, pores, and other features occurring on length scales large compared to atomic sizes. The goal of OOF is to use data from a micrograph of a real or simulated material to compute its macroscopic behavior via finite element analysis.

The OOF user loads images into the program, assigns material properties to the features of the image, generates a finite element mesh that matches the geometry of the features, chooses which physical properties to solve for, and performs virtual experiments to determine the effect of the microstructural geometry on the material. OOF is intended to be a general tool, applicable to a wide variety of microstructures in a wide variety of physical situations. It is currently used by academic, industrial, and government researchers worldwide.

There are two versions of OOF, OOF2 and OOF3D, each freely available on the OOF website. OOF2 starts with two dimensional images of microstructures and solves associated two-dimensional differential equations, assuming that the material being simulated is either a thin freely suspended film or a slice from a larger volume that is unvarying in the third dimension (generalizations of plane stress and plane strain, respectively). OOF3D starts with three dimensional images and solves equations in three dimensions. Development this year continued on multiple fronts.

Adam Creuziger of the NIST Material Measurement Laboratory wishes to use OOF2 to analyze metallic samples consisting of many misoriented grains. The orientations of the grains are critical for determining the material properties and are obtained experimentally at each pixel using electron backscatter diffraction (EBSD). OOF2 previously had the ability to use EBSD data when solving equations, but many operations, such as image segmentation and mesh generation, did not use the orientations. After S. Langer's modifications, OOF2 can now use crystal orientations in almost every situation in which it previously used only pixel colors. For example, it can now select all pixels with orientation within a given range, or automatically divide an image into groups where each group contains only similarly oriented pixels. In addition, OOF2's output routines were enhanced to make it easier to correlate local material properties with computed quantities. Where appropriate, upgrades to OOF2 were applied to OOF3D as well.

EBSD maps are often noisy and incomplete; orientation measurements are missing in some locations, and some measurements contain errors. G. Doğan worked with Prof. Prashant Athavale from Clarkson University to develop a new algorithm to regularize and complete such EBSD map images. The algorithm performs nonlinear diffusion to correct erroneous noisy orientation values. It also completes the missing values by diffusing the information from available neighboring values into missing locations. Preliminary results on synthetic images and empirical maps provided by Creuziger are very promising. Once the regularization algorithm is completed, the output EBSD maps will be fed into a

customized segmentation algorithm that will extract the individual grains from the EBSD images.

OOF2 and OOF3D still rely on some old third-party programs and libraries that will soon become obsolete. S. Langer has continued to work on the switch to the new versions of the aging software. Upgrading from gtk+2 to gtk+3 (used for the graphical user interface) must be done before the switch from Python 2 to Python 3 (used for high level programming and scripting) because there is no support for gtk+2 in Python 3. However, the graphics window in OOF2 (used for displaying and interacting with images, meshes, and results) uses a library (libgnomecanvas) that works with gtk+2 and has no equivalent in gtk+3. Therefore, the first step in must be to write a new canvas library. This is almost complete and is being written in a way that will make it useful outside of the OOF project.

Last year S. Langer and A. Reid added a new, robust method of computing the intersection of a finite element and a set of voxels to OOF3D, solving a long-standing problem with the code. The new routines have been repackaged to make them easier to use in other situations in which one wants to compute the intersection of a set of voxels and any convex polyhedron and are now available as a library called "VSB" (for Voxel Set Boundary)[16]. A paper on the method has been submitted to *Computing and Visualization in Science*.

To the authors' surprise, after years of use with no issues, OOF2 exhibited the same pathology in its element-pixel intersection algorithm that caused problems with OOF3D. OOF2 was modified to use a method akin to the new 3D technique. The new method is slower than the old but was sped up by dividing the image into bins. The ideal bin size depends on the size of the element, but binning is cheap, so OOF2 now creates bins at a number of scales and chooses the appropriate one for each element. Applying the same multiple binning technique to OOF3D might help there as well, but that has yet to be investigated.

During this year, A. Reid and S. Keshavarz completed the implementation of the crystal-plastic constitutive rule in the OOF code, and the construction of the corresponding divergence equation object. Challenges, some expected and some not, arose in executing the time-evolution of this equation. Plasticity has a history-dependence, which necessitated an incremental time-stepping scheme which was not present in the existing OOF code base. In addition, the plastic constitutive rule stores local state information at individual integration points, whereas the OOF infrastructure is geared towards managing state data in nodal fields. The near-term solution to this problem will be to complete implementation of the incremental stepper, which will allow plasticity problems to actually be solved in OOF. This does not realize the full promise of OOF, which includes scenarios where multiple interacting problem types may need to be re-started in order to be self-consistently solved. Plasticity problems' richer state data complicates the re-starting process and will likely pose additional architectural challenges.

OOF2 and OOF3D continue to be used externally. OOF2 was downloaded about 650 times this past year, and OOF3D was downloaded about 200 times. OOF2 can also be run on the NSF nanoHUB facility[17], where it was used between 10 and 100 times each month this past year.

A. Reid gave presentations about the OOF code and its emerging capabilities at the SIAM Computational Science and Engineering meeting in Spokane, Washington, and the Integrated Computational Materials Engineering (ICME) conference in Indianapolis, Indiana in July.

Microstructure Coarsening with Stochastic Particle Systems

Joseph Klobusicky
Robert Pego (Carnegie Mellon University)
Govind Menon (Brown University)

Material microstructures in the form of networks can be found in polycrystalline metals, porcelains, and soap foams. Through the heating of metal or the diffusion of gas through cell walls, network microstructures are transformed as a result of an energy minimization process. In the case of isotropic surface tension, grain boundaries evolve with respect to mean-curvature flow. For two dimensional networks, the von Neumann rule gives a relation between the topology of a grain and its geometry. Specifically, a grain with area A grows at the constant rate

$$\frac{dA}{dt} = c(n-6),$$

where c is a material constant, and n is the number of sides in the grain. As a consequence of the von Neumann rule [1], grains with fewer than six sides can vanish to a point (see Figure 53). When this occurs, an immediate addition or deletion of sides occurs for the grain's neighbors, which subsequently changes their growth rate.

Understanding the coupling of topology, geometry, and grain deletion is a complicated question. Several previous studies [2, 3] have derived kinetic equations for understanding statistical properties of the network. In [4], which is currently under review, we have derived a system of nonlinear kinetic equations for area and topology evolution covering a wide range of mean field assumptions. Using a fixed-point argument, these equations were shown to be well-posed, and several

[16] https://www.ctcms.nist.gov/oof/vsb/

[17] https://nanohub.org/tools/oof2

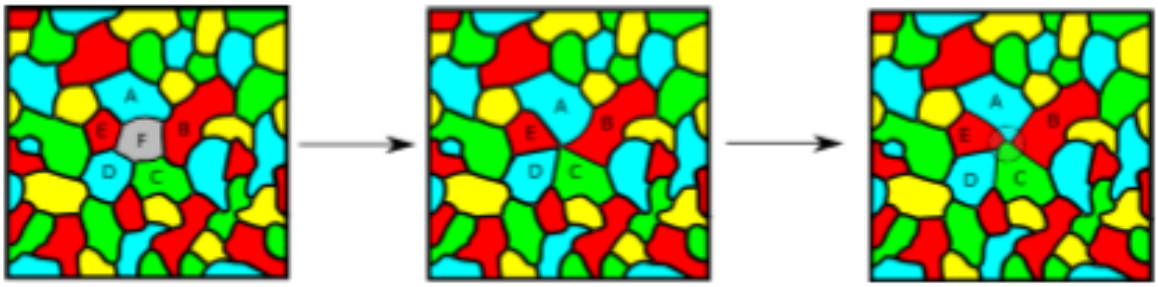

Figure 53. *The vanishing of a five-sided grain. Left: A network before deletion of a five-sided face, labeled F. Center: The annihilation step, in which F is contracted to a point. Right: The creation step, in which a tree is glued at the degree five vertex, recovering the requirement that all vertices are degree three.*

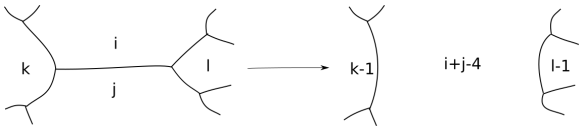

Figure 54. *A foam network before and after wall rupture. Letters in cells denote the number of sides in each grain.*

conserved quantities were also rigorously established. However, a much more challenging question is proving convergence rates of the stochastic particle system to their hydrodynamic limits. Progress in this area has been incremental, focusing on several minimal models which incorporate the major behaviors of grain coarsening, such as area advection, removal, and mutation [5, 6].

Along with curvature driven coarsening, we may also study the coarsening of foams due to wall rupture. Although several experiments and simulations have examined various statistics of aged foams, there is currently no set kinetic equations for estimating statistical topology. This is likely due to the nature of side reassignment for wall rupture, which is fundamentally different from a vanishing grain under gas diffusion. Let C_n denote a cell with n sides. Then a typical "reaction" of four faces from wall rupture is then

$$C_i + C_j + C_k + C_l \to C_{i+j-4} + C_{k-1} + C_{l-1}.$$

See Figure 54 for an illustration. Coarsening through wall rupture, as opposed to curvature flow, does not produce quasi-stationary statistics for a network's topology. Instead, we observe gelation phenomena, in which several grains rapidly gain sides. Currently, we are deriving coagulation equations to explain the onset and rate of gelation and comparing solutions of these equations to Markov models on networks.

[1] C.S. Smith, and C. Stanley. *Grain Shapes and Other Metallurgical Applications of Topology*. American Society for Metals, 1951.

[2] H. Flyvbjerg. Model for Coarsening Froths and Foams. *Physical Review E* **47** (1993), 4037.

[3] M. Marder. Soap-bubble Growth. *Physical Review A* **36** (1987), 438.

[4] J. Klobusicky, G. Menon, and R. Pego. Two-Dimensional Grain Boundary Networks: Stochastic Particle Models and Kinetic Limit. In review.

[5] J. Klobusicky and G. Menon. Concentration Inequalities for a Removal-Driven Thinning Process. *Quarterly of Applied Mathematics* **75** (2017), 677–696.

[6] J. Klobusicky and G. Menon, Hydrodynamic limit theorems for a piecewise deterministic Markov process with two species. In process.

Theory and Uncertainty Quantification of Coarse-Grained Molecular Dynamics

Paul N. Patrone
Andrew Dienstfrey
Geoffrey McFadden

In materials modeling, industrial R&D teams are increasingly reliant on computational tools such as molecular dynamics (MD) to speed up development and market insertion of next-generation materials. The ultimate dream of this strategy is to realize an "atoms-to-airplane" paradigm in which structural components such as wings can be designed in silico to meet certain strength requirements, given only knowledge of the underlying material composition. However, MD is generally limited to simulating systems with millions of atoms or less over timescales of nanoseconds, far short of the sizes and timescales required for macroscopic component-level models. To overcome this problem, modelers have proposed a variety of coarse graining strategies that attempt to "project-out" unnecessary degrees-of-freedom and thereby reach larger scales. But to date, no one technique has been accepted as a practical solution for coarse-grained (CG) modeling in high-throughput industrial settings.

From a mathematical standpoint, a key problem with many CG strategies is that they remove microscopic information about systems in an ad-hoc manner

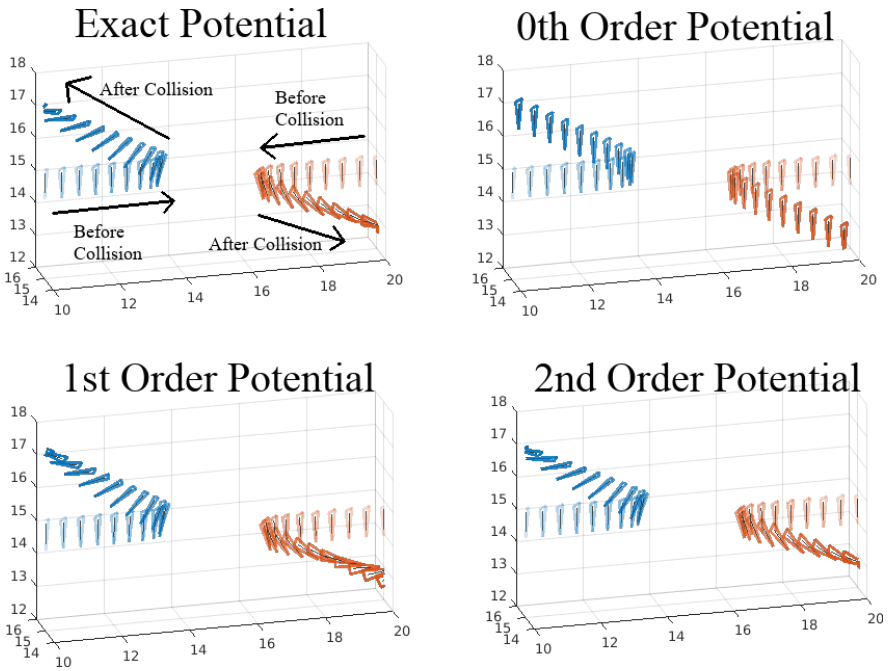

Figure 55. *Collision between triangular particles computed using an exact, atomistic potential, as well as the multipole potential truncated at various orders. Note that the trajectories agree more closely with increasing orders of approximation.*

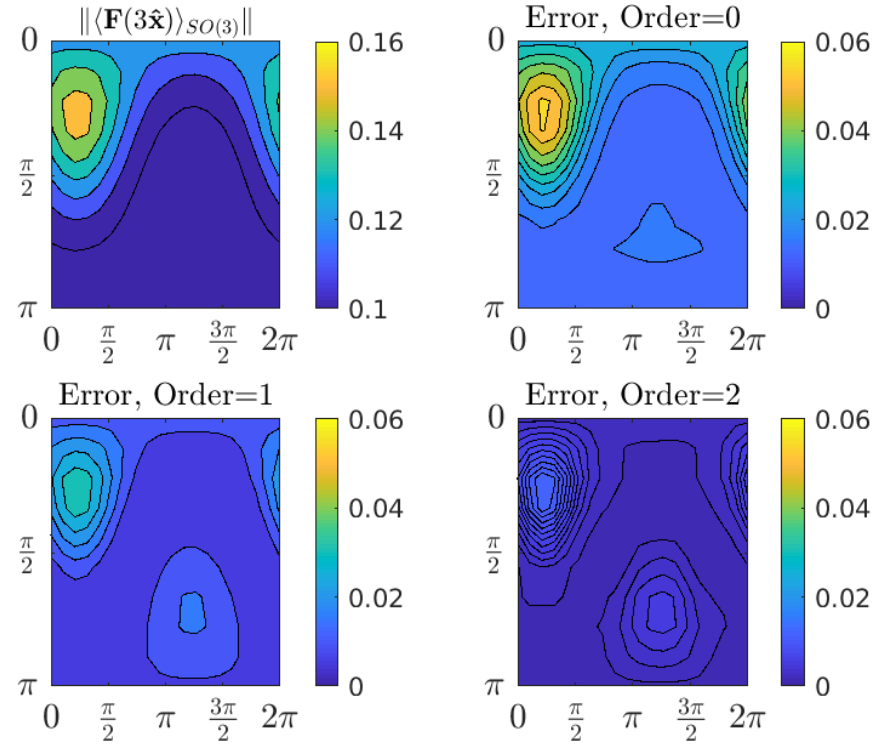

Figure 56. *Comparison between the exact, atomistic potential and various multipole approximations for the triangular particles shown in the figure above. Here the potential has been averaged over all orientational degrees of freedom associated with one of the particles at a fixed center-of-mass separation distance. The horizontal and vertical axes correspond to the two remaining orientational degrees of freedom. Note that the upper left plot is the average of the exact potential, whereas the remaining three plots are relative errors in various multipole approximations; moreover, the latter decreases with increasing order of approximation*

and without any reference to limiting processes or quantitative error estimates. This has created a situation in which it is impossible to know beforehand how accurate a CG method is, so that expensive all-atom simulations are still necessary for validation purposes. More problematic, such approaches do not provide a theoretical framework to address the fundamental question of how much information a CG model can preserve about its atomistic counterpart. Thus, the materials science community does not have clear perspective on what can be achieved through such techniques.

To address these issues, ACMD staff have been developing a hierarchy of approaches that link models with increasing degrees of complexity to their all-atom counterparts. The first of these is a method of course graining rigid-body molecules by reformulating their interaction potential in terms of a generalized multipole expansion. The benefit of this approach is that it allows one to explicitly control the order of approximation through truncation of the expansion at any given order. It also provides a connection to a popular class of CG techniques that project the molecular structure onto point particles. Importantly, our analysis reveals that such approaches introduce unphysical symmetries and eliminate energetic and physical effects due, e.g., to angular momentum. These results have been published in a pair of manuscripts and presented at an international workshop on uncertainty quantification and coarse graining [1, 2].

Current work aims to extend this hierarchy by connecting rigid-body models

to their fully flexible atomistic counterparts. In this context, we are pursuing a pair of asymptotic methods that treat coarse graining of thermodynamics and dynamics separately. The goal is to determine the extent to which these techniques are consistent with one another, which would address the question of how much information can be preserved in a CG model. We anticipate that this work will lead to additional publications and open-source implementations.

[1] P. N. Patrone, A. Dienstfrey, and G. B. McFadden. Model Reduction of Rigid-body Molecular Dynamics via Generalized Multipole Potentials. *Physical Review E* **100** (2019), 063302. DOI: 10.1103/PhysRevE.100.063302

[2] P. N. Patrone, A. Dienstfrey, and G. B. McFadden. Towards A Priori Uncertainty Quantification of Coarse-Grained Molecular Dynamics: Generalized Multipole Potentials. In *Proceedings of the AIAA SciTech 2019 Forum*, San Diego, California, January 7-11, 2019. DOI: 10.2514/6.2019-0971.

The Effect of Vacancy Creation and Annihilation on Grain Boundary Motion

Geoffrey McFadden
William Boettinger (NIST MML)
Yuri Mishin (George Mason University)

Many important applications in materials science involve the interaction of stress and grain boundary behavior in crystalline solids. A crystalline solid typically consists of grains with given crystal orientations that are separated by grain boundaries (GBs) where the orientation changes. Typical grain sizes can range from hundreds of micrometers to large single crystals that can be on the order of centimeters. Of particular interest is the development of appropriate boundary conditions that are used in models of moving grain boundaries.

The interaction of vacancies with grain boundaries is involved in many processes occurring in materials, including radiation damage healing, diffusional creep, and solid-state sintering. We have recently developed a model [1] that describes a set of processes occurring at a GB in the presence of a non-equilibrium, non-homogeneous vacancy concentration. Such processes include vacancy diffusion toward, away from, and across the GB, vacancy generation and absorption at the GB, and GB migration. Numerical calculations based on this model [2] reveal that the coupling among the different processes gives rise to interesting phenomena, such as vacancy-driven GB motion and accelerated vacancy generation/absorption due to GB motion.

In the numerical treatment of the model the motion of grain boundaries is simulated using a mapping to a fixed computational domain which is computed along with the evolution of the diffusion fields from various initial conditions. The dynamics can also be studied analytically by considering small-amplitude perturbations to equilibrium states which can described by a normal mode analysis of the linearized governing equations, illustrating the roles played by the various terms in the boundary conditions. Future work is anticipated to include the effects of surface energy and surface stress in curved geometries during grain growth, as well as the implementation of related phase-field models [3] that could aid in the description of more complicated geometries.

[1] Y. Mishin, G. B. McFadden, R. F. Sekerka, and W. J. Boettinger. Sharp Interface Model of Creep Deformation in Crystalline Solids. *Physical Review B* **92** (2015) 064113. DOI: 10.1103/PhysRevB.92.064113

[2] G. B. McFadden, W. J. Boettinger, and Y. Mishin. The Effect of Vacancy Creation and Annihilation on Grain Boundary Motion. *Acta Materialia* **185** (2020) 66-79. DOI: 10.1016/j.actamat.2019.11.044

[3] Y. Mishin, J. A. Warren, R. F. Sekerka, and W. J. Boettinger. Irreversible Thermodynamics of Creep in Crystalline Solids. *Physical Review B* **88** (2013) 184303. DOI: 10.1103/PhysRevB.88.18430

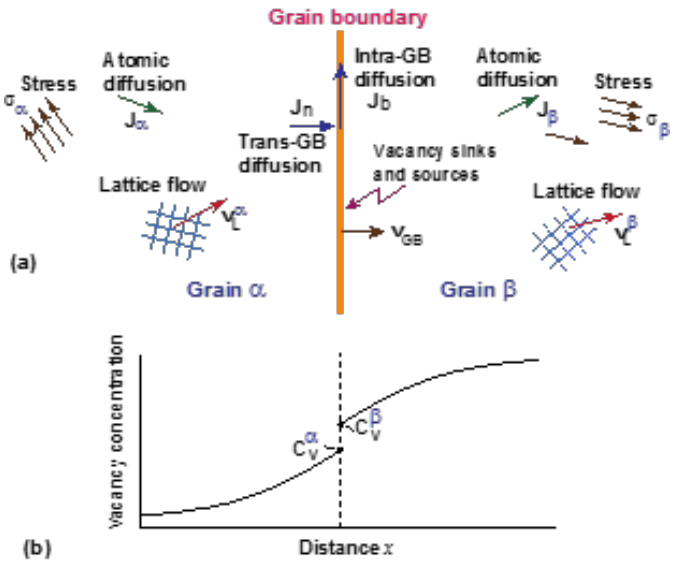

Figure 57. *The physical processes occurring at the grain boundary and in the grains within the proposed model.*

Shear Localization in Bulk Metallic Glasses

Timothy Burns

Bulk metallic glass (BMG), a.k.a. amorphous metal, is a promising new material for a variety of applications [1, 2, 10]. It is twice as strong as titanium, has excellent resistance to wear and corrosion, and is tougher and more elastic than ceramics. In a conventional metallic alloy, as the mixture is cooled from the liquid state, the atoms of the metal arrange themselves into a pattern of crystals, called grains, which typically have different sizes and shapes. Such structures are produced by the nucleation and growth of crystalline phases from the molten alloy during solidification. By contrast, in certain oxide mixtures (e.g., silicate glasses), the nucleation and growth kinetics are significantly slower, with the result that the liquid can be readily undercooled far below the melting point of crystals (e.g., a quartz crystal) [2].

At sufficiently deep undercooling, both oxide melts and some metallic liquids undergo a *glass transition* and freeze as vitreous solids. As a result, the microstructure of metallic glass is very different from that of conventional metals. Instead of arranging themselves into a polycrystalline granular structure, the atoms of metallic glasses become "frozen" into a random, disordered structure. It is this amorphous structure that gives metallic glasses remarkable toughness, hardness, elasticity, strength, and resistance to corrosion and wear. These properties of BMG's have stimulated research into the use of these new materials for important structural applications, including medical devices, such as prosthetics [2, 10].

Unfortunately, when these materials flow plastically at room temperature, the flow rapidly tends to become highly localized into narrow shear bands, with a thickness on the scale of nanometers [1, 2, 5-10]. This initiation and growth of shear bands can lead to catastrophic fracture in a BMG, which severely limits the material's usefulness. Thus, an important problem is to understand the physical mechanisms that control this process, such as the production and transport of heat, free volume, and momentum.

Some theoretical studies have argued that this strain localization is controlled not by rapid heating, as is the case with adiabatic shear band formation in polycrystalline metals [3, 4], but rather by a change in the concentration of free volume in the material [8, 9], while others argue that it is controlled by a combination of heating and free volume effects [5]. Numerical simulation of the linear ordinary differential equations that model perturbed shear flow in a BMG (Figure 58) shows that the controlling term is $\partial f/\partial \xi$, the rate of change of plastic strain with respect to free volume (see Figure 59). In this sense, the instability is driven by the free volume, not the temperature. Furthermore, the simulations indicate that there is a large increase in the perturbed temperature associated with the growth in the free volume, which implies that shear bands are associated with rapid heating [9]. Current work has been focused on using asymptotic methods to elucidate the dependence of the perturbation equations on the perturbation wavelength ω.

$$\frac{d\delta_\gamma}{dt} = \frac{\partial f}{\partial \xi}\delta_\xi + \frac{\partial f}{\partial \theta}\delta_\theta$$

$$\frac{d\delta_\xi}{dt} = -\beta_4 (L\omega)^2 \delta_\xi + \frac{\partial g}{\partial \xi}\delta_\xi + \frac{\partial g}{\partial \theta}\delta_\theta$$

$$\frac{d\delta_\theta}{dt} = -(L\omega)^2 \delta_\theta + \beta_3 \tau \left(\frac{\partial f}{\partial \xi}\delta_\xi + \frac{\partial f}{\partial \theta}\delta_\theta\right)$$

$$\beta_3 \approx 0.5, \;\; \beta_4 \approx 10^{-10}, \;\; max(\tau) \approx 10, \;\; L \approx 10^{-5}$$

Figure 58. *Linearization of nondimensionalized continuum model of shear flow in a BMG. Dominant term is $\partial f/\partial \xi$, the rate of change of plastic strain with respect to free volume. Subscripts γ and θ correspond to shear strain and temperature. τ is the shear stress.*

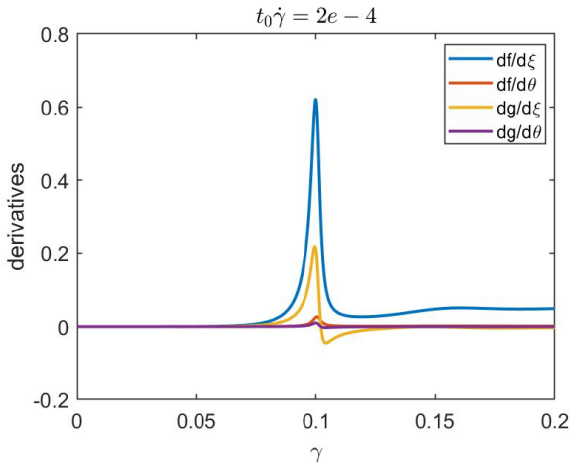

Figure 59. *Derivatives of constitutive functions for plastic flow $\boldsymbol{f}(\boldsymbol{\xi}, \boldsymbol{\theta}, \boldsymbol{\tau})$ and free volume $\boldsymbol{g}(\boldsymbol{\xi}, \boldsymbol{\theta}, \boldsymbol{\tau})$, with respect to a simple shearing deformation at a constant rate of strain.*

[1] M. F. Ashby and A. L. Greer. Metallic Glasses as Structural Materials. *Scripta Materialia* **54** (2006), 321-326.

[2] E. Axinte Metallic Glasses from "Alchemy" to Pure Science: Present and Future of Design, Processing and Applications of Glassy Metals. *Materials and Design* **35** (2012), 518-556.

[3] T. J. Burns. Approximate Linear Stability Analysis of a Model of Adiabatic Shear Band Formation. *Quarterly of Applied Mathematics* **43** (1985), 65-84.

[4] M. A. Davies and T. J. Burns. Thermomechanical Oscillations in Material Flow During High–Speed Machining. *Philosophical Transactions of the Royal Society of London, A* **359** (2001), 821-846.

[5] L. H. Dai and Y. L. Bai. Basic Mechanical Behaviors and Mechanics of Shear Banding in BMGs. *International Journal of Impact Engineering* **35** (2008), 704-716.

[6] Y. F. Gao, B. Yang, and T. G. Nieh. Thermomechanical Instability Analysis of Inhomogeneous Deformation in Amorphous Alloys. *Acta Materialia* **55** (2007), 2319-2327.

[7] R. Huang, Z. Suo, J. H. Prevost, and W. D. Nix. Inhomogeneous Deformation in Metallic Glasses. *Journal of the Mechanics and Physics of Solids* **50** (2002), 1011-1027.

[8] M. Q. Jiang and L. H. Dai. On the Origin of Shear Banding Instability in Bulk Metallic Glasses. *Journal of the Mechanics and Physics of Solids* **57** (2009), 1267-1292.

[9] F. Spaepen. Must Shear Bands Be Hot? *Nature Materials* **5** (2006), 7-8.

[10] M. M. Trexler and N. N. Thadhani. Mechanical Properties of Bulk Metallic Glasses. *Progress in Materials Science* **55** (2010), 759-839.

Generalizing Zeno

John Nolan
Jack Douglas (NIST MML)
Debra Audus (NIST MML)

Zeno[18] is a widely used program to examine the structure of complex objects, e.g., DNA, proteins, polymers and other objects. Zeno uses random walk simulations to hit the object of interest. The classical theory connects hitting probabilities of Brownian motion with the capacity of the object. Our research aims to generalize this approach by replacing Brownian motion with Levy alpha-stable motions and accurately calculate the alpha capacity of an object. This would give an alternative view of these objects. Our expectation is that using different alpha values will give multiple views of an object, revealing more about its structure.

This work involves a mixture of new methods and computer codes to simulate these stable motions. The first approach was to generate many random paths using simulation methods for isotropic stable laws. The second method is to generalize the "walk on spheres" method used in Zeno to improve the efficiency of the simulations. Luc Devroye at McGill University and J. Nolan have developed algorithms to simulate first hitting times and hitting locations for stable processes. Nolan has implemented them in an R package. The exact connection between hitting probabilities for stable motions and alpha capacity is not as direct as in the Brownian case; we are currently using simulation methods to quantify this relationship.

[18] https://zeno.nist.gov/

High Performance Computing and Visualization

Computational capability continues to advance rapidly, enabling modeling and simulation to be done with greatly increased fidelity. Doing so often requires computing resources well beyond what is available on the desktop. Developing software that makes effective use of such high-performance computing platforms remains very challenging, requiring expertise that application scientists rarely have. We maintain such expertise for application to NIST problems. Such computations, as well as modern experiments, typically produce large volumes of data, which cannot be readily comprehended. We are developing the infrastructure necessary for advanced interactive, quantitative visualization and analysis of scientific data, including the use of 3D immersive environments, and applying the resulting tools to NIST problems.

Simulation of Dense Suspensions: Cementitious Materials

William George
Nicos Martys (NIST EL)
Clarissa Ferraris (NIST EL)
Steven Satterfield
Judith Terrill

A suspension is a collection of solid inclusions embedded in a fluid matrix. Suspensions play an important role in a wide variety of applications including paints, cement-based materials, slurries, and drilling fluids. Understanding the flow properties of a suspension is necessary in many such applications. However, measuring and predicting flow properties of suspensions remains challenging.

Suspensions can be quite complex, as the inclusions may have a wide range of shapes and a broad size distribution. Further complicating matters is that different matrix fluids may have quite disparate flow behavior. While the simplest type of matrix fluid is Newtonian, where the local stress is proportional to the shear rate, the matrix fluid can also be non-Newtonian, exhibiting quite complex behavior including shear thinning (viscosity decreases with shear rate), shear thickening (viscosity increases with shear rate), viscoelasticity (exhibiting both viscous and elastic properties), or even have a time dependent viscosity (thixotropic).

We have two on-going studies on the rheology of cementitious materials, which are dense suspensions in non-Newtonian matrix fluids.

SRMs for Mortar and Concrete. Rotational rheometers, devices that measure fluid properties such as viscosity, are routinely used for homogeneous materials such as oils, but their use on dense suspensions, such as concrete, is a relatively new phenomenon. Since measurements with rheometers involve flow in a complex geometry, it is important that they are calibrated with a well characterized standard reference material (SRM). We are developing such SRMs in collaboration with the NIST Engineering Laboratory.

NIST produced an SRM for cement paste (SRM 2492) as the first step in the development of a reference material for concrete rheometers. The second step, the development of an SRM for mortar (SRM 2493), was completed in 2017 and is currently available. The material properties of the mortar SRM, such as viscosity, could not be measured in fundamental units with certainty. Thus, simulation was used to determine the viscosity of the mortar. To obtain the necessary fidelity in the simulations, a high-performance computing facility was used. Results of these simulations were compared with physical experiments as validation.

In 2019 we released SRM 2497, a standard reference concrete for rheological measurements [1]. The concrete SRM is comprised of the previously released mortar SRM with the addition of suspended 10 mm diameter hard glass spheres. The certified values for SRM 2497 were determined using the simulation results previously computed for the mortar SRM. As an indication of the impact of this work, the use of the cement paste and mortar SRMs are referenced in the new ASTM standard test method for measuring the rheological properties of cementitious materials [2].

We are currently running a suite of simulations of the cement SRM using the cement paste as the matrix fluid in which both 1 mm and 10 mm diameter hard spheres are suspended. The results of these simulations should match the results from simulations comprising the mortar SRM as the matrix fluid with suspended 10 mm hard spheres. Depending on the outcome of these simulations, the concrete SRM certification may need to be updated. The current suite of concrete simulations is expected to complete in the next year.

Flow of Dense Suspensions in Pipes. Understanding the flow of suspensions in pipes is important for a wide variety of applications. For example, in the construction industry, concrete is often placed by pumping it through extensive pipe systems. However, research on predicting the pumpability of concrete has been limited due to the heavy equipment and large amounts of material

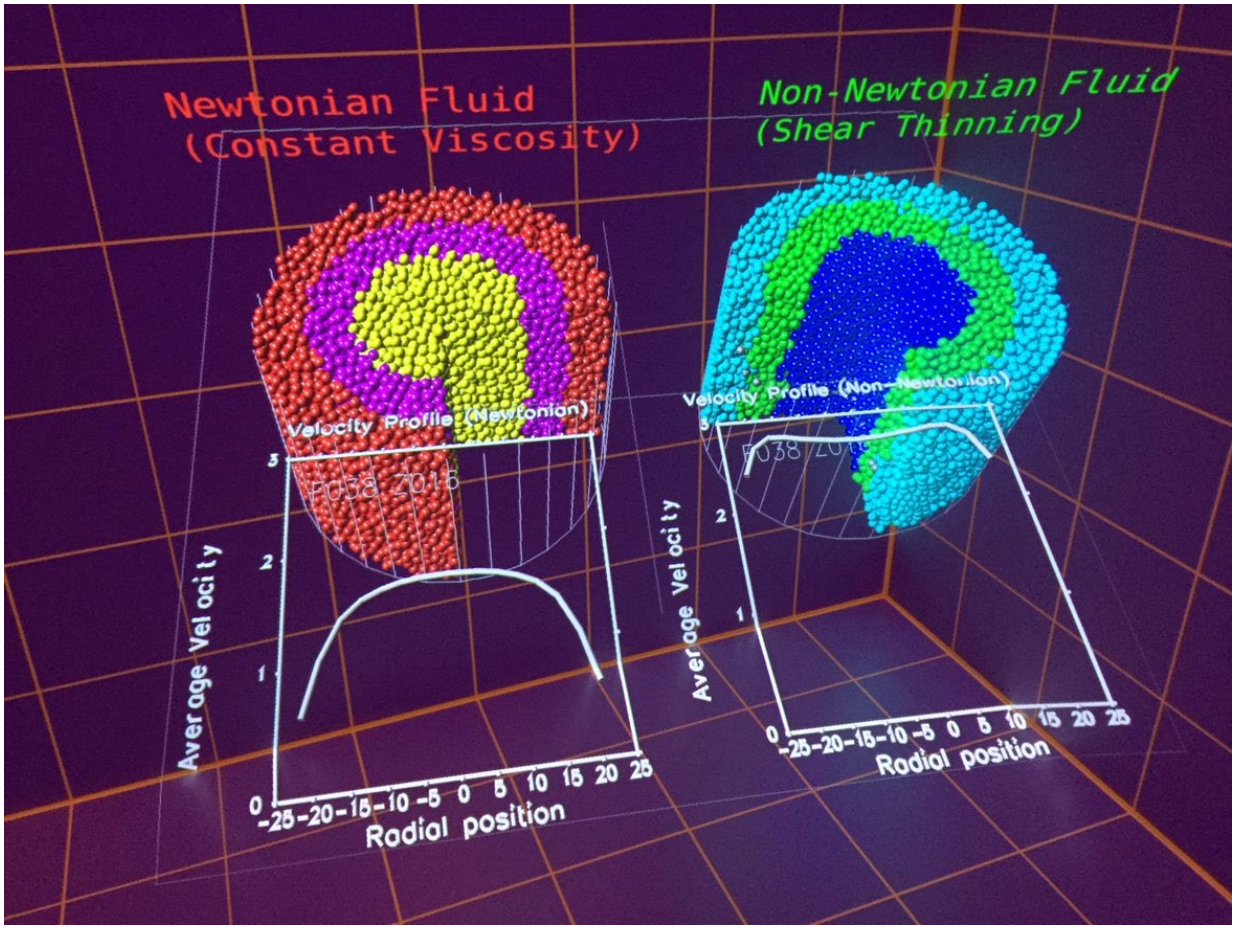

Figure 60. *Side-by-side comparison of identical systems with only a single property of the matrix fluid changed, one Newtonian and the other non-Newtonian (shear thinning)*

needed. Suspension flow in pipes is also important in the developing field of 3D additive manufacturing.

Predicting the flow of this complex fluid, which is composed of a non-Newtonian matrix fluid with suspended solid inclusions flowing under pressure, is challenging. Flow in these systems is also complicated by variety of phenomena such as slip at the wall and shear induced migration, which has only been studied for the simpler case of a suspensions with a Newtonian matrix fluid. A detailed discussion of this topic is available in a NIST Technical Note [3]. It is also the case, especially in the case of 3D additive manufacturing, that the placement of these materials is time sensitive, from the time the material is initially mixed to the time it is pumped and placed [4].

We have been conducting detailed simulations of the flow of suspensions through pipes to enable the development of predictive flow models and to advance measurement science in this field. Through quantitative analysis and visualization of results, we have gained insight into shear-induced migration and slip behavior in these systems. For example, Figure 60 shows a side-by-side comparison of identical systems with only a single property of the matrix fluid changed, one Newtonian and the other non-Newtonian (shear thinning). Over the last year we have been conducting a suite of simulations of shear thinning and shear thickening suspensions, varying the properties of the matrix fluid and the driving force.

Using computations to study the flow velocity fields as a function of driving force, we have discovered a useful scaling relationship. Given that the matrix fluids have a viscosity, μ, that relates to the strain rate, $\dot{\gamma}$, such that

$$\mu \propto \dot{\gamma}^n$$

we have determined that the system velocity in the pipe, v, is related to the driving force, g, as

$$v \propto g^{1/(1+n)}$$

So, for example, with a shear thinning matrix fluid with $n = -0.5$, we have

$$v \propto g^{1/(1-0.5)} = g^2$$

and with a matrix fluid which is shear thickening, with $n = 0.5$, we have

$$v \propto g^{1/(1+0.5)} = g^{2/3}$$

Notice that this scaling relation depends on the power-law behavior of the non-Newtonian matrix fluid. As a consequence, given a few measurements of the flow velocity versus the driving force of the suspension, one can determine the power law behavior of the suspension, and indeed we can then also determine the power law behavior of the matrix fluid.

In the last year, before our simulations completed, we presented some preliminary results [5]. In the fall of 2019, each of our pipe-flow simulations reached a steady state. Final results showed agreement with the model predictions to within 15 %. In November 2019 we submitted a paper detailing our findings to the Journal of Rheology [6].

Nanoscale Suspension Flow. New instrumentation at NIST's NCNR allows for the study of flow in nanoscale parallelepiped channels using neutron scattering. In support of this study, we are extending the capability of the NIST Quaternion-based Dissipative Particle Dynamics (QDPD) dense-suspension code to model similar flows, matching interparticle interactions and flow rates, for comparison to these new scattering experiments. This work will also be extended to include suspensions of monoclonal antibodies and other extended or non-spherical objects in the flow geometry.

[1] N. S. Martys, W. L. George, R. P. Murphy, and K. Weigandt. Certification of SRM 2497: Standard Reference Concrete for Rheological Measurements. NIST Special Publication 260-194, April 2019, 116 pages. DOI: 10.6028/NIST.SP.260-194

[2] ASTM Standard C1874, 2019, "New Test Method for Standard Test Method for Measuring the Rheological Properties of Cementitious Materials using a Coaxial Rotational Rheometer." ASTM International, West Conshohocken, PA, 2019. DOI: 10.1520/C1874-2019

[3] M. Choi, C. F. Ferraris, N. S. Martys, V. K. Bui, H. R. Trey Hamilton, and D. Lootens. Research Needs to Advance Concrete Pumping Technology. NIST Technical Note 1866, 2015. DOI: 10.6028/NIST.TN.1866

[4] S. Z. Jones, D. P. Bentz, N. S. Martys, W. L. George, and A. Thomas. "Rheological Control of 3D Printed Cement Paste." Digital Concrete 2018: First International Conference on Concrete and Digital Fabrication, Zurich Switzerland, September 9-12, 2018.

[5] N. S. Martys, W. L. George, S. G. Satterfield, and S. Z. Jones. "Computational Modelling of Suspension Flow in Pipes: Application to Cement Based Materials." 90th Annual Meeting of The Society of Rheology, Houston, TX October 14-18, 2018.

[6] Nicos S. Martys, William L. George, Ryan P. Murphy, and Kathleen Weigandt. Pipe Flow of Sphere Suspensions having a Power-Law-Dependent Fluid Matrix. In review.

Monoclonal Antibodies Under High Shear

William George
Nicos Martys (NIST EL)
Steven Satterfield
Judith Terrill

Recent advances at the NIST Center for Neutron Research (NCNR) have enabled neutron scattering experiments for the study of the development of long-range structure and phase transitions under pressure-driven flow conditions in a tube geometry. This capability was developed, in part, to study therapeutic proteins, such as monoclonal antibodies, as they flow under high shear rate, such as would be encountered during direct injection via a hypodermic needle.

Such direct injection is desired because it would simplify the delivery of these therapeutic proteins, which are currently only administered intravenously. However, since such injections can lead to shear rates on the order of $10^6/s$, there is concern that this could lead to structural degradation of the molecules. Even small distortions of the molecular structure could cause aggregation of the protein. The most dangerous potential consequence of such distortion and agglomeration is that the patient may develop an allergic reaction to the medication. Recorded fatalities have occurred where immunogenic response to such aggregates is suspected. For these reasons it is necessary for the pharmaceutical companies to demonstrate that the structure of protein therapeutics is not degrading before high shear rate delivery methods can be utilized.

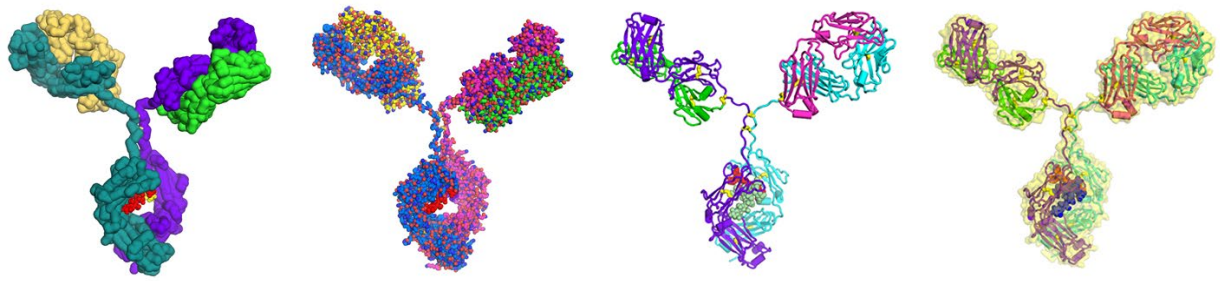

Figure 61. *Simulation of the NIST monoclonal antibody (NIST mAb) Reference Material (SRM 8671).*

In support of this research, we have been extending the capabilities of our dense-suspension simulator, QDPD, to match the physical experiments being performed at the NCNR. Recent experiments are in good agreement with preliminary QDPD simulations of similar systems, that is, the flow of suspensions in a tube.

The extensions to QDPD will enable the simulation of suspensions of the NIST monoclonal antibody (NIST mAb) Reference Material (SRM 8671) shown in Figure 61. In collaboration with NCNR, the NIST Engineering Lab, and the NIST Material Measurement Lab, we plan to carry out a suite of simulations designed to determine the effect of the flexibility within monoclonal antibodies on the suspension's viscosity for a set of volume fractions and shear rates like that studied at NCNR.

In addition to the rheological studies, we will also modify QDPD to generate pertinent data from our NIST mAb simulations that will assist in the analysis of neutron scattering data from NCNR experiments on such systems. This is needed since experimental neutron scattering results so far have been shown to be difficult to interpret, primarily due to their complexity.

HydratiCA, In Situ Analysis and Machine Learning

Judith Terrill
Justyna Zwolak
James Filliben
Jeffrey Bullard (Texas A&M University)

With the extremely long running times and the very large simulations that we now work on, it is not possible to write out detailed data during the runs. But there are things that need to be studied in the simulations while they are running. The only way forward is to do the needed analysis during the runs. The disadvantage is that the analyses need to be done locally in each cell of the simulation and without outside interaction.

We are using a large-scale simulation code, HydratiCA [1], to develop and test our techniques. HydratiCA is a stochastic reaction-diffusion model of cement hydration. Hydration transforms paste from a fluid suspension (e.g., cement powder mixed with water) into a hardened solid. This process involves complex chemical and microstructural changes. Understanding and predicting the rates of these changes is a longstanding goal.

HydratiCA integrates a PDE forward in time using small time steps on a 3D lattice of sites, and data analysis is challenging because a single timestep generates a large, many-dimensional data set. Furthermore, there are large parts of that data that are either empty or not interesting to the scientists. Our original goal was to try to understand and predict the conditions when a lattice site either runs out of material or space and causes the simulation to greatly reduce the time step to resolve phenomena which are, in fact, negligible, and thus substantially increasing the simulation time with no benefit.

To address this issue, we first searched for a good descriptor (something which can be used to characterize something else; i.e., a dimension of representation space). We discovered that reaction saturation index [2, 3], a quantitative measure of how far a reaction is from equilibrium and also a measure of the thermodynamic driving force for growth, provided valuable information on the state of the simulation at each site. We successfully modeled the saturation index vs simulation time using Chebyshev polynomials and achieved a dramatic reduction in data because more than a million time steps could easily be reduced to 20 coefficients. This had the additional benefit of smoothing the data which enabled us to calculate reliable first and second derivatives. Now the simulation data could be reduced to a few states. It was then straightforward to find the peaks in the curve that indicated when and where the simulation was running short of resources [4].

Evaluating the Quality of the Fits. Curve fitting goes on in each cell of the simulation. But the goal for real-world runs consists of sizes of the order of 1000^3 cells. Because of the size, it is not possible to look at this data. So, the fits need to be done locally at each cell and without outside intervention. And this means the quality of these fits needs to be evaluated locally. There are recognized ways of doing this. But as Matejka and Fitzmaurice [5, 6] and others have demonstrated, single number statistics are not robust enough for this to be relied upon. The solution is to use images of plots and have a trained classifier "look" at them and report a classification. In the coming year, we will be using data from decades of experiments at NIST[19] to create datasets that we compute statistics on and convert into images. Using these, we will build deep learning classifiers that we can use to provide us with information on the quality of fits.

Relationship to Laboratory Experiments. After finding the peaks in the saturation index, it was remembered that these peaks have also been seen in some laboratory experiments [7] and still are not well understood. This opens up an avenue to design laboratory experiments and corresponding simulation runs to do direct comparisons between the experiments and simulation outputs.

[1] J. W. Bullard, E. Enjolras, W. L. George, S. G. Satterfield, and J. E. Terrill. A Parallel Reaction-Transport Model Applied to Cement Hydration and Microstructure Development. *Modelling and Simulation in Materials Science and Engineering* **18**:2 (2010), 18.

[19] https://www.itl.nist.gov/div898/software/dataplot/homepage.htm

[2] J. W. Bullard, G. W. Scherer, and J. J. Thomas. Time dependent Driving Forces and the Kinetics of Tricalcium Silicate Hydration. *Cement Concrete Research* **74** (2015), 26–34.

[3] A. E. Nielsen and J. M. Toft. Electrolyte Growth in Crystals. *Journal of Crystal Growth* **67** (1984) 278-288.

[4] J. E. Terrill. ''Curve Fitting with Validation as a First Step to the Discovery of Physical Laws.'' Workshop III: Validation, Guarantees in Learning Physical Models: from Patterns to Governing Equations to Laws of Nature, UCLA Institute for Pure, and Applied Mathematics (IPAM), Los Angeles, CA, October 28, 2019.

[5] A. Cairo. Download the Datasaurus: Never Trust Summary Statistics Alone; Always Visualize Your Data. Albert Cairo's www.functionalart.com, A Weblog about Information Design and Visualization, August 29, 2016. URL: http://www.thefunctionalart.com/2016/08/download-datasaurus-never-trust-summary.html

[6] J. Matejka and G. Fitzmaurice. Same Stats, Different Graphs: Generating Datasets with Varied Appearance and Identical Statistics through Simulated Annealing. In *Proceedings of the 2017 ACM SIGCHI Conference on Human Factors in Computing Systems*, May 6-11, 2017, Denver, CO.

[7] J. M. Makar, G. W. Chan, and Y. Esseghaier. A Peak in the Hydration Reaction at the End of the Cement Induction Period. *Journal of Material Science* **42** (2007), 1388–1392.

Nanostructures and Nano-Optics

James S. Sims
Judith Terrill
Garnett W. Bryant (NIST PML)
Jian Chen (OSU)
Henan Zhao (UMBC)

Research and development of nanotechnology, with applications ranging from smart materials to quantum computation to biolabs on a chip, remains a national priority. Semiconductor nanoparticles, also known as nanocrystals and quantum dots (QDs), are one of the most intensely studied nanotechnology paradigms. Nanoparticles are typically 1 nm to 10 nm in size, with a thousand to a million atoms. Precise control of particle size, shape and composition allows one to tailor charge distributions and control quantum effects to obtain properties completely different from the bulk and from small clusters. Due to enhanced quantum confinement effects, nanoparticles act as artificial, man-made atoms with discrete electronic spectra that can be exploited as light sources for novel enhanced lasers, discrete components in nanoelectronics, qubits for quantum information processing, and enhanced ultrastable fluorescent labels for biosensors to detect, for example, cancers, malaria or other pathogens, and to do cell biology.

We are working with the NIST Physical Measurement Laboratory to develop computationally efficient large-scale simulations of such nanostructures, and also to develop immersive visualization techniques and tools to enable analysis of highly complex computational results of this type. The electrical, mechanical, and optical properties of semiconductor nanocrystals and quantum dots are studied. In the most complex structures this entails modeling with on the order of a million atoms. Highly parallel computational and visualization platforms are critical for obtaining the computational speeds necessary for a systematic, comprehensive study.

Our current code creates a wave function with maximum spin up, one with maximum spin down, and two intermediate ones. The addition of a magnetic field provides a probe to split excitonic states, providing a more complete spectroscopy of quantum dot optics. This allows us to isolate contributions from spin-orbit coupling, Zeeman and spatial motion. Magnetic field response depends sensitively on the QD size and shape.

It is the addition of a magnetic field which allows for the intrinsic spins of the electrons to lead to different effects in a magnetic field depending on the QD size and shape, and it is necessary to be able to see the effect of spin in different QD arrangements. Without visualization, it becomes very difficult to understand what this distribution is and how it changes for different magnetic fields, electric fields or strain. This distribution is critical for understanding exchange interactions or electron/nucleus interactions in quantum devices. These properties are intimately connected with the performance of these structures in quantum information processing. In the most complex structures this entails modeling structures with on the order of a million atoms.

As the device size in Si electronics continues to decrease, the devices are rapidly approaching the atomic scale where a change in only a few atoms can make a significant change in device performance. At the same time, the ability to make Si nanodevices with only a few, deterministically placed dopant atoms opens up the possibility of creating quantum information processing devices with these structures. We are currently participating in a research program to make, characterize and model both traditional and quantum Si devices at this few-dopant atom limit.

During the past year, we have focused on using the atomistic tight-binding simulation tool and the visualization tools to analyze the electronic and spin properties of quantum dot systems where alloy effects in the barrier between dots are critical. This includes studies of InGaAs quantum dots with bismuth added to the GaAs barrier to enhance hole spin mixing. This could lead to novel ways to use these hole spins as qubits with ultrafast, optical control. This work was done in collaboration with students from the Joint Quantum Institute and with researchers at the University of Delaware who are trying to make these structures. This

work has been published in *Physical Review B* and a second publication is being prepared.
The current serial codes used to simulate dopant-based devices in silicon were extended this past year to be a parallel code to exploit the computing power of NIST's Linux cluster. The current parallel simulation tool is being used as a template for implementing the parallel version of this new code. These simulation tools have also been applied to atomic-scale dopant-based Si electronic, quantum and photonic devices.

At the same time, ongoing analysis of results from the simulations of various nanodevices are supported by enhanced visualization tools developed in ITL. The significant speedup of these visualization tools makes them practical to use on data from million-atom device simulations both for visualization at the desktop and for 3D visualization. This has greatly facilitated analysis of these systems with large amounts of data. This is especially important for systems for random alloys. These tools allow one to determine which results are configuration specific and which apply to all random configurations of the same structure. Additional work was done on the on how separable versus integral feature dimensions affect the perception of magnitudes across a variety of tasks [1].

[1] H. Zhao and J. Chen. Bivariate Separable-Dimension Glyphs can Improve Visual Comparison of Holistic Features for Large-Range Magnitude Vector Data Visualization. In review.

High Precision Calculations of Fundamental Properties of Few-Electron Atomic Systems

James Sims
Stanley Hagstrom (Indiana University)
Maria Ruiz (University of Erlangen, Germany)
Bholanath Padhy (Khallikote College, India)

NIST has long been involved in supplying critically evaluated data on atomic and molecular properties such as the atomic properties of the elements contained in the Periodic Table and the vibrational and electronic energy level data for neutral and ionic molecules contained in the NIST Chemistry WebBook. Fundamental to this endeavor is the ability to predict, theoretically, a property more accurately than even the most accurate experiments. It is our goal to be able to accomplish this for few-electron atomic systems.

While impressive advances have been made over the years in the study of atomic structure, in both experiment and theory, the scarcity of information on atomic energy levels is overwhelming, especially for highly ionized atoms. The availability of high precision results tails off as the state of ionization increases, not to mention higher angular momentum states. In addition, atomic anions have more diffuse electronic distributions, thus representing more challenging computational targets than the corresponding ground states.

In the past two decades, there have been breathtaking improvements in computer hardware and innovations in mathematical formulations and algorithms, leading to "virtual experiments" becoming a more and more cost-effective and reliable way to investigate chemical and physical phenomena. Our contribution in this arena has been undertaking the theoretical development of our hybrid Hylleraas-CI (Hy-CI) wave function method to bring sub-chemical accuracy to atomic systems with more than two electrons.

Hy-CI has from its inception been an attempt to extend the success of the Hylleraas (Hy) method to systems with more than three electrons, and hence is an attempt to solve not just the three-body problem but the more general N-body problem [1]. Fundamental to the method is the restriction of one interelectronic coordinate r_{ij} per configuration state function (CSF). For atomic systems with greater than four electrons, all relatively precise calculations nowadays adopt the Hy-CI methodology of one r_{ij} term per CSF. In the case of three electron lithium systems, we have computed four excited states of the lithium atom to two orders of magnitude greater than has ever been done before [2]. At the four-electron level, to get truly accurate chemical properties like familiar chemical electron affinities and ionization energies, it is important to get close to the nanohartree level we achieved for the three-election atom, a significantly more difficult problem for four electrons than for three. By investigating more flexible atomic orbital basis sets and better configuration state function filtering techniques to control expansion lengths, we have been able to successfully tackle the four-electron case.

Progress to date has included computing the non-relativistic ground state energy of not only beryllium, but also many members of its isoelectronic sequence to 8 significant digit accuracy. With the results from our calculations and a least squares fit of the calculated energies, we have been able to compute the entire beryllium ground state isoelectronic sequence for Z = 4 through Z = 113 [3]. Li^- (with Z=3), nominally the first member of this series, has a decidedly different electronic structure and was not included in those calculations and subsequent discussions, but that "omission" has been corrected and we have subsequently carried out large, comparable calculation for the Li^- ground state [4].

The first member of the Be isoelectronic ground state sequence, the negative Li^- ion, is also a four-electron system in which correlation plays a very

important part in the binding. However due to the reduced nuclear charge, it is a more diffuse system in which one of its outer two L shell electrons moves at a greater distance from the nucleus than the other, and hence its nodal structure is different from that of a coupled L shell with an identical pair of electrons. The ground state of the singlet S state of Li^- is the same type of problem as the first excited state of Be; it is like Be(2s3s), not Be(2s2s). Completing this calculation has provided the necessary insight to enable the calculation of the Be first excited state of singlet S symmetry, Be(2s3s), to an order of magnitude better than previous calculations. Armed with this result, we have been able to continue this level of precision to the Be(2s4s) excited state, and have calculated the higher, more diffuse Be(2s5s) through Be(2s7s) states as well this past year, and in the process have demonstrated that Hy-CI can calculate the higher, more diffuse Rydberg states with more complicated nodal structures to the same level of accuracy as the less excited states.

While our work has demonstrated the efficacy of Hy-CI as a solution to the N-body problem for four or more electrons, this work has also shown the presence of a "double cusp" $r_{12}r_{34}$ term type slow convergence problem at the nanohartree accuracy level which is ultimately built into Hy-CI for four or more electrons. We are currently investigating whether a generalization of the Hy-CI method to an exponentially correlated Hy-CI (E-Hy-CI) method in which the single r_{ij} of an Hy-CI wave function is generalized to a form which pairs an exponential r_{ij} factor with linear r_{ij}. Since this type of correlation factor has the right behavior in the vicinity of the r_{ij} cusp, and also as r_{ij} goes to infinity, the hope is that this will overcome the eventual slow convergence of the double cusp and hence enable calculations for N > 4 to proceed with the same level of accuracy of the four electron calculations, for both ground and excited states.

[1] J. S. Sims and S. A. Hagstrom. Combined Configuration Interaction – Hylleraas Type Wave Function Study of the Ground State of the Beryllium Atom. *Physical Review A* **4**:3 (1971), 908. DOI: 10.1103/PhysRevA.4.908

[2] J. S. Sims and S. A. Hagstrom. Hy-CI Study of the 2 Doublet S Ground State of neutral Lithium and the First Five Excited Doublet S States. *Physical Review A* **80** (2009), 052507. DOI: 10.1103/PhysRevA.80.052507

[3] J. S. Sims and S. A. Hagstrom. Hylleraas-Configuration Interaction Nonrelativistic Energies for the Singlet S Ground States of the Beryllium Isoelectronic Series up Through Z = 113. *Journal of Chemical Physics* **140** (2014), 224312. DOI: 10.1063/1.4881639

[4] J. S. Sims. Hylleraas-Configuration Interaction Study of the Singlet S Ground State of the Negative Li Ion. *Journal of Physics B: Atomic, Molecular and Optical Physics* **50** (2017), 245003. DOI: 10.1088/1361-6455/aa961e

Machine Learning Enhanced Dark Soliton Detection in Bose-Einstein Condensates

Justyna P. Zwolak
Justin Elenewski (University of Maryland)
Amilson R. Fritsch (University of Maryland)
Ian B. Spielman (NIST PML)

Solitary waves (solitons) are non-dispersing spatially localized traveling waves that retain their size, shape, and speed as they move, and even when they collide with one another. Solitons appear naturally in oceans and water channels. In optical fibers, solitons have found commercial application for long-distance, high speed transmission lines. Since solitons can propagate without loss of energy for long distances, it has also been suggested that they can be used for communication technology and quantum switches and gates [1].

In repulsively interacting quasi-1D Bose-Einstein condensates (BECs), the soliton velocity governs its width, depth, and also other properties. Solitons can collide like hard spheres whose effective "radius" depends on the soliton velocity or pass through each other like "invisible" particles. Additionally, a soliton's velocity has been shown to determine its stability in three-dimensional traps. In any experiment involving solitons dynamics, a large amount of data needs to be analyzed. Absorption imaging is by far the most popular imaging technique used in ultracold atom experiments (see Step 1 in Figure 62). It can provide information about spatial distribution of atoms, their number, and average temperature. The image of the cloud of atoms with images of the probe and the background, can be combined to form the optical depth

$$O.D. = -\ln\frac{I_A - I_{BG}}{I_P - I_{BG}}$$

which is proportional to the local density of atoms (here, I_A denotes the probe light with a fraction absorbed by the atoms, I_P is the probe beam without the atoms, and I_{BG} is the residual light in the experiment when the probe beam is off). The challenge is identifying the location of one or many solitons from such images. While semi-scripted protocols can be used to process the data, in many cases the final decision about the number and position of the solitons within BEC has to be done manually [2].

We are developing an automated protocol for detecting and positioning dark solitons in BECs. Our proposed algorithm combines an automated data processing software with three convolutional neural networks (CNNs) pre-trained to identify the number of solitons present in a BEC (Step 2 in Figure 62) and, if solitons are detected, determine their position (Step 3 in

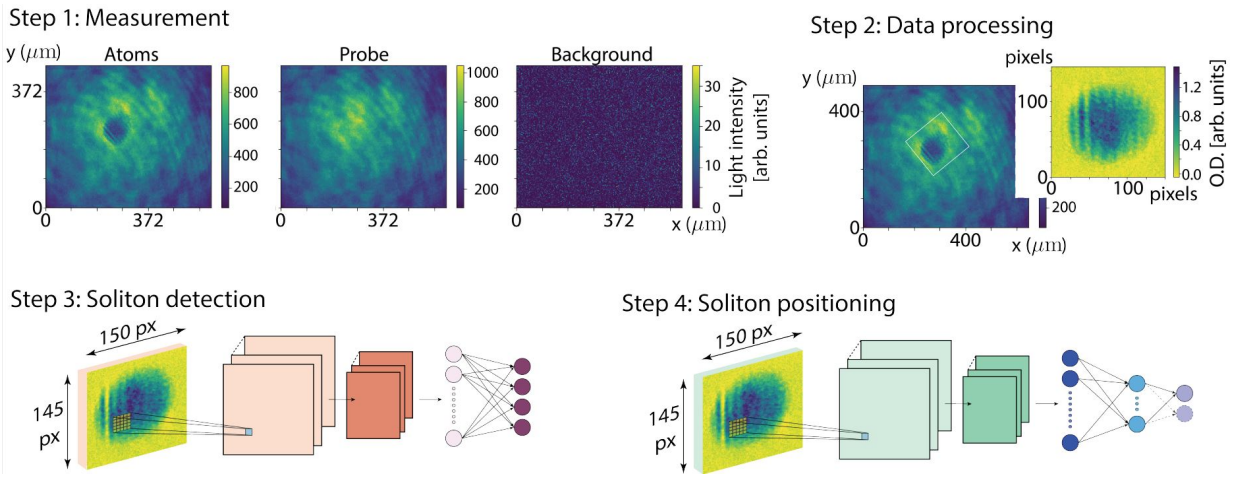

Figure 62. *Visualization of the soliton classification protocol. In Step 1, we show the experimental procedure to image the atoms. Left image (I_A) shows the probe light with a fraction absorbed by the atoms, center (I_P) shows the probe beam without the atoms, and right (I_{BG}) shows the residual light in the experiment when the probe beam is off). In Step 2, these three measurements are combined through Eq. (1) to obtain the final absorption image which is used for the analysis. Two machine learning algorithms are then used to identify the solitons, one to determine the number of solitons present (Step 3) and second one to determine the relative position of each soliton (Step 4) within a given cloud. The size of the last layer in the positioning network depends on the outcome of the classifier network.*

Figure 62). The four possible outcomes of the classifying network are

- no solitons,
- one soliton,
- two solitons, and
- other (e.g., more than two solitons, partial soliton).

If either the "no solitons" or "other" class is detected, the protocol terminates and returns the appropriate class. Otherwise, it proceeds to the positioning phase, selecting an appropriate positioning CNN based on the expected number of solitons.

Currently, we are developing the classifier network. To train it, we have manually labeled 1057 experimentally measured absorption images. Data augmentation enabled us to increase the size of the training data set to 1898 images. Using this data set, we were able to train a CNN to an accuracy of 79.5 % (with 90 % of data used for training and 10 % for validation). To further improve the performance of the classifier, we need more labeled data. As the manual annotation of experimental data is a very time-consuming procedure, we are developing a custom simulation protocol for BEC solitons that will allow us to generate a training set based on theory alone. By evolving condensate dynamics in real-time, we can produce a large set of absorption images for both single- and multi-soliton configurations in a trapped BEC. Most importantly, these configurations are intrinsically labelled based on the physical parameters of the underlying model.

While this research project is still at an early stage, the automated soliton detector that we have already tested highlights the applicability of machine learning-driven feature detection, rather than traditional curve fitting, to streamline cold atom research.

[1] L. M. Aycock, H. M. Hurst, D. K. Efimkin, D. Genkina, H-I Lu, V. M. Galitski, and I. B. Spielman. Soliton Diffusion in Bose–Einstein Condensates. *Proceedings of the National Academy of Sciences* **114** (2017), 2503-2508.

[2] A. R. Fritsch, Mingwu Lu, G. H. Reid, A. M. Piñeiro, and I. B. Spielman. Creating Solitons with Controllable and Near Zero Velocity in Bose-Einstein Condensates. arXiv:2004.04200.

WebVR Graphics

Sandy Ressler
Matthew Hoehler (NIST EL)
Frankie Willard (Poolesville High School)
Justin Slud (University of Maryland)
Adam Lenker (Messiah College)

WebVR continues to gain traction in the wider Web. In late 2019 the Immersive Web Working Group of the World Wide Web Consortium (W3C) introduced a new overarching standard that will eventually be supported by all major browser vendors. WebXR encompasses virtual reality (VR), augmented reality (AR), and mixed reality (MR). The W3C has a strong history of introducing standards which go on to be widely and successfully used. Mozilla's Firefox currently supports WebXR and we expect to see widespread adoption. Our work supports this trend by utilizing WebVR and will fully transition to WebXR in the coming year. Web based technologies remain the best method to distribute our work to the public, simplifying the process by eliminating the need for specialized software installations.

We continue work on new applications of VR to the Digital Library of Mathematical Functions, creating a DLMF Graphics Gallery, and a new application that enables users to interact with data associated with controlled fires.

Interactive 360 Fire Videos. This new area of research, done in collaboration with Matt Hoehler of EL, records dramatic fire scenes which the user can see from inside the fire itself. These remarkable videos are produced by a device Hoehler has developed, known as a Burn Observable Bubble (BOB). BOB sounds simple enough— place a waterproof camera inside a sphere filled with recirculating water—however the practicalities mandate taking quite a bit of care in the design, using materials that can withstand intense heat. Several cameras were sacrificed to achieve the correct combination of materials and water cooling.

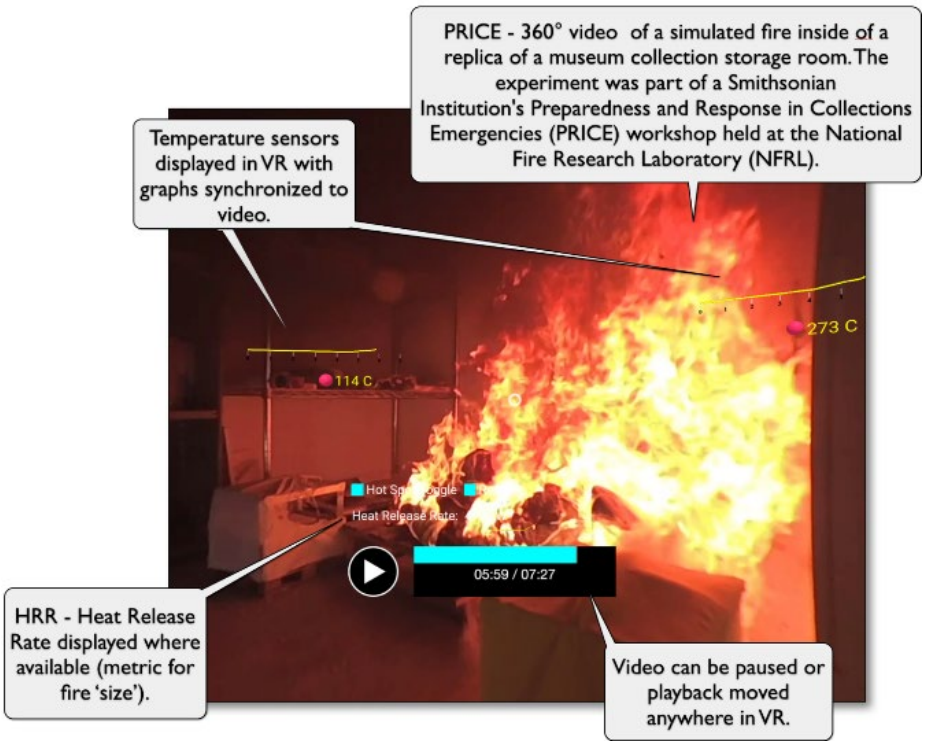

Figure 63. *Interactive 360-degree fire video with temperature data and graphs.*

The main exemplar fire we are working with is known as the PRICE fire[20]. It was a controlled burn in a closet meant to simulate what would happen if a closet at the Smithsonian Institution caught on fire. Approximately a half dozen temperature sensors were placed throughout the environment and a continuous log of data was recorded along with the 360-degree video itself. Our main task is to create a WebVR environment that allows the user to see the associated data synchronized with the video. This allows fire researchers and trainees the ability to see the location of the sensors with the temperature displayed floating above them. As a user you are able to move the location of the temperature data and interact (e.g., rewind, fast forward) with the playback of the video. We continue to experiment with the functionality of the data interaction and its visualization. Much of this work was accomplished by our SURF and SHIP students, Frankie Willard and Adam Lenker.

DLMF Function Gallery. We have created a DLMF function gallery[21], a web page where users can view and download all of the surfaces visualized in the NIST Digital Library of Mathematical Functions (DLMF)[22] book and web site.

Each surface of the gallery has associated data available in a wide variety of formats. These are: ctm, dae, dxf, fbx, glb, gltf, json, obj, off, ply, stl, wrl, x3d and xyz. The user can get all of these formats in a convenient zip file. The files were created by a scripting process that uses MeshLab and NodeJS. This work was primarily accomplished by SURF student Justin Slud over the summer of 2019. Our near-term goal is to make these surfaces available to the public as a general computer graphic resource. They could be used for 3D printing, game backgrounds or surfaces, mathematical education and whatever else users can imagine.

[1] S. Ressler. "Hot Stuff: Using Web3D to Examine Fire from the Inside." EPICentre, University of New South Wales, Sydney Australia, September 18, 2019. URL: https://slides.com/sressler/hotstuff#/

[2] S. Ressler. "Too Hot to Handle: Web3D for Fire Data Exploration." SIGGRAPH Asia 2019, Brisbane, Australia, October 24, 2019. URL: https://slides.com/sressler/sigasia2019#/

[20] http://snippet.cam.nist.gov/~sressler/webvrfire/fireapp/

[21] https://math.nist.gov/~SRessler/jas23/MAINPROJECT/gallery.html

[22] http://dlmf.nist.gov/

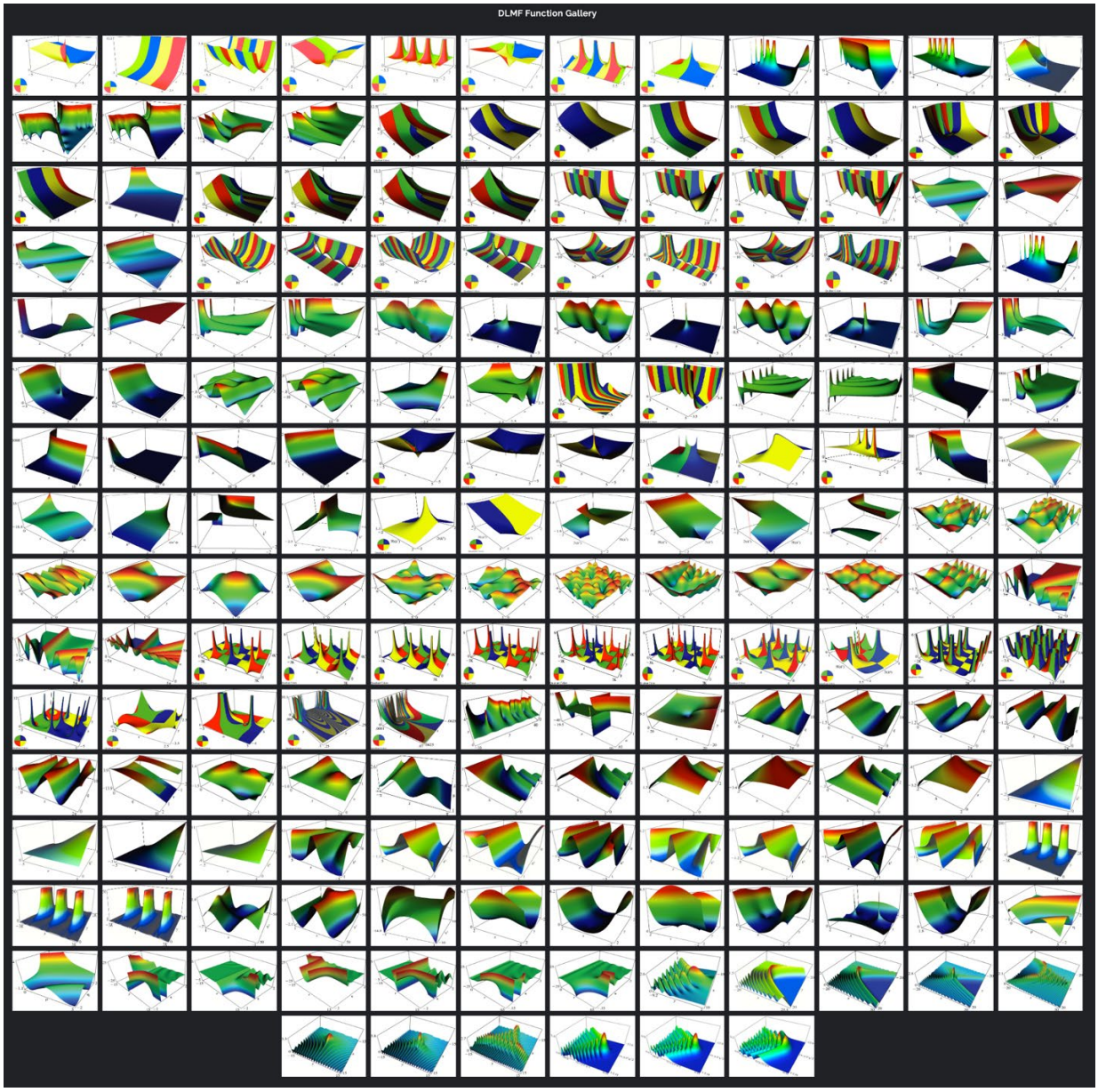

Figure 64. *Digital Library of Mathematical Functions function gallery.*

Quantum Information

An emerging discipline at the intersection of physics and computer science, quantum information science is likely to revolutionize 21st century science and technology in the same way that lasers, electronics, and computers did in the 20th century. By encoding information into quantum states of matter, one can, in theory, enable phenomenal increases in information storage and processing capability. At the same time, such computers would threaten the public-key infrastructure that secures all of electronic commerce. Although many of the necessary physical manipulations of quantum states have been demonstrated experimentally, scaling these up to enable fully capable quantum computers remains a grand challenge. We engage in (a) theoretical studies to understand the power of quantum computing, (b) collaborative efforts with the multi-laboratory experimental quantum science program at NIST to characterize and benchmark specific physical realizations of quantum information processing, and (c) demonstration and assessment of technologies for quantum communication.

Quantum Information Science

Scott Glancy
Emanuel Knill
Sae Woo Nam (NIST PML)
Ezad Shojaee (University of Colorado)
Arik Agavayan (University of Colorado)
Mohammad Alhejji (University of Colorado
Shawn Geller (University of Colorado
Alex Kwiatkowski (University of Colorado)
Karl Mayer (University of Colorado)
James R. van Meter (University of Colorado)
Lynden K. Shalm (University of Colorado)
Yanbao Zhang (NTT Corporation)
Abu Ashik Md. Irfan (Indiana University)
Gerardo Ortiz (Indiana University)

Figure 65. *Paulina Kuo of ACMD (left) moderates the session Building Quantum Computers: Why and How at the AAAS Annual Meeting held in Washington, DC in January 2019. Panelists were (l. to r.) Christopher Monroe (University of Maryland), Debbie Leung (Institute for Quantum Computing, Waterloo, Canada), and Matt Reagor (Rigetti Computing).*

The last few years have seen rapid growth in the number of quantum bits (qubits) that can be used for quantum information processing in one device. While these qubits are still too few and too noisy for use in fault-tolerant architectures, some are claimed to have already demonstrated subtle quantum advantages. ACMD researchers are contributing to the effort of making practical and useful quantum information processing and communication possible. Recently they have developed the currently most data-efficient method for device-independent quantum randomness generation and expansion, generalized methods for universal computing with decoherence-free subspaces to higher-dimensional physical systems, determined a method for self-testing Majorana-mode states, and are studying entanglement swapping in quantum networks with high loss or added noise.

Randomness Generation. Randomness is an important resource in computation and communication, with secure randomness required for safe internet interactions and transactions. Quantum mechanics enables device-independent randomness generation, where the randomness is certified without needing to trust our quantum devices. We have developed randomness generation protocols based on a statistical framework [1, 2, 3], where our protocols dramatically improve the amount of randomness obtained from a given amount of data. We implemented a spot-checking randomness expansion protocol that generated 24 % more randomness than was consumed by the random choices that are required for certification. The implementation used NIST's loophole-free Bell-test setup. Our randomness expansion capabilities make it possible to demonstrate cross-feeding randomness generation, whereby it is possible to generate an unbounded amount of randomness given a fixed amount of initial randomness.

Fault Tolerant Quantum Computing. One way to dramatically reduce noise acting equally on nearby qubits and to enable quantum computing on quantum-dot qubits is to encode information in decoherence-free subsystems of identical physical systems supporting logic gates generated by readily available exchange interactions. We have determined that universal computation using only exchange-based gates is possible for any number of levels of the physical systems used, and we devised simpler methods for implementing entangling gates based on decoupling strategies normally used to suppress coherent noise [4]. Next steps include further

development of our methods for practical implementations and demonstrations in available quantum devices.

One proposed technology for quantum computing is based on Majorana modes, which are emergent fermionic subsystems localized at ends of special nanowires in contact with a superconductor. These modes are more resilient to some errors than typical qubits are. Verifying the existence of such Majorana mode is an ongoing, international experimental effort that is producing increasingly convincing evidence. Our goal is to verify the operational behavior of these modes using self-testing methods, which can provide much stronger evidence that Majorana modes are present. We developed such a method that can certify Majorana mode states and operations with minimal assumptions on compatibility of measurements [5]. Our method is robust to noise and introduces a new self-testing scenario that does not assume a preexisting subsystem decomposition. We hope to extend the method from one that verifies static states and measurements to one that can certify the dynamics of the system.

Quantum Networks. Realizing the full power of quantum information processing requires quantum networks that enable quantum communication between quantum computing nodes. NIST is advancing quantum networking with efforts to build quantum repeaters and testbeds for developing and testing protocols. We are contributing to these efforts by studying entanglement swapping protocols in the presence of loss and noise. For example, we have determined that it is not possible to swap entanglement if the two modes used for swapping experienced an average loss of at least 50 % and only Gaussian operations and quadrature measurements are allowed. We are exploring other methods for generating shared entanglement between nodes, focusing on methods with states and measurements readily accessible in superconducting devices with mechanical oscillators for transduction between microwave and optical modes for communication over optical fiber.

[1] Y. Zhang, E. Knill, and P. Bierhorst. Certifying Quantum Randomness by Probability Estimation. *Physical Review A* **98** (2018), 040304(R). DOI: 10.1103/PhysRevA.98.040304

[2] Y. Zhang, L. K. Shalm, J. C. Bienfang, M. J. Stevens, M. D. Mazurek, S. W. Nam, C. Abellan, W. Amaya, M. W. Mitchell, H. Fu, C. A. Miller, A. Mink, and E. Knill. Experimental Low-Latency Device-Independent Quantum Randomness. *Physical Review Letters*, to appear.

[3] Y. Zhang, H. Fu, and E. Knill. Efficient Randomness Certification by Quantum Probability Estimation. *Physical Review Research*, to appear.

[4] J. R. van Meter and E. Knill. Approximate Exchange-Only Entangling Gates for the Three-Spin- Decoherence-Free Subsystem. *Physical Review A* **99** (2019), 042331. DOI: 10.1103/PhysRevA.99.042331

[5] A. A. M. Irfan, K. Mayer, G. Ortiz, and E. Knill. Certified Quantum Measurements of Majorana Fermions. arXiv:1904.12207, (2019).

Quantum Characterization Theory and Applications

Scott Glancy
Emanuel Knill
Alexey Gorshkov (NIST PML)
Dietrich Leibfried (NIST PML)
Alan Migdall (NIST PML)
Trey Porto (NIST PML)
Daniel Slichter (NIST PML)
Kartik Srinivisan (NIST PML)
Andrew Wilson (NIST PML)
Sarah Aguasvivas-Manzano (University of Colorado)
Arik Avagyan (University of Colorado)
Dan Cole (University of Colorado)
Stephen Erickson (University of Colorado)
Panyu Hou (University of Colorado)
Shawn Geller (University of Colorado)
Hannah Knaack (University of Colorado)
Alex Kwiatkowski (University of Colorado)
Michael Lauria (University of Colorado)
Jieying Li (University of North Carolina)
David Phillips (University of Oxford)
Sam Showalter (DePauw University)
Raghavendra Srinivas (University of Colorado)
Jenny Wu (University of Colorado)

Many emerging technologies will exploit quantum mechanical effects to enhance metrology, computation, and communication. Developing these technologies requires improved methods to characterize the performance of quantum devices. This characterization requires solving statistical problems such as estimating an underlying quantum state, measurement, or process by using a collection of measurements made on the quantum system. Alternatively, one may also want to estimate figures-of-merit such as fidelity, error rates, and entanglement measures from that data. Accurate quantum characterization allows experimentalists to answer questions like "What is happening in my quantum experiment?" or "How well will my system perform some quantum information protocol?" and to characterize uncertainty in that answer.

NIST's Ion Storage Group has pioneered one of the world's most successful quantum computer development projects. To keep pace with their recent advances in qubit preparation, logical operation, and measurement fidelities, ACMD researchers are developing more advanced statistical techniques to characterize trapped ion quantum computers. An ion qubit is measured by counting the number of photons the ion releases when illuminated by a fluorescent laser. A random number of photons will be produced, but the probability distribution depends on the ion's state. Distinguishing the $|0\rangle$ and $|1\rangle$ states requires differentiating between two slightly overlapping probability distributions. ACMD

researchers are developing a hidden Markov model of the fluorescent measurement process, a strategy for manipulating the ion during the measurement, and a Bayesian system inferring the ion's state at the start of the measurement process. These tools will enable higher fidelity ion qubit measurement and a better understanding of measurement error.

Randomized benchmarking is a popular tool for estimating an effective error-per-logic-gate for a small quantum computer. In a randomized benchmark measurement, one applies random strings of logic gates to the qubits and observes how the error probability depends on the length of the strings. The gates must be chosen from a "2-design," a probability distribution over logic gates that sufficiently randomize the quantum states. ACMD researchers have constructed a new 2-design that allows experimenters to apply each random gate with a fixed pattern of laser pulses. The new 2-design will give more consistent and reliable randomized benchmarking results. ACMD researchers are working with the Ion Storage Group to perform randomized benchmark measurements of a new ion trap using this 2-design.

ACMD researchers are contributing to the Metrology with Interacting Photons project, which is funded by the NIST Innovations in Measurement Science program. This project's goals are to demonstrate photon-photon interactions that are mediated by Rydberg atoms and to exploit those for metrology and quantum information processing. ACMD researchers have theoretically explored adapting traditional homodyne detection so that they can verify that the photons have actually interacted with one another despite noise, loss, and a strict limit on the power of the homodyne reference field (or "local oscillator"). They have characterized what properties of optical quantum states can be inferred from the measured data even when the signal is contaminated by noise photons in nearby modes, when the reference field is very weak, and when the reference phase and power can be varied [1]. ACMD researchers have partnered with PML to demonstrate this measurement strategy in an optical experiment. They have collected data and are analyzing it.

Characterizing uncertainty in the estimates provided by quantum state tomography remains challenging. Without computationally tractable and statistically rigorous methods to produce confidence intervals for parameters characterizing quantum states, interpreting experimental results can be problematic. To address this problem, most researchers use bootstrap-based methods to characterize uncertainty. However, the probability distributions involved are complicated, and bootstrap estimates are biased, so bootstrap confidence intervals may not achieve the desired coverage probabilities. ACMD researchers have studied several bootstrap-based methods for constructing confidence intervals. The studies show that none of these methods reliably provide confidence intervals with the correct coverage probabilities. Some are useful for relatively low confidence levels ≈68 %, but they are not reliable for high confidence levels ≈95 %. ACMD researchers have now also begun testing algorithms to construct Bayesian credible intervals.

[1] Arik Avagyan, Emanuel Knill, Scott Glancy, and Hilma Vasconcelos. State Tomography with Photon Counting after a Beam Splitter. In preparation.

Correlated Noise in Quantum Devices

Yi-Kai Liu
Mohammad Hafezi (University of Maryland)
Kaixin Huang (University of Maryland)
Alireza Seif (University of Maryland)
Travis Scholten (IBM)
Robin Blume-Kohout (Sandia National Labs)
Kevin Young (Sandia National Labs)

Noise and decoherence are an important concern in the development of quantum devices for metrology and computation. These problems are becoming increasingly challenging, as experimentalists start to build so-called NISQ (noisy intermediate-scale quantum) devices, which have tens to hundreds of qubits, with noise levels that are low but not insignificant. In order to use NISQ devices effectively, one must mitigate the effects of noise, using techniques such as quantum control, and active quantum error correction.

To this end, it is important to develop mathematical models that can accurately describe noise processes on many qubits over fairly long timescales, including phenomena such as temporal correlations (e.g., non-Markovian memory effects), and spatial correlations (e.g., crosstalk between qubits). In addition, one needs statistical methods for fitting these noise models to experimental data, as well as computational techniques for simulating these noise models efficiently.

We are developing various approaches to these problems. First, we are developing a model of sparse correlated dephasing noise on many qubits. Correlated dephasing can occur when two or more qubits are coupled to the same environmental degrees of freedom, which may happen for a variety of reasons, including physical proximity, and spectral (frequency) crowding. This can occur in various physical systems, such as superconducting qubits. Here, we consider a model of anomalous pairwise correlations, described by a graph G, which is unknown, but is promised to be sparse. We are developing methods to fit this model to experimentally accessible data, by preparing many-body entangled states, observing their decay, and using compressed sensing measurements to reconstruct the graph G.

Second, we are developing more efficient methods for noise spectroscopy for learning models of non-Markovian noise. As a simple example, we consider a single qubit coupled to a bosonic bath (the spin-boson model). We are developing novel pulse sequences for estimating different features of the spectral density function of the bath. As an application, we use these techniques to learn so-called 1-D chain representations of the bath, which allows for faster numerical simulations of the qubit coupled to the bath.

Third, we are investigating the use of machine learning algorithms for estimating or predicting qualitative features of the noise. In particular, we have found that machine learning classifiers (such as support vector machines), combined with commonly available quantum measurement techniques (such as gate set tomography), can be trained to distinguish between different types of noise (stochastic or coherent) on a single qubit. This gives a novel way of characterizing quantum noise, by learning from examples, without relying on an explicit model of the noise [1].

[1] T. L. Scholten, Y.-K. Liu, K. Young, and R. Blume-Kohout. Classifying Single-qubit Noise using Machine Learning. arXiv 1908.11762, August 2019.

Quantum-Inspired Techniques for Explainable AI

Yi-Kai Liu
Lucas Brady

Many techniques for machine learning and artificial intelligence seem to involve a tradeoff between "expressiveness" (the degree to which they can solve complicated problems) and "explainability" (the ease with which a human being can understand or interpret their behavior). For instance, state-of-the-art deep neural networks are highly expressive, while more traditional methods (such as probabilistic graphical models and sparse regression) are human-interpretable. But there are few methods that excel in both expressiveness and explainability. Such methods are needed for many practical applications where safety and reliability are important, such as computer-assisted medical diagnoses and self-driving cars.

We are investigating how ideas from quantum information theory, such as tensor networks, can be applied to the problem of constructing explainable AI. Tensor networks have been widely used to describe entangled many-body quantum states in condensed matter physics; some prototypical examples are matrix product states (MPS) for 1-D gapped spin chains, multiscale entanglement renormalization ansatz (MERA) states for 1-D critical spin chains, and projected entangled pair states (PEPS) for 2-D spin chains.

In some ways, tensor networks are similar to latent variable models and hidden Markov models. They have some of the same nice features that aid with explainability, such as sparsity and graph structure. However, tensor networks generate a different class of probability distributions than classical latent variable models, and they are trained using different algorithms. We are investigating certain situations where tensor networks may be more expressive than latent variable models, while still being efficiently learnable.

As a first step in this direction, we are studying a class of quantum-inspired models that imitate probabilistic graphical models. These models are constructed using the ground states of so-called stoquastic Hamiltonians. These models generate multivariate probability distributions that maximize an entropy-like objective function, subject to constraints on the marginals of the distribution. Prediction and inference in these models can be performed using adiabatic evolution on a quantum computer or quantum Monte Carlo simulations on a classical computer. This work is still preliminary, but it suggests a possible way of reducing the computational costs of probabilistic graphical models.

Analog Quantum Algorithms

Lucas Brady
Chris Baldwin (NIST PML)
Alexey Gorshkov (NIST PML)
Roberto Gorbea (University of Puerto Rico)
Aniruddha Bapat (University of Maryland)
Jake Bringewatt (University of Maryland)
Yaroslav Kharkov (University of Maryland)
Itay Hen (University of Southern California)

As quantum computers and quantum technologies begin to be realized and become more powerful, it is important to develop algorithms that can exploit these small devices to best utilize any quantum advantage. Such devices are usually noisy and prone to errors, making it difficult to implement many circuit-based quantum algorithms that require a specific sequence of quantum operations. Another class of quantum algorithms that is thought to be more suitable to these small noisy devices is analog quantum algorithms. Rather than being described in terms of discrete quantum operations or gates, these algorithms are described in terms of how the system or Hamiltonian evolves with time.

One of the most promising algorithmic approaches to utilizing small quantum devices involves applying a variational approach. Here, we use classical computation to pick some set of parameters for a quantum calculation or state preparation, using the small quantum computer to sample from the distribution of outputs that results from those parameters. This output is then used

to update the classical algorithm, leading to a loop until a desired problem is solved or the state is prepared.

For instance, one of the most prominent quantum variational algorithms is the Quantum Approximate Optimization Algorithm (QAOA) [2]. In this algorithm, a system of quantum bits, or qubits, are exposed to two alternating Hamiltonians. These Hamiltonians are applied for p alternations, with the times for each pulse being fed to the classical computer as its variational parameters. The goal is to approximately prepare the ground state of one of the Hamiltonians (or any other desired state), and the output of sampling the quantum computer for a given parameter set is used in a classical loop to optimize the energy of the produced state (or another desired quantity).

As a proof-of-principle, we recently participated in the theory support for an experimental implementation of a QAOA algorithm on a small, 40-qubit, quantum computer [1] with experimentalists at the University of Maryland. This project not only implemented the small quantum algorithm but succeeded in characterizing the quantum device, showing the full control landscape of the variational algorithm experimentally.

The outer loop of a variational algorithm requires significant computational resources, and one of the big open questions is how best to choose initial parameters as the size of the problem or the number of allowed parameters is increased. We see that an optimized set of QAOA parameters for p steps can be used to make good initial guesses at the optimal parameters for a larger number of steps. We are currently working on an analytic proof of this fact, and we are also using machine learning techniques to try to predict these patterns and the resulting quantum states' energies.

While classical analogues exist for many quantum algorithms, no known classical algorithm quite captures the dynamics of QAOA. In some cases, classical analogues have even been found that match quantum algorithms in terms of computational runtimes, so discovering whether a classical analogue for QAOA exists is exciting. We developed ideas for a classical simulation of imaginary-time QAOA (as opposed to the normal real-time version) and looked at how this imaginary-time domain algorithm could be simulated through Monte Carlo techniques, comparing it, with initially favorable results, to another classical algorithm derived to be analogous to quantum analog computation.

Another important class of analog quantum algorithms is Quantum Adiabatic Optimization (QAO) [3] or its slightly more generalized form, Quantum Annealing (QA). In this algorithm, the system is initialized in the ground state of some initial Hamiltonian. If the Hamiltonian changes slowly enough, the quantum adiabatic theorem says that the system will stay in the ground state, allowing us to find the ground state of desired Hamiltonians that encodes some classical problem.

Of key interest is whether QAOA or QA performs better in a time-restricted setting. We have explored a time-restricted version of QAOA numerically and using the framework of optimal control theory. Our results show that an intermediate form is often preferred, for instance doing a QAOA-like algorithm at the beginning and end but a smoother annealing-like curve in the middle. Furthermore, QAOA attempts to form a discrete analog of this true optimal procedure.

Classical simulation of QAO is hindered by what is known as the sign problem. A classical Monte Carlo can be derived for any QAO problem, but for all but a specific class of so-called "sign-problem free" Hamiltonians the resulting Monte Carlo probabilities are both positive and negative, leading to an exponential slow-down in the classical simulation. We explored two different approaches to mitigating or bypassing this sign-problem for specific classes of Hamiltonians. In one approach, we utilize the structure of the Hamiltonian itself, grouping positive and negative probabilities separately. In another approach on-going approach, we are examining how deformation of the Monte Carlo integration domain into the complex plane and the path of stationary phase can lead to a mitigation of these computational slowdowns.

[1] G. Pagano, A. Bapat, P. Becker, K. S. Collins, A. De, P. W. Hess, H. B. Kaplan, A. Kyprianidis, W. L. Tan, C. Baldwin, L. T. Brady, A. Deshpande, F. Liu, S. Jordan, A. V. Gorshkov, and C. Monroe. Quantum Approximate Optimization with a Trapped-Ion Quantum Simulator. arXiv:1906.02700, 2019.

[2] Edward Farhi, Jeffrey Goldstone, and Sam Gutmann. A Quantum Approximate Optimization Algorithm. arXiv:1411.4028, 2014.

[3] Edward Farhi, Jeffrey Goldstone, Sam Gutmann, and Michael Sipser. Quantum Computation by Adiabatic Evolution, arXiv:0001106, 2000.

Quantum Coin-Flipping [23]

Carl Miller (NIST ITL)
Aarthi Sundaram (University of Maryland, Microsoft)
Yusuf Alnawakhtha (University of Maryland)

Classical cryptography relies on computational hardness assumptions: "if problem X cannot be solved efficiently, then protocol Y is a secure cryptographic protocol." Quantum cryptography began in the 1980's with the observation that if one uses quantum devices, it is possibly to carry out cryptography using only physical

[23] This work, which was performed in the ITL Computer Security Division, is included here in to provide a more complete accounting of work in quantum information science being undertaken in ITL.

assumptions instead of computational assumptions. The first fully realized application was quantum key distribution (that is, secure communication using a quantum channel). In the decades since then, number of other cryptographic tasks have been explored.

A fundamental cryptographic task is *two-party coin-flipping*. Suppose that Alice and Bob are communicating across an electronic channel, and they wish to fairly flip a coin. Alice wants the outcome to be "heads," and Bob wants it to be "tails." Neither one trusts the other to do the coin flip, and they have no trusted third party to do it for them. Is it possible to fairly flip a coin in a way that will satisfy both of them?

In a classical (non-quantum) setting, without computational assumptions, there is a simple argument to that shows that two-party coin-flipping is impossible. (Either Alice or Bob will always be able to cheat.) But work that began in the 1990's showed that two-party coin-flipping *is* possible if Alice and Bob share a quantum channel. Early results showed that the bias (a numerical measure of the unfairness of the coin-flip) can be brought down to 21 % using a simple multi-round quantum communication protocol between Alice and Bob. Then, starting in 2004, physicist Carlos Mochon produced a series of papers [1-3] which ultimately showed (with some remarkable theoretical creativity) that there is a family of quantum coin-flipping protocols in which the bias can be made arbitrarily close to zero.

Mochon's work left at least one question unanswered: Can coin-flipping be done efficiently? The protocols that Mochon used to show vanishing bias involved a huge (in fact, slightly worse than exponential) number of communication rounds between Alice and Bob. In the 12 years since it was completed, there have been no major improvements on the asymptotic performance of Mochon's protocol. It is curious to see such a long halt on a central problem.

Recent work by Carl Miller [4] introduced new theoretical tools to help us understand the problem of optimizing the resource cost of quantum coin-flipping. This work delivered some unfortunate news: *efficient quantum coin-flipping is impossible*. Any quantum coin-flipping protocol must use an exponential number of communication rounds. Miller's work has finally explained the mystery of why efficient quantum coin-flipping has been out of reach for so long. The proof works by making a surprising connection to tools from complex analysis. It was featured at the Quantum Information Processing (QIP) conference in Shenzhen, China in January 2020.

The good news is that insight gained in [4] may eventually lead to positive results. We are currently interested in seeing how central theoretical constructions in [4] can be used to optimize coin-flipping if we allow a constant (rather than vanishing) level of bias. There is hope that these same tools could also be used to address other cryptographic tasks between mutually mistrustful players. Additionally, efficient quantum coin-flipping may become possible if we change the underlying physical model (for example, by taking relativity and the speed of light into account).

[1] C. Mochon. Quantum Weak Coin Flipping with Bias of 0.192. In *Proceedings of the 45th Annual IEEE Symposium on the Foundations of Computer Science*, October 2004, 2-11.

[2] C. Mochon. Large Family of Quantum Weak Coin-Flipping Protocols. *Physical Review A* **72**:2 (2005), 022341.

[3] C. Mochon. Quantum Weak Coin Flipping with Arbitrarily Small Bias. arXiv:0711.4114, 2007.

[4] C. Miller. The Impossibility of Efficient Quantum Weak Coin Flipping. arXiv:1909.10103, 2019.

Post-Quantum Cryptography

Yi-Kai Liu
Gorjan Alagic (NIST/ITL Computer Security Division)
Jacob Alperin-Sheriff (NIST/ITL Comp. Security Div.)
Daniel Apon (NIST/ITL Computer Security Division)
Lily Chen (NIST/ITL Computer Security Division)
David Cooper (NIST/ITL Computer Security Division)
Quynh Dang (NIST/ITL Computer Security Division)
John Kelsey (NIST/ITL Computer Security Division)
Carl Miller (NIST/ITL Computer Security Division)
Dustin Moody (NIST/ITL Computer Security Division)
Rene Peralta (NIST/ITL Computer Security Division)
Ray Perlner (NIST/ITL Computer Security Division)
Angela Robinson (NIST/ITL Computer Security Div.)
Daniel Smith-Tone (NIST/ITL Computer Security Div.)

NIST is currently engaged in a formal process to develop standards for post-quantum cryptosystems. The goal of this process is to standardize one or more cryptosystems that could replace those currently used schemes that are vulnerable to attack by quantum computers, including RSA, Diffie-Hellman and elliptic curve cryptosystems. These play a crucial role in Internet commerce and cybersecurity. While large quantum computers have not yet been built, NIST believes it is prudent to begin preparing for that possibility.

NIST is focusing on three main functionalities: public-key encryption, key exchange, and digital signatures. These are fundamental cryptographic primitives that enable a variety of applications, including secure web browsing, digital certificates, and secure software updates.

There are a number of candidate cryptosystems that are believed to be quantum secure. These are based on a variety of mathematical techniques, including high-dimensional lattices, coding theory, systems of multivariate polynomial equations, elliptic curve isogenies, hash-based signatures, and many others. However,

further research is needed in order to increase confidence in the security of these schemes, and to improve their practical performance.

In December 2016, NIST solicited proposals for post-quantum cryptosystems, and in November 2017, NIST began the first round of the review process, with 82 proposals. In January 2019, based on input from the post-quantum cryptography community, NIST selected 26 of the proposed cryptosystems to move onto the second round of the standards development process [1]. These candidates are now undergoing further analysis. It is hoped that, by focusing on a smaller number of candidate cryptosystems, NIST and the research community will be able to get a deeper understanding of their security properties, and any potential vulnerabilities. In addition, there are ongoing efforts to develop (and test) high-quality software implementations of these cryptosystems, on a variety of computing platforms.

To assist with these efforts, NIST organized the Second PQC Standardization Conference, on August 22-25, 2019, co-located with the CRYPTO conference in Santa Barbara, California. The event included presentations on the candidate cryptosystems and related topics, as well as open-ended discussion. In addition, NIST hosts the "PQC Forum" mailing list, which has served to communicate a large amount of feedback and technical analysis on the proposed post-quantum cryptosystems. NIST is also carrying out independent research on post-quantum cryptography and quantum cryptanalysis.

NIST anticipates that there will be a third round of analysis and evaluation, beginning sometime around June 2020, which will focus on a smaller number of candidate cryptosystems. At the end of the third round, NIST may select some of these cryptosystems for standardization or further study.

[1] G. Alagic, J. M. Alperin-Sheriff, D. C. Apon, D. A. Cooper, Q. H. Dang, C. A. Miller, D. Moody, R. C. Peralta, R. A. Perlner, A. Y. Robinson, D. C. Smith-Tone, and Y.-K. Liu. Status Report on the First Round of the NIST Post-Quantum Cryptography Standardization Process. NISTIR 8240, January 2019, 27 pages. DOI: 10.6028/NIST.IR.8240

Quantum Channel Modeling [24]

Michael Frey (NIST ITL)

Quantum channel identification (QCI) is the metrological determination of one or more parameters of a quantum channel. In [1] Frey proposed indefinite causal ordering (ICO) as a scheme for QCI. QCI refers to copies of a quantum channel physically or logically arranged so that the path through them is a superposition of different possible paths. ICO is called pure when the path superposition is a pure quantum state. Frey [1] showed that channel probing, in which probes in prepared quantum states are passed through copies of the channel to estimate one or more channel parameters, is in a strong sense aided by ICO. Specifically, pure ICO is known to increase the quantum Fisher information (QFI) in the processed probe state about the unknown parameter(s).

In [2] Frey considered the case complementary to pure ICO in which the path state is maximally mixed for a given indefiniteness. Deriving the QFI under this condition by a new approach, Frey found that mixed ICO-assisted QCI, while not as beneficial as pure ICO-assisted QCI, still yields greater QFI than does the comparable scheme with definite causal order. The d-dimensional quantum depolarizing channel was used as the channel model for these studies. These studies further revealed for probing the depolarizing channel that the relative effectiveness of both mixed and pure ICO decreases with probe dimension, each scheme being most effective for qubit probes.

The investigations described above considered just superpositions of forward and reverse channel orderings; for example, three channels, A, B, and C, in a superposition of orderings A-B-C and C-B-A. Alternatively, these channels could be cyclically ICOed: A-B-C, B-C-A, and C-A-B. Study is underway to determine the relative effectiveness of disparate ICOs for QCI. More speculatively, a possible connection between the hierarchy of qubit entanglement classes and that of ICOs of quantum channels is being sought.

[1] M. Frey. Indefinite Causal Order Aids Quantum Depolarizing Channel Identification. *Quantum Information Processing* **18** (2019), 96. DOI: 10.1007/s11128-019-2186-9

[2] M. Frey. Probing the Quantum Depolarizing Channel with Mixed Indefinite Causal Order. In Proceedings of the SPIE **10984** (2019), *Quantum Information Science, Sensing, and Computation XI*, 109840D. DOI: 10.1117/12.2520395

[24] This work, which was performed in the ITL Statistical Engineering Division, is included here to provide a more complete accounting of work in quantum information science being undertaken in ITL.

Joint Center for Quantum Information and Computer Science

Matthew Coudron
Yi-Kai Liu
Carl Miller (NIST ITL)
Jacob Taylor (NIST PML)
Andrew Childs (University of Maryland)

http://quics.umd.edu/

Established in October 2014, the Joint Center for Quantum Information and Computer Science (QuICS) is a cooperative venture of NIST and the University of Maryland (UMD) to promote basic research in understanding how quantum systems can be effectively used to store, transport and process information. QuICS brings together researchers from the University of Maryland Institute for Advanced Computer Studies (UMIACS) and the UMD Department of Physics and Computer Science with NIST's Information Technology and Physical Measurement Laboratories, together with postdocs, students and a host of visiting scientists.

QuICS has quickly established itself as a premier center for research in quantum information science. Thirteen Fellows, one Adjunct Fellow, 13 postdocs, and 32 graduate students are currently associated with the center. In CY 2019 a total of 117 research papers were produced by those associated with the center. Some 31 seminars were held through the year, many by visiting researchers.

This year Matthew Coudron of ACMD joined Yi-Kai Liu of ACMD and Carl Miller of the ITL Computer Security Division as QuICS Fellows, each holding research appointments at the University where they mentor students and postdocs. Jacob Taylor of NIST PML currently serves as Co-Director of the center along with Andrew Childs of the UMD Computer Science Department. Yi-Kai Liu is slated to replace Taylor as Co-Director in 2020.

In June 2019, QuICS organized the 14th Conference on the Theory of Quantum Computation, Communication and Cryptography (TQC 2019), a large three-day conference with competitive submissions across a wide range of quantum information topics; and the first Workshop on Noisy Intermediate Scale Quantum (NISQ), a two-day satellite event of TQC with an outstanding set of invited speakers covering potential applications of near-term quantum computers.

QuICS' success has resulted in it outgrowing its original space in the Atlantic Building on the College Park Campus. Happily, it is in the process of doubling its footprint there, obtaining 5400 square feet of additional space, which will include 15 new offices and an expanded seminar room.

Quantum Communications and Networking R&D

Oliver Slattery
Lijun Ma
Xiao Tang
Anouar Rahmouni (MASCIR, Morocco)
Summit Bhushan (Indian Institute of Technology)

http://www.nist.gov/quantum

The Quantum Communication and Networks Project develops and studies quantum devices for use in quantum communications and networking applications. Our goal is to bridge the gap between fundamental quantum mechanics/information theory and their practical applications in information technology. Our research covers two areas:

1. Creation, transmission, interfacing, storage, processing and measurement of optical qubits – the quantum states of single photons. We build and study quantum devices, such as entangled-photon sources, single-photon detectors, optical quantum memory and quantum interfaces. A long-term goal is to use these devices in quantum systems such as a quantum repeater or quantum network.
2. Implementation of a quantum network testbed in which the suitability and performance of new and existing quantum devices and systems can be studied in a real-life network environment. The testbed will lead to the development of best-practices and protocols for quantum networks.

Quantum networks of the future will consist of a wide range of devices that in turn will be tied to different technologies and materials; see Figure 66. Ensuring that these disparate technologies can function within the same network is a major challenge for quantum network research and development. For example, quantum memories based on atomic ensembles operating at very precise frequencies may need to serve a quantum computer using trapped ions at greatly different, yet equally ridged, frequencies.

Quantum Memories. Quantum memory is an essential device for quantum communication, computing and networking [1]. In optical quantum memory, the quantum states of photons are transferred to the quantum spin-state of the atoms for storage. Clouds of atoms in a vacuum cell are commonly used to maximize the interaction between the atoms and the signal. As the atoms in the cell move around (randomly since they are warm and have energy), they naturally bounce off the walls of the cell and this impact causes many atoms to lose their coherence and the quantum spin state to be destroyed. In recent work, we have experimentally studied different cell wall coatings to alleviate this effect. We had the

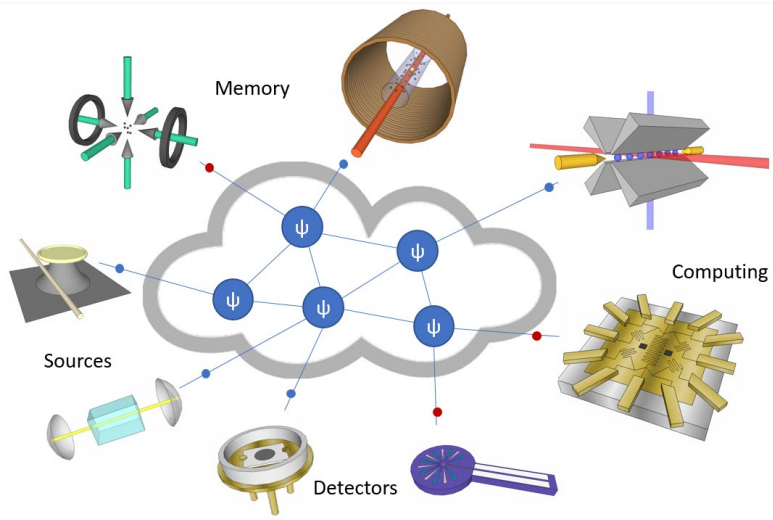

Figure 66. *A Quantum Network will consist of multiple systems based on different technologies and materials.*

walls of the cell coated with Alkene instead of the more traditional Paraffin, which greatly reduced the impact of the atom/wall collision (effectively cushioning the wall). Therefore, many more atoms return from collisions with their coherence and spin-state intact and are available for reconversion to the photon quantum state when required.

Quantum Interfaces. Any comprehensive quantum communications system, especially a quantum network, will use a mixture of technologies and frequencies for its key components that are based on different technologies. In this case, the interface between these various components becomes an essential consideration. A set of interfaces can, for example, convert the frequency of a signal from a shared single photon source to be compatible with different quantum memory frequencies or different quantum computing technologies. An interface can convert a telecommunications frequency that is suitable for long-distance transmission to a more optimal detection frequency while preserving the quantum characteristics of the signal. Quantum interfaces will also enable hybrid quantum networks that operate at different frequencies for different target applications. Recently, we implemented a cascaded interface connecting three essential frequencies for quantum communications, computing and networks including 1540 nm for long-distance transmission, 895 nm for Cesium quantum memory and 369 nm for Ytterbium ion quantum computing applications [2]; see Figure 67

Single photon sources. We have previously implemented a narrow linewidth single photon source based on cavity enhanced spontaneous parametric down-conversion (SPDC) [3]. We are also continuing our research and development of single photon sources based on spontaneous four-wave-mixing (SFWM) in a high-quality factor (high-Q) micro-resonator. These high-Q micro-resonators have the potential to generate very narrow linewidth sources that can be tailored to connect to atomic systems. However, coupling light into and out of a micro-resonator has long been a challenge for researchers. Current solutions include using refractive optics (such as a prism) to direct light from the tip of a fiber into the micro-resonator and again back into another fiber. Another existing technique is to use a highly tapered (stretched) fiber and to transfer light between the fiber and the micro-resonator by way of their overlapping evanescent waves. These and similar solutions have certain advantages and disadvantages. During this year, we designed a novel technique to couple light both ways between a micro-resonator and a fiber that we expect to be reproducible and robust. We are currently implementing this scheme to test its performance.

Quantum Network Research: As the development of component quantum devices in the laboratories continues, more attention is being paid to testing these components in connected systems such as quantum networks. We are working with our colleagues in other ITL and NIST divisions to implement a field testbed for quantum communication and quantum networks on the NIST campus. The system will be developed for field testing components, devices and systems related to quantum communications, and for studying the compatibility of quantum and conventional optical communication. This is an important priority because integrating into existing fiber-optic infrastructure is an economic and practical choice for deployment of quantum communication systems in the future.

[1] L. Ma, O. Slattery, and X. Tang. Optical Quantum Memory Based on Electromagnetically Induced Transparency. *Journal of Optics* **19**:4 (2017), 043001.

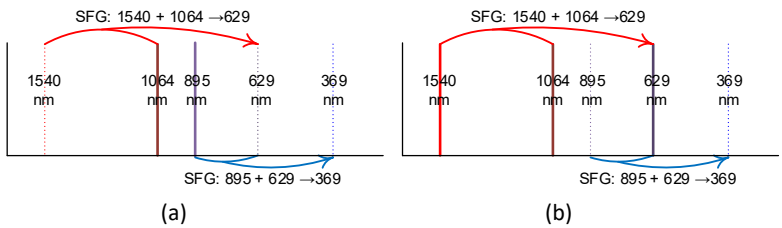

Figure 67. *The cascaded interface can convert (a) single photons in a fiber (at 1540 nm) to single photons for computing (at 369 nm) or (b) from single photons in a quantum memory (at 895 nm) to single photons for computing (at 369 nm).*

[2] O. Slattery, L. Ma, and X. Tang. A Cascaded Interface to Connect Quantum Memory, Quantum Computing and Quantum Transmission Frequencies. In *Frontiers in Optics + Laser Science APS/DLS*, OSA Technical Digest, Optical Society of America, 2019, W3A.125.

[3] O. Slattery, L. Ma, K. Zong, and X. Tang. Background and Review of Cavity-Enhanced Spontaneous Parametric Down-Conversion. *Journal of Research of the National Institute of Standards and Technology* **124** (2019), 1-18.

New Entangled Photon-Pair Sources

Paulina Kuo
Brian Alberding (NIST PML)
Varun Verma (NIST PML)
Thomas Gerrits (NIST PML)
Sae Woo Nam (NIST PML)
Martin Fejer (Stanford University)
Peter Schunemann (BAE Systems)
Mackenzie Van Camp (BAE Systems)

Entangled photon-pairs are critical building blocks for quantum networks, quantum communications and quantum-enhanced sensing. Entangled photons are used to distribute entanglement and quantum information across a quantum network. For metrology and sensing, entangled photons have been shown to enable increased sensitivity to optical phase [1]. Many techniques exist for generating entangled photon-pairs. We explored new techniques for entangled photon-pair generation, which may offer new functionality compared to existing photon-pair sources.

We developed a monolithic, aperiodically poled lithium niobate crystal for producing polarization-entangled photons-pairs [2]. This crystal is engineered to simultaneous generate photon pairs with $|H_sV_i\rangle$ and $|V_sH_i\rangle$ polarizations, where the subscripts *s* and *i* represent signal and idler photons, respectively. We performed measurements on this pair source and observed excellent polarization-entanglement visibility (see Figure 68). This technique is well-suited for integrated quantum optics in materials such as thin-film lithium niobate.

We also investigated photon-pair generation in new materials, such as zincblende crystals. Zincblende crystals (such as GaAs, GaP, and ZnSe) have high symmetry and no birefringence, which allows nonlinear optical mixing of a diverse set of polarization states [3]. For polarization-entangled photon-pair generation, these crystals can easily produce the desired $|H_sV_i\rangle$ and $|V_sH_i\rangle$ polarization states in a single, uniform quasi-phase-matched (QPM) grating. In collaboration with BAE Systems, we set up an experiment and performed preliminary measurements of parametric down-conversion

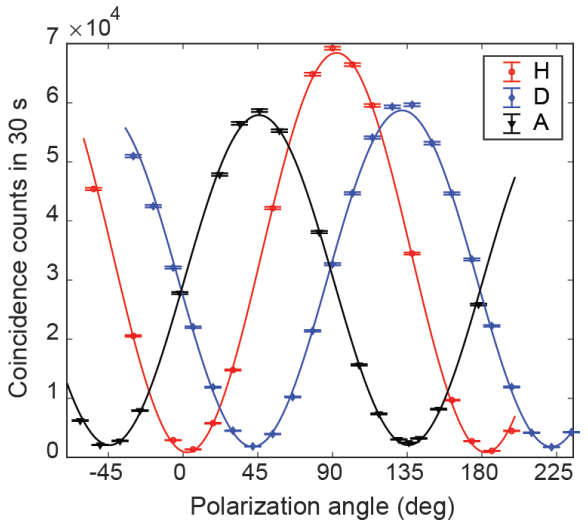

Figure 68. *Coincidence counts as a function of idler polarization angle with the signal polarization angle set to horizontal (H), diagonal (D) and anti-diagonal (A). We observed entanglement visibilities of 97 % (H), 94 % (D) and 93 % (A).*

in QPM GaP [4]. We used silica-fiber-coupled superconducting nanowire single-photon detectors [5] to sense the infrared down-converted photons.

Results of these investigations were presented at the 2019 Conference on Lasers and Electro-Optics (CLEO) [2, 4] and at the Photonics West conference. Paulina Kuo gave three invited talks during the year on entangled photon generation and applications.

[1] J. P. Dowling. Quantum Optical Metrology – the Low-down on High-NOON States. *Contemporary Physics* **49**:2 (2008) 125.

[2] P. S. Kuo, V. B. Verma, T. Gerrits, S. W. Nam, and R. P. Mirin. Generating Polarization-Entangled Photon Pairs in Domain-Engineered PPLN. In *Conference on Lasers and Electro-Optics OSA Technical Digest*, San Jose, CA, May 5-10, 2019. DOI: 10.1364/CLEO_AT.2019.JTu2A.42

[3] P. S. Kuo and M. M. Fejer. Mixing of Polarization States in Zincblende Nonlinear Optical Crystals. *Optics Express* **26**:21 (2018) 26971. DOI: 10.1364/OE.26.026971

[4] P. S. Kuo, P. G. Schunemann, M. Van Camp, V. B. Verma, T. Gerrits, S. W. Nam, and R. P. Mirin. Towards a Source of Entangled Photon Pairs in Gallium Phosphide. In *Conference on Lasers and Electro-Optics OSA Technical Digest*, San Jose, CA, May 5-10, 2019. DOI: 10.1364/CLEO_QELS.2019.FTh1D.5

[5] P. S. Kuo. Using Silica Fiber Coupling to Extend Superconducting Nanowire Single-Photon Detectors into the Infrared. *OSA Continuum* **1**:4 (2018) 1260. DOI: 10.1364/OSAC.1.001260

Foundations of Measurement Science for Information Systems

ITL assumes primary responsibility within NIST for the development of measurement science infrastructure and related standards for IT and its applications. ACMD develops the mathematical foundations for such work. This can be very challenging. For example, many large-scale information-centric systems can be characterized as an interconnection of many independently operating components (e.g., software systems, communication networks, the power grid, transportation systems, financial systems). A looming new example of importance to NIST is the Internet of Things. Exactly how the structure of such large-scale interconnected systems and the local dynamics of its components leads to system-level behavior is only weakly understood. This inability to predict the systemic risk inherent in system design leaves us open to unrealized potential to improve systems or to avoid potentially devastating failures. Characterizing complex systems and their security and reliability properties remains a challenging measurement science problem for ITL.

Network Modeling and Analysis Algorithm Toolbox

Brian Cloteaux

Studying interactions within systems, such as biological, social or communications, is an active area of pursuit in the research community. Commonly, such interactions are modeled as networks or graphs. As these areas of investigation mature, researchers increasingly need to be domain specialists, not experts in programming and graph algorithms. Providing such researchers with a tool set of fast and efficient algorithms for network modeling and analysis is the central idea behind this project. As a byproduct of this research, there have been a number of theoretical discoveries.

Recent results coming from this project have produced extremely efficient algorithms for testing if a sequence is graphic [1], and for generating random instances of a network with a given degree sequence [2]. In addition to these new algorithms, we have been looking at approaches to improving existing algorithms. We found several new bounds that have direct algorithmic application [3, 4], leading to faster modeling algorithms, and interesting applications in graph theory.

As an example of the results from this project, we recently worked on the problem of random graph generation. The most common approach used for this problem is to create a non-random instance and then to modify it using a Monte Carlo Markov chain approach. A serious problem with this approach is that it requires holding an entire graph in memory. For random graph generation, sequential importance sampling methods have also been developed, but suffer from slow run times. We introduced a new algorithm for creating random instances [2], which overcomes the space and speed limitations of earlier methods. We also published results that can be used to speed-up some instances of the traditional Monte Carlo Markov chain approach [4].

This past year we continued to give attention to the problem of generating random graphs created using a

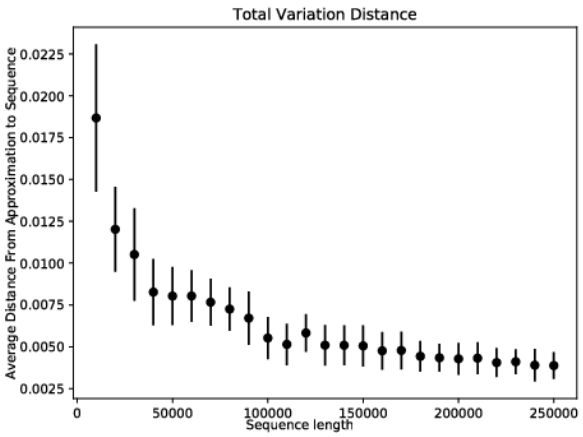

Figure 69. *This figure represents the average difference between a non-graphic sequence selected from a power-law distribution with exponent of 2 and its approximation created from our new algorithm. Each point represents the average distance for 30 sequences created at a given length. The error bars represent one standard deviation.*

graphic degree sequence selected from some given probability distribution. More specifically, how do we deal with a randomly drawn integer sequence that is not graphic (i.e., a degree distribution that is not realized in any graph)? There have been two approaches to this problem. The first is to simply discard the sequence and repeatedly select a new sequence until a graphic sequence is found. This approach has been used by various graph libraries. A disadvantage to this approach is that for some probability distributions, such as a power-law distribution, the probability of selecting a graphic sequence can be very small. For these distributions, we have a very small chance of finding a graphic sequence in reasonable time.

In response to this difficulty, an alternative is to find the closest graphic sequence to the original non-graphic degree sequence using a given distance measure. The published algorithms that try this approach have been either very slow or require a large amount of memory. These algorithms construct these sequences by first building an entire graph and then extracting the degree

sequence from this graph. For very large graphs, this approach quickly becomes impractical.

We introduced two algorithms for graphic approximation that are extremely fast and do not require constructing a graph to compute the new sequence [5]. One method gives a graphic sequence that minimizes the discrepancy metric (essentially the L_1 distance). The second method, under some minor conditions, minimizes the probability distribution distance, and specifically the total variation distance, between the original sequence and the approximation. We showed that under the total variation distance, the quality of the result from this approximation algorithm for many sequences actually improves as the size of the sequences increases. In fact, this distance goes to zero as the length of the sequence increases. Figure 69 shows how the average total variation distance between the original sequences and their approximations from the algorithm approach zero as the sequence length grows. Our work is the first practical approximation for extremely large sequence generation.

We are currently publishing these new algorithms and enhancements for the benefit of the public. In addition, we are continuing to examine other fundamental algorithms needed by the network research community.

[1] B. Cloteaux. Is This for Real? Fast Graphicality Testing. *Computing in Science & Engineering* **17**:6 (2015), 91-95. DOI: 10.1109/MCSE.2015.125

[2] B. Cloteaux. Fast Sequential Creation of Random Realizations of Degree Sequences. *Internet Mathematics* **12** (2016). DOI: 10.1080/15427951.2016.1164768

[3] B. Cloteaux. A Sufficient Condition for Graphic Lists with Given Largest and Smallest Entries, Length and Sum. *Discrete Mathematics and Theoretical Computer Science* **20**:1 (2018), paper 25. DOI: 10.23638/DMTCS-20-1-25

[4] B. Cloteaux. Forced Edges and Graph Structure. *Journal of Research of NIST* **124** (2019), paper 22. DOI: 10.6028/jres.124.022

[5] B. Cloteaux. Fast Graphic Approximation of Very Large Integer Sequences. In review.

Robustness of Complex Systems and Finding Nodes Vulnerable to Cascading Failures

Richard J. La

Many complex engineered systems providing critical services comprise heterogeneous, interdependent component systems (CSs). Intricate dependence among CSs makes the analysis of such complex systems challenging. Moreover, due to the interdependence among the CSs, in many cases, even a local failure of a small number of CSs can lead to widespread failures in the system, potentially compromising the function of the overall system. For instance, an outage in one part of an electrical grid, such as a transmission line failure, can trigger cascading failures and lead to a large-scale blackout, affecting millions of people (e.g., Northeast blackout of 2003 and India blackouts of 2012).

With increasing reliance of modern societies on such complex yet fragile systems, there is a growing interest in understanding their robustness and discovering susceptible CSs whose failures can cause widespread failures and economic losses. The goal of this project is two-fold: (i) investigate how underlying dependence structure among CSs shapes the robustness of complex systems; and (ii) design computationally efficient methods for identifying vulnerable CSs that may serve as the weak links in critical systems. The expected outcomes will help researchers and engineers better understand the fragility/robustness of complex systems and develop new guidelines for enhancing their resilience.

To this end, we adopted the probability of cascading failures (PoCF) as a metric for quantifying both the robustness of the overall system and that of individual CSs. The PoCF of the system is the likelihood of experiencing widespread failures, starting with a random initial failure in the system and is a good indicator of how susceptible a complex system is to random failures. The PoCF of a CS is the probability that its failure will trigger cascading failures in the system and helps us quickly identify vulnerable CSs that pose greater risks to the system and, hence, require attention.

Adopting the PoCF as a robustness metric, we first investigated how clustering (or transitivity) displayed by real networks affects the PoCF of a system. Second, we proposed two computationally efficient methods for discovering vulnerable nodes when limited historical data are available.

Our study revealed that (a) there is an intriguing relationship between network clustering and the PoCF of the system [1]. Moreover, in the critical regime where a complex system can suffer widespread failures, network clustering is beneficial in that it tends to keep failures localized in a small neighborhood, thus diminishing the PoCF in complex systems; and (b) when the Perron-Frobenius eigenvalue of the associated weighted Hashimoto matrix is close to one, there is a close relation between the PoCFs of CSs and their non-backtracking centralities, which serve as a measure of their importance in the network [2].

In addition, our proposed methods for identifying vulnerable nodes (eigenvector-based approach and optimization-based approach) suggest that, even in the absence of sufficient historical data or detailed simulation, we may be able to identify many, if not most, of vulnerable nodes that are more prone to trigger cascading failures in complex systems [2, 3]. However, the eigenvector-based approach [2] can suffer considerable

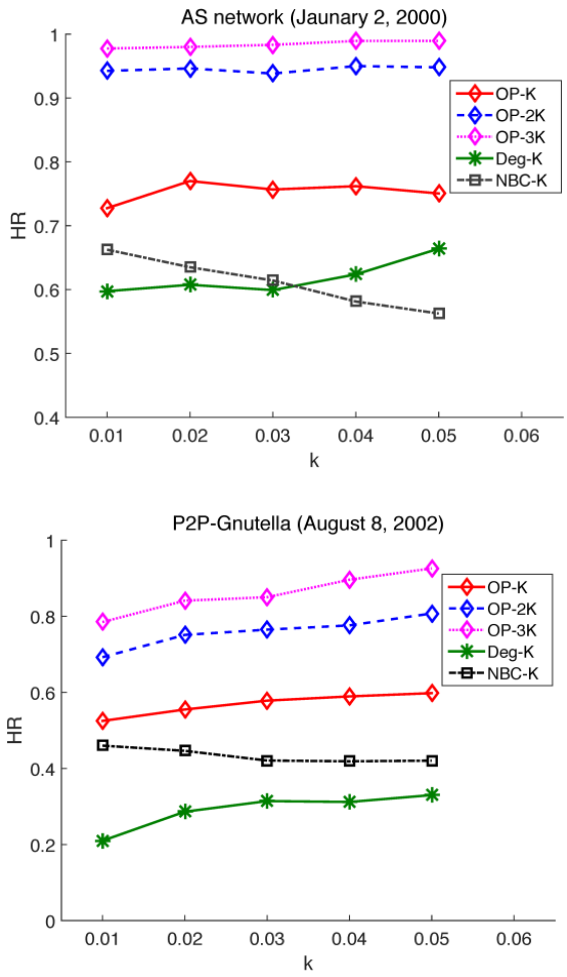

Figure 70. *Plots of average hit rates for (a) the connectivity of autonomous systems in the Internet and (b) the connectivity of Gnutella peer-to-peer network.*

performance degradation when the Perron-Frobenius eigenvalue of the associated Hashimoto matrix is not close to one.

The performance of the proposed methods is shown in Figure 70, using two real networks – the connectivity of autonomous systems (AS) in the Internet and that of Gnutella peer-to-peer (P2P) network. Here, we aim to identify the top $K = k \times n$ most vulnerable CSs, where n is the number of CSs in the system and k is varied from 0.01 to 0.05. The hit rate (HR) shown in the figure is the fraction of K most vulnerable CSs that are in the list of K candidates suggested by the proposed methods, hence correctly discovered. For a simple comparison, if we randomly choose K CSs, the expected hit rate is k. The black line (NBC-K) and the red line (OP-K) plot the hit rate for the eigenvector-based approach [2] and the optimization-based approach [3], respectively.

In addition, the figure plots the fraction of K most vulnerable nodes correctly identified when we consider the list of $2K$ and $3K$ candidates (instead of only K), which are labeled OP-2K and OP-3K, respectively. The plots suggest that the optimization-based approach outperforms all other compared approaches. Furthermore, the list of $3K$ candidates identified by the optimization-based approach contains virtually all of the K most vulnerable CSs in the AS network and 80 to 90 percent of the CSs in the P2P network [3]. Together with the finding in [4] that a number of vulnerable CSs tends to be small, this suggests that if we harden a moderately small number of CSs suggested by our proposed method, it may be possible to drastically reduce the likelihood of suffering widespread failures in complex systems.

[1] R. J. La. Influence of Clustering on Cascading Failures in Interdependent Systems. *IEEE Transactions on Network Science and Engineering* **6**:3 (2019), 351-363.

[2] R. J. La. Identifying Vulnerable Nodes to Cascading Failures: Centrality to the Rescue. In *Complex Networks and Their Applications VII* (L. Aiello, C. Cherifi, H. Cherifi, R. Lamboitte, P. Lio, and L. Roch, eds.), *Studies in Computational Intelligence* **812** (2018), Springer.

[3] R. J. La. Identifying Vulnerable Nodes to Cascading Failures: Optimization-Based Approach. In *Complex Networks and Their Applications VIII* (H. Cherifi, S. Gaito, J. Mendes, E. Moro, and L. Rocha, eds.), *Studies in Computational Intelligence* **881** (2019), Springer.

[4] Y. Yang, T. Nishikawa, and A. E. Motter. Small Vulnerable Sets Determine Large Network Cascades in Power Grids. *Science* **358** (2017), 6365.

Algorithms for Identifying Important Network Nodes for Communication and Spread

Fern Y. Hunt
Roldan Pozo

The identification of nodes in a network that enable the fastest spread of information is an important if not fundamental problem in network control and design. It is applicable to the optimal placement of sensors, the design of secure networks, and the problem of control when network resources are limited. Our approach to this problem has its origins in models of opinion dynamics and the spread of innovation in social networks. The mode of communication between nodes is described by simple models of random or deterministic propagation of information from a node to its neighbors. During the past few years, we have made progress in understanding the structural requirements for sets of nodes for effective spread in networks and have developed scalable algorithms for constructing these sets in real world networks.

We consider a discrete time model of information spread (represented by a variable assigned to each node) in a network with a set of nodes V and a subset $A \subseteq V$ of k nodes representing leaders or stubborn agents that are initially assigned a single value. Propagation occurs

by iterated averaging or diffusion defined by a stochastic matrix P. All node values will eventually converge to the single value at a speed determined by the sub-stochastic matrix $P_{\sim A}$, the matrix P restricted to the complement of A. An effective spreader in this situation is then a set of nodes for which convergence to this single value is fastest, i.e., the set A for which the Perron-Frobenius eigenvalue of $P_{\sim A}$ is largest. Using a classical result of Markov chain theory, the problem can be recast in terms of finding the set A of cardinality k that minimizes the mean first hitting time, i.e., the average or expected time a random walker reaches the target set A for the first time.

Previously we considered a polynomial time algorithm for finding an approximation to the optimal set. It is an extension of the classic greedy algorithm and it begins with a class of optimal and near optimal starter sets of smaller cardinality rather than the conventional choice of a best singleton set. Direct comparison of the algorithm results with the actual optimal solution and lower bounds on the performance ratio can be obtained because $F(A)$, the sum of mean first arrival times to A by random walkers that start at nodes outside of A, is a supermodular set function [2]. However, for large complex networks commonly encountered in applications, another approach is needed.

Recently, we developed a set of fast heuristics that work well on graphs with large hubs, a common feature of complex networks. When the desired set cardinality is k, subsets of hub vertices are rapidly screened to produce candidate sets. Each set consists of k nodes whose first (or higher order) neighborhoods have minimal overlap. After further screening, the offered approximation is selected by ranking the results of a Monte Carlo calculation of F for each candidate. This process allows us to find near optimal and optimal spreaders in networks with millions of nodes and dozens of millions of edges in less than a few seconds on a typical laptop. After conducting tests on real world graphs from diverse application areas including molecular biology, traffic control and social networks, we hypothesize that the method is most effective in terms of speed and quality of offered solutions when it is used on graphs with a large ratio of maximal degree to average degree.

This past year, we continued our investigation of the accuracy of this procedure. After realizing that the resulting offered set was an approximate solution of a discrete stochastic optimization problem, we established sufficient conditions that imply that it is also an approximate solution of the original problem. The first step was to establish the accuracy of the Monte Carlo calculation of F. The fact that the first hitting time to a set A has a distribution with exponential tails means that a sample average of simulated hitting times produces a consistent estimate of F in the limit of large sample size i.e. number of simulations. Establishing the degree of optimality of any offered solution is very difficult since supermodularity cannot be used and the size of the graphs are so large. However, the methods we use make it possible to rapidly sample the distribution of possible F values. We suppose the screening and ranking procedures produce candidate sets with F values that rank in the highest percentile of a distribution of such values over all subsets of fixed cardinality. Independent repetition of the heuristic calculation enables us to produce an estimate of a fixed percentile value along with a confidence interval for that estimate. The latter follows from an application of Chebyshev's inequality. Note that the resulting interval contains both the offered solution value and the optimal value of the original problem. Even in the case of a large number of repetitions, this approach is promising because it takes very little time to perform a single execution. The results of our work are reported in a paper in preparation [3].

[1] F. Hunt. Using First Hitting Times to Maximize the Rate of Convergence to Consensus. arXiv:1812.08881.

[2] F. Hunt. An Algorithm for Identifying Optimal Spreaders in a Random Walk Model of Network Communication. *Journal of Research of the National Institute of Standards and Technology* **121** (2016), 180-195. DOI: 10.6028/jres.121.008

[3] F. Hunt and R. Pozo. Algorithms for Effective Spread and Communication in Real Complex Networks. In preparation.

Reinforcement Learning for Efficient Virtual Machine Placement in Network Clouds

Richard J. La
Yang Guo (NIST ITL)
Xinquan Tian (NIST ITL)

Emerging and diverse network applications and dynamically changing demands for different network services have led to increasing complexity and a need for more flexible network architecture and management. As a result, virtualization of necessary network functions on shared network resources, as opposed to static provisioning of dedicated hardware for different network functions, has gained popularity in software defined networks and 5G systems. A key advantage of this new paradigm is that new network functions can be dynamically instantiated on available network resources as they are needed, and the associated network resources will be released upon the termination of network functions as they expire.

Although network function virtualization (NFV) offers greater flexibility and potential for more efficient utilization of network resources, it requires a network controller capable of managing the resources in a much

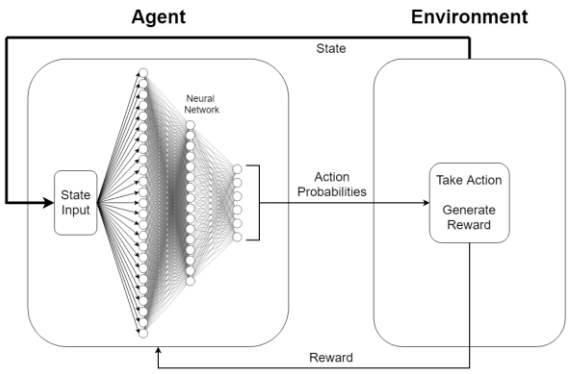

Figure 71. *Overall architecture of the machine learning-based approach to network management policy design.*

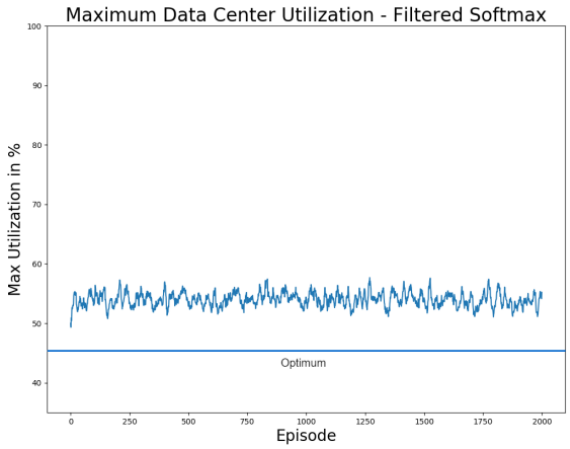

Figure 72. *Maximum data center utilization.*

more dynamical fashion via a more sophisticated network resource scheduling policy. To this end, researchers have proposed several different potential solutions, ranging from simple heuristics to more complicated policies, for instance, obtained from solving simple Markov decision processes (MDPs).

There are several challenges to designing an efficient policy. First, as the size of the network state space increases rapidly with features, so called the curse of dimensionality, maintaining a large table for the policy which specifies the action to be taken at each state becomes impractical, if not infeasible. Second, identifying a (near) optimal policy, for example, by solving an MDP, becomes computationally demanding when the state space is large.

For these reasons, researchers have been searching for an alternative approach to designing a good policy. The overarching goal of this project is to identify a new framework for designing good policies that can efficiently utilize network resources, without requiring a large volume of existing data.

It is well known that a sufficiently large neural network can be used to approximate any function in a class of functions. For this reason, we employ a deep neural network (DNN) as a function approximator in order to address the first challenge [1]. To tackle the second challenge, we turn to reinforcement learning (RL). RL is well suited for designing a good policy in a non-stationary environment without requiring much prior information. Instead of assuming that the necessary statistical information is known to solve an MDP, RL relies on the realized rewards achieved by different actions to induce a desirable policy. For this reason, we adopt RL for training the DNN, which is then used to choose an appropriate action based on the network state.

The overall architecture for which we propose to design a network management policy is shown in Figure 71. Given a network state, the DNN determines the probability distribution over the set of admissible actions at the state. Once an action is chosen, it causes a transition in the network state in accordance with prescribed transition probabilities and produces a reward, on the basis of the current state, the chosen action, and the next state. This reward is then used to update the weights of the DNN.

We applied our approach to the problem of designing a policy for virtual machine (VM) placement. In our study, requests arrive according to some stochastic process, and each request, based on its type, requires a certain amount of computational resources for a random duration. If the policy admits a request, it must either find a VM with adequate resources or create a new instance of VM at some data center if no existing VM has sufficient resources to accommodate the request. The goal of the policy is to minimize the maximum utilization among the data centers.

Figure 72 shows the maximum utilization among the data centers, along with the theoretical optimum (in the static case). The figure suggests that, although there is some gap between our policy produced by the proposed framework and the theoretical optimum, which is in practice not achievable, our policy maintains the maximum utilization reasonably close to the theoretical optimum, demonstrating its effectiveness.

In the future, we plan to apply our framework to designing a service function chain resource allocation policy in 5G networks, in which service function chain (SFC) requests must be embedded in NFV infrastructure. Each SFC consists of multiple workloads that can be distributed at more than one VM. However, when workloads are distributed, communication between the workloads and, hence, VMs is necessary, and the communication network must be able to support the necessary communication, introducing an additional layer of constraints that must be respected.

[1] I. Goodfellow, Y. Bengio, and A. Courville. *Deep Learning.* The MIT Press, 2016.

[2] R. S. Sutton and A. G. Barto. *Reinforcement Learning: An Introduction*. 2nd ed., The MIT Press, 2018.

Defining Ground Truth for Aggregated Security Metrics

Assane Gueye (Prometheus Computing)
Peter Mell (NIST ITL)

In security, we know how to make measurements of very specific features (e.g., number of infected hosts) but we don't know how to aggregate multiple metrics into meaningful indicators. However, executives desperately need aggregate measures in order to direct their funding decisions for securing an enterprise. Security officers need aggregate measurements to focus their scarce resources in improving the security posture of their systems. The security research field has largely given up on aggregating security measures because there is no ground truth for such measures. There is no provably correct answer. However, answers must be obtained in order to make security decisions and to evaluate whether or not a security posture has improved or declined.

In this work, we propose to define (not discover) a ground truth for such measurements. For physics, the ground truth comes from the physical world. For security, we don't have any ground truth, but we need something upon which to build aggregated security measurements. While not at all satisfactory, the best we have is human expert opinion. And such opinions will change over time as the humans learn and as the technology and threat landscape change. The result is that our ground truth and our metrics will change over time. While unsatisfying, this is the reality of metrics in computer security. We should embrace this reality instead of ignoring it and doing nothing.

The research question is how to harness human expert opinion in order to develop aggregated security metrics. We believe that a combination of human expert polling/voting with the training of machine learning algorithms can produce such aggregated security metrics that can evolve and improve over time given the changing threat landscape. We would mature such approaches from initially being able to order the severity of vulnerabilities to later provide actual aggregated metrics from individual inputs.

This could be used, for example, to create a metric that takes as input the set of system security plan controls and outputs an indication of the level of security of the system (at a much finer granularity than FIPS 199 [1]). Another example would be to input disparate measurements regarding the security state of a network and rate the security of that network. A final example would be a metric that takes as input the set of characteristics of a vulnerability and outputs a vulnerability score (note that such a metric exists as the Common Vulnerability Scoring System (CVSS)[25], but it has significant limitations). This latter example will be our initial test case.

The project will be divided in three major phases. In the first phase (our initial test case), we have focused on the CVSS, analyzing scores collected from 2005 to 2019. Our analysis has focused on three main subjects of interest. First, we have analyzed the evolution of the threat landscape over the years. Then, we studied the most frequent metric values and analyzed their rankings over the years. Finally, we used *association rule mining* techniques to derive the most prevalent patterns of co-occurrence of the metrics.

The analysis of the data has shown that the vulnerability threat landscape has been dominated by a few vulnerability types and has not evolved over the years. The overwhelming majority of software vulnerabilities are exploitable over the network (i.e., remotely). Successfully exploiting these vulnerabilities is not difficult, and very little authentication to the target victim is necessary for a successful attack. Moreover, most of the flaws require very limited interaction with users. The damage of these vulnerabilities has however mostly been confined in the scope of the compromised systems with very moderate spill-over.

With respect to co-occurrences of the metrics, we have derived a number of frequent association rules. By exploiting these relations and aligning them with human expert opinions, one may be able to establish some "ground truth" that can be used as a basis for sound software vulnerability metrics. Such a ground truth will certainly need to be regularly re-evaluated and updated as more vulnerabilities are discovered, and more technologies become available. The definition of the ground truth shall be considered in follow-on studies of the present one. A paper describing the current results is in process [2].

In the second phase, we will build the data collection tool which will be a computer program that automates the harnessing of human expert opinion. We will then leverage this data and develop the machine learning algorithms that shall enable us to build the proof-of-concept of the "moving ground truth" needed for aggregated security metrics. The last phase of the project will focus on generalizing our algorithms and results to cover other existing (and new) security metrics.

[1] Standards for Security Categorization of Federal Information and Information Systems, Federal Information Processing Standards (FIPS) Pub 199, NIST, February 2004. URL: https://nvlpubs.nist.gov/nistpubs/FIPS/NIST.FIPS.199.pdf

[2] P. Mell and A. Gueye. A Suite of Metrics for Calculating the Most Serious Security Relevant Software Flaw Types. In review.

[25] https://www.first.org/cvss/

Towards Pricing-Based Resource Management in Virtualized Radio Access Networks

Vladimir Marbukh
Kamran Sayrafian
Behnam Rouzbehani (University of Lisbon, Portugal)
Luis M. Correia (University of Lisbon, Portugal)

The objective of this project is developing a distributed, low complexity cross-layer optimization scheme for resource management in virtualized Radio Access Networks. The optimization should be subject to the Virtual Network Operators (VNOs) guarantee of the contracted Service Level Agreements (SLAs) to the users. In [1] we proposed an approach which uses weighted proportional fairness as a basis for allocation of the system capacity. This allocation is achieved by a distributed pricing-based solution to a two-layer convex optimization problem. Through this mechanism, some of the key functionalities of the centralized virtualization platform are transferred to the individual VNOs and users. This allows for a drastic reduction in the complexity of the system management compared to the previously proposed centralized approaches. Another advantage of the proposed distributed cross-layer optimization is the enhanced level of isolation among different VNOs.

In [2] we extended this scheme by combining Radio Resource Management (RRM) in virtualized Radio Access Networks (RANs) [1] with admission control. The system architecture follows the concept of network slicing proposed in the latest release of 3GPP standards for 5G service-oriented architectures [3]. The proposed distributed resource management approach overcomes the scalability issues of the centralized RRM. It maximizes the aggregate system utility using a two-stage distributed optimization with pricing adaptation on *fast* and *slow* time scales. At the faster time scale, assuming that VNO capacities do not change, users adjust their rates based on the congestion pricing. At the slower time scale each VNO adjusts its own capacity according to the congestion price at this VNO. This optimization is subject to the total capacity of the system. The decentralization is due to the dual role of congestion prices that are used for both adjustment of the users' rates and VNO capacity expansion/reduction.

We evaluated the proposed optimization scheme by simulating a scenario with three types of VNOs and differentiated SLAs sharing radio resources from an underlying physical heterogeneous network. Results for the four types of service classes confirm that the proposed combination of admission control and capacity allocation ensures that all SLAs are satisfied, the entire aggregated capacity is utilized, and the residual available capacity is shared among the users proportionally.

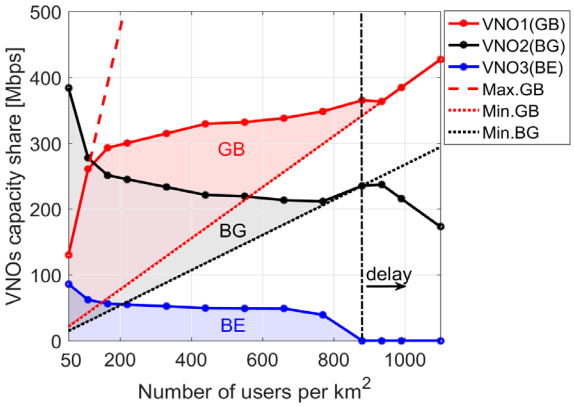

Figure 73. *Capacity share of virtual radio resource management among the virtual network operator.*

Figure 73 demonstrates the ability of the proposed algorithm to correct imbalances in the VNO capacities subject to the total and minimum capacity constraints. As the number of users in the system increases, a VNO providing Guaranteed Bitrate (GB) services experiences higher congestion than other VNOs. The proposed algorithm corrects this imbalance by increasing VNO GB capacity at the expense of the capacities of other VNOs. However, the capacity share of VNO providing Best Effort (BE) with minimum Guaranteed rate (BG) services does not drop below the minimum contracted SLA threshold.

In our future research we plan to address the fundamental assumption of time scale separation, including viability of this assumption in practical situations, performance loss in situations of comparable time scales in rate/capacity adaptation, and mechanisms to mitigate this inefficiency. Another potential direction of research is accounting for users with latency-sensitive services, which are described by a S-type utility function. The corresponding utility maximization problem is non-convex, and thus may require an approximate solution.

[1] B. Rouzbehani, V. Marbukh, K. Sayrafian, and L.M. Correia. Towards Cross-Layer Optimization of Virtualized Radio Access Networks. In *Proceedings of the 2019 IEEE European Conference on Networks and Communications (EUCN'19)*, Valencia, Spain, June 18-21, 2019.

[2] B. Rouzbehani, V. Marbukh, and K. Sayrafian. A Joint Admission Control & Resource Management Scheme for Virtualized Radio Access Networks. In *Proceedings of the 2019 IEEE Conference on Standards for Communications and Networking (CSCN'19),* Granada, Spain, October 28-30, 2019.

[3] G3GPP TS 29.500. 5G System; Technical Realization of Service Based Architecture, July 2018. Granada, Spain, October 28-30, 2019.

A Machine Learning Approach to Maximize Output Power of Kinetic-Based Micro Energy-Harvesters

Kamran Sayrafian
Masoud Roudneshin (Concordia University, Canada)
Amir G. Aghdam (Concordia University, Canada)

Wearable and implantable medical sensors are considered a key component of future telemedicine systems, allowing clinicians to have remote access to real-time patient's data. These devices typically operate by using small batteries; therefore, frequent recharge or battery replacement might be necessary to keep the device functioning properly. Prolonging the lifetime of these batteries and reducing their frequency of recharge could have a paramount impact on their everyday use. This is especially important for implanted devices, where battery replacement is not easily possible.

Energy harvesting refers to the process of scavenging energy from external sources (ambient environment such as solar power, wind and kinetic energy). For wearable devices, kinetic energy can be a reliable solution for power generation in medical sensors. For cases of non-stationary vibrations (for example, as a result of the human body motion), a Coulomb force parametric generator (CFPG) architecture has been proposed as a promising solution to extract power from human movements [1]. In this type of system, a proof mass can move within a space with upper and lower bounds $\pm X_l$. The summation of the device motion to the inertial frame $\xi(t)$ and the relative motion of the proof mass with respect to the device $x(t)$ make the absolute motion of the proof mass equal to $y(t) = \xi(t) + x(t)$. The dynamics of the proof mass motion in CPFG has been modeled by the following nonlinear differential equation [2]

$$m\ddot{y}(t) = -m\ddot{x}(t) - F \times Relay(x(t))$$

where m is the proof mass, $\ddot{y}(t)$is the acceleration of the frame of the CPFG with respect to the inertial frame, $\ddot{x}(t)$ is the relative acceleration of the proof mass with respect to the frame of the CFPG, F is the electrostatic holding force which acts against the motion of the proof mass, and *Relay* models a hysteresis function that switches between +1 and -1. The generated mechanical power of the system is equal to the product of the electrostatic holding force and the relative velocity of the proof mass with respect to frame and is calculated as

$$P(t) = F \times \dot{x}(t)$$

In [2], we demonstrate that the output power of a CFPG micro-harvester can be maximized by proper adjustment or adaptation of the electrostatic force F. A methodology for optimizing F by observing the input acceleration in the previous time interval was also proposed. In this project, we propose a novel method for the estimation of the suboptimal value of the electrostatic force in a micro energy-harvester, according to the current absolute acceleration of the CFPG frame. We use the frequency spectrum of the human body acceleration data in our analysis. Eight different machine learning classification schemes are then used and their performances are compared in terms of accuracy in estimating the suboptimal value of the holding force in the next time step for power maximization [3].

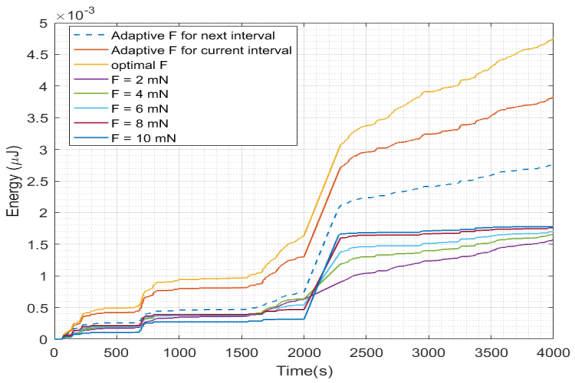

Figure 74. *Comparison of the harvested energy for the optimal value of F, using KNN algorithm and for various constant holding forces.*

Figure 74 displays the gain in the harvested energy for a 4000 s time interval using the basic machine learning K-Nearest Neighbors (KNN) Algorithm. The harvested energy for several constant holding forces is also plotted. In addition, for this example, we have included the amount of harvested energy using the optimal value of the holding force as a reference. The curve corresponding to the optimal F serves as an upper bound for the amount of energy that can be generated. As observed, the net output energy using the KNN technique could lead to a significant gain in the harvested power. The exact amount of the gain depends on many parameters such as the dimensions of the mass-spring-damper inside the harvester, adaptation time interval, and the classification algorithm. The impact of these parameters will be studied in more detail in future research.

Although it is desirable for the adaptive holding force methodology to be as close as possible to the optimal curve, one should also take into consideration the computational complexity of the algorithms used. The higher this complexity, the more energy it requires to perform, leading to less (or even no) gain in the harvested power. Therefore, a thorough analysis of the implementation complexity and the resulting power consumption of the added hardware is required to justify the addition of the optimization methodology to the micro harvester circuitry.

[1] P. D. Mitcheson, T. Sterken, C. He, M. Kiziroglou, E. Yeatman, and R. Puers. Electrostatic Microgenerators. *Measurement and Control* **41**:4 (2008), 114–119.

[2] M. Dadfarnia, K. Sayrafian, P. Mitcheson, and J. S. Baras. Maximizing Output Power of a CFPG Micro Energy-Harvester for Wearable Medical Sensors. In *Proceedings of the 4th International Conference on Wireless Mobile Communication and Healthcare*, 2014, 218–221.

[3] M. Roudneshin, K. Sayrafian, and A. Aghdam. A Machine Learning Approach to the Estimation of Near-Optimal Electrostatic Force in Micro Energy-Harvesters. In *Proceedings of the 7th Annual IEEE International Conference on Wireless for Space and Extreme Environments (WISEE 2019)*, Ottawa, Canada, October 16-18, 2019.

Combinatorial Testing for Software-based Systems

Raghu N. Kacker
D. Richard Kuhn (NIST ITL)
Yu Lei (University of Texas at Arlington)
Dimitris E. Simos (SBA-Research, Austria)
Mohammad S. Raunak (Loyola University, Maryland)
Nicky Mouha (NIST ITL)
Eric Wong (University of Texas at Dallas)
James F. Lawrence
Itzel Dominguez-Mendoza (CENAM, Mexico).

https://csrc.nist.gov/projects/automated-combinatorial-testing-for-software

In 1997, the Mars Pathfinder began experiencing system resets at seemingly unpredictable times soon after it landed and began collecting data. Fortunately, engineers were able to deduce and correct the problem, which occurred only when (1) a particular type of data was being collected, and (2) intermediate priority tasks exceeded a certain load, resulting in a blocking condition that eventually triggered a reset. Situations of this type are known as *interaction faults*. Many real-time failures of software-based systems have been traced to interaction faults. These are often insidious in that they may remain hidden until the unfortunate combination is encountered during system operation.

Combinatorial testing (CT) is a versatile methodology for detecting interaction faults. CT began as pairwise (2-way) testing in which all pairs of the test values for all pairs of test factors are checked. Thus, pairwise testing can detect faults involving single factors or interactions between two factors. CT is based on an empirical observation, referred to as the *interaction rule*, that while the behavior of a software system may be affected by many factors, only a few are involved in any given failure. NIST investigations of failures in actual systems have shown that while most faults involved a single factor or interaction between two factors, some faults involved three or more factors [1]. (A fault involving more than six factors has not yet been reported.) Thus, pairwise testing is useful, but it may not be adequate for detecting interaction faults involving more than two test factors.

More than a decade ago, NIST took the initiative to extend pairwise (2-way) CT to higher strength t-way CT for $t > 2$. NIST has helped make CT practical by developing research tools and techniques for generating combinatorial test suites. CT has now gained significant interest from the international software testing community. Many successful results from the use of CT in aerospace, automotive, and financial service industries, as well as defense, security, and electronic medical systems have since been reported.

A suite of test cases for combinatorial t-way testing includes (covers) at least once all possible t-tuples of the test values for every set (combination) of t factors out of the complete set of all k factors that are tested ($k > t$). Use of mathematical objects called covering arrays makes it possible to check all t-tuples of the test values with a small number of test cases. Table 1 shows a covering array of 13 rows and 10 columns each having two possible values, 0 and 1. Columns correspond to the factors and the rows correspond to the test cases. The number of possible sets (combinations) of 3 out of 10 test factors is $(10 \times 9 \times 8)/(3 \times 2 \times 1) = 120$. When each factor has two possible values, each set of 3 factors can have $2^3 = 8$ possible triples of test values ((0, 0, 0), (0, 0, 1), (0, 1, 0), (0, 1, 1), (1, 0, 0), (0, 0, 1), (1, 1, 0), (1, 1, 1)). So, the total number of possible triples of values for all 10 factors is $120 \times 8 = 960$. A test suite based on Table 1 includes (covers) at least once all 960 distinct triples of the test values of ten factors.

One wants a minimal covering array, which covers all possible t-tuples of the test values for every set of t out of all k factors with the least number of rows (test cases). In practice, many factors have dependencies and constraints, with the consequence that not all combinations of the test values may be logically or physically valid. A combinatorial test suite must avoid such forbidden combinations. Generating minimal covering arrays that avoid forbidden combinations is a difficult mathematical and computational problem [2]. A great deal of research has been done to develop mathematical and computational methods to generate minimal covering arrays of this type. NIST and its collaborators have developed several such algorithms.

NIST-Developed Tools: NIST has developed several research tools to make CT practical. ACTS (for Automated Combinatorial Testing for Software), which was developed in cooperation with the University of Texas at Arlington, includes several algorithms to generate high strength test suites for CT. The ACTS algorithms are optimized to efficiently avoid forbidden combinations of test settings. More than 3500 users have downloaded executable versions of the ACTS algorithms from the NIST webpage for CT. (It is difficult to ascertain the number of users because some users have

Table 1. *A covering array of 13 rows includes all eight triplets (000, 001, 010, 011, 100, 101, 110, and 111) of the possible values (0 and 1) for every one of the 120 possible sets of 3 out of 10 test factors represented by the columns (for example, see colored entries)*

	Columns									
Rows	**1**	**2**	**3**	**4**	**5**	**6**	**7**	**8**	**9**	**10**
1	0	0	0	0	0	0	0	0	0	0
2	1	1	1	1	1	1	1	1	1	1
3	1	1	1	0	1	0	0	0	0	1
4	1	0	1	1	0	1	0	1	0	0
5	1	0	0	0	1	1	1	0	0	0
6	0	1	1	0	0	1	0	0	1	0
7	0	0	1	0	1	0	1	1	1	0
8	1	1	0	1	0	0	1	0	1	0
9	0	0	0	1	1	1	0	0	1	1
10	0	0	1	1	0	0	1	0	0	1
11	0	1	0	1	1	0	0	1	0	0
12	1	0	0	0	0	0	0	1	1	1
13	0	1	0	0	0	1	1	1	0	1

redistributed to others and some are students who may have used it only once for a single project.)

A second research tool, CCM (for Combinatorial Coverage Measurement), developed jointly by NIST and a guest researcher from CENAM, the national metrology institute of Mexico, describes the incompleteness of a test suite that may not have been developed from a CT viewpoint. Basic combinatorial coverage measurements describe the incompleteness of a test suite relative to a test suite based on a covering array that includes all possible *t*-tuples of values for every *t*-factor combination for various values of *t*. The combinatorial deficiency of a test suite can be remedied by additional tests. Thus, CCM can help guide the expansion of a test suite to satisfy stated combinatorial requirements [3]. The latest version of CCM supports constraints which exclude forbidden combinations of values. A parallel processing version is also available.

Impact of NIST Research: NIST efforts have sparked a surge of research and application of combinatorial testing technology. A 2010 NIST Special Publication on CT was downloaded more than 30 000 times by end 2014 [4]. In 2013, we published a book with CRC Press on this topic [5]. One of the first large-scale users that we worked with is a group at the U.S. Air Force Base in Eglin, Florida. The behavior of one of their systems depended on the sequential order of certain events. This led to the problem of testing sequences of events, which required development of new mathematical objects called *sequence covering arrays* [6, 7, 8]. Lockheed-Martin, a large U.S. defense contractor, reported (based on eight projects) that use of CT reduced cost of testing by about 20 % with 20 % to 50 % improvement in test coverage [9]. CT methods are now being used in diverse areas such as financial services, automotive, automation, avionics, video coding standards, and for security testing. The NIST webpage for CT cites over forty application papers.

For testing a software-based system, no single approach is enough. Multiple approaches are generally needed at various stages of software development and installation. CT complements other approaches for testing, verification, and validation of software-based systems. CT is now included in software engineering courses taught in more than 18 U.S. universities and two Austrian universities. NIST efforts on technology transfer of CT tools and techniques received the 2009 Excellence in Technology Transfer Award from the Federal Laboratory Consortium-Mid Atlantic Region.

CT has also gained significant interest from the research community. In 2012, NIST took the lead in organizing a workshop on CT[26] in conjunction with the IEEE International Conference on Software Testing, Verification, and Validation (ICST), a premier conference in this field[27]. Since then, an International Workshop on Combinatorial Testing (IWCT) has become an annual event for sharing advancements in CT tools and techniques, as well as results from practical industrial use of CT. The eighth such IWCT was held on April 23, 2019 in Xian, China (https://iwct2019.sba-research.org/) in conjunction with ICST 2019 (http://icst2019.xjtu.edu.cn/). Four of us (Kacker, Kuhn, Lei, and Simos) were among the co-organizers. The IWCT 2019 received 19 submission, from which the Program Committee selected 14 papers (6 full papers, 6 short papers, and 2 extended abstracts for poster presentations). The program contained research papers as well as on applications and use cases of CT. IWCT is now the largest of the workshops associated with ICST in both the number of papers and the number of participants.

Recent accomplishments and current projects include the following.

- *Cryptographic hash functions* are security-critical algorithms with many practical applications, notably in digital signatures. We used combinatorial testing methods to detect bugs in implementations of cryptographic hash functions. One bug had remained undetected despite extensive testing over a period of seven years. The results are reported in a paper in the IEEE Transaction on Reliability [10].
- *Fault localization* is a generic problem in testing software-based systems. It refers to detecting from the pass/fail results of testing an error (bug) that triggers a failure. Our research paper on tools and techniques for fault localization from combinatorial

[26] http://www.research.ibm.com/haifa/Workshops/ct2012/

[27] http://icst2012.soccerlab.polymtl.ca/Content/home/index.php?language=english

testing has been accepted for publication in the IEEE Transactions on Software Engineering [11].

- CT has been found to be effective in testing and verifying *Rule-based Security Systems*. A paper on this topic appeared in the proceedings of the 30th International Conference on Software Engineering and Knowledge Engineering (SEKE 2018) [12].
- *Combinatorial Sequence Testing for Browser Fingerprinting*: We investigated the applicability of combinatorial sequence testing to the problem of fingerprinting browsers based on their behavior during a Transport Layer Security (TLS) handshake [13].
- We have investigated *practical issues in using CT* in five real-life studies. A paper entitled 'How does Combinatorial Testing Perform in the Real World: An Empirical Study' has been submitted for publication to the journal Empirical Software Engineering.
- In collaboration with researchers from Adobe and SBA-Research, a leading Austrian research center for information security, we showed that CT is an effective way to validate the *data collection, compression and processing components of Adobe analytics* [14]. Moreover, we performed combinatorial coverage measurements to evaluate the effectiveness of the *validation framework for the Adobe Analytics reporting engine*. The results of this evaluation show that combinatorial coverage measurements are an effective way to supplement existing validation for several objectives [15].

Our on-going research projects include the following:

- *Combinatorial Security Testing for IoT systems*: In collaboration with a team of researchers from the SBA-Research, we are testing for the security of Internet of Things home automation systems using combinatorial methods. We created an input parameter model to be used with a combinatorial test case generation strategy. We evaluated the generated test cases on a real-world IoT appliance settings compatible with the created abstract model. We implement an automated test execution framework which includes automated test oracles for evaluation purposes.
- *Combinatorial Fuzzing for Smart Contracts*: A blockchain is a decentralized computer system that uses cryptographic and distributed consensus technologies to record information in a permanent and verifiable manner. A smart contract is a computer program that executes one or more transactions on a blockchain. When some conditions are met, the transactions are automatically executed, and their results are recorded on the blockchain in a way that cannot be changed. We are investigating a combination of CT and a basic testing approach called fuzzing to improve code coverage in testing smart contracts. We are investigating eight real-life smart contracts. Our initial results show about 20 % improvement of code coverage.
- *CT for Multiple Input Models*: Existing work on CT is mainly concerned with test generation for a single input model (selection of test factors and their values). We are investigating test generation for multiple input models with shared parameters (test factors). This problem arises in finite state machine (FSM)-based testing and graphical user interface (GUI) testing.

[1] D. R. Kuhn, D. R. Wallace, and A. M. Gallo, Jr. Software Fault Interactions and Implications for Software Testing. *IEEE Transactions on Software Engineering*, **30** (June 2004), 418-421. DOI: 10.1109/TSE.2004.24

[2] L. Kampel and D. E. Simos. A Survey on the State of the Art of Complexity Problems for Covering Arrays. *Theoretical Computer Science* **800** (2019), 107-124. DOI: 10.1016/j.tcs.2019.10.019

[3] D. R. Kuhn, R. N. Kacker, and Y. Lei. Combinatorial Coverage as an Aspect of Test Quality. *CrossTalk: The Journal of Defense Software Engineering*, March/April 2015, 19-21.

[4] D. R. Kuhn, R. N. Kacker, and Y. Lei. Practical Combinatorial Testing, Special Publication 800-142, National Institute of Standards and Technology, October 2010. URL:http://nvlpubs.nist.gov/nistpubs/Legacy/SP/nistspecialpublication800-142.pdf

[5] D. R. Kuhn, R. N. Kacker, and Y. Lei. *Introduction to Combinatorial Testing*. CRC Press, 2013.

[6] D. R. Kuhn, J. M. Higdon, J. F. Lawrence, R. N. Kacker and Y. Lei. Combinatorial Methods for Event Sequence Testing. In *Proceedings of the 5-th IEEE International Conference on Software Testing, Verification and Validation Workshops* (ICSTW), Montreal, Quebec, Canada, April 17-21, 2012, 601-609. DOI: 10.1109/ICST.2012.147

[7] D. R. Kuhn, J. M. Higdon, J. F. Lawrence, R. N. Kacker and Y. Lei. Efficient Methods for Interoperability Testing using Event Sequences. *CrossTalk: The Journal of Defense Software Engineering*, July/August 2012, 15-18. URL: https://apps.dtic.mil/docs/citations/ADA566540

[8] Y. M. Chee, C. J. Colbourn, D. Horsley, and J. Zhou. Sequence Covering Arrays. *SIAM Journal of Discrete Mathematics* **27** (2013), 1844-1861. DOI: 10.1137/120894099

[9] J. Hagar, D. R. Kuhn, R. N. Kacker, and T. Wissink. Introducing Combinatorial Testing in a Large Organization. *IEEE Computer* **48** (April 2015), 64-72. DOI: 10.1109/MC.2015.114

[10] N. Mouha, M. S. Raunak, D. R. Kuhn, and R. N. Kacker. Finding Bugs in Cryptographic Hash Function Implementations. *IEEE Transactions on Reliability* **67** (September 2018), 870-884. DOI: 10.1109/TR.2018.2847247

[11] L. S. Ghandehari, Y. Lei, R. N. Kacker, D. R. Kuhn, T. Xie, and D. Kung. A Combinatorial Testing-Based Approach to Fault Localization, *IEEE Transactions on Software Engineering*, to appear. DOI: 10.1109/TSE.2018.2865935

[12] D. R. Kuhn, D. Yaga, R. N. Kacker, Y. Lei, and V. Hu. Pseudo-exhaustive Verification of Rule Based Systems. In *Proceeding of the International Conference on Software Engineering and Knowledge Engineering* (SEKE 2018), Redwood City, CA, July 1-3, 2018, 586-591. DOI: 10.1109/TR.2018.2847247

[13] B. Garn, D. E. Simos, S. Zauner, D. R. Kuhn, and R. N. Kacker. Browser Fingerprinting using Combinatorial Sequence Testing, In *Proceedings of the 2019 Conference on Hot Topics in the Science of Security (HoTSoS 2019),* Nashville, TN, April 2-3, 2019, Article 7. DOI: 10.1145/3314058.3314062

[14] R. Smith, D. Jarman, R. Kuhn, R. N. Kacker, D. E. Simos, L. Kampel, M. Leithner, and G. Gosney. Applying Combinatorial Testing to Large-scale Data Processing at Adobe. In *Proceedings of the 12-th IEEE International Conference on Software Testing, Verification and Validation Workshops* (ICSTW), Xian, China, April 22-27, 2019, 190-193. DOI: 10.1109/ICSTW.2019.00051

[15] R. Smith, D. Jarman, J. Bellows, R. Kuhn, R. N. Kacker, and D. E. Simos. Measuring Combinatorial Coverage at Adobe. In *Proceedings of the 12-th IEEE International Conference on Software Testing, Verification and Validation Workshops* (ICSTW), Xian, China, April 22-27, 2019, 194-197. DOI: 10.1109/ICSTW.2019.00052

Mathematical Knowledge Management

We work with researchers in academia and industry to develop technologies, tools, and standards for representation, exchange, and use of mathematical data. Of particular concern are semantic-based representations which can provide the basis for interoperability of mathematical information processing systems. We apply these representations to the development and dissemination of reference data for applied mathematics. The centerpiece of this effort is the Digital Library of Mathematical Functions, a freely available interactive and richly linked online resource, providing essential information on the properties of the special functions of applied mathematics, the foundation of mathematical modeling in all of science and engineering.

Digital Library of Mathematical Functions

Barry I. Schneider
Daniel W. Lozier
Bruce R. Miller
Bonita V. Saunders
Howard S. Cohl
Marjorie A. McClain
Ronald F. Boisvert
Adri B. Olde Daalhuis (University of Edinburgh)
Charles W. Clark (NIST PML)
Brian Antonishek (NIST EL)

http://dlmf.nist.gov/

Progress in science has often been catalyzed by advances in mathematics. More recently, developments in the physical sciences, such as investigations into string theory, have influenced pure mathematics. This symbiotic relationship has been extremely beneficial to both fields. Mathematical developments have found numerous applications in practical problem-solving in all fields of science and engineering, while cutting-edge science has been a major driver of mathematical research**.** Often the mathematical objects at the intersection of mathematics and physical science are mathematical functions. Effective use of these tools requires ready access to their many properties, a need that was capably satisfied for more than 50 years by the *Handbook of Mathematical Functions with Formulas, Graphs, and Mathematical Tables*, which was published by the National Bureau of Standards (NBS) in 1964 [1].

The 21st century successor to the NBS Handbook, the freely accessible online Digital Library of Mathematical Functions (DLMF) together with the accompanying book, the *NIST Handbook of Mathematical Functions* [2], published by Cambridge University Press in 2010, are collectively referred to as the DLMF. The DLMF continues to serve as the gold standard reference for the properties of what are termed the special functions of applied mathematics.

The DLMF has considerably extended the scope of the original handbook as well as improving accessibility

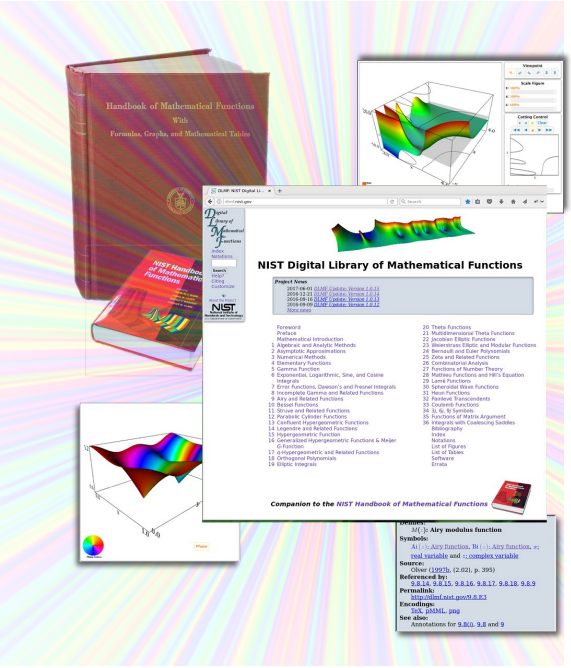

Figure 75. *A visual history of the DLMF from its roots in the 1964 NBS Handbook to the eye catching and informative graphical contents of the present DLMF.*

to the worldwide community of scientists and mathematicians. To cite a few examples, the new handbook contains more than twice as many formulas as the old one, coverage of more functions, in more detail, and an up-to-date list of references. The website covers everything in the handbook and much more: additional formulas and graphics, math-aware search, interactive zooming and rotation of 3D graphs, internal links to symbol definitions and cross-references, and external links to online references and sources of software.

In order to help assess the impact of the DLMF project, the NIST library has undertaken a project to track citations to the DLMF, as well as to the original NBS Handbook. While the original Handbook still receives an enormous number of citations, citations to the DLMF are steadily growing in relation to the original handbook. Google Scholar now reports more than 5 500 citations to

the DLMF. During calendar year 2019 the DLMF website served up some 5.4M pages to more than 324 000 visitors in some 508 000 sessions. This is roughly a 20 % increase over 2018, in spite of the fact that the DLMF was shut down for much of January 2019 due to the government-wide lapse in appropriations.

Today's DLMF is the product of many years of effort by more than 50 contributors. Its initial release in 2010, however, was not the end of the project. Corrections to errors, clarifications, bibliographic updates, and addition of new material all need to be made on a continuing basis. And, new chapters covering emerging subject areas need to be added, to assure the continued vitality of the DLMF deep into the 21st century. In the past year, there were four DLMF releases, 1.0.22 (2019-03-15), 1.0.23 (2019-06-15), 1.0.24 (2019-09-15) and 1.0.25 (2019-12-15) which kept us on our quarterly release schedule.

The updating of various DLMF chapters and the development of new ones continues. These include a new chapter on Orthogonal Polynomials of Several Variables and substantial updates to the chapters on Orthogonal Polynomials, Algebraic Methods, and Painlevé Transcendents. Four authors were identified to carry out the work. Drafts are now available and are being internally reviewed. External validation of the chapters will follow in much the same manner as the original DLMF.

One of the design goals for the DLMF was that each formula would be connected to a proof in the literature. This data, visible as annotations on the website, provides either a proof for the formula, a reference to the proof for the formula or, for definitions, a reference which gives that definition. Unfortunately, this information was not provided in all cases. We are working to systematically verify the completeness and traceability to published proofs for DLMF formulae. This audit has been completed for Chapter 25 (Zeta and Related Functions) and is actively continuing for Chapters 1-5 and 22-30. In addition, work has progressed to make proof-related information visible in metadata at the equation level. Improvements in markup to more accurately identify the nature of the added material have been developed and deployed (see Chapter 9, Airy and Related Functions).

A major step that was taken this year was the migration of the DLMF from the CVS repository to Github. This has enabled a far more thorough approach to updating the DLMF, reporting and dealing with bugs and correcting mistakes.

Finally, in recognition of both past accomplishments and excellent service to the goals of the DLMF project, Howard Cohl was named Technical Editor and Marjorie McClain Associate Technical Editor of the DLMF.

[1] M. Abramowitz and I. Stegun, eds. *Handbook of Mathematical Functions with Formulas, Graphs and Mathematical Tables*. Applied Mathematics Series 55, National Bureau of Standards, Washington, DC 1964.

[2] F. Olver, D. Lozier, R. Boisvert and C. Clark, eds. *NIST Handbook of Mathematical Functions*. Cambridge University Press, 2010.

Visualization of Complex Functions Data

Bonita Saunders
Bruce Miller
Brian Antonishek (NIST EL)
Sandy Ressler
Qiming Wang (NIST retired)

Our visualization of complex functions data is motivated by a desire to help researchers obtain a clear understanding of mathematical functions arising as solutions to problems in the physical and mathematical sciences. The goal is to design informative and accurate web visualizations that are freely accessible to users on most computer platforms. Our general approach consists of four distinct, but essential components. First, we use reliable sources, such as the NIST Digital Library of Mathematical Functions (DLMF) and other published references, to study function definitions and properties to determine the function's behavior. Second, we search for trustworthy numerical software that can be used to compute plot data or validate its accuracy. Next, we create custom designed computational meshes to capture key function features such as zeros, branch cuts, poles, and other discontinuities; and finally, we utilize or expand existing technology for 3D web graphics to develop interactive surface visualizations that spur user exploration.

Since the DLMF provided the impetus for this project, our work was initially driven by a quick results-oriented approach. Now that the DLMF is well established we are re-examining some components to determine how our work might be improved to enhance the DLMF visualizations or generalized to benefit a larger research community. Our current work on adaptive meshes to improve our underlying computational grids supports our design process, but it may also interest other researchers in the fields of mesh generation, optimization, approximation theory, or any area related to the design of curves and surfaces for mathematical or physical applications. For this reason, we continue to publish and present our results at universities, conferences, and workshops [1-8].

To facilitate the recent move of DLMF files to a GitHub repository we reorganized or purged DLMF graphics files to decrease the storage needed. Large executable files were replaced with scripts that quickly regenerate visualization executables whenever the

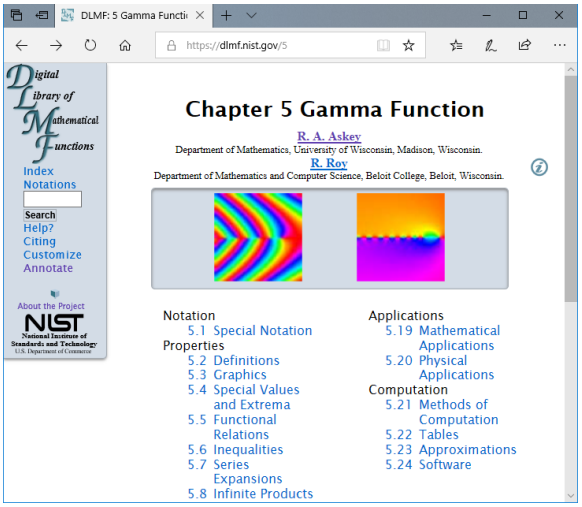

Figure 76. *Title web page of the DLMF chapter on the gamma function. Two gallery images show density plots of the complex gamma and digamma functions. The images link to a sidebar providing additional descriptive information*

DLMF website is rebuilt. Similarly, we may want to store scripts that regenerate the computational grids and plot data, but this is not a trivial task. We can store the grid sizes and parameters that define the grid generation mappings, but significant grid modifications will require extensive preprocessing work. Accessibility to the numerical software needed to compute the plot data is another issue. Preferably, it should also be stored in the repository, but this may involve dealing with C++, Fortran and other languages, or commercial computer algebra packages.

As time permits, we will continue to explore opportunities to increase the visibility of our work. The NIST Public Affairs Office recently placed our DLMF inspired image of the gamma and digamma functions in the Executive Conference Room at NIST. The picture was originally part of a NIST art gallery display at the Johns Hopkins University Montgomery County Campus [9]. We also want to increase visibility inside the DLMF site. Currently, some DLMF chapters display chapter related images on the title page as shown in Figure 76. Creating a gallery of images for all chapters would add visual interest to the DLMF. Each image would link to a short descriptive sidebar that could include links to the chapter's application section or related function visualizations. New and updated DLMF chapters currently under development can provide a test bed for this work.

[1] B. Saunders. Complex Variables, Mesh Generation, and 3D Web Graphics: Research and Technology Behind the Dynamic Visualizations in the NIST Digital Library of Mathematical Functions. In *Proceedings of the National Association of Mathematicians (NAM) 50th Anniversary Celebration*, AMS Contemporary Mathematics Series, to appear.

[2] B. Saunders. "Mathematics, Mesh Generation, & 3D Graphics on the Web and Finding a Career at NIST." MD-DC-VA Fall Section Meeting, Mathematical Association of America, Norfolk State University, November 9, 2019.

[3] B. Saunders. "B-Splines and 3D Web Graphics: Mathematics and Technology Behind the Visualizations of the NIST Digital Library of Mathematical Functions." George Mason University, Fairfax, VA, October 25, 2019.

[4] B. Saunders. "B-Spline Mesh Generation, 3D Web Graphics and the NIST Digital Library of Mathematical Functions." Lafayette College, Easton, PA, September 25, 2019.

[5] B. Saunders. "An Adaptive Curvature and Gradient Based Grid Generation Method." 15th Meeting on Applied Scientific Computing and Tools (MASCOT 2018), Rome, Italy, October 5, 2018.

[6] B. Saunders, "Adaptive Curvature-Based Grid Generation for 3D Web Graphics", Curves and Surfaces 2018, Arcachon, France, July 3, 2018.

[7] B. Schneider, B. Miller, B. Saunders. NIST's Digital Library of Mathematical Functions. *Physics Today,* **71**:2 (2018), 48-53. DOI: https://doi.org/10.1063/PT.3.3846

[8] B. Saunders. "NIST's Digital Library of Mathematical Functions and the Digital Age." MD-DC-VA Spring Section Meeting, Mathematical Association of America, Virginia Military Institute/Washington & Lee University, Lexington, VA, April 14, 2018.

[9] C. Clark, B. Saunders, and B. Miller. DLMF Gamma, Digamma Phase Plot Display. MICRO/MACRO: Big Images of Small Things from NIST Labs. Johns Hopkins University Montgomery County Campus, Rockville, MD, September 6 – November 11, 2016.

Towards a Machine-Readable Digital Library of Mathematical Functions

Bruce Miller
Deyan Ginev (Chakra Consulting)
Tom Wiesing (University of Erlangen, Germany)

The principal initial goal of the Digital Library of Mathematical Functions (DLMF) project was to present useful definitions, relationships, properties and other information about the special functions for use by scientists and engineers; that is, directly to people. In the medium term, we have striven to develop procedures for DLMF enhancements, maintenance and corrections. While we feel we have been successful so far, the longer-term goal of putting all data into a fully machine-readable form has been slower in coming, given the scale and complexity of the material. This form would improve the findability, accessibility, reuse, and, in particular, computability of the mathematics.

While one can imagine a sufficiently rich set of semantic LaTeX macros allowing the author to specify not

only the printed form of the formula, but completely specify the exact semantic meaning of every symbol and expression as well, this approach is so cumbersome as to be impractical. Conversely, one might imagine eventual artificial intelligence able to infer the meaning from any given TeX markup along with the document's full text and context, but that is hardly feasible as yet. We seek the sweet spot between those extremes where the author supplies just enough clarity via semantic macros so that follow-up analysis can resolve any remaining ambiguities.

Fully implementing this strategy is still very much a work in progress, particularly the latter inference aspect, even scaled down. Progress is being made in several fundamental components, however, and there are many benefits to even partly annotated and disambiguated data in terms of web services and information discovery.

Short of fully explicit author markup, the mathematical formula must be parsed at least to determine the expression structure. We are cataloging the range of mathematical notations both within and outside of DLMF and have continued to enhance the mathematical grammar to increase the coverage. Additionally, we are exploring parsing frameworks which provide multiple parses to cover cases where the notation has several possible interpretations. Techniques for pruning these possibilities according to consistency or partial knowledge are being developed.

We have developed and made use internally of a set of semantic macros for DLMF's special functions and the more notationally complex concepts. Focusing here resolves some of the most glaring ambiguities, both syntactic and semantic. (There are so many different *f*'s!) This even provides a convenience to authors to simplify and regularize the typing required. As the benefits of machine-readable mathematical data on the web become realized and more apparent, a much broader audience of authors is likely to find these tools useful. For our macro set to be more palatable to that audience, it needs to be appropriately simplified and yet generalized. We are working towards this with the goal of publishing and making available our semantic macro set.

A common basis is also necessary for effective interoperability. Are the functions treated in DLMF actually the same as those in Mathematica, or Maple or the NAG libraries? As it turns out, usually they are, but sometimes they are not, and the differences can be subtle. Establishing these correspondences is exactly the purpose of the Special Function Concordance activity of the International Mathematical Knowledge Trust (IMKT) established by the Global Digital Mathematical Library (GDML) working group of the International Mathematical Union. We are participating in this effort to establish this concordance between the various special functions, in all their flavors, as used within various handbooks, such as the DLMF, and software systems, such as Mathematica, Maple and NAG, to assure interoperability.

For our part, we are developing a catalog of the special functions as defined in DLMF. Obviously, we start by listing those formulas which we consider to be the defining ones for each function. However, the key is to focus on those aspects, those choices, that potentially distinguish our version of a particular function from those of other systems. Choices of argument conventions (e.g., elliptic functions sn(u,k) vs. sn(u,m)) are significant. Patterns of singularities and type signatures help distinguish different extensions and generalizations of functions. A trickier class of difference are the choices made for the location of branch-cuts or which value is taken on the cuts, or indeed the choice made to avoid them entirely as multi-valued functions. Given this set of distinguishing features, we are collecting and encoding that information for each of the DLMF's functions in the form of OpenMath Content Dictionaries.

Scientific Document Corpora for Natural and Mathematical Language Research

Bruce Miller
Deyan Ginev (Chakra Consulting)
Tom Wiesing (University of Erlangen, Germany)

Recent advances in machine learning have opened up new possibilities for harvesting large collections of scientific documents to find, understand and reuse information. There is much research and development still to be carried out in Natural Language Processing (NLP) as well as extending this research to the unique characteristics of mathematical and scientific language and notation. To enable such research, it is important to have a set of documents available in a form appropriate for processing to use as both training and test data. In order to provide a statistical foundation for further work, the larger the data set the better. To that end, we have applied our LaTeXML tool to the massive corpus at arXiv.org[28]. We have then carried out initial experiments on statement classification using that data set.

LaTeXML[29] was originally developed for use in converting the LaTeX sources of the Digital Library of Mathematical Functions (DLMF)[30] into web format, namely HTML and MathML. Most of arXiv.org is also in LaTeX format, albeit using a significantly less disciplined markup style and a wide variety of support

[28] https://arXiv.org/

[29] https://dlmf.nist.gov/LaTeXML/

[30] https://dlmf.nist.gov/

packages, including uncommon or very complex ones. By continuing to refine and develop LaTeXML, to make it more robust as well as to increase the coverage of new or evolving TeX packages, we have managed to convert 96 % of arXiv's 1.4M documents into HTML+MathML with a 69 % success rate (documents producing, at worst, warnings).

Although the markup used in LaTeX documents found in the wild seldom emphasizes semantics, there are nevertheless a number of macros and environments which can be taken to reflect the author's intent. Such markup may indicate theorems, proofs, definitions as well as introductions and acknowledgments and so on. We were able to extract some 10M such annotated paragraphs in 50 categories from our conversion of arXiv [1]. Using 80 % of the documents as a training set, we discovered that many categories were too similar. For example, theorems, lemmas and propositions share language patterns. Combining these "confusion nests" yielded 13 clear cut categories into which the paragraphs could be reliably categorized with a 0.91 F1 score.

[1] D. Ginev and B. R. Miller. Scientific Statement Classification over arXiv.org. arXiv:1908.10993

Mathematical Language Processing

Abdou Youssef
Bruce Miller
Howard S. Cohl
Moritz Schubotz (Karlsruhe - Leibniz-Institute for Information Infrastructure, Germany)
André Greiner-Petter (Technische Universität Berlin, Germany)

Math concepts, expressions and equations permeate articles and documents in all STEM fields, since they express scientific and technical knowledge precisely and concisely. As the volumes of knowledge in STEM fields are already enormous and growing at an exponential rate, it has become imperative to automate the processing of STEM manuscripts to identify and extract knowledge, and to use that knowledge in high-end computer applications.

Math language processing (MLP) is a new discipline that is emerging to meet the above-stated goal and to address all the challenges involved. In ACMD we have been involved in several MLP projects to create basic and applied methods, software tools, annotated datasets, and ultimately full-fledged systems and applications, for students, researchers, scientists and practitioners in math, science and engineering areas. Our projects utilize a whole spectrum of technologies and techniques, including machine learning (ML), deep learning (DL), natural language processing (NLP), computational linguistics, and mathematical knowledge management.

The following two ongoing projects represent some of what we are currently doing in MLP.

Deep Learning for Math and Science Processing. This project, now in its third year, is using the latest in machine learning, deep learning, and natural language processing techniques and technologies to develop methods and software for extracting and disambiguating semantics from text and equations in math and science documents, and to leverage those methods and software to create new tools and applications. Supported by three successive annual grants from the ITL Building the Future Program, the project contributes to progress in knowledge discovery and use, and to the synthesis of large and exponentially growing volumes of technical text in STEM fields.

We have already created new, first-of-a-kind labeled and unlabeled datasets of math content, that are used by us and the research community for training and testing powerful ML/DL models for extracting and classifying knowledge in STEM documents, and turning that knowledge to something useful for general users in education, research, engineering, and technology.

In the next phase, the project will:

- Enhance our part-of-math tagger that we have been developing, so it provides the unambiguous in-context meaning/role of every math term in an equation.
- Start to develop and evaluate DL-based math-specific summarization systems. They will be both extractive (for selected equations and key phrases) and abstractive (for more concise paraphrasing), single- and multi-document, and personalizable to better serve the individual users' needs.
- Leverage NIST's Digital Library of Mathematical Functions (DLMF) and the papers/textbooks referenced by the DLMF, to create a technical summarization labeled-dataset of document-summary pairs. Such a labeled dataset will be greatly useful for training and testing math-specific summarization systems like the ones mentioned above.
- Continue development of enhanced techniques and declarative information within the DLMF source files, leading to a fully disambiguated dataset, and to Content-MathML representation of the math that can be used in further computation.

Automated Presentation-to-Computation (P2C) Conversion. STEM students, researchers and practitioners often need to compute with mathematical expressions and equations. To do so, they traditionally have to write software (*aka*, code), one for each expression or equation. That takes considerable human effort and time and is error prone. To increase the efficiency

and productivity of STEM users, and to improve reliability and accuracy of computations, it is desirable to have computer systems that automatically convert math expressions into code that computes those math expressions, that is, to automate the process of *presentation-to-computation* (P2C) *conversion*.

In this project, using the part-of-math tagger that we have built and continue to enhance, and in collaboration with a number of outside researchers, as well as local high school summer interns, we have developed P2C techniques and software to convert a fairly large set of mathematical expressions (written in LaTeX and some pre-defined macros) to Maple and Mathematica code, with considerable success. Maple and Mathematica are two widely used mathematical computation platforms (also known as computer algebra systems). Examples of math expressions that can now be automatically converted to code include long functional summations and products, derivatives, and integrals, to name a few. P2C conversion of more kinds of expressions is currently underway.

Performance evaluations of our conversion techniques have been conducted and have shown that the resulting output code is quite accurate. Further advancement is planned using more sophisticated versions of the part-of-math tagger that will result from applying deep learning techniques to MLP.

[1] A. Youssef and B. Miller. Explorations into the Use of Word Embedding in Math Search and Math Semantics. In *Intelligent Computer Mathematics* (C. Kaliszyk, E. Brady, A. Kohlhase, and C. Sacerdoti Coen, eds.), CICM 2019, *Lecture Notes in Computer Science* **11617** (2019), Springer.

[2] H. Cohl, M. Schubotz, A. Youssef, A. Greiner-Petter, J. Gerhard, B. V. Saunders, M. A. McClain, J. Bang and K. Chen. Semantic Preserving Bijective Mappings of Mathematical Formulae Between Word Processors and Computer Algebra Systems *Lecture Notes in Artificial Intelligence* **10383** (2017), Springer.

[3] A. Greiner-Petter, H. Cohl, A. Youssef, M. Schubotz, A. Trost, R. Dey, A. Aizawa, and B. Gipp. Comparative Verification & Validation of Digital Mathematical Libraries and Computer Algebra Systems. In review.

DLMF Standard Reference Tables on Demand

Bonita Saunders
Bruce Miller
Marjorie McClain
Annie Cuyt (U. Antwerp)
Stefan Becuwe (U. Antwerp)
Franky Backeljauw (U. Antwerp)
Chris Schanzle

http://dlmftables.uantwerpen.be/

DLMF Standard Reference Tables on Demand (DLMF Tables) is a collaborative project between ACMD and the University of Antwerp Computational Mathematics Research Group (CMA) [1-5]. The goal is to develop an online system for generating tables of special function values with an error certification for comparison with software for computing special functions. The system might be used by software developers or researchers to test their own code or to confirm the accuracy of results obtained from a commercial or publicly available package. User-specified precision of the computed function values will be a key feature.

A beta site based on CMA's MpIeee, a multiprecision IEEE 754/854 compliant C++ floating point arithmetic library, is already available at the University of Antwerp, but work is underway to prepare for the eventual movement of the site to NIST. We are currently standardizing the structure and documentation of the codes that compute the function values. This task began in summer 2019 in Belgium when DLMF Tables project leader B. Saunders spent several weeks working directly with the Antwerp team. Since all project members at NIST and Antwerp are heavily involved in multiple projects, carving out time to dedicate to DLMF Tables is a concern. We are working to alleviate this problem through an improved distribution of tasks, regular local meetings among the ACMD team, and frequent communication with CMA in Antwerp by email or teleconference.

We are also looking for additional personnel to work on the project. A postdoc interested in the validated computation of special functions would be an ideal addition to the team. We have submitted advertisements and articles to various technical mailing lists, newsgroups, and newsletters, and discussed our work in several talks and technical publications [6-11]. To date no suitable candidates with direct experience have been found, and we are expanding our search to mathematicians, computational scientists, and physical scientists in related fields. We are also working to bring more diversity into the field. This summer B. Saunders is leading the project "Validated Numerical Computations of Mathematical Functions" at the African Diaspora Joint

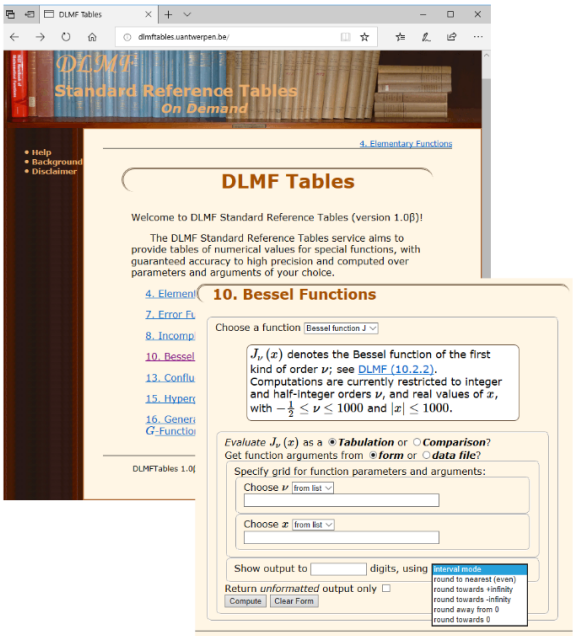

Figure 77. *DLMF Tables generates tables of special function values at user specified precision. Users input real values and parameters where the function is to be evaluated. The user may request output in interval mode, where the output is shown as a table of intervals that bound the true results or may request output in one of several rounding modes. Users may also choose to compare their own table of values to the reference values generated by the system.*

Mathematics Workshop (ADJOINT 2020) at the Mathematical Sciences Research Institute (MSRI) in Berkeley, California. The workshop is designed to establish and promote research collaborations among U.S. mathematicians, especially those of sub-Saharan African descent.

[1] F. Backeljauw, S. Becuwe, A. Cuyt, J. Van Deun, and D. Lozier. Validated Evaluation of Special Mathematical Functions. *Science of Computer Programming* **10** (2013), 1016.

[2] M. Colman, A. Cuyt and J. Van Deun. Validated Computation of Certain Hypergeometric Functions. *ACM Transactions on Mathematical Software* **38**:2 (January 2012), Article 11.

[3] F. Backeljauw. A Library for Radix-independent Multiprecision IEEE-compliant Floating-point Arithmetic. Technical Report 2009-01, Department of Mathematics and Computer Science, Universiteit Antwerpen, 2009.

[4] A. Cuyt, V. B. Petersen, B. Verdonk, H. Waadeland and W. B. Jones. *Handbook of Continued Fractions for Special Functions*. Springer, New York, 2008.

[5] A. Cuyt, B. Verdonk, H. Waadeland. Efficient and Reliable Multiprecision Implementation of Elementary and Special Functions. *SIAM Journal of Scientific Computing* **28** (2006), 1437-1462.

[6] B. Schneider, B. Miller, and B. Saunders. NIST's Digital Library of Mathematical Functions. *Physics Today*, **71**:2 (2018), 48-53. DOI: https://doi.org/10.1063/PT.3.3846

[7] B. Saunders. Bridging the Cultural Divide to Lead the NIST DLMF Tables Project. *National Association of Mathematicians Newsletter* **L**:4 (2019), 12-13.

[8] B. Saunders, B. Miller, F. Backeljauw, S. Becuwe, M. McClain, and A. Cuyt. DLMF Standard Reference Tables on Demand: A Software Testing System. In preparation.

[9] B. Saunders. "Research in Computational and Applied Mathematics at NIST." Worcester Polytechnic Institute, Worcester, MA, April 18, 2019.

[10] B. Saunders. "Mathematics, Mesh Generation, and 3D Graphics on the Web, and Finding a Career at NIST." MAA MD-DC-VA Fall Section Meeting, Norfolk State University, Norfolk, VA, November 9, 2019.

[11] B. Saunders. "Who Needs Standard Reference Tables on Demand?" Mathematical Association of America, MD-DC-VA Spring Section Meeting, Frostburg State University, Frostburg, MD, April 29, 2017.

NIST Digital Repository of Mathematical Formulae

Howard S. Cohl
Marjorie A. McClain
Bonita V. Saunders
Abdou Youssef
Moritz Schubotz (University of Konstanz)
André Greiner-Petter (Technische Universität Berlin)
Alan Sexton (University of Birmingham)
Avi Trost (Poolesville HS)
Rajen Dey (Montgomery Blair HS)

The NIST Digital Repository of Mathematical Formulae (DRMF) is an online compendium of formulae for orthogonal polynomials and special functions (OPSF) designed to a) facilitate interaction among a community of mathematicians and scientists interested in OPSF; b) be expandable, allowing the input of new formulae from the literature; c) provide information for related linked open data projects; d) represent the context-free full semantic information concerning individual formulas; e) have a user friendly, consistent, and hyperlinkable viewpoint and authoring perspective; f) contain easily searchable mathematics; and g) take advantage of modern MathML tools for easy-to-read, scalably rendered content-driven mathematics.

Our DRMF implementation, previously built using MediaWiki (the wiki software used by Wikipedia), is currently in migration to a different software platform, namely the platform used by the NIST Digital Library of Mathematical Functions (DLMF). See Figure 78 for the current draft of the DRMF home page, and Figure 79 for a sample DRMF formula page.

The DRMF has been described in a series of papers and talks [1-9]. A key asset in the development of DRMF context free semantic content is the utilization of

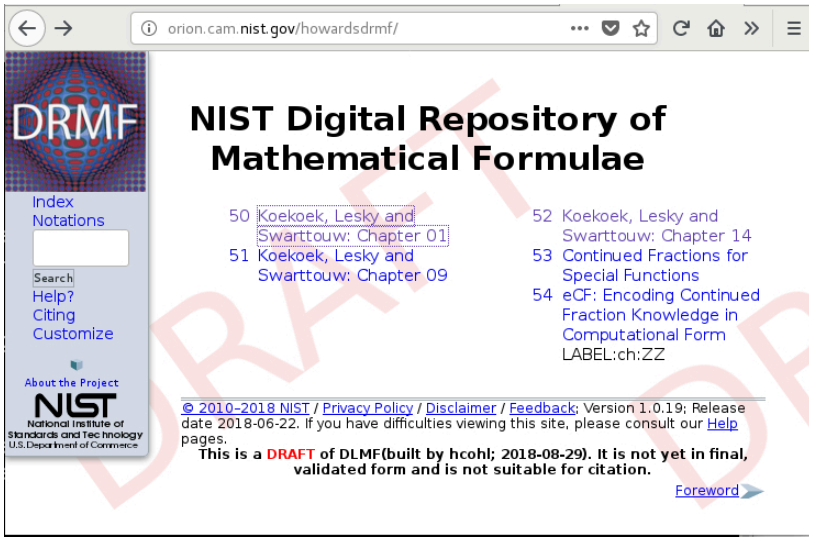

Figure 78. *Current draft of the DRMF home page displaying the current table of contents.*

a set of LaTeX macros and macro call functionality created by Bruce Miller (ACMD) to achieve the encapsulation of semantic information within the DLMF [10]. These macros give us the capability to tie LaTeX commands in a mostly unambiguous way to mathematical functions defined in an OPSF context. There are currently 540 DLMF LaTeX macros, as well as an additional 156 which have been created specifically for the DRMF. Most if not all DLMF macros have at least one DLMF web page associated with them. One goal is to have definition pages for all additional DRMF macros. The use of DLMF and DRMF macros guarantees mathematical and structural consistency throughout the DRMF. We refer to LaTeX source with incorporated DLMF and DRMF macros as semantic LaTeX.

DRMF formula seeding is currently focused on

(1) Koekoek, Lesky, and Swarttouw (KLS) chapters 1 (Definitions and Miscellaneous Formulas), 9 (Hypergeometric Orthogonal Polynomials), and 14 (Basic Hypergeometric Orthogonal Polynomials [11];

(2) Koornwinder KLS addendum LaTeX data [12];

(3) Wolfram Computational Knowledge of Continued Fractions Project (eCF) [3];

(4) Continued Fractions for Special Functions (CFSF) Maple dataset hosted by the University of Antwerp [3,14];

(5) Bateman Manuscript Project (BMP) books [13]; and

(6) Magnus, Oberhettinger, and Soni (MOS) books [13].

For these seed projects, we are developing (have developed) Python and Java software to incorporate DLMF and DRMF macros into the corresponding LaTeX source. Our coding efforts have also focused on extracting formula data from LaTeX source as well as generating DRMF semantic LaTeX. We have developed Java software for the seeding of the eCF and CFSF projects which involve conversion from Mathematica and Maple format to DLMF and DRMF macro incorporated semantic LaTeX [3]. Moreover, in [4] we developed the VMEXT visualization that helps us to investigate the content structure of MathML expressions without reading the verbose parallel MathML markup; see Figure 80.

In August 2014, the DRMF Project obtained permission and license to use BMP material as seed content for the DRMF from Caltech. Caltech has loaned us copies of the BMP. In February 2018, we received permission and license to use the KLS and MOS material as seed content for the DRMF from Springer Nature. We have forwarded the copies of BMP and MOS to A. Sexton, Scientific Document Analysis Group, School of Computer Science, University of Birmingham, UK. Sexton has scanned the BMP and MOS and is developing software to perform mathematical optical character recognition to obtain LaTeX source. To enhance the development process of the OCR software, we have developed an automated testing framework that uses visual diffs of the original scanned source and the rendering of the generated LaTeX source.

Current and future DRMF development projects include the production of formula output representations (such as semantic LaTeX, MathML, Mathematica, Maple, and Sage); incorporation of sophisticated DLMF and DRMF macro related formula search; and the development of capabilities for user community formula input. In this vein, A. Youssef has written a grammar-based mathematical language processor (MLP) that uses JavaCC to parse mathematical LaTeX expressions [15]. Based on the MLP, A. Greiner-Petter has developed a Java tool to convert mathematical LaTeX expressions, which contain DLMF and DRMF macros, to a given computer algebra system source format. This Java tool provides further information for the conversion about possible ambiguities and differences in definitions, domains and branch cuts between the semantic LaTeX source and the CAS source. Furthermore, it is designed to be easily extendable to other computer algebra systems and currently supports Maple and Mathematica input sources.

ACMD summer student Avi Trost worked on the project “Semantic Enhancement for Wronskians and Prime Derivative Notation,” and ACMD summer student Rajen Dey worked on the project “Semantic

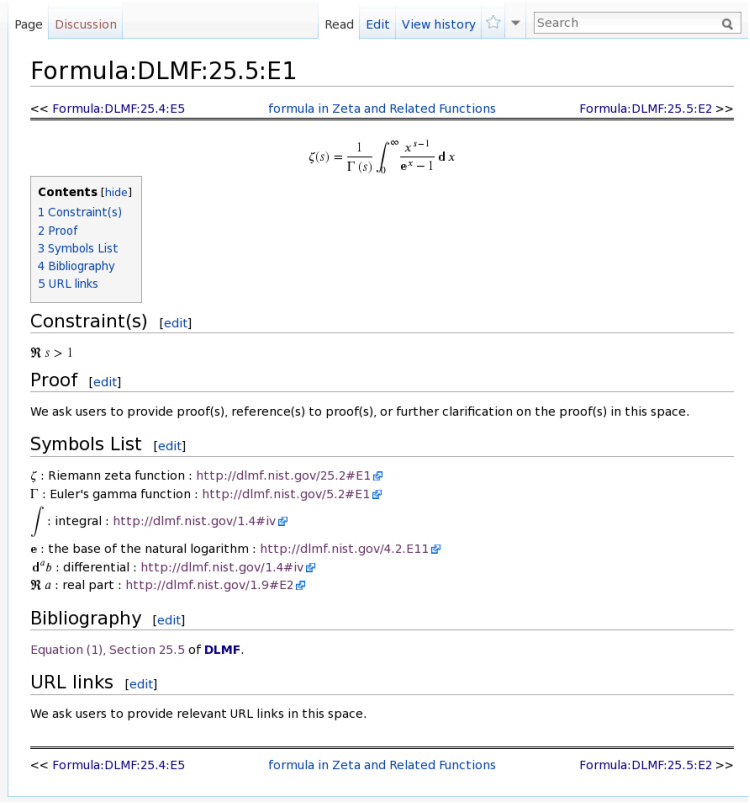

Figure 79. *Sample DRMF formula page, taken from the KLS Chapter 1 dataset.*

Enhancement for Sums and Products." Cohl was a member of the program committee for the 12th Conference on Intelligent Computer Mathematics (CICM 2019). Prague, Czech Republic, July 8-12, 2019.

The KLS datasets have been uploaded to our DLMF platform as well as the CFSF and eCF datasets. By working with Andrea Fisher-Scherer, Rights Administrator, Artists Rights Society, New York, NY, we have received permission from Foundation Vasarely, to use an image of one of Victor Vasarely's paintings as the DRMF logo; see Figure 81.

[1] H. S. Cohl, M. A. McClain, B. V. Saunders, M. Schubotz and J. C. Williams. Digital Repository of Mathematical Formulae. *Lecture Notes in Artificial Intelligence* **8543** (2014), Proceedings of the Conferences on Intelligent Computer Mathematics 2014, Coimbra, Portugal, July 7-11, 2014, (S. M. Watt, J. H. Davenport, A. P. Sexton, P. Sojka, and J. Urban, eds.), Springer, 419-422.

[2] H. S. Cohl, M. Schubotz, M. A. McClain, B. V. Saunders, Cherry Y. Zou, Azeem S. Mohammed, and Alex A. Danoff. Growing the Digital Repository of Mathematical Formulae with Generic LaTeX Sources. *Lecture Notes in Artificial Intelligence* **9150** (2015), Proceedings of the Conference on Intelligent Computer Mathematics 2015, Washington DC, USA, July 13-17, 2015, (M. Kerber, J. Carette, C. Kaliszyk, F. Rabe, and V. Sorge, eds.), Springer, 280-287.

[3] H. S. Cohl, M. Schubotz, A. Youssef, A. Greiner-Petter, J. Gerhard, B. V. Saunders, M. A. McClain, J. Bang, and K. Chen. Semantic Preserving Bijective Mappings of Mathematical Formulae between Word Processors and Computer Algebra Systems. *Lecture Notes in Computer Science* **10383** (2017), Proceedings of the Conference on Intelligent Computer Mathematics 2017, Edinburgh, Scotland, U.K., July 17-21, 2017, (H. Geuvers, M. England, O. Hasan, F. Rabe, O. Teschke, eds.), Springer, 115-131.

[4] M. Schubotz, N. Meuschke, T. Hepp, H.S. Cohl, and B. Gipp. VMEXT: A Visualization Tool for Mathematical Expression Trees. *Lecture Notes in Computer Science* **10383** (2017), Proceedings of the Conference on Intelligent Computer Mathematics 2017, Edinburgh, Scotland, U.K., July 17-21, 2017, (H. Geuvers, M. England, O. Hasan, F. Rabe, O. Teschke, eds.), Springer, 340-345.

[5] M. Schubotz and H.S. Cohl. "Content Dictionary Description: Select Symbols from Chapter 9 of the KLS Dataset in the DRMF." OpenMath Workshop, Conference on Intelligent Computer Mathematics 2017, Edinburgh, Scotland, U.K., July 17-21, 2017.

[6] M. Schubotz, A. Greiner-Petter, P. Scharpf, N. Meuschke, H. S. Cohl, and B. Gipp. Improving the Representation and Conversion of Mathematical Formulae by Considering their Textual Context. In *Proceedings of the Joint Conference on Digital Libraries* (JCDL 18), Fort Worth, Texas, USA, June 3-6, 2018, 233-242.

[7] H. S. Cohl, A. Greiner-Petter, and M. Schubotz. Automated Symbolic and Numerical Testing of DLMF Formulae using Computer Algebra Systems. *Lecture Notes in Computer Science* **11006** (2018), Proceedings of the Conference on Intelligent Computer Mathematics 2018, Hagenberg, Austria, August 13-17, 2018, (F. Rabe, W. Farmer, G.O. Passmore, A. Youssef, eds.), Springer, 39-52.

[8] A. Greiner-Petter, M. Schubotz, H. S. Cohl, and B. Gipp. MathTools: An Open API for Convenient MathML Handling. *Lecture Notes in Computer Science* **11006** (2018), Proceedings of the Conference on Intelligent Computer Mathematics 2018, Hagenberg, Austria, August 13-17, 2018, (F. Rabe, W. Farmer, G.O. Passmore, A. Youssef, eds.), Springer, 104-110.

[9] A. Greiner-Petter, M. Schubotz, H. S. Cohl, and Bela Gipp. Semantic Preserving Bijective Mappings for Expressions involving Special Functions between Computer Algebra Systems and Document Preparation Systems, *Aslib Journal of Information Management*, **71**:3 (2019), 415. DOI: 10.1108/AJIM-08-2018-0185

[10] B. Miller. "Drafting DLMF Content Dictionaries." OpenMath Workshop, 9th Conference on Intelligent Computer Mathematics (CICM 2016), Bialystok, Poland.

[11] R. Koekoek, P. A. Lesky, and R. F. Swarttouw. *Hypergeometric Orthogonal Polynomials and their q-Analogues*. Springer Monographs in Mathematics, Springer-Verlag, Berlin, 2010.

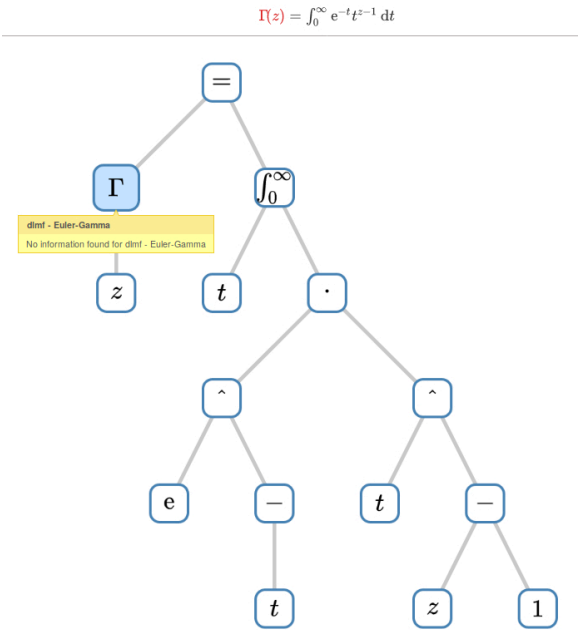

Figure 80. *VMEXT visualization of Equation 5.2.1 in the DLMF. The corresponding MathML XML file is 89 lines and 6293 characters long.*

[12] T. H. Koornwinder. Additions to the Formula Lists in Hypergeometric Orthogonal Polynomials and their *q*-analogues by Koekoek, Lesky and Swarttouw. arXiv:1401.0815, June 2015.

[13] A. Erdelyi, W. Magnus, F. Oberhettinger, and F. G. Tricomi. *Higher Transcendental Functions*. Vols. I, II, III, Robert E. Krieger Publishing Co., Melbourne, FL, 1981.

[14] A. Cuyt, V. Petersen, H. Waadeland, W. B. Jones, F. Backeljauw, C. Bonan-Hamada, and S. Becuwe. *Handbook of Continued Fractions for Special Functions*. Springer, New York, 2008.

[15] A. Youssef. Part-of-Math Tagging and Applications. *Lecture Notes in Computer Science* **10383** (2017), Proceedings of the Conference on Intelligent Computer Mathematics 2017, Edinburgh, Scotland, U.K., July 17-21, 2017, (H. Geuvers, M. England, O. Hasan, F. Rabe, O. Teschke, eds.), Springer, 356-374.

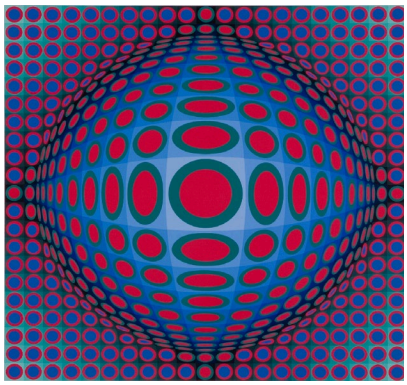

Figure 81. *DRMF logo.*

Fundamental Solutions and Expansions for Special Functions and Orthogonal Polynomials

Howard S. Cohl
Roberto S. Costas-Santos (University of Alcala)
Hans Volkmer (University of Wisconsin-Milwaukee)
Gestur Olafsson (Louisiana State University)
T. Mark Dunster (San Diego State University)
Mourad E. H. Ismail (University of Central Florida)
Jessica E. Hirtenstein (University of California Davis)
Philbert R. Hwang (University of Maryland)
Thinh H. Dang (George Washington University)
Tanay Wakhare (University of Maryland)
Justin Park (Poolesville High School)
Jason Zhao (University of California Los Angeles)
Linus Ge (University of Rochester)

The concept of a function expresses the idea that one quantity (the input) completely determines another quantity (the output). Our research concerns special functions and orthogonal polynomials. A special function is a function that has appeared in the mathematical sciences so often that it has been given a name. Green's functions (named after the British mathematician George Green, who first developed the concept in the 1830s) describe the influence of linear natural phenomena such as electromagnetism, gravity, heat and waves. For example, in electrostatics, a Green's function describes the influence of a point charge, called the source, over all of space. The inputs for fundamental solutions (Green's functions) are all of space (with the exception of a singular region), and the output is the "force" exerted from the point throughout space. Green's functions are fundamental to the study of inhomogeneous partial differential equations and are powerful in that they provide a mechanism for obtaining their solutions.

We investigate fundamental solutions of linear partial differential equations on highly symmetric Riemannian manifolds (harmonic, rank-one symmetric spaces) such as real, complex, quarternionic, and octonionic Euclidean, hyperbolic, and projective spaces. Our recent focus has been on applications of fundamental solutions for linear elliptic partial differential operators on spaces of constant curvature. With Dunster and Dang, we have constructed closed-form expressions of a fundamental solution for the Helmholtz equation in *d*-dimensional, *R*-radius spaces of constant positive and negative curvature. These were in the hyperboloid model of hyperbolic geometry, in terms of associated Legendre functions, and on the *d*-dimensional hypersphere, in terms of Ferrers functions [1].

With Olafsson, we are preparing work on fundamental solutions for the Laplace-Beltrami operator on rank one symmetric spaces of compact and noncompact type [2]. Cohl is working with Hirtenstein on deriving

Gegenbauer expansions and addition theorems for binomial and logarithmic fundamental solutions of the polyharmonic equation in even-dimensional space with powers of the Laplacian greater than or equal to the dimension divided by two [3]. In conjunction with Park and Volkmer, Cohl is computing all Gauss hypergeometric representations of Ferrers functions of the second kind by starting with the full list of 18 Gauss hypergeometric representations for the associated Legendre function of the second kind [4].

In the following works, we derive and use properties of hypergeometric and basic hypergeometric orthogonal polynomials to derive their properties and properties of the hypergeometric and basic hypergeometric functions themselves. In particular, we compute generalizations of generalized and basic hypergeometric orthogonal polynomial generating functions as well as corresponding definite integrals using orthogonality. With Costas-Santos and Wakhare, using a generalization of the Rogers generating function for continuous q-ultraspherical/Rogers polynomials derived by Ismail and Simeonov in terms of Askey-Wilson polynomials specialized to continuous q-ultraspherical/Rogers polynomials [5] and a different generalization of the same generating function, we have derived several results [6] using the series-rearrangement technique. For instance, we derive a hierarchy of generalized generating functions starting from the Ismail/Simeonov expansion limiting to some classical/q-classical expansions including Gegenbauer's generating function for Gegenbauer polynomials, Heine's formula for Legendre polynomials, and Hein's reciprocal square root identity for Chebyshev polynomials of the first kind (hereafter Chebyshev polynomials). We also derived several expansion of Jacobi polynomials and limiting expansions in terms of Chebyshev polynomials and Laguerre polynomials and a new quadratic transformation for basic hypergeometric series, and a Wilson polynomial expansion. With Costas-Santos, Hwang and Wakhare, our series-rearrangement technique is extended to generalizations of other generating functions for basic hypergeometric orthogonal polynomials in [7]. Here, we derive generalizations of generating functions for Askey-Wilson, q-ultraspherical/Rogers, q-Laguerre, and little q-Laguerre/Wall polynomials.

With Costas-Santos and Wakhare, we obtained q-analogues of the Sylvester, Cesàro, Pasternack, and Bateman polynomials and generating functions for these polynomials in [8]. With Costas-Santos and Zhao, we derived generalized linearization formulas for generalized and basic hypergeometric orthogonal polynomials by applying connection relations to them [9]. Here, we generalize linearization formulae for continuous q-ultraspherical/Rogers, Jacobi, and continuous q-Jacobi polynomials. With Costas-Santos and Zhao, in [10], we derived generalizations of linearization formulae for Gegenbauer and Laguerre polynomials using connection relations for these polynomials.

With Ismail, we derived 5-term contiguous relations for linearization coefficients of generalized and basic hypergeometric orthogonal polynomials such as Laguerre, Gegenbauer, Hermite, Jacobi, continuous q-ultraspherical/Rogers, and continuous q-Jacobi polynomials [11]. In work with Costas-Santos and Ge [12], we derived terminating and non-terminating transformations of basic hypergeometric functions using representations of the Askey-Wilson polynomials and their symmetric and q-inverse sub-families in the q-Askey scheme. These include the continuous dual-q-Hahn, Al-Salam-Chihara, continuous big q-Hermite and continuous q-Hermite polynomials and their q-inverse representations.

Cohl served on the Scientific and Local Organizing committees for the Orthogonal Polynomials and Special Functions Summer School 6 (OPSF-S6) workshop which was held on June 17-23, 2016 at the Norbert Wiener Center for Harmonic Analysis and Applications at the University of Maryland. The OPSF-S6 lecture notes will be published by Cambridge University Press, edited by Cohl and Ismail, including lecture notes by Duran, Ismail, Koelink, Rosengren, and Zeng [13].

Because of the news that Richard Askey, a giant in the OPSF field from the University of Wisconsin, entered hospice care, Cohl and Ismail worked with 63 colleagues to prepare a *Liber Amicorum for Dick Askey* which was presented to him and his family at an event held on September 4, 2019 in Madison, Wisconsin [14]. Unfortunately, Askey passed away on October 9, 2019. Cohl and Ismail are currently preparing an extended version of the Liber Amicorum which will be printed and sent to members of Dick's family and his very close colleagues which will be composed of the remembrances from 83 of his colleagues. Cohl, Ismail, and H-H. Wu have been invited to prepare a 20-page memorial article which will be submitted to *The Notices of the American Mathematical Society* in 2020 [15].

Cohl and Costas-Santos co-organized a special session on special functions and orthogonal polynomials at the 2nd International Conference on Symmetry, September 1-7, 2019, Benasque, Spain. Cohl remains editor or co-editor for OP-SF NET, the SIAM Activity Group on Orthogonal Polynomials and Special Functions Newsletter, *The Ramanujan Journal,* and a special issue on symmetry in special functions and orthogonal polynomials in the journal *Symmetry*.

[1] H. S. Cohl, T. H. Dang, and T. M. Dunster. Fourier and Gegenbauer Expansions for a Fundamental Solution of the Helmholtz Operator in Riemannian Spaces of Constant Curvature. *Symmetry, Integrability and Geometry: Methods and Applications* **14**:136 (2018), Special Issue on Orthogonal Polynomials, Special Functions and Applications (OPSFA14), 45 pages. DOI: 10.3842/SIGMA.2018.136

[2] G. Olafsson and H. S. Cohl. Fundamental Solutions for the Laplace-Beltrami Operator on the Rank One Symmetric Spaces. In preparation.

[3] H. S. Cohl and J. E. Hirtenstein. Binomial and Logarithmic Gegenbauer Expansions for the Even-dimensional Polyharmonic Equation. In preparation.

[4] H. S. Cohl, J. Park, and H. Volkmer. Gauss Hypergeometric Representations of Ferrers Functions of the Second Kind. In preparation.

[5] M. E. H. Ismail and P. Simeonov. Formulas and Identities Involving the Askey-Wilson Operator, *Advances in Applied Mathematics* **76** (2016). DOI: 10.1016/j.aam.2016.02.002

[6] H. S. Cohl, R. S. Costas-Santos, and T. V. Wakhare. On a Generalization of the Rogers Generating Function, *Journal of Mathematical Analysis and Applications* **475**:2 (2019), 1019. DOI: 10.1016/j.jmaa.2019.01.068

[7] H. S. Cohl, R. S. Costas-Santos, P. R. Hwang, and T. V. Wakhare. Generalizations of Generating Functions for Basic Hypergeometric Orthogonal Polynomials. In review.

[8] H. S. Cohl, R. S. Costas-Santos, and T. V. Wakhare. Some Generating Functions for q-polynomials. *Symmetry* **10**:12 (2018), 758. DOI: 10.3390/sym10120758

[9] H. S. Cohl, R. S. Costas-Santos, and J. Zhao. Generalizations of Linearization Formulae for Continuous Hypergeometric Orthogonal Polynomials. In preparation.

[10] H. S. Cohl, R. S. Costas-Santos and J. Zhao. Generalized Linearization Coefficients for Laguerre and Gegenbauer Polynomials. In preparation.

[11] H. S. Cohl, M. E. H. Ismail. Two-dimensional Contiguous Relations for Linearization Formulae. In preparation.

[12] H. S. Cohl, R. S. Costas-Santos and L. Ge. Basic Hypergeometric Transformations from Symmetric and q-inverse Sub-families of the Askey-Wilson Polynomials in the q-Askey-scheme. In preparation.

[13] M. E. H. Ismail and H. S. Cohl, eds. *Lecture Notes from the Sixth Orthogonal Polynomials and Special Functions Summer School 2016*. Cambridge University Press, in preparation.

[14] H. S. Cohl and M. E. H. Ismail, eds. *Liber Amicorum, a Friendship Book for Dick Askey*. First and Second Editions, in preparation.

[15] M. E. H. Ismail, H. S. Cohl and H.-H. Wu, eds. The Life and Mathematics of Richard A. Askey. In preparation.

Outreach

ACMD staff engage in a variety of efforts that serve to educate the general public about the work of the division and to encourage students to consider careers in science and engineering. Some of those are described here. Also see Table 2 on page 121.

Student Internships in ACMD

Ronald Boisvert

ACMD is committed to helping to prepare the next generation of scientific researchers by providing internships of various types to students at each of the graduate, undergraduate, and high school levels. The NIST programs used to enable such internships include the following:

- *Foreign Guest Researcher Program.* Provides stipends to support visits of guest researchers from foreign institutions for periods of a few weeks to several years.
- *Pathways Program.* Provides temporary Federal appointments to students, typically 1-2 years. Allows easy conversion to full-time permanent status. (Restricted to US Citizens.)
- *Professional Research Experience Program (PREP)*[31]. A cooperative agreement with nine universities[32] that provides a mechanism for NIST to support internships for students from those institutions on the Gaithersburg campus throughout the year. A similar agreement with four universities[33] exists for the NIST Boulder Labs.
- *Student Volunteer Program.* A mechanism that provides unpaid internships for students.
- *Summer High School Internship (SHIP) Program*[34]. SHIP uses the Student Volunteer Program to organize a competitive summer volunteer program for high school students.
- *Summer Undergraduate Research Fellowship (SURF) Program*[35]. A competitive program providing undergraduates a 10-week research experience at NIST.

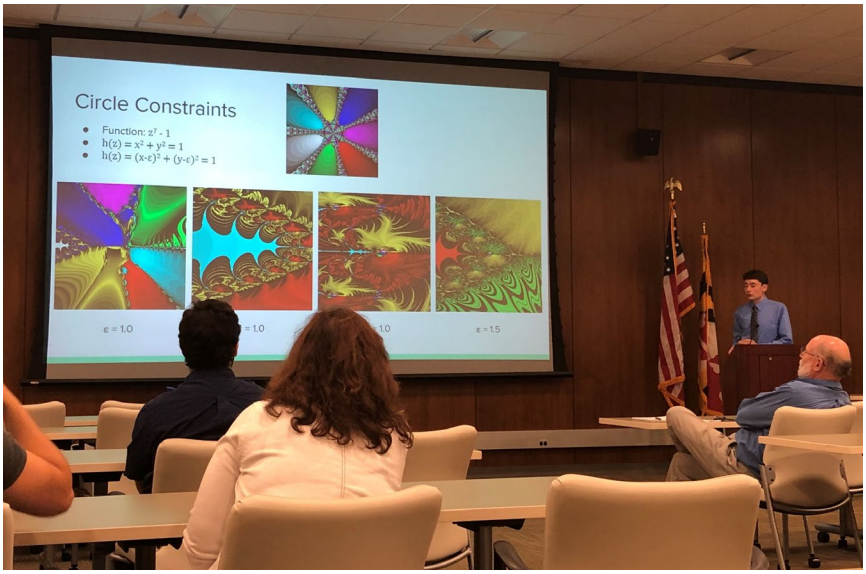

Figure 82. *Daniel De Leon, a NIST SURF student from the University of Maryland gives a presentation at the annual SURF symposium held in the last week of the summer program.*

Funding for all of these programs comes from the Division hosting the student. The Pathways Program, the PREP Program, and the Foreign Guest Researcher Program can also be used to support postdoctoral researchers.

During the last 15 months, ACMD supported the work of 39 student interns, including 15 graduate students, 14 undergraduates, and 11 high school students. See Table 2 for a complete listing.

ACMD staff members are also active in the education of graduate students, serving both as Ph.D. advisers and as members of thesis committees; see page 142.

[31] https://www.nist.gov/iaao/academic-affairs-office/nist-professional-research-experience-program-prep

[32] Brown University, Georgetown University, Montgomery College, Towson University, the University of the District of Columbia, the University of Maryland College Park, and a consortium of Johns Hopkins University, Morgan State University, and the State University of New York at Binghamton.

[33] Brown University, the Colorado School of Mines, the University of Colorado Boulder, and the University of Colorado Denver

[34] https://www.nist.gov/careers/student-opportunities/summer-high-school-intern-program

[35] https://www.nist.gov/surf

Practitioner's Guide to Social Network Analysis for Education Researchers

Justyna P. Zwolak
Remy Dou (Florida International University)

It has long been recognized that to advance our economy and our society we need to develop a strong workforce of experts in science, technology, engineering, and mathematics (STEM) [1]. Yet, of all students who enter a four-year college intending to major in a STEM field, over 30 % fail to graduate with a STEM degree. The situation for students from historically underrepresented groups in STEM is even more alarming: of all the STEM bachelor's degrees awarded nationwide, only 12.8 % go to Hispanic students, 8.7 % to Black or African American students, and 0.5 % to American Indian or Alaska Native students [2]. These percentages are not commensurate with the demographic distribution of the U.S. national population. One pathway to address this issue and move toward equity in STEM is by making systemic changes to classes and departments that promote the retention (the successful completion of a course) and persistence (the successful completion of a sequence of courses) of students from all socio-economic and demographic groups.

It has been suggested as early as mid-1970s that both retention and persistence are linked with student engagement and that insufficient interactions with others lead to a low commitment to the university and, ultimately, affects one's decision about whether to drop out [3]. More recent studies suggest that students' persistence, engagement, and also performance are all interlinked and that active learning environments offer key advantages over traditional lecture in all these domains [4].

Over the past five years, we have been performing mathematical modeling, optimization, and statistical and complex network analyses of students' network data to understand correlations between social and academic integration and other factors affecting student academic well-being, such as engagement and its evolution over time, academic performance, self-efficacy, and anxiety, and to understand how these factors affect the odds of students' persistence in the context of students coming from historically underrepresented minority groups. Our studies further support the benefits of dynamic group formation strategies that give students an opportunity to interact with many peers throughout a semester both during class time and outside of class.

To provide the education research community with proper tools to reproduce research using network analysis in their own classrooms, and to enable studies on a larger scale, earlier this year we published an invited article providing a practical guide to using network analysis on classroom data [5]. In this work, we discuss the practical aspects of designing network studies, such as development of the data collection instruments, setting up protocols for gathering data, identifying network methodologies relevant to a given research question, and conducting the analysis. We illustrate these techniques using student anxiety data from active-learning physics classrooms at a large Hispanic-Serving Institution. To complement the guide to network analysis in education

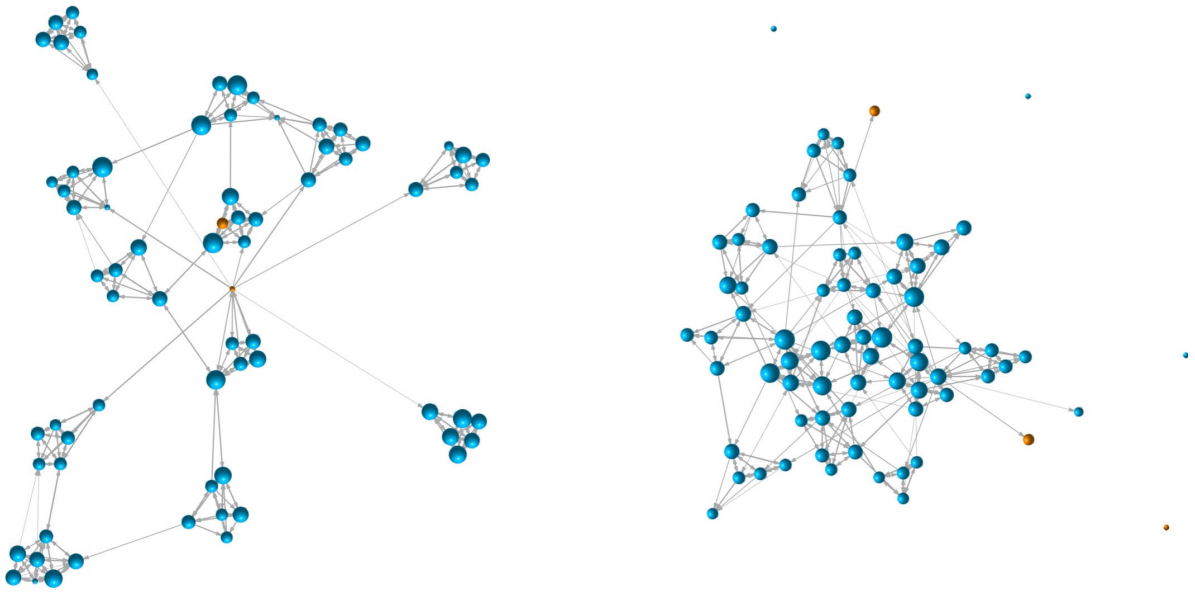

Figure 83. *Network visualization for two different collection times done using code provided by the SNA toolbox (left: 2nd week of the semester; right: 11th week of the semester). The node size is proportional to the closeness centrality measure. Orange nodes represent students who failed the class.*

research, we provide (and maintain) a set of tools for other researchers to use this approach in their work—the *SNA toolbox*—that can be accessed on GitHub [6].

[1] President's Council of Advisors on Science and Technology. *Engage to Excel: Producing One Million Additional College Graduates with Degrees in Science, Technology, Engineering, and Mathematics.* Executive Office of the President, 2012. URL: https://eric.ed.gov/?id=ED541511 (accessed: May 8, 2017)

[2] National Science Board. *Science and Engineering Indicators 2018*. NSB-2018-1, National Science Foundation, 2018. URL: https://www.nsf.gov/statistics/2018/nsb20181/report (accessed: May 10, 2019)

[3] V. Tinto. Dropout from Higher Education: A Theoretical Synthesis of Recent Research. *Review of Educational Research* **45**:89 (1975), 89-125. DOI: 10.3102/00346543045001089

[4] S. Freeman, S. L. Eddy, M. McDonough, M. K. Smith, N. Okoroafor, H. Jordt, and M. P. Wenderoth. Active Learning Increases Student Performance in Science, Engineering, and Mathematics. *Proceedings of the National Academy of Sciences of the USA* **111**:8410 (2014). DOI: 10.1073/pnas.1319030111

[5] R. Dou and J. P. Zwolak. Practitioner's Guide to Social Network Analysis: Examining Physics Anxiety in an Active-Learning Setting. *Physical Review Physics Education Research* **15** (2019), 020105. (In *Focused Collection on Quantitative Methods in PER: A Critical Examination* series.) DOI: 10.1103/PhysRevPhysEducRes.15.020105

[6] J. P. Zwolak. SNA toolbox, 2018. URL: https://github.com/jpzwolak/SNA-toolbox

Computations in Physics: A Quest to Integrate Computer Methods in STEM Courses

Justyna P. Zwolak
Judith Terrill
Aleksandra Słapik (University of Silesia)

Over the last fifty years, computers have been utilized in almost every field of human activity. Today, computer technologies enable steady progress and new scientific discoveries, playing a major role in how science in done. Along with experiment, computer-based methods became an important research tool – from controlling the apparatus and course of the experiments to visualizations to carrying out complicated analysis of collected data to suggesting new research directions. Likewise, computer technologies are moving into traditionally blue-collar fields. According to a recent article in the Wall Street Journal [1], "Within three years, U.S. manufacturing workers with college degrees will outnumber those without".

To ensure the continuous improvement and further development of technology, it is necessary to provide students in science, technology, engineering, and mathematics disciplines with sufficient exposure to hands-on experience with employing computations in problem solving [2]. Yet, although one can no longer imagine scientific work without computers, these technologies are still often missing from curricula. A survey from 2016 reported that in more than 75 % of the surveyed departments more than half of the faculty reported not using any interactive engagement activities with computation [3].

In this project, we are investigating the problem of teachers' skills with and attitudes towards adapting computational methods in teaching. A pilot study conducted among high school science teachers and science teachers-in-training revealed that, at the high school level, computers are used (or expected to be used) mainly as a visualization tool to either draw a graph of a given function or to graphicly represent data. While students are encouraged to use computer technologies while working on homework assignments, they are not given information about the available technologies nor are they offered any training opportunities on how to use them. Even more alarmingly, the vast majority of respondents could not even identify the meaning of computer algebra system or numerical methods.

While this preliminary work is just a first step towards answering the question about teachers experiences with computation as well as any perceived barriers towards the greater use of computation, is confirms the great need to further support the implementation of computer technologies in classrooms if the next generation of STEM graduates is to be prepared to keep pace with the current trends in research and industry.

[1] A. Hufford. American Factories Demand White-Collar Education for Blue-Collar Work. *The Wall Street Journal* [Front Page Print Edition], December 10, 2019.

[2] American Association of Physics Teachers (AAPT). *Recommendations for Computational Physics in the Undergraduate Physics Curriculum*. URL: https://www.aapt.org/Resources/upload/AAPT_UCTF_CompPhysReport_final_B.pdf

[3] M. D. Caballero and L. Merner. Prevalence and Nature of Computational Instruction in Undergraduate Physics Programs Across the United States. *Physical Review Physics Education Research* **14** (2018), 020129. DOI: 10.1103/PhysRevPhysEducRes.14.020129

Table 2. *Student interns in ACMD.*

Name	From	Program		Mentor	Topic
Alhejji, Mohammad	U. Colorado Boulder	G	PREP	E. Knill	Quantum randomness protocols
Anyanwu, Joy	Richard Montgomery H.S.	H	SHIP	S. Satterfield	Scientific visualization and analysis
Ariori, Rukayat	Morgan State U.	G	PREP	S. Satterfield	High end visualization
Avagyan, Arik	U. Colorado Boulder	G	PREP	E. Knill	Quantum information processing
Berman, Joseph	McLean H.S.	H	SVP	J. Terrill	Visualization of robot wayfinding
Bhaskaran, Aadya	Emory U.	U	SVP	B. Cloteaux	Generating synthetic networks
Conerly, Azizah	Morgan State U.	U	PREP	J. Kauffman	Numerical turbulence modeling
Converse, Joseph	Miami U. of Ohio	U	SURF	P. Kuo	Quantum frequency conversion
Crise, Owen	Maret School	H	SHIP	P. Patrone	Geometric optics for microfluidics
De Leon, Daniel	U. of Maryland	U	SURF	A. Kearsley	Fractals and Lagrange multiplier estimates
Dey, Rajen	Montgomery Blair H.S.	H	SVP	H. Cohl, A. Youssef	DRMF semantic capture enhancement
Eruslu, Hasan	U. of Delaware	G	FGR	G. Doğan S. Langer	Algorithms 3D image and shape analysis
Ge, Linus	U. of Rochester	U	SURF	H. Cohl, A. Youssef	Symmetric and inverse sub-families of the Askey-Wilson polynomials
Geller, Shawn	U. of Colorado	G	PREP	E. Knill	Characterization of quantum state preparation and measurement errors
Gorbea Finalet, Roberto	U. of Puerto Rico	U	SURF	L. Brady	Quantum-inspired classical algorithms
Hafken, Emily	McLean H.S.	H	SVP	R. Kacker	Applications of experiment design
Hu, Mingyu	University of Colorado	G	FGR	M. Donahue	Modeling of antiferromagnets
Joshi, Rakshan	Poolesville H.S.	H	SHIP	S. Satterfield	Scientific visualization and analysis
Khrac, Katjana	U. Zagreb, Croatia	G	FGR	K. Sayrafian	Positioning metrology in the human body
Kwiatkowski, Alexander	U. of Colorado	G	PREP	E. Knill	Quantum networking
Landgren, Elizabeth	Macalester College	U	SURF	S. Satterfield	Voice commands for the NIST CAVE
Lauria, Michael	U. of Colorado	G	PREP	E. Knill	Characterization of quantum computers
Li, Jieying	U. of NC, Chapel Hill	U	SURF	S. Glancy	Characterization of quantum computers
Li, Shuang	USC	G	FGR	G. Doğan S. Langer	Algorithms 3D image and shape analysis
Lin, Angelica	College of William and Mary	U	SURF	A. Kearsley	Chemometric methods for monoclonal antibody classification
Mayer, Karl	U. Colorado Boulder	G	PREP	E. Knill	Protocols for quantum optics
Murali, Anita	William G. Enloe H.S.	H	SHIP	S. Satterfield	Scientific Visualization and Analysis
Northcutt, Lily	U. of Maryland	U	SURF	M. Mascagni	Walk on spheres processes
Ornstein, Joel	U. of Colorado	G	PREP	S. Glancy	Quantum Information Journal Club
Schaffer, Scott	McLean H.S.	H	SVP	J. Terrill	Visualization of Robot Wayfinding
Slud, Justin	U. of Maryland	U	SURF	S. Ressler	VR and AR for the DLMF
Stein, Peter	UMBC	U	SURF	S. Satterfield	CHIMeS: CAVE and HMD Interactive Menu System
Su, Kevin	Princeton U.	U	PW	G. Doğan S. Langer	Image analysis
Trost, Avi	Poolesville H.S.	H	SVP	H. Cohl, A. Youssef	DRMF Semantic Capture Enhancement
Van Meter, James	U. Colorado Boulder	G	PREP	E. Knill	Quantum measurement of space-time
Wiesing, Tom	Jacobs U. Bremen	G	FGR	B. Miller	Digital Library of Math Functions
Willard, Frank	Poolesville H.S.	H	SHIP	S. Ressler	VR for mathematical functions
Xiao, Selena	Thomas Wootton H.S.	H	SHIP	J. Kauffman	GUIs for scientific software testing
Zhao, Henan	UMBC	G	FGR	J. Terrill	Understanding metrology datasets
Zong, Kevin	U. of Maryland	U	SURF	O. Slattery	Software for single photon counters

Legend

G Graduate Student
U Undergraduate
H High School

PREP Professional Research Experience Program
FGR Foreign Guest Researcher
PW Pathways
SVP Student Volunteer Program
SURF Summer Undergraduate Research Fellowship
SHIP Student High School Internship Program

Figure 84. *NIST sponsored a booth at the ACM Richard Tapia Celebration of Diversity in Computing San Diego, CA, September 18-21, 2019. Shown here Leticia Velazquez (Rice University), Anthony Kearsley (ACMD), Richard Tapia (Rice University), Katie Boeckl (NIST ITL), Danielle Santos (NIST ITL)*

Part IV

Activity Data

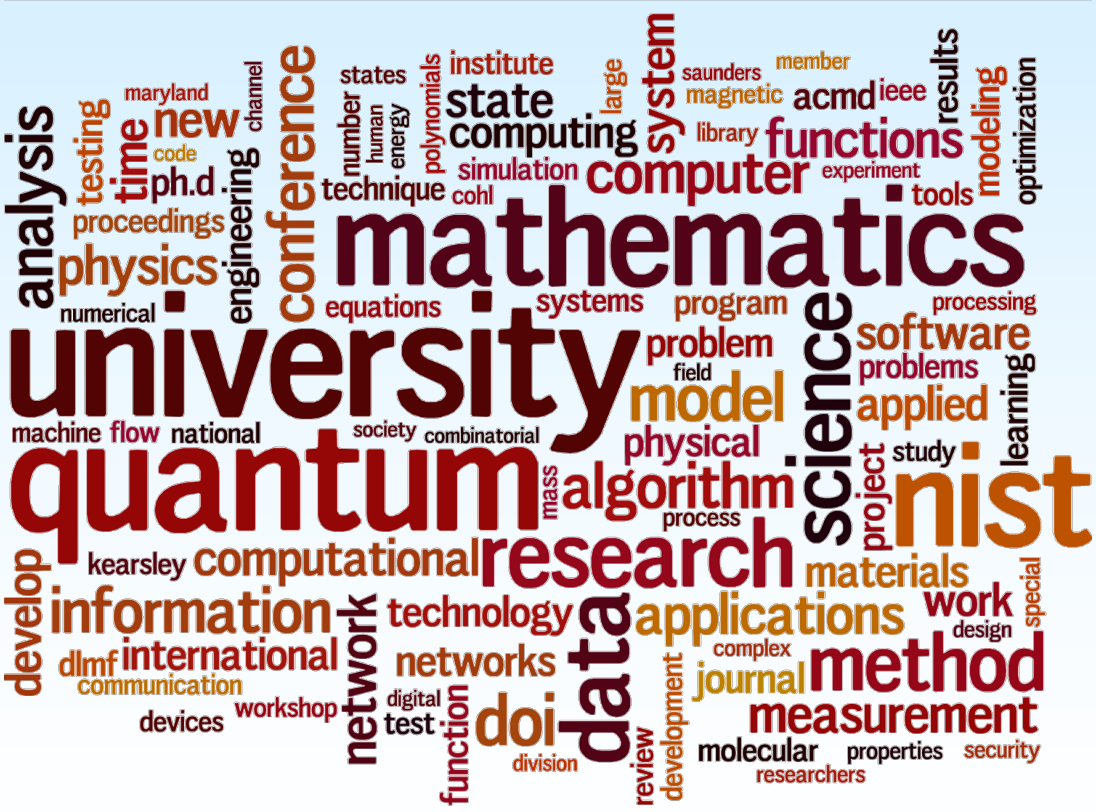

Publications

Note: Names of (co-)authors with a Division affiliation during this reporting period are underlined.

Appeared

Refereed Journals

1. D. Anderson, J. Benson, and A. Kearsley. Foundations of Modeling in Cryobiology II: Heat and Mass Transport in Bulk and at Cell Membrane and Ice-Interfaces. *Cryobiology* **91** (2019), 3-7. DOI: 10.1016/j.cryobiol.2019.09.014
2. D. Anderson, J. Benson, and A. Kearsley. Numerical Solution of Inward Solidification of a Dilute Ternary Solution Towards a Semi-Permeable Spherical Cell. *Mathematical Biosciences* **316** (2019), 108240. DOI: 10.1016/j.mbs.2019.108240
3. I. Bell and B. Alpert. Exceptionally Reliable Density-Solving Algorithms for Multiparameter Mixture Models from Chebyshev Expansion Root-finding. *Fluid Phase Equilibria* **476** Part B, (2018), 89-102. DOI: 10.1016/j.fluid.2018.04.026
4. J. Bernal and J. Lawrence. Characterization and Computation of Matrices of Maximal Trace Over Rotations. *Journal of Geometry and Symmetry in Physics* **53** (2019), 21-53. DOI: 10.7546/jgsp-53-2019-21-53
5. R. Brinson, J. Marino, F. Delaglio, L. Arbogast, R. Evans, A. Kearsley, G. Gingras, H. Ghasriani, Y. Aubin, G. Pierens, X. Jia, M. Mobli, H. Grant, D. Keizer, K. Schweimer, J. Ståhle, G. Widmalm, E. Zartler, C. Lawrence, P. Reardon, J. Cort, P. Xu, Feng Ni, S. Yanaka, K. Kato, S. Parnham, D. Tsao, A. Blomgren, T. Rundlöf, N. Trieloff, P. Schmieder, A. Ross, K. Skidmore, K. Chen, D. Keire, D. Freedberg, T. Suter-Stahel, G. Wider, G. Ilc, J. Plavec, S. Bradley, D. Baldisseri, M. Sforça, A. de Mattos Zeri, J. Wei, C. Szabo, C. Amezcua, J. Jordan, and M. Wikström. Enabling Adoption of 2D-NMR for the Higher Order Structure Assessment of Monoclonal Antibody Therapeutics. *mAbs* **11**:1 (2019), 94-105. DOI: 10.1080/19420862.2018.1544454
6. J. Bullard, J. Hagedorn, T. Ley, Q. Hu, W. Griffin, and J. Terrill. A Critical Comparison of 3D Experiments and Simulations of Tricalcium Silicate Hydration. *Journal of the American Ceramic Society* **101**:4 (2018), 1453–1470. DOI: 10.1111/jace.15323
7. J. W. Bullard, E. J. Garboczi, P. E. Stutzman, P. Feng, A. S. Brand, L. Perry, J. Hagedorn, W. Griffin, and J. E. Terrill. Measurement and Modeling Needs for Microstructure and Reactivity of Next-Generation Concrete Binders. *Cement and Concrete Composites* **101** (2019), 24-31. DOI: 10.1016/j.cemconcomp.2017.06.012
8. A. Carasso. Computing Ill-Posed Time-Reversed 2D Navier-Stokes Equations Using a Stabilized Explicit Finite Difference Scheme Marching Backward in Time. *Inverse Problems in Science and Engineering*, December 2019. DOI: 10.1080/17415977.2019.1698564
9. H. Cohl, R. Costas-Santos, and T. Wakhare. Some Generating Functions for *q*-Polynomials. *Symmetry* **10**:12 (2018), 758. DOI: 10.3390/sym10120758
10. H. Cohl, T. Dang, and T. Dunster. Fundamental Solutions and Gegenbauer Expansions of Helmholtz Operators in Riemannian Spaces of Constant Curvature. *Symmetry, Integrability and Geometry: Methods and Applications (SIGMA)* **14** (2018), 136-181. DOI: 10.3842/SIGMA.2018.136
11. H. Cohl, R. Costas-Santos, and T. Wakhare. On a Generalization of the Rogers Generating Function. *Journal of Mathematical Analysis and Applications* **475**:2 (2019), 1019-1043. DOI: 10.1016/j.jmaa.2019.01.068
12. G. Cooksey, P. Patrone, J. Hands, S. Meek, and A. Kearsley. Dynamic Measurement of Nanoflows: Realization of an Optofluidic Flow Meter to the Nanoliter-per-Minute Scale. *Analytical Chemistry* **91** (2019), 10713-10722. DOI: 10.1021/acs.analchem.9b02056
13. R. Dou and J. Zwolak. Practitioner's Guide to Social Network Analysis: Examining Physics Anxiety in an Active-Learning Setting. Physical Review Physics Education Research 15 (2019), 020105. DOI: 10.1103/PhysRevPhysEducRes.15.020105
14. R. Evans, A. Balijepalli, and A. Kearsley. Diffusion-Limited Reaction in Nanoscale Electronics. *Methods and Applications of Analysis* **26**:2 (2019), 149-166. DOI: 10.4310/MAA.2019.v26.n2.a4
15. J. Fong, N. Heckert, J. Filliben, and S. Freiman. Uncertainty in Multi-Scale Fatigue Life Modeling and a New Approach to Estimating Frequency of In-service Inspection of Aging Components. *Strength, Fracture and Complexity* **11** (2018), 195-217. DOI: 10.3233/SFC-180223
16. J. T. Fong, N. A. Heckert, J. J. Filliben, and S. W. Freiman. A Multi-Scale Failure-Probability-Based Fatigue or Creep Rupture Life Model for Metal Alloys. *International Journal of Pressure Vessels and Piping* **173** (2019) 79-93. DOI: 10.1016/j.ijpvp.2019.04.003
17. J. Fowler, C. Pappas, B. Alpert, W. Doriese, G. O'Neil, J. Ullom, and D. Swetz. Approaches to the Optimal Nonlinear Analysis of Microcalorimeter

Pulses. *Journal of Low Temperature Physics* **193** (2018), 539-546. DOI: 10.1007/s10909-018-1892-5

18. H. Gharibnejad, M. Leadingham, H. Schmale, and B. Schneider. A Comparison of Numerical Approaches to the Solution of the Time-Dependent Schrödinger Equation in One Dimension. *Computer Physics Communications* (2019), 106808. DOI: 10.1016/j.cpc.2019.05.019

19. H. Gharibnejad and B. Schneider. Numerical Methods Every Atomic and Molecular Theorist Should Know. *Nature Reviews Physics* **2** (2020), 89-102. DOI: 10.1038/s42254-019-0126-3

20. A. Greiner-Petter, H. Cohl, M. Schubotz and B. Gipp. Semantic Preserving Bijective Mappings for Expressions Involving Special Functions Between Computer Algebra Systems and Document Preparation Systems. *Aslib Journal of Information Management* **71**:3 (2019), 415-439. DOI: 10.1108/AJIM-08-2018-0185

21. S. Houston, T. Cravens, D. Schultz, H. Gharibnejad, W. Dunn, D. Haggerty, A. Rymer, B. Mauk, G. Gladstone, and N. Ozak. Jovian Auroral Ion Precipitation: X-Ray Production from Oxygen and Sulfur Precipitation. *Journal of Geophysical Research Space Physics* **125**:2 (2020). DOI: 10.1029/2019JA027007

22. S. Kalantre, J. Zwolak, S. Ragole, X. Wu, N. Zimmerman, M. Stewart, and J. Taylor. Machine Learning Techniques for State Recognition and Auto-Tuning in Quantum Dots. *npj Quantum Information* **5**:6 (2019), 6. DOI: 10.1038/s41534-018-0118-7

23. R. Kacker. Measurement Uncertainty and its Connection with True Value in the GUM Versus JCGM Documents. *Measurement* **127** (2018), 525-532. DOI: 10.1016/j.measurement.2018.05.105

24. K. Keenan, Z. Gimbutas, A. Dienstfrey, and K. Stupic. Assessing Effects of Scanner Upgrades for Clinical Studies. *Journal of Magnetic Resonance Imaging* **50**:6 (2019), 1948-1954. DOI: 10.1002/jmri.26785

25. A. Keith, C. Baldwin, S. Glancy, and E. Knill. Joint Quantum-State and Measurement Tomography with Incomplete Measurements. *Physical Review A* **98** (2018), 042318. DOI: 10.1103/PhysRevA.98.042318

26. L. Kocia and P. Love. The Non-disjoint Ontic States of the Grassmann Ontological Model, Transformation Contextuality, and the Single Qubit Stabilizer Subtheory. *Journal of Physics A* **52** (2019), 095303. DOI: 10.1088/1751-8121/aafca7

27. P. Kuo and M. Fejer. Mixing of Polarization States in Zincblende Nonlinear Optical Crystals. *Optics Express* **26**:21 (2018), 26971-26984. DOI: 10.1364/OE.26.026971

28. P. Kuo. Using Silica Fiber Coupling to Extend Superconducting Nanowire Single-Photon Detectors into the Infrared. *OSA Continuum* **1**:4 (2018), 1260-1266. DOI: 10.1364/OSAC.1.001260

29. R. La. Influence of Clustering on Cascading Failures in Interdependent Systems. *IEEE Transactions on Network Science and Engineering* **6**:3 (2019), 351-363. DOI: 10.1109/TNSE.2018.2805720

30. G. Lesaja and F. Potra. Adaptive Full Newton-Step Infeasible Interior-Point Method for Sufficient Horizontal LCP. *Optimization Methods and Software* **34**:5 (2019), 1014–1034. DOI: 10.1080/10556788.2018.1546857

31. D. Li, B. Alpert, D. Becker, D. Bennett, G. Carini, H. Cho, W. Doriese, J. Dusatko, J. Fowler, J. Frisch, J. Gard, S. Guillet, G. Hilton, M. Holmes, K. Irwin, V. Kotsubo, S. Lee, J. Mates, K. Morgan, K. Nakahara, C. Pappas, C. Reintsema, D. Schmidt, S. Smith, D. Swetz, J. Thayer, C. Titus, J. Ullom, L. Vale, D. Van Winkle, A. Wessels, and L. Zhang. TES X-ray Spectrometer at SLAC LCLS-II. *Journal of Low Temperature Physics* **193** (2018), 1287-1297. DOI: 10.1007/s10909-018-2053-6

32. K. Mayer and E. Knill. Quantum Process Fidelity Bounds from Sets of Input States. *Physical Review A* **98** (2018), 052326. DOI: 10.1103/PhysRevA.98.052326

33. G. McFadden, W. Boettinger, and Y. Mishin. Effect of Vacancy Creation and Annihilation on Grain Boundary Motion. *Acta Materialia* **185** (2020), 66-79. DOI: 10.1016/j.actamat.2019.11.044

34. N. Mouha, M. Raunak, D. Kuhn, and R. Kacker. Finding Bugs in Cryptographic Hash Function Implementations. *IEEE Transactions on Reliability* **67**:3 (2018), 870-884. DOI: 10.1109/TR.2018.2847247

35. A. Nucciotti, B. Alpert, M. Balata, D. Becker, D. Bennett, A. Bevilacqua, M. Biasotti, V. Ceriale, G. Ceruti, D. Corsini, M. De Gerone, R. Dressler, M. Faverzani, E. Ferri, J. Fowler, G. Gallucci, J. Gard, F. Gatti, A. Giachero, J. Hays-Wehle, S. Heinitz, G. Hilton, U. Köster, M. Lusignoli, J. Mates, S. Nisi, A. Orlando, L. Parodi, G. Pessina, A. Puiu, S. Ragazzi, C. Reintsema, M. Ribeiro-Gomez, D. Schmidt, D. Schuman, F. Siccardi, D. Swetz, J. Ullom, and L. Vale. Status of the HOLMES Experiment to Directly Measure the Neutrino Mass. *Journal of Low Temperature Physics* **193** (2018), 1137-1145. DOI: 10.1007/s10909-018-2025-x

36. P. Patrone, A. Dienstfrey, and G. McFadden. Model Reduction of Rigid-Body Molecular Dynamics via Generalized Multipole Potentials. *Physical Review E* **100** (2019), 063302. DOI: 10.1103/PhysRevE.100.063302

37. P. Patrone, G. Cooksey, and A. Kearsley. Dynamic Measurement of Nanoflows: Analysis and Theory of an Optofluidic Flowmeter. *Physical Review Applied* **11** (2019), 034025. DOI: 10.1103/PhysRevApplied.11.034025

38. C. Petra and F. Potra. A Homogeneous Model for Monotone Mixed Horizontal Linear Complementarity Problems. *Computational Optimization and Applications* **72** (2019), 241–267. DOI: 10.1007/s10589-018-0035-x

39. I. Roth, R. Kueng, S. Kimmel, Y. Liu, D. Gross, J. Eisert, and M. Kliesch. Recovering Quantum Gates from Few Average Gate Fidelities. *Physical Review Letters* **121** (2018), 170502. DOI: 10.1103/PhysRevLett.121.170502

40. D. Schultz, H. Gharibnejad, T. Cravens, and S. Houston. Data for Secondary-Electron Production from Ion Precipitation at Jupiter III: Target and Projectile Processes in H+, H, and H- + H_2 Collisions. *Atomic Data and Nuclear Data Tables* 132 (2020), 101307. DOI: 10.1016/j.adt.2019.101307

41. E. Smith, J. Zwolak, and C. Manogue. Isolating Approaches: How Middle-Division Physics Students Coordinate Forms and Representations in Complex Algebra. *Physical Review Physics Education Research* **15**:1 (2019), 010138. DOI: 10.1103/PhysRevPhysEducRes.15.010138

42. J. van Meter and E. Knill. Approximate Exchange-Only Entangling Gates for the Three-Spin-½ Decoherence-Free Subsystem. *Physical Review A* **99** (2019), 042331. DOI: 10.1103/PhysRevA.99.042331

43. Y. Wan, D. Kienzler, S. Erickson, K. Mayer, T. Tan, J. Wu, H. Vasconcelos, S. Glancy, E. Knill, D. Wineland, C. Andrew, and D. Leibfried. Quantum Gate Teleportation Between Separated Qubits in a Trapped-Ion Processor. *Science* **364** (2019), 875-878. DOI: 10.1126/science.aaw9415

44. J. Wu, A. Martin, and R. Kacker. Monte Carlo Studies of Bootstrap Variability in ROC Analysis with Data Dependency. *Communications in Statistics – Simulation and Computation* **48** (2019), 317-333. DOI: 10.1080/03610918.2018.1521974

45. D. Yeo, F. Potra, and E. Simiu. Tall Building Database-Assisted Design: A Review of NIST Research. *International Journal of High-Rise Buildings* **8**:4 (2019), 265-273. DOI: 10.21022/IJHRB.2019.8.4.1

46. Y. Zhang, E. Knill, and P. Bierhorst. Certifying Quantum Randomness by Probability Estimation. *Physical Review A* **98** (2018), 040304(R). DOI: 10.1103/PhysRevA.98.040304

Journal of Research of NIST

1. B. Cloteaux. Forced Edges and Graph Structure. *Journal of Research of NIST*, **124** (2019), 124022. DOI: 10.6028/jres.124.022

2. J. Lawrence, J. Bernal, and C. Witzgall. A Purely Algebraic Justification of the Kabsch-Umeyama Algorithm. *Journal of Research of NIST* **124** (2019), 124028. DOI: 10.6028/jres.124.028

3. O. Slattery, L. Ma, K. Zong and X. Tang. Background and Review of Cavity-Enhanced Spontaneous Parametric Down-Conversion. *Journal of Research of NIST* **124** (2019), 124019. DOI: 10.6028/jres.124.019

Book Chapters

1. J. Fong, J. Filliben, N. Heckert, D. Leber, P. Berkman, and R. Chapman. Uncertainty Quantification of Failure Probability and a Dynamic Risk Analysis of Decision-Making for Maintenance of Aging Infrastructure. In *Risk Based Technologies* (P. Varde, R. Prakash, and N. Joshi, eds.), Springer, 2018, 65-80. DOI: 10.1007/978-981-13-5796-1_5

2. P. Patrone and A. Dienstfrey. Uncertainty Quantification for Molecular Dynamics. *Reviews in Computational Chemistry* **31** (2019), 115-169. DOI: 10.1002/9781119518068.ch3

In Conference Proceedings

1. B. Cloteaux and V. Marbukh. SIS Contagion Avoidance on a Network Growing by Preferential Attachment. In *Proceedings of the 2nd Joint International Workshop on Graph Data Management Experiences & Systems and Network Data Analytics (GRADES-NDA'19),* Amsterdam, Netherlands, July 30, 2019. DOI: 10.1145/3327964.3328502

2. G. Cooksey, P. Patrone, J. Hands, S. Meek, and A. Kearsley. Dynamic Measurement of Nanoliter per Minute Flow by Scaled Dosage of Fluorescent Solutions. In *Proceedings of the 22nd International Conference on Miniaturized Systems for Chemistry and Life Sciences (MicroTas 2018)*, Kaohsiung, Taiwan, November 11-15, 2018. URL:https://tsapps.nist.gov/publication/get_pdf.cfm?pub_id=926590

3. F. Duan, Y. Lei, R. Kacker, and D. Kuhn. An Approach to T-way Test Sequence Generation with Constraints. In *Proceedings of the 2019 IEEE International Conference on Software Testing, Verification, and Validation Workshops (ICSTW),* Xi'an, China, April 22-23, 2019. DOI: 10.1109/ICSTW.2019.00059

4. H. Feng, J. Chandrasekaran, Y. Lei, R. Kacker, and D. R. Kuhn. A Method-Level Test Generation

Framework for Debugging Big Data Applications. In *Proceedings of the 2018 IEEE International Conference on Big Data*, Seattle, WA, December 10-13, 2018. DOI: 10.1109/BigData.2018.8622248

5. J. Fong, P. Marcal, R. Rainsberger, N. Heckert, and J. Filliben. Design of an Intelligent Python Code for Validating Crack Growth Exponent by Monitoring a Crack of Zig-Zag Shape in a Cracked Pipe. In *Proceedings of ASME 2019 Pressure Vessels & Piping Conference*, San Antonio, TX, July 14-19, 2019. DOI: 10.1115/PVP2019-93502

6. J. Fong, N. Heckert, J. Filliben, P. Marcal, S. Berweger, T. Wallis, K. Genter, and P. Kabos. Design of an Intelligent Python Code to Run Coupled and License-Free Finite-Element and Statistical Analysis Software for Calibration of Near-Field Scanning Microwave Microscopes. In *Proceedings of the 2019 International COMSOL Users Conference*, Boston, MA, October 2-4, 2019.

7. J. Fong, N. Heckert, J. Filliben, and S. Freiman. A Co-Reliability-Target-Based Fatigue Failure Probability Model for Implementing the New ASME Boiler & Pressure Vessel Section XI Division 2 Reliability and Integrity Management Code: A Technical Brief. In *Proceedings of the ASME 2019 Pressure Vessels & Piping Conference*, San Antonio, TX, July 27-31, 2019. DOI: 10.1115/PVP2019-93508

8. B. Garn, D. Simos, S. Zauner, D. Kuhn, and R. Kacker. Browser Fingerprinting Using Combinatorial Sequence Testing. In *Proceedings of the 6th Annual Symposium on Hot Topics in the Science of Security (HoTSoS 2019),* Nashville, TN, April 2-3, 2019. DOI: 10.1145/3314058.3314062

9. L. Hu, W. Wong, D. Kuhn, and R. Kacker. MCDC-Star: A White-Box Based Automated Test Generation for High MC/DC Coverage. In *Proceedings of the 5th International Conference on Dependable Systems and Their Applications (DSA)*, Dalian, China, September 22-23, 2018. DOI: 10.1109/DSA.2018.00027

10. R. Kacker. True Value and Uncertainty in the GUM. In *Proceedings of the XXII World Congress of the International Measurement Confederation (IMEKO)*, Belfast, Ireland, September 3-6, 2018. DOI: 10.1088/1742-6596/1065/21/212003

11. J. Kauffman, W. George, and J. Pitt. An Overset Mesh Framework for an Isentropic ALE Navier-Stokes HDG Formulation. In *Proceedings of the AIAA SciTech Forum*, San Diego, CA, January 7-11, 2019. DOI: 10.2514/6.2019-1986

12. K. Krhac, K. Sayrafian, G. Noetscher, and D. Simunic. A Simulation Platform to Study the Human Body Communication Channel. In *Proceedings of the 41st Annual International Conference of the IEEE Engineering in Medicine and Biology Society (EMBC)*, Berlin, Germany, July 23-27, 2019. DOI: 10.1109/EMBC.2019.8857883

13. P. Kuo, P. Schunemann, M. Van Camp, V. Verma, T. Gerrits, S. Nam, and R. Mirin. Towards a Source of Entangled Photon Pairs in Gallium Phosphide. In *Proceedings of the CLEO: QELS Fundamental Science 2019*, San Jose, CA, May 5-10, 2019. DOI: 10.1364/CLEO_QELS.2019.FTh1D.5

14. P. Kuo, V. Verma, T. Gerrits, S. Nam, and R. Mirin. Generating Polarization-Entangled Photon Pairs in Domain-Engineered PPLN. In *Proceedings of the CLEO: Applications and Technology 2019*, San Jose, CA, May 5-10, 2019. DOI: 10.1364/CLEO_AT.2019.JTu2A.42

15. R. La. Identifying Vulnerable Nodes to Cascading Failures: Centrality to the Rescue. In *Proceedings of the International Conference on Complex Networks and their Applications*, Cambridge, England, December 11-13, 2018. DOI: 10.1007/978-3-030-05411-3_69

16. R. La. Identifying Vulnerable Nodes to Cascading Failures: Optimization-Based Approach. In *Proceedings of the International Conference on Complex Networks and their Applications*, Lisbon, Portugal, December 10-12, 2019. DOI: 10.1007/978-3-030-36687-2_64

17. M. Lotfi, R. La, and N. Martins. Bayesian Congestion Game with Traffic Manager: Binary Signal Case. In *Proceedings of the 2018 IEEE Conference on Decision and Control (CDC)*, Miami Beach, FL, December 17-19, 2018. DOI: 10.1109/CDC.2018.8618652

18. L. Ma, X. Tang, A. Battou and O. Slattery. A Testbed for Quantum Communication and Quantum Networks. In *Proceedings of the SPIE Conference on Defense and Commercial Sensing*, Baltimore, MD, April 14-18, 2019. DOI: 10.1117/12.2519081

19. L. Ma, X. Tang and O. Slattery. Optical Quantum Memory Applications in Quantum Communication. In *Proceedings of the SPIE Optical Engineering and Applications*, San Diego, CA, August 11-15, 2019. DOI: 10.1117/12.2528786

20. V. Marbukh. Towards Fog Network Utility Maximization (FoNUM) for Managing Fog Computing Resources. In *Proceedings of the 2019 IEEE International Conference on Fog Computing (ICFC),* Prague, Czech Republic, June 24-26, 2019. DOI: 10.1109/ICFC.2019.00032

21. P. Marcal, R. Rainsberger, and J. Fong. Pure Plastic Behavior and the Assumption of Zero Elasticity at the Limit Load. In *Proceedings of the ASME 2019*

Pressure Vessels & Piping Conference, San Antonio, TX, July 14-19, 2019. DOI: 10.1115/PVP2019-93699

22. P. Patrone, A. Dienstfrey, and G. McFadden. Towards a Priori Uncertainty Quantification of Coarse-Grained Molecular Dynamics: Generalized Multipole Potentials. In *Proceedings of the AIAA SciTech 2019 Forum*, San Diego, California, January 7-11, 2019. DOI: 10.2514/6.2019-0971

23. S. Perez-Simbor, K. Krhac, C. Garcia-Pardo, K. Sayrafian, D. Simunic, and N. Cardona. Impact of Measurement Points Distribution on the Parameters of UWB Implant Channel Model. In *Proceedings of the 2018 IEEE Conference on Standards for Communications and Networking (CSCN),* Paris, France, October 29-31, 2018. DOI: 10.1109/CSCN.2018.8581808

24. S. Pugh, M. Raunak, D. Kuhn, and R. Kacker. Systematic Testing of Post-Quantum Cryptographic Implementations Using Metamorphic Testing. In *Proceedings of the 2019 IEEE/ACM 4th International Workshop on Metamorphic Testing (MET),* Montreal, Canada, May 26, 2019. DOI: 10.1109/MET.2019.00009

25. F. Potra. Equilibria and Weighted Complementarity Problems. In *Numerical Analysis and Optimization (*M. Al-Baali, L. Grandinetti, and A. Purnama, eds.), Springer Proceedings in Mathematics and Statistics **235** (2018), 249-275. DOI: 10.1007/978-3-319-90026-1_12

26. C. Rao, N. Li, Y. Lei, R. Kacker, and D. Kuhn. Using Parameter Mapping to Avoid Forbidden Tuples in a Covering Array. In *Proceedings of the 12th IEEE International Conference on Software Testing, Verification, and Validation Workshop (ICSTW-2019)*, Xian China, April 22-27, 2019. DOI: 10.1109/ICSTW.2019.00060

27. M. Roudneshin, K. Sayrafian, and A. Aghdam. A Machine Learning Approach to the Estimation of Near-Optimal Electrostatic Force in Micro Energy-Harvesters. In *Proceedings of the 7th Annual IEEE International Conference on Wireless for Space and Extreme Environments (WISEE 2019),* Ottawa, Canada, October 16-18, 2019. DOI: 10.1109/WiSEE.2019.8920332

28. B. Rouzbehani, V. Marbukh, and K. Sayrafian. A Joint Admission Control & Resource Management Scheme for Virtualized Radio Access Networks. In *Proceedings of the 2019 IEEE Conference on Standards for Communications and Networking (CSCN'19)*, Granada, Spain, October 28-30, 2019. DOI: 10.1109/CSCN.2019.8931373

29. B. Rouzbehani, V. Marbukh, K. Sayrafian, and L. Correia. Towards Cross-Layer Optimization of Virtualized Radio Access Networks. In *Proceedings of the IEEE European Conference on Networks and Communications (EuCNC)*, Valencia, Spain, June 18-21, 2019. DOI: 10.1109/EuCNC.2019.8801989

30. P. Scharpf, M. Schubotz, H. Cohl, and B. Gipp. Towards Formula Concept Discovery and Recognition. In *Proceedings of the 4th Joint Workshop on Bibliometric-enhanced Information Retrieval and Natural Language Processing for Digital Libraries (BIRNDL),* co-located with the 42nd International ACM SIGIR Conference on Research and Development in Information Retrieval (SIGIR 2019), Paris, France, July 25, 2019, 108-115. URL:http://nbn-resolving.de/urn:nbn:de:bsz:352-2-8baaql3vz7aw5

31. A. Scrinzi, B. Schneider, F. Martin. I. Bray, J. Gorfinkiel, J. Tennyson, K. Bartschat, M. Klinker, O. Zatarinny, and S. Pamidighantam. A Science Gateway for Atomic and Molecular Physics. In *Proceedings of the Practice and Experience in Advanced Research Computing (PEARC 19)*, Chicago, IL, USA, July 28 - August 1, 2019. arXiv: abs/2001.02286v1

32. O. Slattery, L. Ma and X. Tang. A Cascaded Interface to Connect Quantum Memory, Quantum Computing and Quantum Transmission Frequencies. In *Proceedings of the 2019 OSA Conference on Frontier in Optics (FIO),* Washington, DC., September 15-19, 2019. DOI: 10.1364/FIO.2019.JW3A.125

33. R. Smith, D. Jarman, J. Bellows, D. Kuhn, R. Kacker, and D. Simos. Measuring Combinatorial Coverage at Adobe. In *Proceedings of the 12th IEEE International Conference on Software Testing, Verification, and Validation Workshop (ICSTW-2019)*, Xian China, April 22-27, 2019. DOI: 10.1109/ICSTW.2019.00052

34. R. Smith, D. Jarman, D. Kuhn, R. Kacker, D. Simos, L. Kampel, M. Leithner, and G. Gosney. Applying Combinatorial Testing to Large-scale Data Processing at Adobe. In *Proceedings of the 12th IEEE International Conference on Software Testing, Verification, and Validation Workshop (ICSTW-2019)*, Xian, China, April 22-27, 2019. DOI: 10.1109/ICSTW.2019.00051

35. A. Youssef and B. Miller. Explorations into the Use of Word Embedding in Math Search and Math Semantics. In *Proceedings of the 12th Conference on Intelligent Computer Mathematics (CICM)*, Prague, Czech Republic, July 2019, Lecture Notes in Computer Science **11617** Springer, Cham. DOI: 10.1007/978-3-030-23250-4_20

Technical Reports

1. G. Alagic, J. Alperin-Sheriff, D. Apon, D. Cooper, Q. Dang, C. Miller, D. Moody, R. Peralta, R. Perlner, A. Robinson, D. Smith-Tone, and Y. Liu. Status Report on the First Round of the NIST Post-Quantum Cryptography Standardization Process. NISTIR 8240, January 2019, 27 pages. DOI: 10.6028/NIST.IR.8240
2. R. F. Boisvert (ed.), Applied and Computational Mathematics Division, Summary of Activities for Fiscal Year 2017, NISTIR 8208, April 2018, 143 pages. DOI: 10.6028/NIST.IR.8208
3. L. Kocia and P. Love. Stationary Phase Method in Discrete Wigner Functions and the Classical Simulation of Quantum Circuits. ArXiv preprint 1810.03622, October 8, 2018. arXiv: 1810.03622
4. N. Martys, W. George, R. Murphy, and K. Weigandt. Certification of SRM 2497: Standard Reference Concrete for Rheological Measurements. NIST Special Publication 260-194, April 2019, 116 pages. DOI: 10.6028/NIST.SP.260-194
5. T. Scholten, Y. Liu, K. Young, and R. Blume-Kohout. Classifying Single-Qubit Noise Using Machine Learning. ArXiv preprint 1908.11762, August 2019, 20 pages. arXiv:1908.11762v1
6. H. Zhao, G. W. Bryant, W. Griffin, J. E. Terrill, and J. Chen. What Do People See in a Twenty-Second Glimpse of Bivariate Vector Field Visualizations? ArXiv preprint 1905.02366, May 7, 2019. arXiv: 1905.02366

Accepted

1. C. Agarwal, J. Klobusicky, and D. Schonfeld. Convergence of Back Propagation with Momentum for Network Architectures with Skip Connections. *Journal of Computational Mathematics*.
2. F. Ahmadi, Y. Sozer, M. Donahue, and I. Tsukerman. A Low-loss and Lightweight Magnetic Material for Electrical Machinery. *IET Electric Power Applications*.
3. F. Ahmadi, M. Donahue, Y. Sozer, and I. Tsukerman. Micromagnetic Study of Magnetic Nanowires. *AIP Advances*.
4. D. Becker, B. Alpert, D. Bennett, M. Croce, J. Fowler, J. Gard, A. Hoover, Y. Joe, K. Koehler, J. Mates, G. O'Neil, M. Rabin, C. Reintsema, D. Schmidt, D. Swetz, P. Szypryt, L. Vale, A. Wessels, and J. Ullom. Advances in Analysis of Microcalorimeter Gamma-Ray Spectra. *IEEE Transactions on Nuclear Science*.
5. I. Beichl and A. Jensen. A Sequential Importance Sampling Algorithm for Counting Linear Extensions. *ACM Journal of Experimental Algorithmics*.
6. M. Donahue, ed. *Electrostatic and Magnetic Phenomena: Particles, Macromolecules, Nanomagnetics.* World Scientific Publishing.
7. L. Ghandehari, Y. Lei, R. Kacker, D. Kuhn, T. Xie, and D. Kung. A Combinatorial Testing-Based Approach to Fault Localization. *IEEE Transactions on Software Engineering.* DOI: 10.1109/TSE.2018.2865935
8. Z. Gimbutas, S. Jiang, and L. Luo. Evaluation of Abramowitz Functions in the Right Half of the Complex Plane. *Journal of Computational Physics*.
9. L. Ma, X. Tang, and O. Slattery. Optical Quantum Memory and its Applications in Quantum Communication Systems. *Journal of Research of NIST*.
10. D. Porter and M. Donahue. Standard Problems in Micromagnetics. In *Electrostatic and Magnetic Phenomena: Particles, Macromolecules, Nanomagnetics* (M. J. Donahue, ed.), World Scientific Publishing.
11. B. Saunders. Complex Variables, Mesh Generation, and 3D Web Graphics: Research and Technology Behind the Dynamic Visualizations in the NIST Digital Library of Mathematical Functions. In *Proceedings of the National Association of Mathematicians (NAM) 50th Anniversary Celebration,* AMS Contemporary Mathematics Series.
12. J. Sims. Hylleraas-Configuration-Interaction (Hy-CI) Non-Relativistic Energies for the 3 ^{1}S, 4 ^{1}S, 5 ^{1}S, 6 ^{1}S, and 7 ^{1}S Excited States of the Beryllium Atom. *Journal of Research of NIST.*
13. E. Williams, J. Zwolak, R. Dou, and E. Brewe. Linking Engagement and Performance: The Social Network Analysis Perspective. *Physical Review Physics Education Research*.
14. P. Wills, E. Knill, K. Coakley, and Y. Zhang. Performance of Test Super Martingale Confidence Intervals for the Success Probability of Bernoulli Trials. *Journal of Research of NIST*.
15. Y. Zhang, H. Fu, and E. Knill. Efficient Randomness Certification by Quantum Probability Estimation. *Physical Review Research*.
16. Y. Zhang, L. Shalm, J. Bienfang, M. Stevens, M. Mazurek, S. Nam, C. Abellan, W. Amaya, M. Mitchell, H. Fu, C. Miller, A. Mink, and E. Knill. Experimental Low-Latency Device-Independent Quantum Randomness. *Physical Review Letters*.

In Review

1. S. Ambroziak and K. Sayrafian. IoT for Healthcare Applications.
2. S. Asadi, Z. Darvay, G. Lesaja, N. Mahdavi-Amiria and F. Potra. A Full-Newton Step Interior-Point Method for Weighted Linear Complementarity Problem.
3. S. Bhushan, L. Ma, X. Tang, and O. Slattery. Terahertz Electromagnetically Induced Transparency in Cesium Atoms.
4. B. Cloteaux. Fast Graphic Approximation of Very Large Integer Sequences.
5. R. Evans, A. Balijepalli, and A. Kearsley. Transport Phenomena in Biological Field Effect Transistors.
6. J. Fong, N. Heckert, J. Filliben, P. Marcal, and S. Freiman. A Distribution Selection and Scale Uncertainty-Based Approach to Estimating a Minimum Allowable Strength for a Full-Scale Component or Structure of Engineering Materials.
7. J. Fowler, B. Alpert, Y. Joe, G. O'Neil, D. Swetz, and J. Ullom. A Robust Principal Component Analysis for Messy Microcalorimeter Data.
8. Z. Gimbutas, N. Marshall, and V. Rokhlin. A Fast Simple Algorithm for Computing Potential Charges on a Line.
9. A. Greiner-Petter, A. Youssef, T. Ruas, B. Miller, M. Schubotz, A. Aizawa, and B. Gipp. Math-Word Embedding in Math Search and Semantic Extraction.
10. L. Hu, W. Wong, D. Kuhn, and R. Kacker. How Does Combinatorial Interaction Testing Perform in the Real World: An Empirical Study on Five Industrial Systems?
11. F. Hunt. A First Hitting Time Approach to Finding Effective Spreaders in a Network.
12. E. Kim, G. McFadden, and A. Cerfon. Elimination of MHD Current Sheets by Modifications to the Plasma Wall in a Fixed Boundary Model.
13. J. Klobusicky, G. Menon, and R. Pego. Two-Dimensional Grain Boundary Networks: Stochastic Particle Models and Kinetic Limits.
14. S. Langer and A. Reid. Calculating Voxel-Polyhedron Intersections for Meshing Images.
15. K. Mayer and E. Knill. Bounding the Quantum Process Fidelity with a Minimal Set of Input States.
16. J. Majikes, P. Patrone, D. Schiffels, M. Zwolak, A. Kearsley, S. Forry, and J. Liddle. Revealing Thermodynamics of DNA Origami Folding via Affine Transformations.
17. N. Martys, W. George, R. Murphy, and K. Weigandt. Pipe Flow of Sphere Suspensions Having a Power-Law-Dependent Fluid Matrix.
18. G. Pagano, A. Bapat, P. Becker, K. Collins, A. De, P. Hess, H. Kaplan, A. Kyprianidis, W. Tan, C. Baldwin, L. Brady, A. Deshpande, F. Liu, S. Jordan, A. Gorshkov, and C. Monroe. Quantum Approximate Optimization with a Trapped-Ion Quantum Simulator.
19. P. Patrone, A. Kearsley, J. Majikes, and J. Liddle. Analysis and Uncertainty Quantification of DNA Fluorescence Melt Data: Applications of Affine Transformations.
20. C. Titus, D. Li, B. Alpert, H. Cho, J. Fowler, S. Lee, K. Morgan, D. Swetz, J. Ullom, A. Wessels, and K. Irwin. Count Rate Optimizations for TES Detectors at a Femtosecond X-ray Laser.
21. P. Wills, E. Knill, K. Coakley, and Y. Zhang. Performance of Test Super Martingale Confidence Intervals for the Success Probability of Bernoulli Trials.
22. Y. Zhang, E. Knill, and P. Bierhorst. Quantum Randomness Generation by Quantum Probability Estimation with Quantum Side Information.
23. J. Zwolak, T. McJunkin, S. Kalantre, J. Dodson, E. MacQuarrie, D. Savage, M. Lagally, S. Coppersmith, M. Eriksson, and J. Taylor. Auto-Tuning of Double Dot Devices in Situ with Machine Learning.

Inventions

Patents

1. G. Cooksey, P. Patrone, and A. Kearsley. Optical Flow Meter for Determining a Flow Rate of a Liquid. US15/967,966.
2. L. Ma, O. Slattery and X. Tang. Direct Absolute Spectrometer for Direct Absolute Spectrometry. US Publication US 2019/0376846 A1. Published: December 12, 2019.

Invention Disclosures

1. G. Cooksey and P. Patrone. Zero Flow Detector
2. B. Alpert, et al. Table-Top Apparatus for the Time-Resolved X-Ray Absorption and Emission Spectroscopy Using an Array of X-Ray Microcalorimeter Sensors.

Presentations

Note: When multiple presenters are listed, names of co-presenters with a Division affiliation during this reporting period are underlined.

Invited Talks

1. D. A. Anderson, J. D. Benson, and A. J. Kearsley. "Modeling Heat and Mass Transport in Cryobiology." School of Mathematical and Natural Sciences, Arizona State University, November 8, 2018.
2. R. F. Boisvert. "ACM Digital Library: How We Got Here." ACM Digital Library Workshop, New York, NY, January 30, 2019.
3. R. F. Boisvert. "Reproducibility and Badging at ACM." International Federation for Information Processing (IFIP) Working Group 2.5, Valencia, Spain, July 20, 2019.
4. T. Burns. "Closed-Form Projection Method for Regularizing a Function Defined by a Discrete Set of Noisy Data and for Estimating its Derivative and Fractional Derivative." Eleventh IMACS International Conference on Nonlinear Evolution Equations and Wave Phenomena: Computation and Theory, University of Georgia, April 17-19, 2019.
5. A. Carasso. "Computing 2D Incompressible Navier-Stokes Equations Backward in Time." 2019 Inverse Problems Symposium, Purdue University, May 29-31, 2019.
6. G. Doğan. "Variational Shape Optimization for Image Analysis." Applied Mathematics Seminar, Colorado State University, Fort Collins, CO, October 19, 2018.
7. G. Doğan. "Boundary Shape Optimization to Detect Objects and Regions in Images." Clarkson University, Potsdam, NY, March 8, 2019.
8. G. Doğan. "An Optimization Algorithm for Elastic Shape Distances Between 2d Object Boundaries." AMS Joint Mathematics Meeting, Baltimore, MD, January 16-19, 2019.
9. R. Evans, A. Balijepalli, and A. Kearsley. "Transport Phenomena in Field Effect Transistors." Applied and Computational Math Seminar, George Mason University, Fairfax, VA, November 1, 2019.
10. R. Evans, A. Balijepalli, and A. Kearsley. "Transport Phenomena in Field Effect Transistors." 2020 International Congress of Industrial and Applied Mathematics, Valencia, Spain, July 19, 2019.
11. J. Fong. "Artificial Intelligence (AI) For Validating Crack Growth Exponent by Monitoring a Crack of Zig-Zag Shape in Pressure Vessel & Piping." University of Texas at Arlington Research Institute, Arlington, TX, July 12, 2019.
12. S. Glancy. "Supposed Loopholes in Loophole-Free Tests of Local Realism." Quantum Information Revolution: Impact to Foundations, Växjö, Sweden, June 10, 2019.
13. S. Glancy. "NIST's Best Practices for Quantum Tomography." IEEE Quantum Initiative Workshop, Gaithersburg, MD, May 2, 2019.
14. A. Kearsley. "Survey of PDE Constrained Optimization at NIST." Arizona State University, November 7, 2018.
15. A. Kearsley. "Solidification in Cryobiology." Arizona State University, November 7, 2018.
16. A. Kearsley. "Control of Inward Solidification in Cryobiology." Society of Mathematical Biology Annual Meeting, Montreal Canada, July 25, 2019.
17. A. Kearsley. "A Survey of Applied Mathematics and Computational Science at NIST." Workshop on Mathematics Departments and the Explosive Growth of Computational and Quantitative Offerings in Higher Education, American Mathematics Society, Washington DC, October 3, 2019.
18. A. Kearsley and A. Moorthy. "Identifying Seized Drugs with Mass Spectral Library Searching." Shippensburg University Colloquium, Shippensburg University, Shippensburg, PA, October 3, 2019.
19. A. Kearsley. "Mathematical Issues in Cryobiology: Notes on Simulation and Control." Biomolecular Measurement Division Seminar, NIST Gaithersburg, November 19, 2019.
20. P. Kuo. "Entangled Photons for Quantum Information Applications." Department of Applied Physics Seminar, Royal Institute of Technology, Stockholm, Sweden, June 13, 2019.
21. P. Kuo. "Zincblende Nonlinear Crystals for Quantum Information Applications." IEEE Photonics Conference, San Antonio, TX, October 2, 2019.
22. P. Kuo. "Entangled Photons for Quantum Information Applications." Institute for Optical Science Seminar, Ohio State University, Columbus, OH, November 8, 2019.
23. L. Ma, X. Tang, and O. Slattery. "From Quantum Cryptography to the Quantum Internet: An Overview of Quantum Communications and Networks." Joint Seminar of iQUIST and iOptics, University of Illinois, Champaign-Urbana, IL, October 9, 2019.

24. L. Ma, X. Tang, and O. Slattery. "Optical Quantum Memory and Quantum Communication Systems." 2019 SPIE Conference on Optics and Photonics, San Jose, CA, August 11-15, 2019.
25. P. Patrone, A. Dienstfrey, and G. McFadden. "Uncertainty Quantification for Coarse-Grained Molecular Dynamics: The Role of Asymptotics in Model Reduction." Workshop on Computational Mathematics for Model Reduction and Predictive Modelling in Molecular and Complex Systems, EPFL / CIB, Lausanne, Switzerland, May 28, 2019.
26. P. Patrone. "Mathematics and Metrology at NIST: Applications for Microfluidics and Biological Systems [translated from Italian]." National Institute of Metrology Research (INRIM), Turin, Italy, June 3, 2019.
27. P. Patrone, A. Kearsley, and G. Cooksey. "Mathematics for Microfluidic Measurements of Flow & Cell-based Properties." CYTO 2019, Vancouver, Canada, June 24, 2019.
28. D. Porter. "Tcl Core Team Year in Review." 25th Annual Tcl/Tk Conference, Houston, TX, October 18, 2018.
29. D. Porter. "Tcl Core Team Year in Review." 26th Annual Tcl/Tk Conference, Houston, TX, November 7, 2019.
30. F. Potra. "A Homogeneous Model for Monotone Mixed Horizontal Linear Complementarity Problems." 30th European Conference on Operations Research (EURO 2019), Dublin, Ireland, June 23-26, 2019.
31. R. Pozo. "A Network Measure for the Analysis of Large-Scale Graphs" American University, October 30, 2018.
32. S. Ressler. "Hot Stuff: Using Web3D to Examine Fire from the Inside." EPICentre, Sydney, Australia, September 18, 2019.
33. B. Saunders. "Research in Computational and Applied Mathematics at NIST." Worcester Polytechnic Institute, Worcester, MA, April 18, 2019.
34. B. Saunders. "B-Spline Mesh Generation, 3D Web Graphics and the NIST Digital Library of Mathematical Functions." Lafayette College, Easton, PA, September 25, 2019.
35. B. Saunders. "Mathematics Behind the 3D Visualizations of the NIST Digital Library of Mathematical Functions." George Mason University, Fairfax, VA, October 25, 2019.
36. B. Saunders. "Mathematics, Mesh Generation, and 3D Graphics on the Web, and Finding a Career at NIST." MAA MD-DC-VA Fall Section Meeting, Norfolk State University, Norfolk, VA, November 9, 2019.
37. J. Zwolak. "Auto-Tuning and Rays-Based Learning of Quantum Dot Devices." The Centre for Quantum Computation and Communication Technology, Sydney, Australia, November 15, 2018
38. J. Zwolak, J. Taylor, S. Kalantre, and X. Wu. "True Machine Learning for Quantum Dot Tune-up." American Physical Society, Boston, MA, March 8, 2019.
39. J. Zwolak. "CNN-Supported Auto-Tuning of Devices in Quantum Dot Experiments." University of Oxford, Oxford, United Kingdom, May 14, 2019.
40. J. Zwolak. "Students Experiences in a Classroom. The Social Network Perspective." Jackson State University, Jackson, MS, May 17, 2019.
41. J. Zwolak. "Machine Learning for Automated Formation of Quantum Dot Arrays." The Northwest Workshop on Quantum Transduction, Seattle, WA, November 15, 2019.
42. J. Zwolak. "Machine Learning Supported Auto-Tuning of Quantum Dot Devices: Two Dots and Beyond." Center for Integrated Nanotechnologies, Sandia National Laboratories, Albuquerque, NM, December 2, 2019.
43. J. Zwolak. "Rays-Based Learning and Auto-Tuning of Devices in Quantum Dot Experiments." R. G. Herb Condensed Matter Seminar at the University of Wisconsin-Madison, Madison, WI, December 17, 2018.

Conference Presentations

1. S. Ressler and K. Chen. "NIST Digital Library of Math Functions Meets Virtual Reality." Mixed/Augmented/Virtual Reality Innovation Conference (MAVRIC), College Park, MD, October 18, 2018.
2. B. Saunders. "An Adaptive Curvature and Gradient Based Grid Generation Method." 15th Meeting on Applied Scientific Computing and Tools (MASCOT 2018), Rome, Italy, October 5, 2018.
3. A. Biacchi, E. De Lima Correa, F. Zhang, T. Moffat, W. Tew, M. Donahue, S. Woods, C. Dennis, and A. Hight Walker. "Tuning the Properties of Colloidal Magnetic Particles for Thermometry on the Nanoscale." 64th Annual Conference on Magnetism and Magnetic Materials (MMM 2019), Las Vegas, NV, November 8, 2019.

4. T. Burns. “Shear Band Formation in Bulk Metallic Glasses.” 55th Annual Technical Meeting of the Society of Engineering Science, Engineering School of the University Carlos III, Madrid, Spain, October 10-12, 2018.
5. T. Burns. “Estimation of the Derivative and Fractional Derivative of a Function Specified by Noisy Data.” 3rd Fractional Calculus Meeting, University of Zaragoza, Zaragoza, Spain, September 25-27, 2019.
6. B. Cloteaux. “SIS Contagion Avoidance on a Network Growing by Preferential Attachment.” GRADES-NDA’19, Amsterdam, Netherlands, July 30, 2019.
7. H. Cohl. “Fundamental Solutions and Gegenbauer Expansions of the Helmholtz Equations on d-Dimensional Riemannian Spaces of Constant Curvature.” 2018 Canadian Mathematical Society Meeting, Vancouver, Canada, December 10, 2018.
8. H. Cohl. “More Precise Symmetric Descriptions for Properties of the Askey-Wilson Polynomials and their Symmetric Sub-Families.” 15th International Symposium on Orthogonal Polynomials, Special Functions and Applications (OPSFA-15) Hagenberg, Austria, July 24, 2019.
9. H. Cohl. “More Precise Symmetric Descriptions for Properties of the Askey-Wilson Polynomials and their Symmetric Sub-Families.” 2nd International Conference on Symmetry, Centro de Ciencias de Benasque Pedro Pascual, Benasque, Spain, September 2, 2019.
10. H. Cohl. “More Precise Symmetric Descriptions for Properties of the Askey-Wilson Polynomials and their Symmetric Sub-Families.” Fall Central Sectional Meeting of the American Mathematical Society, University of Wisconsin-Madison, Madison, Wisconsin, September 14, 2019.
11. H. Cohl. “More Precise Symmetric Descriptions for Properties of the Askey-Wilson Polynomials and their Symmetric Sub-Families.” University of Wisconsin-Milwaukee, Milwaukee, Wisconsin. September 20, 2019.
12. N. Douguet, H. Gharibnejad, B. Schneider, and L. Argenti. “Ab Initio Numerical Methods for Attosecond Molecular Spectroscopy.” Annual Meeting of the American Physical Society Division of Atomic, Molecular, and Optical Physics (DAMOP), Milwaukee, WI, May 27-31, 2019.
13. J. Fong. “A Partial Verification of a COMSOL Example Problem on the Fluid-Structure Interaction in a Network of Blood Vessels.” International COMSOL Users Conference, Boston, MA, October 4, 2018.
14. J. Fong. “A Failure-Predicting Intelligent Python (IP) Code for Monitoring a Crack of Irregular Shape in a Pipe.” International Conference on Computational and Experimental Engineering and Sciences, Tokyo, Japan, March 26, 2019.
15. J. Fong. “Pure Plastic Behavior and the Assumption of Zero Elasticity at the Limit Load.” 2019 ASME International Pressure Vessel and Piping Division Conference, San Antonio, TX, July 16, 2019.
16. J. Fong. “Design of an Intelligent Python Code for Validating Crack Growth Exponent by Monitoring a Crack of Zig-Zag Shape in a Cracked Pipe.” 2019 ASME International Pressure Vessel and Piping Division Conference, San Antonio, TX, July 18, 2019.
17. J. Fong. “A Co-Reliability-Target-Based Fatigue Failure Probability Model for Implementing the Proposed ASME Boiler & Pressure Vessel Code Section XI Division 2 Reliability and Integrity Management (RIM) Code.” 2019 ASME International Pressure Vessel and Piping Division Conference, San Antonio, TX, July 18, 2019.
18. H. Gharibnejad, M. Leadingham, H. Schmale, and B. Schneider. “A Comparison of Numerical Approaches to the Solution of the Time-Dependent Schrödinger Equation in One Dimension.” Annual Meeting of the American Physical Society Division of Atomic, Molecular, and Optical Physics (DAMOP), Milwaukee, WI, May 27-31, 2019.
19. Z. Gimbutas. “Optimized Quadratures for the Sommerfeld Representations of Acoustic and Electromagnetic Fields.” SIAM Conference on Computational Science and Engineering (CSE19), Spokane, WA, March 1, 2019.
20. Z. Gimbutas. “High Order Methods for the Evaluation of Layer Potentials in Three Dimensions.” International Congress on Industrial and Applied Mathematics (ICIAM), Valencia, Spain, July 16, 2019.
21. S. Glancy. “Tomography of Quantum Gate Teleportation Between Separated Zones of a Trapped-Ion Processor.” Assessing the Performance of Quantum Computers, Estes Park, CO, September 25, 2019.
22. R. Kacker, D. Kuhn, Y. Lei, and D. Simos. “Factorial Experiments, Covering Arrays, and Combinatorial Testing.” 2019 Joint Statistical Meetings, Denver, Colorado, July 27-August 1, 2019.

23. J. Kauffman, W. George, and J. Pitt. "An Overset Mesh Framework for the Hybridizable Discontinuous Galerkin Method." 14th Symposium on Overset Composite Grids and Solution Technology, College Park, MD, October 1, 2018.
24. J. Kauffman, W. George, and J. Pitt. "An Overset Mesh Framework for an Isentropic ALE Navier-Stokes HDG Formulation." AIAA Science and Technology Forum, San Diego, CA, January 7, 2019.
25. D. R. Kuhn, D. Simos, and R. Kacker. "Combinatorial Methods for Testing and Analysis of Critical Software and Security Systems." DATA-Works 2019, Springfield, VA 22150, April 9-11, 2019.
26. P. Kuo. "Nonlinear Mixing of Polarization States in Non-Birefringent Crystals." SPIE Photonics West, San Francisco, CA, February 2-7, 2019.
27. P. Kuo, P. Schunemann, M. Van Camp, V. Verma, T. Gerrits, S. Nam, and R. Mirin. "Towards a Source of Entangled Photon Pairs in Gallium Phosphide." Conference on Lasers and Electro-Optics, San Jose, CA, May 5-10, 2019.
28. Y.-K. Liu. "Lectures on Quantum Algorithms (Parts 1, 2 and 3)." Illinois Quantum Computing Summer School, Chicago, IL, June 17-20, 2019.
29. L. Ma, X. Tang, A. Battou, and O. Slattery. "A Testbed for Quantum Communication and Networks." 2019 SPIE Conference on Defense and Commercial Sensing, Baltimore, MD, April 14-18, 2019.
30. V. Marbukh. "Towards Fog Network Utility Maximization (FoNUM) for Managing Fog Computing Resources." Workshop on Efficient Data Movement in Fog Computing, Prague, Czech Republic, June 24, 2019.
31. V. Marbukh. "Towards Robust Access for Internet of Things in Uncertain/Adverse Communication Environment." Workshop on Internet of Things for Adversarial Environments, Paris, France, April 29, 2019.
32. N. Martys and W. George. "Computational Modelling of Suspension Flow in Pipes: Application to Cement Based Materials." Society of Rheology 90th Annual Meeting, Houston, TX, October 14, 2018.
33. A. Moorthy, A. Kearsley, W. Mallard, W. Wallace, and S. Stein. "Evaluation of NIST Library Search Software." 67th American Society of Mass Spectrometry Conference on Mass Spectrometry and Allied Topics, Atlanta, GA, June 2-6, 2019.
34. S. Ressler. "WebXR: Immersing Yourself in Science." SIGGRAPH Birds of a Feather, Los Angeles CA, July 13, 2019.
35. S. Ressler. "Too Hot to Handle: Web3D for Fire Data Exploration." SIGGRAPH Asia 2019, Brisbane, Australia, October 24, 2019.
36. B. Saunders. "An Adaptive Curvature and Gradient Based Grid Generation Method.", 15th Meeting on Applied Scientific Computing and Tools (MASCOT 2018), Rome, Italy, October 5, 2018.
37. K. Sayrafian. "Impact of Measurement Points Distribution on the Parameters of UWB Implant Channel Model." 4th Annual IEEE Conference on Standards for Communications and Networking (CSCN 2018), Granada, Spain, October 29-31, 2018.
38. K. Sayrafian. "A Simulation Platform to Study the Human Body Communication Channel." 41st International Engineering in Medicine and Biology Conference (IEEE EMBC 2019), Berlin, Germany, July 23-27, 2019.
39. K. Sayrafian. "An Overview of IoT-Health." IoT-Health 2019: Second International Workshop on IoT Enabling Technologies in Healthcare, Istanbul, Turkey, September 8, 2019.
40. B. Schneider. "A Science Gateway for Atomic and Molecular Physics." Practice and Experience in Advanced Research Computing (PEARC) on Rise of the Machines, Chicago, IL, July 28 - August 01, 2019
41. A. Youssef. "Explorations into the Use of Word Embedding in Math Search and Math Semantics." 12th Conference on Intelligent Computer Mathematics (CICM) 2019, Prague, Czech Republic, July 2019.
42. Y. Zhang, H. Fu, K. Shalm, J. Bienfang, M. Stevens, M. Mazurek, S. Nam, C. Abellan, W. Amaya, M. Mitchell, C. Miller, A. Mink and E. Knill. "Efficient Randomness Certification by Quantum Probability Estimation." International Conference on Quantum Cryptography (QCRYPT 2019), Montreal, Canada, August 26 – 30, 2019.
43. J. Zwolak, S. Kalantre, X. Wu, and J. Taylor. "Vector-Supported Learning and Auto-Tuning of Devices in Quantum Dot Experiments." Silicon Quantum Electronics Workshop 2018, Sydney, Australia, October 15, 2018.
44. J. Zwolak, S. Kalantre, T. McJunkin, E. MacQuarrie, D. Savage, M. Lagally, M. Eriksson, and J. Taylor. "Ray-based State Learning of Double

Quantum Dot Systems." Silicon Quantum Electronics Workshop, San Sebastian, Spain, October 14, 2019.

Poster Presentations

1. F. Ahmadi, M. Donahue, Y. Sozer, and I. Tsukerman. "Micromagnetic Study of Soft Magnetic Nanowires." 64th Annual Conference on Magnetism and Magnetic Materials (MMM 2019), Las Vegas, NV, November 7, 2019.
2. P. Armstrong and W. Griffin. "Virtual Reality for Cell Microscopy." Mixed/Augmented/Virtual Reality Conference (MAVRIC), College Park, MD, October 17-18, 2018.
3. J. Biggins and S. Ressler. "Virtual Tours: Experiments in Monoscopic and Stereoscopic Virtual Reality." The Mixed/Augmented/Virtual Reality Innovation Conference (MAVRIC), College Park, MD, October 18, 2018.
4. L. Brady and A. Bapat. "A Path Sum Approach To QAOA." Software Tailored Architechtures for Quantum codesign (STAQ) Kickoff Meeting, Durham, NC, December 4, 2018.
5. L. Brady, A. Bapat, and A. Gorshkov. "QAOA Digitizes an Asymptotic Curve: A Path Sum Approach." Southwest Quantum Information and Technology Workshop, Albuquerque, NM, February 11, 2019.
6. L. Brady, C. Baldwin, A. Bapat, and A. Gorshkov. "Limiting Behavior of QAOA vs. QAO." Theoretical Quantum Computation, Communication, and Cryptography Conference, College Park, MD, June 3, 2019.
7. L. Brady, C. Baldwin, A. Bapat, and A. Gorshkov. "Limiting Behavior of QAOA vs. QAO." Adiabatic Quantum Computing Conference, Innsbruck, Austria, June 27, 2019.
8. B. Cloteaux and V. Marbukh. "SIS Contagion Avoidance on a Network Growing by Preferential Attachment." 2nd Joint International Workshop on Graph Data Management Experiences & Systems and Network Data Analytics (GRADES-NDA'19), Amsterdam, Netherlands, July 30, 2019.
9. G. Cooksey, P. N. Patrone, J. R. Hands, S. E. Meek, and A. J. Kearsley. "Dynamic Measurement of Nanoliter per Minute Flow by Scaled Dosage of Fluorescent Solutions." 22nd International Conference on Miniaturized Systems for Chemistry and Life Sciences (MicroTas 2018), Kaohsiung, Taiwan, November 11-15, 2018.
10. G. Doğan. "Scikit-Shape: Python Toolbox for Shape Analysis and Segmentation." SIAM Conference on Computational Geometric Design, Vancouver, Canada, July 17-19, 2019.
11. M. Donahue and D. Porter. "Quantitative Evaluation and Reduction of Error in Computation of the Demagnetization Tensor." 64th Annual Conference on Magnetism and Magnetic Materials (MMM 2019), Las Vegas, NV, November 7, 2019.
12. W. Griffin, K. Sayrafian, and K. Krhac. "Sample Location Selection for Statistical Pathloss Modeling of Wireless Capsule Endoscopy." IEEE Visualization Conference, Vancouver, Canada, October 20-25, 2019.
13. S. Glancy. "Deterministic Teleportation of a Controlled-NOT Gate in a Trapped Ion System." Southwest Quantum Information Technology Workshop, Albuquerque, NM, February 10, 2019.
14. S. Kalantre, J. Zwolak, T. McJunkin, J. Dodson, E. MacQuarrie, D. Savage, M. Lagally, S. Coppersmith, M. Eriksson, and J. Taylor. "In-Situ Machine Learning Assisted Auto-Tuning of Quantum Dot Devices." Workshop on Noisy Intermediate-Scale Quantum Technologies, College Park, MD, June 6, 2019.
15. S. Kalantre, J. Zwolak, S. Ragole, X. Wu, and J. Taylor. "Machine Learning Techniques for State Recognition and Auto-Tuning in Quantum Dots." Joint Center for Quantum Information and Computer Science (QuICS) Stakeholders Day, College Park, MD, February 11, 2019.
16. J. Kauffman, S. Satterfield, W. Griffin, and M. Donahue. "Visual Analysis of Micromagnetic Magnetization Reversal." IEEE VIS 2019, Vancouver, Canada, October 23, 2019.
17. K. Krhac, K. Sayrafian, and D. Simunic. "A 3D Immersive Platform to Study Wireless Communication and Tracking of Ingestible Electronics." IEEE EMB Special Topic Conference on Healthcare Innovations and Point-of-Care Technologies, National Institute of Health, Bethesda, MD, November 20-22, 2019.
18. K. Krhac, K. Sayrafian, and D. Simunic. "A Preliminary Study of the Human Body Communication Channel." IEEE EMB Special Topic Conference on Healthcare Innovations and Point-of-Care Technologies, National Institute of Health, Bethesda, MD, November 20-22, 2019.
19. P. Kuo, V. Verma, T. Gerrits, S. Nam, and R. Mirin. "Generating Polarization-Entangled Photon Pairs in Domain-Engineered PPLN." Conference on Lasers and Electro-Optics, San Jose, CA, May 5-10, 2019.

20. P. Kuo, V. Verma, T. Gerrits, and S. Nam. "Domain-Engineered PPLN for Generating Polarization-Entangled Photon Pairs." Single Photon Workshop, Milan, Italy, October 21-25, 2019.
21. L. Ma, O. Slattery, and X. Tang. "Quantum Memory in Anti-Relaxation Coated Gas Cell." 2019 Single Photon Workshop, Milan, Italy, October 19-26, 2019.
22. G. McFadden. "Computational Study of Magnetohydrodynamic Equilibria with Emphasis on Fragility of Flux Surfaces." 60th Annual Meeting of the American Physical Society (APS) Division of Plasma Physics, Portland, OR, November 7, 2018.
23. A. Moorthy, A. Kearsley, W. Mallard, W. Wallace, and S. Stein. "Evaluation of NIST Library Search Software." American Society of Mass Spectrometry (ASMS) Annual Meeting, June 4, 2019.
24. A. Moorthy, A. Kearsley, W. Mallard, W. Wallace, and S. Stein. "NIST Software for Drug Analysis: NIST Forensics Research Innovation to Implementation" Spectrometry and Allied Topics, San Diego CA, June 3-7, 2018.
25. A. Rad, J. Zwolak, S. Kalantre, and J. Taylor. "Towards State Recognition of 2D Arrays of Quantum Dots: Device Simulation." Workshop on Noisy Intermediate-Scale Quantum Technologies, College Park, MD, June 6, 2019.
26. A. Rad, J. Zwolak, S. Kalantre, and J. Taylor. "Towards States Recognition in the Two- Dimensional Quantum Dots Array with Machine Learning." Joint Center for Quantum Information and Computer Science (QuICS) Stakeholders Day, College Park, MD, February 11, 2019.
27. O. Slattery, L. Ma, and X. Tang. "Cascaded Interface for Quantum Memory, Computing and Transmission Frequencies." 2019 OSA Conference on Frontier in Optics (FIO), Washington DC, September 15-19, 2019.
28. O. Slattery, L. Ma, and X. Tang. "Key Components of Quantum Communications Networks." 2019 SPIE Conference on Optics and Photonics, San Jose, CA, August 11-15, 2019.
29. J. Terrill. "Curve Fitting with Validation as a First Step to the Discovery of Physical Laws." Workshop III: Validation, Guarantees in Learning Physical Models: from Patterns to Governing Equations to Laws of Nature, UCLA Institute for Pure, and Applied Mathematics (IPAM), Los Angeles, CA, October 28, 2019.
30. X. Wu, J. P. Zwolak, S. S. Kalantre, A. R. Mills, J. R. Petta, and J. M. Taylor. "Experimental Implementation of Machine Learning Assisted Auto Tuning of Quantum Dot Devices." Silicon Quantum Electronics Workshop, Sydney, Australia, November 15, 2018.
31. J. Zwolak, S. Kalantre, and J. Taylor. "Rays-Based Learning and Auto-Tuning of Devices in Quantum Dot Experiments." At the Crossroad of Physics and Machine Learning Conference, Santa Barbara, CA, February 11, 2019.

Web Services

Note: ACMD provides a variety of information and services on its website. Below is a list of major services provided that are currently under active maintenance.

1. *Digital Library of Mathematical Functions:* a repository of information on the special functions of applied mathematics.
2. *Digital Repository of Mathematical Formulae*: a repository of information on special function and orthogonal polynomial formulae.
3. *DLMF Standard Reference Tables on Demand*: an online software testing service providing tables of values for special functions, with guaranteed accuracy to high precision.
4. DLMF in VR: Experiments using WebVR to display several or sometimes all DLMF surfaces simultaneously in an environment in which the user can grab, scale and throw the surfaces.
5. *muMAG*: a collection of micromagnetic reference problems and submitted solutions.
6. *NIST Adaptive Mesh Refinement Benchmark Problems*: a collection of benchmark partial differential equations for testing and comparing adaptive mesh refinement algorithms.
7. *NIST VR Scanning Tunneling Microscopy Head*: A WebVR capable simulation of the head of a scanning tunneling microscope which you may explore.
8. *Virtual Tours:* A collection of virtual tours suitable for using WebVR equipment for self-guided tours of NIST Library, NIST Shops and NIST Net Zero House.

Software Released

Note: ACMD distributes a large number of software packages that have been developed in the course of its work. Listed below are particular packages which have seen new releases during the reporting period.

1. *ACTS:* Advanced Combinatorial Testing System. Version 3.2. R. Kacker.
2. *Itcl*: C++ inspired object-oriented commands for Tcl. Versions 4.1.2 (11/16/18) and 4.2.0 (11/21/19). D. G. Porter.
3. *LaTeXML*: A LaTeX to XML converter. Continuous access from svn/git repository. B. R. Miller.
4. *OOF2*: Image-Based Analysis of Materials with Complex Microstructures, Versions 2.1.16 (10/19/18), 2.1.17 (4/3/19), and 2.1.18 (11/8/19). S. A. Langer, A. C. E. Reid, and G. Dogan.
5. *OOF3D*: Three-Dimensional Analysis of Materials with Complex Microstructures, Versions 3.2.1 (10/12/18) and 3.2.2 (8/23/19). S. A. Langer, A. C. E. Reid, and G. Dogan.
6. *OOMMF*: The Object Oriented MicroMagnetic Framework, Versions 1.2b3 (9/27/19) and 2.0a2 (9/30/19). M. J. Donahue and D. G. Porter.
7. *QTCode*: Continuous Variable Quantum State Tomography, Version 1.0 (01/02/19). S. Glancy, H. M. Vasconcelos, J. L. E. Silva.
8. *Sqlite3*: bindings to the SQLite database engine for Tcl. Versions 3.25.2 (11/16/18), 3.26.0 (12/11/18), 3.27.2 (4/1/19), 3.28.0 (5/16/19), 3.29.0 (7/11/19), 3.30.1 (11/21/19). D. Porter.
9. *Tcl/Tk*: Extensible scripting language and GUI toolkit. Versions 8.6.9 (11/16/18), 8.6.10 (11/21/19), 8.7a3 and 9.0a1 (11/25/19). D. G. Porter
10. *TDBC*: Database connection commands for Tcl. Versions 1.1.0 (11/16/18) and 1.1.1 (11/21/19). D. G. Porter
11. *Thread*: Thread management commands for Tcl. Versions 2.8.4 (11/16/18), 2.8.5 (11/21/19), and 3.0a1 (11/25/19). D. G. Porter
12. *VSB*: Robustly calculating the intersection of a convex polyhedron and a set of voxels, Version 1.0.1 (5/16/19). S.A. Langer and A.C.E. Reid.

Conferences, Minisymposia, Lecture Series, Courses

ACMD Seminar Series

Stephen Langer served as Chair of the ACMD Seminar Series. There were 22 talks presented during this period; talks are listed chronologically.

1. Adarsh Kumbhari (University of Sydney, Australia). The Importance of Mitochondrial Fission and Fusion in a Beating Heart Cell. October 18, 2018.
2. Sebastian Barillaro (National Institute for Industrial Technology, Argentina). IoT-LPWAN Testing Facility for Security and Trust in Networks of Sensors. October 23, 2018.
3. Alexey Gorshkov (NIST Physical Measurement Laboratory). Optimal Quantum Sensing. October 30, 2018.
4. Sandip Kundu (University of Massachusetts Amherst). Securing Physically Unclonable Functions. December 13, 2018.
5. Luis Melara (Shippensburg University). Optimal Control of Treatments for Retinitis Pigmentosa. April 4, 2019.
6. Evelyn Lunasin (US Naval Academy). Methods for Prediction and Control of Complex Systems. April 18, 2019.
7. Niklas Olmvqist (University of Maryland, College Park). Always Annexing Pixels: On Techniques and Infrastructure for Cross-Device Visualization. May 22, 2019.
8. Prashant Athavale (Clarkson University). Tale of Two Hierarchical Ways of Processing Image Data. June 12, 2019.
9. Mingchao Cai (Morgan State University). Some Fast Solvers for Models of Fluid Flow and Linear Elasticity. June 25, 2019.
10. Robert Harris (University of Maryland School of Pharmacy). Applications of Constant pH Molecular Dynamics Simulations in Drug Design and Materials Science. July 1, 2019.
11. Christopher Rackauckas (MIT). Model-Free Scientific Computing with Neural Differential Equations. July 10, 2019.
12. Natesh Ganesh (University of Massachusetts Amherst). Engineering Energy Efficient Intelligence. July 25, 2019.

13. Wilkie Olin-Ammentorp (SUNY Polytechnic Institute). Investigating Structure and Reliability in Spiking Neural Networks. August 8, 2019.
14. Danielle Middlebrooks (University of Maryland College Park). Quantifying Flows in Time-Irreversible Markov Chains: Application to a Gene Regulatory Network. August 22, 2019.
15. Alfred S. Carasso (ACMD). Computing Ill-Posed Time-Reversed 2D Navier-Stokes Equations using a Stabilized Explicit Finite Difference Scheme Marching Backward in Time. August 27, 2019.
16. Teseo Schneider (Courant Institute, New York University). Black Box Analysis. September 16, 2019.
17. Bimal Roy (Indian Statistical Institute, Kolkata). Matroids and Secret Sharing Schemes. September 25, 2019.
18. Endel Iarve (University of Texas at Arlington). Regularized Finite Element Modeling Methodology for Predicting Discrete Damage-Based Strength and Durability of Laminated Composite Structures. October 8, 2019.
19. Marisabel Rodriguez (Arizona State University). Mathematical Models for Honeybee Population Dynamics. October 21, 2019.
20. Thomas Brown (George Mason University). Two Applications of PDE Constrained Optimization. November 12, 2019.
21. Daniel Nunez (LPI, Inc.). On Entropy Inequality and Ordered Rate Constitutive Theories for Homogeneous, Isotropic, and Compressible Matter Under Finite Deformation with Thermal Effects. December 3, 2019.
22. Hasan Eruslu (University of Delaware). FEM-CQ Approximation of Viscoelastic Waves. December 11, 2019.

Shortcourses

1. J. Fong. "Sect. XI Div. 2 (RIM), and A Method to Estimate Component Co-Reliability: Part I – Why is SBC Incomplete?" ASME/JSME Joint Working Group on RIM Process and System Based Code of the Subgroup on Reliability and Integrity Management (SG-RIM) Program, ASME Boiler & Pressure Vessel Code Section XI Committee, November 14, 2018.
2. J. Fong. "ASME BPVC Sect. XI Div. 2 (RIM), and A Method to Estimate Component Co-Reliability: Part I – Why is SBC Incomplete?" Working Group/Monitoring and NDE (MANDE) of the Subgroup on Reliability and Integrity Management (SG-RIM) Program, ASME Boiler & Pressure Vessel Code Section XI Committee, February 13, 2019.
3. J. Fong. "ASME BPVC Sect. XI Div. 2 (RIM), and A Method to Estimate Component Co-Reliability: Part I – Why is SBC Incomplete?" Subgroup on Reliability and Integrity Management (SG-RIM) Program, ASME Boiler & Pressure Vessel Code Section XI Committee, May 05, 2019.
4. J. Fong. "A Co-Reliability-Target-based Fatigue Failure Probability Model for Implementing the Proposed ASME Boiler & Pressure Vessel Code Section XI Division 2 Reliability and Integrity Management (RIM) Code." ASME/JSME Joint Working Group on RIM Process and System Based Code of the Subgroup on Reliability and Integrity Management (SG-RIM) Program, ASME Boiler & Pressure Vessel Code Section XI Committee, August 5, 2019.

Conference Organization

Leadership

1. W. Griffin. Co-Organizer, Software Engineering and Architectures for Realtime Interactive Systems (SEARIS) Workshop. Osaka, Japan, March 23, 2019.
2. Y.-K. Liu. Member, Steering Committee, International Conference on Quantum Cryptography (QCrypt).
3. M. Mascagni. Co-Organizer, Workshop on Computational Reproducibility at Exascale, SC18, Dallas, TX, November 11, 2018.
4. M. Mascagni. Co-Organizer, Workshop on Computational Reproducibility at Exascale, SC19, Denver, CO, November 17, 2019.
5. B. Miller. Co-Chair, 13th Conference on Intelligent Computer Mathematics, Bertinoro Italy, July 26–31, 2020.
6. L. Orr, W. George, and J. Terrill. Exhibitors, NIST Booth, SC18, Dallas, TX, November 12-15, 2018.
7. L. Orr, W. George, J. Terrill, and R. Boisvert. Exhibitors, NIST Booth, SC19, Denver, CO, November 18-21, 2019.
8. S. Ressler. Demo Chair, ACM SIGGRAPH International Conference on Virtual-Reality Continuum and Its Applications in Industry (VRCAI), Brisbane Australia, November 14-16, 2019.
9. K. Sayrafian. Co-Chair, Internet of Things (IoT) Track, IEEE European Conference on Networks and Communications (IEEE EuCNC 2019), Valencia, Spain, June 18-21, 2019.

10. K. Sayrafian. Lead Organizer and Chair, Second International Workshop on IoT Enabling Technologies in Healthcare (IoT-Health), Istanbul, Turkey, September 8, 2019.
11. K. Sayrafian. Panel Co-Chair, IEEE Conference on Standards for Communications and Networking (IEEE CSCN), Granada, Spain, October 29-31, 2019.
12. K. Sayrafian. Lead Organizer and Co-Chair, Third International Workshop on IoT Enabling Technologies in Healthcare (IoT-Health), Dublin, Ireland, June 11, 2020.
13. K. Sayrafian. Member, International Advisory Board, International Symposium on Medical Information and Communication Technology (ISMICT).
14. B. Schneider. Co-Organizer, A Scientific Gateway for Atomic and Molecular Physics, NIST, Gaithersburg, MD, December 11-13, 2019.

Committee Membership

1. H. Cohl. Member, Program Committee. 12th Conference on Intelligent Computer Mathematics (CICM 2019). Prague, Czech Republic, July 8-12, 2019.
2. W. Griffin. Member, Program Committee. 2018 Workshop on Analysis of Large-scale Disparate Data. Seattle, WA, December 10-13, 2018.
3. W. Griffin. Member, Program Committee. In Situ Infrastructures for Enabling Extreme-scale Analysis and Visualization (ISAV 2018). Dallas, TX, November 12, 2018.
4. S. Glancy. Member, Program Committee. Southwest Quantum Information Technology Workshop, Albuquerque, NM, February 10-12, 2019.
5. S. Glancy. Member, Program Committee. Quantum Information: Impact to Foundations, Linnaeus University, Växjö, Sweden, June 10-13, 2019.
6. R. Kacker. Member, Steering Committee, and Member, Program Committee. 8th International Workshop on Combinatorial Testing (IWCT 2019) in conjunction with the 12-th IEEE International Conference on Software Testing, Verification, and Validation (ICST 2019), Xian China, April 22-27, 2019.
7. V. Marbukh. Member, Technical Program Committee, IEEE European Conference on Networks and Communications (EUCNC), Valencia, Spain, June 17-21, 2019.
8. R. La. Member, Program Committee. ACM International Symposium on Theory, Algorithmic Foundations, and Protocol Design for Mobile Networks and Mobile Computing (MobiHoc), Catania, Italy, July 2-5, 2019.
9. R. La. Member, Program Committee. 18th International Symposium on Modeling and Optimization in Mobile, Ad Hoc and Wireless Networks (WiOpt), Volos, Greece, June 15-19, 2020.
10. R. La. Member, Program Committee. ACM International Symposium on Theory, Algorithmic Foundations, and Protocol Design for Mobile Networks and Mobile Computing (MobiHoc), Shanghai, China, June 30 - July 3, 2020.
11. Y.-K. Liu. Member, Program Committee. 22nd Annual Conference on Quantum Information Processing (QIP 2019). Boulder, CO, January 14-18, 2019.
12. Y.-K. Liu. Member, Program Committee. 10th International Conference on Post-Quantum Cryptography (PQCrypto 2019), Chongqing, China, May 8-10, 2019.
13. O. Slattery. Member, Program Committee. Quantum Communications and Imaging XI, SPIE Optics and Photonics 2019.
14. A. Youssef. Member, Program Committee. 12th Conference on Intelligent Computer Mathematics (CICM) 2019, Prague, Czech Republic, July 2019.

Session Organization

1. H. Cohl. Co-Organizer, Special Session on Special Functions and Orthogonal Polynomials. 2nd International Conference on Symmetry, September 1-7, 2019, Benasque, Spain.
2. R. Evans. Co-Organizer, Minisymposium A6-5-4 10, Analytic and Computational Simulation in Biomedical Engineering and Bioscience. International Congress for Industrial and Applied Mathematics (ICIAM) 2020, Valencia, Spain. July 15-19, 2019.
3. W. Griffin. Co-Organizer, Frontiers Workshop on Immersive Visualization. International Conference & Exhibition on Computer Graphics & Interactive Techniques (SIGGRAPH), Los Angeles, CA, July 28, 2019.
4. A. Kearsley. Co-Organizer, Minisymposium A6-5-4 10, Analytic and Computational Simulation in Biomedical Engineering and Bioscience. International Congress for Industrial and Applied Mathematics (ICIAM), Valencia, Spain, July 15-19, 2019.
5. A. Kearsley. Lead Organizer, Minisymposium on Optimization and Optimal Control in Mathematical

Biology. Society for Mathematical Biology Annual Meeting, Montreal, Canada, July 22-26, 2019.

6. S. Ressler. Organizer, Immersive Analytics Birds of a Feather Session. BoF, SIGGRAPH Asia, Brisbane, Australia, November 17-20, 2019.
7. K. Sayrafian. Co-Organizer and Co-Chair, Special Session on Computational Human Models for In- and On-body Communications. 41st Annual Engineering in Medicine and Biology (EMBC 2019) Conference, Berlin, Germany, July 27, 2019.
8. F. Potra. Chair, Session on Algorithms for Solving Complementarity Problems. 30th European Conference on Operations Research (EURO 2019), Dublin, Ireland, June 23-26, 2019.

Other Professional Activities

Internal

1. B. K. Alpert. Organizer and Lead, Deep Learning Theory Reading Group.
2. R. Boisvert. Member, ITL Diversity Committee.
3. L. Brady. Co-Organizer, Quantum Annealing Seminar, University of Maryland, College Park
4. B. Cloteaux. Member, Washington Editorial Review Board.
5. S. Glancy. Member, Boulder Summer Undergraduate Research Fellowship Committee.
6. S. Glancy. Member, ITL Diversity Committee.
7. A. Kearsley. Chair, ITL Awards Committee.
8. P. Kuo. Member, ITL Space Task Force.
9. P. Kuo. Member, NIST Colloquium Organizing Board.
10. L. Orr. Member, ITL Diversity Committee.
11. D. Porter. Editorial Board, *Journal of Research of NIST*.
12. R. Pozo. Member, Organizing Committee, Spanish Heritage Month, Association of NIST Hispanic Americans (ANHA).
13. S. Ressler. Division Safety Representative, ITL Safety Committee.
14. B. Schneider. Chair, NIST National Strategic Computing Initiative (NSCI) Seminar Series.
15. O. Slattery. Laser Safety Representative, ITL Safety Committee.
16. J. Zwolak. Organizer, Machine Learning Journal Club with Hands-on Coding.

External

Editorial

1. I. Beichl. Member, Editorial Board, *IEEE Computing in Science & Engineering.*
2. R. F. Boisvert. Associate Editor, *ACM Transactions on Mathematical Software*.
3. H. S. Cohl. Member, Editorial Board, *The Ramanujan Journal.*
4. H. S. Cohl. Co-Editor, *OP-SF NET*, The Electronic News Bulletin of the SIAM Activity Group on Orthogonal Polynomials and Special Functions.
5. H. S. Cohl. Co-Editor, *OPSF-S6, 6th Orthogonal Polynomials and Special Functions Summer School Lecture Notes.*
6. H. Cohl. Co-Editor, Liber Amicorum, a Friendship Book for Dick Askey.
7. H. Cohl. Co-Editor, Special Issue on Symmetry in Special Functions and Orthogonal Polynomials. *Symmetry*, 2019.
8. M. J. Donahue. Editor, *Electrostatic and Magnetic Phenomena: Particles, Macromolecules, Nanomagnetics*, World Scientific Publishing.
9. Z. Gimbutas. Member, Editorial Board, *Advances in Computational Mathematics*.
10. R. J. La. Associate Editor, *IEEE Transactions on Information Theory.*
11. R. J. La. Associate Editor, *IEEE/ACM Transactions on Networking.*
12. F. A. Potra. Regional Editor for the Americas, *Optimization Methods and Software*.
13. F. A. Potra. Associate Editor, *Journal of Optimization Theory and Applications.*
14. F. A. Potra. Associate Editor, *Numerical Functional Analysis and Optimization.*
15. F. A. Potra. Associate Editor, *Optimization and Engineering.*
16. B. Saunders. Associate Editor, *Mathematics Magazine*, Mathematical Association of America (MAA).
17. B. Saunders. Webmaster, SIAM Activity Group on Orthogonal Polynomials and Special Functions.
18. B. Saunders. Moderator, *OP-SF Talk*, SIAM Activity Group on Orthogonal Polynomials and Special Functions.
19. K. Sayrafian. Associate Editor, *International Journal on Wireless Information Networks.*

20. K. Sayrafian. Member, Editorial Board, *IEEE Wireless Communication Magazine*.
21. B. Schneider. Associate Editor in Chief, *Computing in Science & Engineering.*
22. B. Schneider. Specialist Editor, *Computer Physics Communications.*

Boards and Committees

1. R. F. Boisvert. Member, ACM Digital Library Committee.
2. R. F. Boisvert. Member, Working Group 2.5 (Numerical Software), International Federation for Information Processing (IFIP).
3. B. Cloteaux. Member, Advisory Board, Department of Computer Science, New Mexico State University.
4. A. Dienstfrey. Member, Working Group 2.5 (Numerical Software), International Federation for Information Processing (IFIP).
5. J. T. Fong. Member, Boiler and Pressure Vessel Code Committee, American Society of Mechanical Engineers (ASME).
6. S. Glancy. Member, IEEE Working Group on Metrics and Benchmarks for Quantum Computing Devices and Systems.
7. W. Griffin. Co-Chair, Software Engineering and Architectures for Realtime Interactive Systems (SEARIS) Working Group.
8. P. Patrone. Member, Applied Math and Scientific Computing Graduate Committee, University of Maryland, College Park.
9. D. G. Porter. Member, Tcl Core Team.
10. S. Ressler. W3C Immersive Web Working Group.
11. B. Saunders. Member, Board of Trustees, Society for Industrial and Applied Mathematics (SIAM).
12. B. Saunders. MD-DC-VA Section Representative, Congress of the Mathematical Association of America (MAA).
13. B. Saunders. Secretary, SIAM Activity Group on Geometric Design.
14. B. Saunders. Member, Selection Committee, Gabor Szego Prize, SIAM Activity Group on Orthogonal Polynomials and Special Functions.
15. K. Sayrafian. Co-Chair, IoT-Health Group, COST CA15104, Inclusive Radio Communication Networks for 5G and Beyond (IRACON).
16. B. I. Schneider. Co-Chair, Networking and Information Technology R&D (NITRD) High End Computing Interagency Working Group.
17. B. Schneider. NIST Representative, National Strategic Computing Initiative Joint Program Office.

Adjunct Academic Appointments

1. M. Coudron. Adjunct Assistant Professor, Department of Computer Science, University of Maryland, College Park, MD.
2. S. Glancy. Lecturer, Department of Physics, Colorado University, Boulder, CO.
3. E. Knill. Lecturer, Department of Physics, Colorado University, Boulder, CO.
4. P. Kuo. Adjunct Associate Professor, Department of Physics, University of Maryland, College Park, MD.
5. Y.-K. Liu. Adjunct Associate Professor, Department of Computer Science, University of Maryland, College Park, MD.
6. K. Sayrafian. Affiliate Associate Professor, Concordia University, Montreal, Canada.
7. X. Tang. Adjunct Professor, University of Limerick, Ireland.

Thesis Direction

1. G. Doğan. Member, Ph.D. Thesis Committee, University of Delaware: H. H. Eruslu.
2. A. Kearsley. Member, Ph.D. Thesis Committee, Drexel University: A. Chen.
3. Y. Liu. Ph.D. Co-Advisor, University of Maryland, College Park: K. Huang.
4. B. Miller. Member, Ph.D. Thesis Committee, University of Erlangen, Germany: D. Ginev.
5. F. Potra. Ph.D. Advisor, University of Maryland Baltimore County: J. Praniewicz.
6. K. Sayrafian. Ph.D. Co-Advisor, University of Zagreb, Zagreb, Croatia: K. Krhac.
7. K. Sayrafian. Ph.D. Co-Advisor, Concordia University, Montreal, Canada, M. Roudneshin.

Community Outreach

1. R. F. Boisvert. Presentation: “Computational Science in a Federal Laboratory,” Career Lecture Series, Keene State College, Keene, NH, April 9, 2019.
2. R. F. Boisvert. Presentation: “Computational Science in a Federal Laboratory,” Department of

Mathematics, Morgan State University, Baltimore, MD, October 3, 2019.

3. A. Kearsley. ITL Representative, ACM Richard Tapia Celebration of Diversity in Computing, San Diego, CA September 18-21, 2019.
4. S. Ressler. Presentation: "WebVR," Gaithersburg High School, December 11, 2018.
5. S. Ressler. Mock Interviews, Gaithersburg High School, April 3, 2019.
6. B. Saunders. Visiting Lecturer, Society for Industrial and Applied Mathematics.
7. B. Saunders. Organizer, Virginia Standards of Learning Tutoring Program, Northern Virginia Chapter (NoVAC), Delta Sigma Theta Sorority, Inc. and the Dunbar Alexandria-Olympic Branch of the Boys and Girls Clubs of Greater Washington, January - May 2019.
8. B. Saunders. Black History Month Profile Display, NIST Public Affairs Office, February 2019.
9. B. Saunders. Featured, Mathematically Gifted & Black Poster, American Mathematical Society (AMS).

Awards and Recognition

1. R. Boisvert. Fellow, Association for Computing Machinery, December 2019.
2. A. Carasso. Award for Excellence in Research in Applied Mathematics, Washington Academy of Sciences, May 2019.
3. A. Carasso, Fellow, Washington Academy of Science, May 2019.
4. A. Carasso. ITL Outstanding Journal Paper Award, August 2019.
5. M. Donahue and D. Porter. Jacob Rabinow Applied Research Award, NIST, December 2018.
6. F. Hunt. Fellow, American Mathematical Society, November 2018.
7. F. Hunt. Fellow, Association for Women in Mathematics, November 2019.
8. K. Krhac and K. Sayrafian. ITL Outstanding Conference Paper Award, Information Technology Laboratory, NIST, August 8, 2019.
9. P. Kuo. Senior Member, Optical Society of America (OSA), June 2019.
10. S. Ressler. 2nd Place, World Standards Day Essay Contest, Society for Standards Professionals, October 2018.
11. B. Saunders. Fellow, Washington Academy of Sciences, May 2019.
12. B. Saunders. Award for Excellence in Research in Mathematics and Computer Science, Washington Academy of Sciences, May 2019.
13. B. Saunders. ITL Outstanding Contribution to Enhance Diversity Award, 2019.
14. K. Sayrafian. Best Paper, IEEE European Conference on Networks and Communications (EuCNC), Valencia, Spain, June 18-21, 2019.
15. K. Sayrafian, S. Perez-Simbor, K. Krhac, C. Garcia Pardo, D. Simunic, and N. Cardona. Best Paper, IEEE Conference on Standards for Communications and Networking, Paris, France, October 2018.

Funding Received

During FY 2019 ACMD's yearly allocation of base funding from the NIST Information Technology Laboratory was supplemented with in funding from a variety of internal and external competitions. Such funding represented 9 % of the Division's FY 2019 budget.

Note: For multi-year awards and joint awards, only projects with new funding received by ACMD during FY 2019 are listed. For joint projects, names of ACMD participants are underlined.

External

1. M. Donahue. NIST Support for DARPA Magnetic Miniaturized and Monolithically Integrated Component (M3IC) Program, DARPA. (Joint with PML)

Internal

1. J. Ullom, G. Hilton, J. Fowler, D. Bennett, R. Doriese, B. Alpert, L. Hudson, and T. Jach. A Thousand-Fold Performance Leap in Ultrasensitive Cryogenic Detectors. NIST Innovations in Measurement Science. (Joint with PML)
2. C. L. Dennis, T. P. Moffat, A. J. Biacchi, A. R. Hight Walker, S. I Woods, W. L. Tew, and M. J. Donahue. Thermal MagIC: An SI-Traceable Method for 3D Thermal Magnetic Imaging and Control. NIST Innovations in Measurement Science. (Joint with PML, MML)
3. A. Dienstfrey, S. Russek, K. Stupic, K. Keenan, Z. Gimbutas, and W. Keyrouz. Deep Learning for MRI Reconstruction and Analysis. Fundamental and Applied Research for AI Program. (Joint with PML)

4. R. Evans, A. Balijepalli, and A. Kearsley. Modeling, Uncertainty Quantification, and Calibration for Biological Field Effect Transistors. Fundamental and Applied Research for AI Program. (Joint with MML)
5. S. Glancy. Neural Networks for Quantum Tomography. ITL Building the Future Program.
6. A. Kearsley and A. Moorthy. AI Forensic Compound Identification. Fundamental and Applied Research for AI Program. (Joint with MML)
7. P. Kuo. Dual-Polarization Quantum Frequency Converter. ITL Building the Future Program.
8. K. Lehnert, K. Silverman, D. Moody, J. Teufel, R. Mirin, S.-W. Nam, E. Knill, P. Hale, and T. Dennis. Establishing the Science of Networks for Superconducting Quantum Computers. NIST Innovations in Measurement Science Program. (Joint with CTL, PML)
9. Y.-K. Liu, Quantum Inspired Techniques for Explainable AI. ITL Building the Future Program.
10. P. N. Patrone, A. Dienstfrey, and G. B. McFadden. Fundamentals and Uncertainty Quantification of Coarse-Grained Simulations III. ITL Building the Future Program.
11. T. Porto, A. Gorshkov, A. Migdall, W. Phillips, S. Glancy, E. Knill, and K. Srinivasan. Metrology with Interacting Photons. NIST Innovations in Measurement Science Program. (Joint with PML)
12. K. Sayrafian. Modeling and Simulation of EFC for Implant-IoT Applications. ITL Building the Future Program.
13. B. I. Schneider, T. Allison, A. J. Kearsley, W. Keyrouz and B. Wallace. ML and AI Applied to Problems in Computational Chemical Physics. ITL Building the Future Program. (Joint with MML)
14. J. Terrill, J. Zwolak, and W. Griffin. In-Situ Machine Learning for Large-Scale Simulation Analysis. ITL Building the Future Program.
15. A. Youssef and B. Miller. Deep Learning Neural Networks for Math & Science Processing. ITL Building the Future Program.

Grants Awarded

ACMD awards a small amount of funding through the NIST Measurement Science Grants Program for projects that make direct contributions to its research programs. During FY 2019 the following cooperative agreements were active.

1. Prometheus Computing LLC: *Security, Resiliency and Dynamics of Interdependent Self-Organizing Networks*. PI: Assane Gueye.
2. Theiss Research: *Algorithms for Image and Shape Analysis in 3d*. PI: Gunay Dogan.
3. Theiss Research: *Exploiting Alternate Computing Technologies*. PI: Alan Mink.
4. University of Edinburgh: *Rigorous and Presentable Asymptotics for Special Functions and Orthogonal Polynomials*. PI: Adri Olde-Daalhuis.
5. University of Maryland: *In-situ Visualization for Immersive Environments*. PI: Amitabh Varshney.
6. University of Maryland: *New Theory and Resilience Metrics for Systems-of-Systems*. PI: Richard J. La.
7. University of Maryland: *Joint Center for Quantum Information and Computer Science (QuICS)*. PI: Andrew Childs.
8. University of Texas at Arlington: *SENTINEL: Security Interaction Testing for IoT Systems and Blockchains*. PI: Yu Lei.

External Contacts

ACMD staff members interact with a wide variety of organizations in the course of their work. Examples of these follow.

Industrial Labs

Amgen Inc.
BAE Systems
Baxter Healthcare
Bernoulli Institute (Switzerland)
Biogen Inc.
The Boeing Company
Bruker Corporation
Deltares (Netherlands)
Eli Lily and Company
EN-FIST Centre of Excellence (Slovenia)
Exxon Mobil
Ford Motor Company
Fraunhoffer IGD (Germany)
Genentech
Gener8
General Electric Global Research Center

Health Canada (Canada)
HC-Photonics Corp.
Hoffmann-La Roche Ltd. (Switzerland)
Honeywell
Intelligent Automation Inc.
Massachusetts General Hospital
Mechdyne
Momenta Pharmaceuticals
NTT Corporation (Japan)
Pfizer Essential Health
Psychometric Research & Development, Ltd. (UK)
Roche Pharmaceutical Research & Early Development
SIKA Technology (Switzerland)
Schrodinger LLC
SUSE
United States Pharmacopeia
Wireless Research Center (North Carolina)

Government/Non-profit Organizations

American Society of Mechanical Engineers
American Telemedicine Association
Argonne National Laboratory
Army Research Laboratory
Association for Computing Machinery
Biosciences National Laboratory (Brazil)
Center for Research in Energy and Materials (Brazil)
CSIRO (Australia)
EN-FIST Centre of Excellence (Slovenia)
Helmholtz-Zentrum (Germany)
IEEE Computer Society
Institute for Applied Mathematics, Italian National Research Council (Italy)
Institute of Molecular Biology and Biophysics (Switzerland)
Institute of Physics and Chemistry of Materials (France)
Pacific Northwest National Laboratory
Leibniz-Forschungsinstitut für Molekulare Pharmakologie (Germany)
Lawrence Livermore National Laboratory
Montgomery County, Maryland
Nanohub.org
NASA Glenn Research Center
NASA Jet Propulsion Laboratory
National Institute of Biomedical Imaging and Bioengineering
National Institute of Chemistry (Slovenia)
National Institutes of Natural Sciences (Japan)
National Institutes of Health
National Physical Laboratory (UK)
National Institute of Research in Metrology (Italy)
National Research Council (Canada)
National Science Foundation
Naval Facilities Engineering Command
Open Math Society
Pacific Northwest National Laboratory
QIMR Berghofer Medical Research Institute (Australia)
Quantum Chemistry Research Institute (Japan)
Quantum Economic Development Consortium
Sandia National Laboratories
Smithsonian Institution
Society for Industrial and Applied Mathematics
Swedish Medical Products Agency (Sweden)
Synchrotron Light Laboratory (Brazil)
Theiss Research
US Department of Energy
US Food and Drug Administration
US Holocaust Memorial Museum
Web3D Consortium
World Wide Web Consortium

Universities

Aalto University (Finland)
Arizona State University
Beijing Institute of Technology (China)
Brown University
California State University, Fullerton
Carnegie Mellon University
Clarkson University
Clemson University
Colorado State University
Columbia University
Concordia University (Canada)
Courant Institute of Mathematical Sciences
Dalian University of Technology (China)
Darmstadt University
Drexel University
Durham University
ETH Zurich (Switzerland)
European University Cyprus (Cyprus)
Federal University of Ceara (Brazil)
Flatiron Institute
Florida State University
Freiburg University (Germany)
Friedrich-Alexander University (Germany)
Gdansk University of Technology (Poland)
George Mason University
George Washington University
Georgia Technological University
Harvard University
Hong Kong Baptist University (China)
Imperial College London (UK)
Indian Institute of Technology (India)
Indiana University
Jacobs University Bremen (Germany)
Khallikote College (India)
Lafayette College
Linnaeus University (Sweden)
Massachusetts Institute of Technology
Medical University of South Carolina
Michigan Technical University

National University of Singapore (Singapore)
Naval Postgraduate School
National Center for Supercomputer Applications
Norfolk State University
Ohio State University
Polytechnic University of Valencia (Spain)
Queensland University of Technology (Australia)
Radford University
Rensselaer Polytechnic University
Rice University
Rochester Institute of Technology
Royal Institute of Technology (Sweden)
Shandong University (China)
Stanford University
Shippensburg University
Stockholm University (Sweden)
Technion, Israel institute of Technology (Israel)
Texas A&M University
Texas Tech University
Tokyo Institute of Technology (Japan)
Tsinghua University (China)
Tufts University
University of Akron
University of Antwerp (Belgium)
University of Bayreuth (Germany)
University of Bergamo (Italy)
University of Bologna (Italy)
University of British Columbia (Canada)
University of California, Berkeley
University of Central Florida
University of Colorado, Boulder
University of Delaware
University of Edinburgh (UK)
University of Erlangen-Nuremberg (Germany)
University of Essex (UK)
University of Houston
University of Illinois, Urbana-Champaign
University of Limerick (Ireland)
University of Lisbon (Portugal)
University of Maryland, Baltimore County
University of Maryland, College Park
University of Maryland, University College
University of Melbourne (Australia)
University of Michigan
University of New Mexico
University of New South Wales (Australia)
University of Notre Dame
University of Oulu (Finland)
University of Petroleum (China)
University of Queensland (Australia)
University of Science and Technology (China)
University of Sheffield (UK)
University of Silesia (Poland)
University of South Carolina
University of Southern California
University of Strathclyde (UK)
University of Sydney (Australia)
University of Texas at Arlington
University of Toronto (Canada)
University of Turin (Italy)
University of Washington
University of Western Ontario (Canada)
University of Windsor (Canada)
University of Wisconsin
University of Zagreb (Croatia)
Virginia Polytechnic Institute
Worcester Polytechnic University
Yale University
Youngstown State University

Part V

Appendix

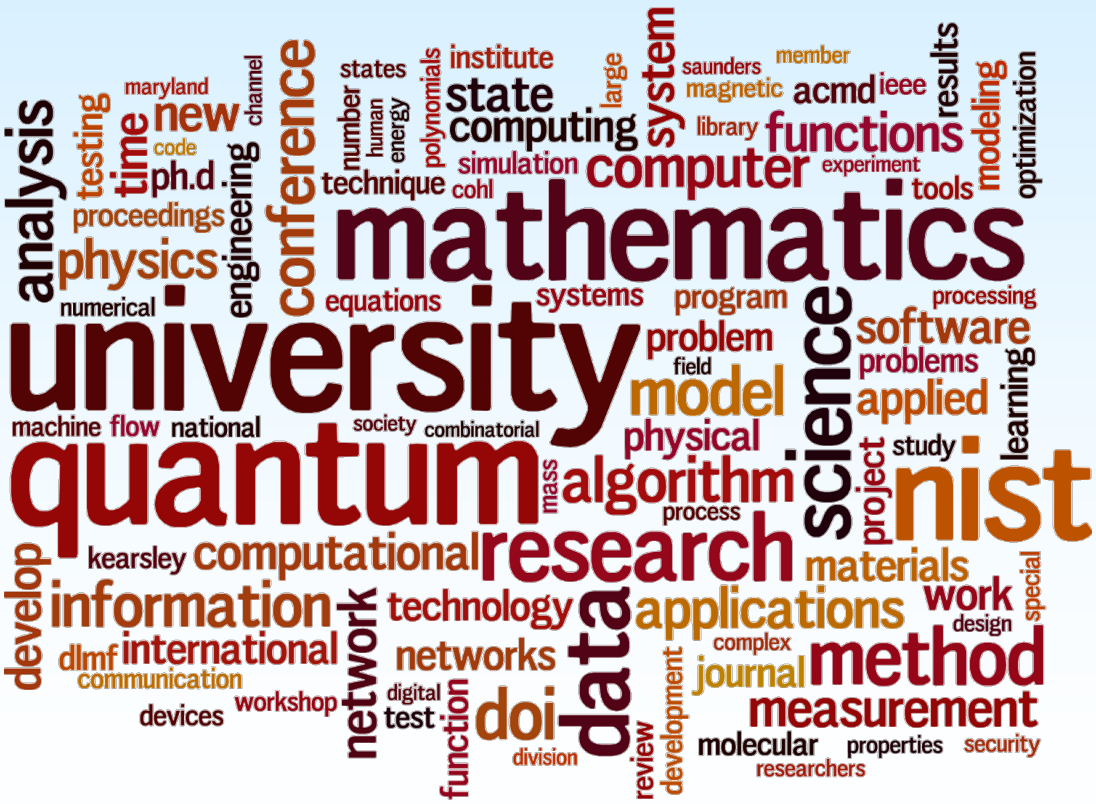

Staff

ACMD consists of full-time permanent Federal staff located at NIST laboratories in Gaithersburg, MD and Boulder, CO. This full-time staff is supplemented with a variety of special appointments. The following list reflects all non-student appointments held during any portion of the reporting period (October 2018 – December 2019). Students and interns are listed in Table 2 page 121.

* Denotes staff at NIST Boulder.
† Denotes part-time Federal staff.

Division Staff

Ronald Boisvert, *Chief*, Ph.D. (Computer Science), Purdue University, 1979
Catherine Graham, *Secretary*
Lochi Orr, *Administrative Assistant*, A.A. (Criminal Justice), Grantham University, 2009
†Alfred Carasso, Ph.D. (Mathematics), University of Wisconsin, 1968
Roldan Pozo, Ph.D. (Computer Science), University of Colorado at Boulder, 1991
Kamran Sayrafian-Pour, Ph.D. (Electrical and Computer Engineering), University of Maryland, 1999
Christopher Schanzle, B.S. (Computer Science), University of Maryland Baltimore County, 1989

Mathematical Analysis and Modeling Group

Timothy Burns, *Leader*, Ph.D. (Mathematics), University of New Mexico, 1977
*Bradley Alpert, Ph.D. (Computer Science), Yale University, 1990
Sean Colbert-Kelly, Ph.D. (Mathematics), Purdue University, 2012
*Andrew Dienstfrey, Ph.D. (Mathematics), New York University, 1998
Ryan Evans, Ph.D. (Applied Mathematics), University of Delaware, 2016
†Jeffrey Fong, Ph. D. (Applied Mechanics and Mathematics), Stanford University, 1966
*Zydrunas Gimbutas, Ph.D. (Applied Mathematics), Yale University, 1999
Fern Hunt, Ph.D. (Mathematics), New York University, 1978
Raghu Kacker, Ph.D. (Statistics), Iowa State University, 1979
Anthony Kearsley, Ph.D. (Computational and Applied Mathematics), Rice University, 1996
Geoffrey McFadden, *NIST Fellow,* Ph.D. (Mathematics), New York University, 1979
Paul Patrone, Ph.D. (Physics), University of Maryland, 2013

Faculty Appointee (Name, Degree / Home Institution)
Daniel Anderson, Ph.D. / George Mason University
Michael Mascagni, Ph.D. / Florida State University
John Nolan, Ph.D. / American University
Florian Potra, Ph.D. / University of Maryland Baltimore County

Guest Researchers (Name, Degree / Home Institution)
Sebastian Barillaro, Ph.D. / Industrial Technology National Institute, Argentina
Diego Andres Bouvier, M.S. / Technological Laboratory of Uruguay
Charles Bezerra Prado, D.Sc. / Instituto Nacional de Metrology, Brazil
Yu (Jeff) Lei, Ph.D. / University of Texas at Arlington
Christoph Witzgall, Ph.D. / *NIST Scientist Emeritus*

Mathematical Software Group

Michael Donahue, *Leader* Ph.D. (Mathematics), Ohio State University, 1991
Javier Bernal, Ph.D. (Mathematics), Catholic University, 1980
Howard Cohl, Ph.D. (Mathematics), University of Auckland, 2010
Stephen Langer, Ph.D. (Physics), Cornell University, 1989

†Daniel Lozier, Ph.D. (Applied Mathematics), University of Maryland, 1979
Marjorie McClain, M.S. (Mathematics), University of Maryland College Park, 1984
Bruce Miller, Ph.D. (Physics), University of Texas at Austin, 1983
William Mitchell, Ph.D. (Computer Science), University of Illinois at Urbana-Champaign, 1988
Donald Porter, D.Sc. (Electrical Engineering), Washington University, 1996
Bonita Saunders, Ph.D. (Mathematics), Old Dominion University, 1985
Barry Schneider, Ph.D. (Physics), University of Chicago, 1969

Faculty Appointees (Name, Degree / Home Institution)
Abdou Youssef, Ph.D. / George Washington University

NRC Postdoctoral Associates
Heman Gharibnejad, Ph.D. (Physics), University of Nevada, 2014

Guest Researchers (Name, Degree / Home Institution)
Günay Doğan, Ph.D. / Theiss Research
Adri Olde Daalhuis, Ph.D. / University of Edinburgh
Deyan Ginev, M.Sc. / Chakra Consulting
Xiaoxu Guan, Ph.D. / Colorado School of Mines
Mark Alexander Henn, Ph.D. / University of Maryland
Todd Martinez, Ph.D. / Stanford University
Chen Qu, Ph.D. / University of Maryland
Moritz Schubotz, Ph.D. / University of Karlsruhe, Germany

Computing and Communications Theory Group

Ronald Boisvert, *Acting Leader*, Ph.D. (Computer Science), Purdue University, 1979
Brian Cloteaux, Ph.D. (Computer Science), New Mexico State University, 2007
Matthew Coudron, Ph.D. (Computer Science), Massachusetts Institute of Technology, 2017
*Scott Glancy, Ph.D. (Physics), University of Notre Dame, 2003
*Emanuel Knill, *NIST Fellow,* Ph.D. (Mathematics), University of Colorado at Boulder, 1991
Paulina Kuo, Ph.D. (Physics), Stanford University, 2008
Yi-Kai Liu, Ph.D. (Computer Science), University of California, San Diego, 2007
Lijun Ma, Ph.D. (Precision Instruments and Machinery), Tsinghua University, 2001
Vladimir Marbukh, Ph.D. (Mathematics) Leningrad Polytechnic University, 1986
Oliver Slattery, *Project Leader*, Ph.D. (Physics), University of Limerick, 2015
†Xiao Tang, Ph.D. (Physics), Chinese Academy of Sciences, 1985

NRC Postdoctoral Associates
Lucas Brady, Ph.D. (Physics), University of California at Santa Barbara, 2018
Lucas Kocia, Ph.D. (Chemistry), Harvard University, 2016

Faculty Appointees (Name, Degree / Home Institution)
James Lawrence, Ph.D. / George Mason University
Richard La, Ph.D. / University of Maryland

Guest Researchers (Name, Degree / Home Institution)
Isabel Beichl, Ph.D. / NIST, Retired
*Peter Bierhorst, Ph.D. / University of Colorado
Sumit Bhushan, Ph.D. / Indian Institute of Technology
*Hilma De Vasconcelos, Ph.D. / Universidade Federal do Ceará, Brazil
*Bryan Eastin, Ph.D. / Northrup Grumman
Assane Gueye, Ph.D. / Prometheus Computing
Stephen Jordan, Ph.D. / Microsoft Research
Alan Mink, Ph.D. / Theiss Research

Anouar Rahmouni, Ph.D. / Moroccan Foundation for Advanced Sci., Innovation and Research
Francis Sullivan, Ph.D. / IDA Center for Computing Sciences

High Performance Computing and Visualization Group

Judith Terrill, *Leader*, Ph.D. (Information Technology), George Mason University, 1998
William George, Ph.D. (Computer/Computational Science), Clemson University, 1995
Terence Griffin, B.S. (Mathematics), St. Mary's College of Maryland, 1987
Wesley Griffin, Ph.D. (Computer Science), University of Maryland Baltimore County, 2016
Sandy Ressler, M.F.A. (Visual Arts), Rutgers University, 1980
Steven Satterfield, M.S. (Computer Science), North Carolina State University, 1975
James Sims, Ph.D. (Chemical Physics), Indiana University, 1969
Justyna Zwolak, Ph.D. (Physics), Nicolaus Copernicus University, Poland, 2011

NRC Postdoctoral Associates

Justin Kauffman, Ph.D. (Engineering Science and Mechanics), Penn State University, 2018

Guest Researchers (Name, Degree / Home Institution)

John Hagedorn, M.S. / NIST, Retired

Glossary of Acronyms

1D	one-dimensional
2D	two-dimensional
3D	three-dimensional
AAAS	American Association for the Advancement of Science
AAPS	American Association of Pharmaceutical Scientists
ACM	Association for Computing Machinery
ACMD	NIST/ITL Applied and Computational Mathematics Division
ACTS	Advanced Combinatorial Testing System
AI	artificial intelligence
AIAA	American Institute for Aeronautics and Astronomics
AMP	atomic and molecular physics
AMS	American Mathematical Society
APS	American Physical Society
AR	augmented reality
AS	autonomous system
ASME	American Society of Mechanical Engineering
ASTM	(formerly) American Society for Testing Materials
AWM	Association for Women and Computing
arXiv	preprint archive housed at Cornell University (http://arxiv.org/)
BCC	body channel communications
BEC	Bose-Einstein condensate
BIM	building information modeling
Bio-FET	biological field effect transistor
BIPM	Bureau International des Poid et Mesures
BMG	bulk metallic glass
BMP	Bateman Manuscript Project
BOB	burn observable bubble
BPVC	ASME Boiler and Pressure Vessel Code
Caltech	California Institute of Technology
CAS	computer algebra system
CAVE	CAVE Automatic Virtual Environment
CCM	Combinatorial Coverage Measurement
CENAM	Center for Metrology of Mexico
CFPG	Coulomb force parametric generator
CG	coarse-grained
CI	configuration interaction
CICM	Conference on Intelligent Computer Mathematics
CLEO	Conference on Lasers and Electro-Optics
CMA	University of Antwerp Computational Mathematics Research Group
CN	Crank-Nicolson method
CNN	convolutional neural network
CNOT	controlled not, a fundamental operation in quantum computing
COMSOL	Multiphysics finite element software
CPU	central processing unit
CS	component system
CFSF	Continued Fractions for Special Functions
CSF	configuration state function
CSIRO	Australia's Commonwealth Scientific and Industrial Research Organization
CT	combinatorial testing
CTL	NIST Communications Technology Laboratory
CTMC	classical trajectory Monte Carlo
CVS	Concurrent Version System (for source code version control)
CVSS	Common Vulnerability Scoring System

CY	calendar year
DAD	database-assisted design
DAMOP	APS Division of Atomic, Molecular, and Optical Physics
DARPA	Defense Advanced Research Projects Agency
DCI	demand-to-capacity index
DL	deep learning
DLMF	Digital Library of Mathematical Functions
DNA	deoxyribonucleic acid
DNN	deep neural network
DOC	Department of Commerce
DOE	Department of Energy
DOI	digital object identifier
DP	dynamic programming
DSO	differential semblance optimization
DRMF	Digital Repository of Mathematical Formulae
EBSD	electron backscatter diffraction
eCF	Wolfram Computational Knowledge of Continued Fractions Project
EL	NIST Engineering Laboratory
ESWL	equivalent static wind loads
FDA	Food and Drug Administration
FDTD	finite difference time domain
FEDVR	finite element discrete variable
FEM	finite element method
FFT	fast Fourier transform
FGR	NIST Foreign Guest Researcher Program
FIPS	Federal Information Processing Standard
FY	fiscal year
GB	grain boundary
GB	guaranteed bitrate
GC	gas chromatography
GDML	Global Digital Mathematical Library
GI	gastrointestinal
GPA	generalized preferential attachment
GUM	Guide to Uncertainty in Measurement
HBC	human body communications
HEC	High End Computing
HMD	head-mounted display
HPCC	High Performance Computing and Communications initiative
HR	hit rate
HTML	hypertext markup language
HVAC	heating, ventilation and air conditioning
HVACSIM+	software package and computing environment for simulating HVAC system
Hy-CI	Hylleraas-Configuration Interaction technique
IARPA	Intelligence Advanced Research Projects Agency
IBBR	UMD-NIST Institute for Bioscience and Biotechnology Research
IBM	intra-body communications
ICIAM	International Congress on Industrial and Applied Mathematics
ICME	Integrated Computational Materials Engineering
ICO	indefinite causal ordering
ICST	International Conference of Software Testing
IDE	integro-differential equation
IEEE	Institute of Electronics and Electrical Engineers
IFIP	International Federation for Information Processing
IMKT	International Mathematical Knowledge Trust
IMS	NIST Innovations in Measurement Science program
IoT	Internet of things
ITAMP	Harvard-Smithsonian Institute for Theoretical Atomic and Molecular Physics

ITL	NIST Information Technology Laboratory
IR	inversion recovery
ISMRM	International Society of Magnetic Resonance in Medicine
IWCT	International Workshop on Combinatorial Testing
JCGM	BIPM Joint Committee for Guides in Metrology
KLS	Koekoek, Lesky and Swarttouw
KNL	Knight's Landing
KNN	K-nearest neighbors' algorithm
KSU	Kansas State University
LaTeX	a math-oriented text processing system
LaTeXML	a LaTeX to Math ML converter
LDA	linear discriminant analysis
M3IC	DARPA Magnetic, Miniaturized, and Monolithically Integrated Components program
MAA	Mathematical Association of America
MathML	Mathematical Markup Language (W3C standard)
MD	molecular dynamics
MDP	Markov decision process
MDS	multi-dimensional scaling
MEMS	micro-electrical mechanical systems
MERA	multiscale entanglement renormalization ansatz
MGGHAT	MultiGrid Galerkin Hierarchical Adaptive Technique (software system)
MHD	magneto-hydrodynamics
ML	machine learning
MLP	mathematical language processing
MML	NIST Material Measurement Laboratory
MOLSSI	Molecular Science Software Institute
MOS	Magnus, Oberhettinger, and Soni
MPI	Message Passing Interface
MR	mixed reality
MRAM	magneto-resistive random-access memory
MRI	magnetic resonance imaging
MSRI	Mathematical Sciences Research Institute (Berkeley)
muMAG	Micromagnetic Activity Group
NASA	National Aeronautics and Space Administration
NBS	National Bureau of Standards
NCNR	National Center for Neutron Research
NDE	non-destructive evaluation
NFV	network function virtualization
NISQ	noisy intermediate-scale quantum
NIST	National Institute of Standards and Technology
NISTIR	NIST Internal Report
NITRD	Networking and Information Technology Research and Development
NLP	natural language processing
NMR	nuclear magnetic resonance
NN	neural network
NRC	National Research Council
NSF	National Science Foundation
NYU	New York University
OCR	optical character recognition
OOF	Object-Oriented Finite Elements (software)
OOF3D	3D version of OOF
OOMMF	Object-Oriented Micromagnetic Modeling Framework (software)
OPSF	orthogonal polynomials and special functions
OSA	Optical Society of America
P2C	presentation to computation conversion
P2P	peer to peer
PA	preferential attachment

PCB	printed circuit board
PCR	polymerase chain reaction
PDE	partial differential equation
PECASE	Presidential Early Career Award for Scientists and Engineers
PH	Powell's hybrid method
PHAML	Parallel Hierarchical Adaptive Multi Level (software)
PI	principal investigator
PML	NIST Physical Measurement Laboratory
PoCF	probability of cascading failures
PPLN	periodically poled lithium nitrate
PQC	post-quantum cryptography
PREP	NIST Professional Research Education Program
PW	NIST Pathways student employment program
QA	quantum annealing
QAO	quantum adiabatic optimization
QAOA	quantum approximate optimization algorithm
QCI	quantum channel identification
QD	quantum dot
QDPD	Quaternion-based Dissipative Particle Dynamics simulation code
QIP	quantum information processing
qMRI	quantitative MRI
QPM	quasi-phase matched
QuICS	UMD-NIST Joint Center for Quantum Information and Computer Science
R&D	research and development
RAN	radio access network
RAVEN	Rapid Analysis of Various Emerging Nanoelectronics
RL	reinforcement learning
RMS	root mean square
RRM	radio resource management
RSA	Rivest-Shamir-Adelman public key cryptographic algorithm
RSP	real-space propagation
SDE	stochastic differential equation
SED	ITL Statistical Engineering Division
SEM	scanning electron microscope
SFC	service function chain
SFWM	spontaneous four-wave mixing
SHIP	Summer High School Internship Program
SIGIR	ACM Special Interest Group on Information Retrieval
SIL	short iterative Lanczos
SIAM	Society for Industrial and Applied Mathematics
SIS	susceptible-infectious-susceptible
SIAM	Society for Industrial and Applied Mathematics
SIGGRAPH	ACM Special Interest Group on Graphics
SLA	service level agreement
SLAC	Stanford Linear Accelerator Center
SO	split operator
SPDC	spontaneous parametric down conversion
SPIE	International Society for Optical Engineering
SRM	standard reference material
STEM	science, technology, engineering, and mathematics
SURF	NIST Student Undergraduate Research Fellowship program
SVD	singular value decomposition
SVP	NIST Student Volunteer Program
TDSE	time domain Schrodinger equation
TES	transition edge sensor
TLS	transport layer security
TQC	Theory of Quantum Computation (conference)

UCF	University of Central Florida
UMBC	University of Maryland Baltimore County
UMD	University of Maryland
UMIACS	University of Maryland Institute for Advanced Computer Studies
UNLV	University of Nevada Las Vegas
UPGMA	unweighted pair group method with arithmetic mean
UQ	uncertainty quantification
URL	universal resource locator
USAF	U.S. Air Force
VEMOS	Visual Explorer for Metric of Similarity (software)
VFA	variable flip angle
VM	virtual machine
VNO	virtual network operator
VR	virtual reality
VSB	voxel set boundary
W3C	World Wide Web Consortium
WAS	Washington Academy of Sciences
XSEDE	NSF eXtreme Science and Engineering Discovery Environment